CLIMATIC VARIABILITY STUDIES OVER PARTS OF INDIA WITH FOCUS ON HYDRO-CLIMATIC VARIABLES

Ph.D. THESIS

by

LITAN KUMAR RAY

DEPARTMENT OF HYDROLOGY
INDIAN INSTITUTE OF TECHNOLOGY ROORKEE
ROORKEE - 247 667 (INDIA)
OCTOBER, 2017

CLIMATIC VARIABILITY STUDIES OVER PARTS OF INDIA WITH FOCUS ON HYDRO-CLIMATIC VARIABLES

A THESIS

Submitted in partial fulfilment of the requirements for the award of the degree

of

DOCTOR OF PHILOSOPHY

in

HYDROLOGY

by

LITAN KUMAR RAY

DEPARTMENT OF HYDROLOGY
INDIAN INSTITUTE OF TECHNOLOGY ROORKEE
ROORKEE – 247 667 (INDIA)
OCTOBER, 2017

INDIAN INSTITUTE OF TECHNOLOGY ROORKEE
ROORKEE

CANDIDATE'S DECLARATION

I hereby certify that the work which is being presented in the thesis entitled "**CLIMATIC VARIABILITY STUDIES OVER PARTS OF INDIA WITH FOCUS ON HYDRO-CLIMATIC VARIABLES**" in partial fulfilment of the requirements for the award of the Degree of Doctor of Philosophy and submitted in the Department of Hydrology of the Indian Institute of Technology Roorkee, is an authentic record of my own work carried out during a period from July, 2012 to May, 2018 under the supervision of Dr. N. K. Goel, Professor, Department of Hydrology, Indian Institute of Technology Roorkee, Roorkee.

The matter presented in this thesis has not been submitted by me for the award of any other degree of this or any other institution.

(LITAN KUMAR RAY)

This is to certify that the above statement made by the candidate is correct to the best of my knowledge.

(Dr N. K. GOEL)
Supervisor

The Ph. D. Viva-Voce Examination of ...., Research Scholar, has been held on ....

Chairman, SRC **Signature of External Examiner**

This is to certify that the student has made all the corrections in the thesis.

Signature of Supervisor **Head of the Department**

Dated:

ABSTRACT

India is a developing country facing tremendous challenges to sustain its fast growing economic growth with the threat of global warming. Global warming or climate change may affect the livelihood of the most vulnerable people living in the country by changing the quality and distribution of India's natural resources. The assessment of climate related changes is most important across India. This can be examined by analysing the hydro-climatic datasets. Therefore, the present work has been taken up to investigate the changes in hydro-climatic variables over parts of the country. The objectives of the present study can be broadly categorised as follows:

(i) Analysis of recent temperature and rainfall datasets to understand the climate induced changes over parts of India.
(ii) Frequency analysis of extreme rainfall and streamflow series considering non-stationarity.

The analysis of temperature datasets cover entire India, while the rainfall analysis covers only east, west, north and central zones of India. Trend and homogeneity in annual and seasonal temperature data of 125 stations for 1941 to 2012 period has been investigated. The Mann-Kendall trend detection test, Theil and Sen's trend slope estimator, Cumulative deviation test, Standard normal homogeneity test and Wilcoxon Rank-Sum test are used for identification of trends and homogeneity in the datasets. The annual average, maximum and minimum temperatures show a rising trend at the rate of 0.44ºC/100 years, 0.51ºC/100 years and 0.19ºC/100 years respectively. All the seasonal temperature variables show a rising trend. Only the minimum temperature of the monsoon season shows the falling trend at the rate of 0.05ºC/100 years. The monsoon maximum temperature depicts a maximum increase at the rate of 0.80ºC/100 years. The homogeneity analysis shows break years around 1972, 1974 and 1977 for the annual average, maximum and minimum temperatures respectively for India. The seasonal analysis shows that the minimum temperatures of winter and monsoon season with the maximum temperature of the post-monsoon season are homogeneous in nature. The magnitude of a trend in all annual and seasonal temperature variables changed significantly

after the break year. The results of the regional analysis also show similar trends as observed in the case of entire India.

Rainfall is one of the most important factors of Indian economy. The estimation of spatio-temporal trends of rainfall on a regional basis will help in understanding the global impact of climatic systems over the region. The Von Neumann ratio, Hurst's coefficient, Mann-Kendall trend and Spearman's rank correlation tests are used for identification of short-term dependence, long-term dependence, trends and the correlation between rainfall of 148 stations with climate change and climate variability indices. Only one-fourth of the station rainfall and rainy day datasets exhibit short-term and long-term dependences on annual and seasonal basis. Most parts of the study area exhibit a decrease of 0 to 200 mm rainfall over the 1951 to 2007 period in annual and monsoon season. In non-monsoon season, the decrease is 0 to 100 mm. The number of rainy days on annual and seasonal basis also show a decrease of 0 to 10 days during the analysis period. Global average temperature and NINO3.4 SST anomaly have indicated good correlation with rainfall indices over the analysis period. Trends in multi-datasets of gridded rainfall also follow the similar pattern. The CRU and GPCC gridded datasets in general do not follow the spatial patterns shown by other gridded datasets.

Frequency analysis of annual maximum rainfall (AMR) data across India and the streamflow series of Narmada river basin has been carried out considering both stationarity and non-stationarity assumptions under recent climatic conditions using GAMLSS model. The annual maximum rainfall datasets of 239 stations, which are well distributed across India are used to see the effect of climate change (global average temperature, GAT), climate variability (NINO and IOD) and local temperature change (RAT) on rainfall quantiles of 25, 50 and 100 years return periods. The results of frequency analysis show that the Gumbel, Lognormal and Generalised Gamma are the most useful distributions for the non-stationarity case. The high values of climate indices, GAT and RAT generally provide higher peaks for annual maximum rainfall and vice versa.

Frequency analysis of annual maximum discharge of six stations of Narmada river basin of India is carried out under stationary and non-stationary conditions using external covariates, like, GAT, NINO, IOD and reservoir index (RI). The results exhibit that in comparison with the non-stationary model; the stationary model either overestimates or underestimates the design flood quantiles. The non-stationary model can also capture the effect of natural variability of any flood process. The results of non-stationary model confirm that the climate variability and construction of reservoirs have a sublime effect on flood process of Narmada river basin. The Hoshangabad station shows a significant influence of reservoir in annual maximum discharge compared to the other stations. The non-stationarity in annual maximum discharge is mainly due to the influence of reservoirs for three out of six stations, while other three stations are showing non-stationarity due to the effect of natural climate variability across the Narmada river basin.

ACKNOWLEDGMENTS

First and foremost, I would like to express my profound gratitude and sincere thanks to my supervisor Dr N. K. Goel**,** Professor, Department of Hydrology, Indian Institute of Technology Roorkee, for his inspiring guidance, valuable suggestions and substantial encouragement throughout the course of this research work. Words would fail to record the invaluable help I was privileged to receive from him on numerous occasions.

I would like to express my sincere thanks to Dr M. Perumal, Chairman, Department Research Committee (DRC), Dr M. L. Kansal and Dr Sumit Sen, members of Student Research Committee (SRC) for providing valuable suggestions while reviewing the work in the SRC meetings.

I express my sincere gratitude to Dr D. S. Arya, Former Head of the Department, and Dr M.K. Jain, Present Head of the Department, for providing necessary facilities for completion of this research work and for all the considerations and timely interventions rendered by him. Besides my research work, I have got a wide range of exposure to involve myself in a numbers of multidisciplinary projects and short term courses. The financial support, as project assistantship, received from the projects sponsored by Ministry of Water Resources, River Development and Ganga Rejuvenation through Bharat Singh Chair for Water Resources, Kalpasar Department, THDCI(L) and many of the other sponsoring agencies is gratefully acknowledged.

I would like to express my gratitude to Dr Himanshu Joshi, Dr B. K. Yadav, present Faculty members of Department of Hydrology and Dr B. S. Mathur, Dr D. K. Srivastava, Dr Ranvir Singh, Dr D. C. Singhal, former Faculty members of Department of Hydrology for their suggestions and help from time to time.

It is my great pleasure to acknowledge the unreserved academic support obtained from Dr Manohar Arora, Scientist, National Institute of Hydrology, Roorkee.

I am also greatly indebted to the Kalpasar Department, Government of Gujarat, Central Water Commission (CWC) and India Meteorological Department (IMD) for providing me with the necessary data required for the study.

I am also thankful to all the supporting staff members of Department of Hydrology, for their valuable support during the course of my research work. My warm thanks are due to Dr Asmita Murumkar, Mr Titas Ganguly, Ms Bratati Chowdhury, research colleagues, Mr Supindra Khatri, Mr Sunil Poudel, Mr Sujan Tamrakar, Mr Jayaram Prajapati, former trainy officiers, Mr Neeraj Kumar Sharma, Mr Rohit Varshney, Ms Khushbu, Ms Divya Ravi Prakash, Project Associates, and Mr Bhanesh, Project Assistant, Department of Hydrology for their valuable support in many ways and welcoming gestures throughout the study period. I am very much grateful to all other research scholars and post graduate students of Department of Hydrology for their encouragement and company during my stay at IIT Roorkee.

There are many friends and people who have been constantly encouraging and supporting me during my research period. I am thankful to all of them. I wish to record my sincere thanks and indebtedness to my friends Dr Subho Upadhaya, Mr Vijay, Mr Ashis, Mr Vikram Kumar, Mr Ajay Vashisht, Mr Jahangeer Ali, Dr Anurag Chauhan, Mr Sangram Bana, Mr Anant Rai, Dr Dinesh Singh at IIT Roorkee, all of whom have rendered selfless help and support in numerous ways during the itinerary of this study.

I recognize with warm appreciation and ever growing blessings of my parents, grandfather, moral support of my sister Lipika, and brother Shekhar. Last but not the least, I wish to thank numerous family members, friends and well-wishers who have contributed, directly or otherwise in making this endeavour an eventuality.

Above all, the greatest of my gratitude is towards the Almighty God who has made all this possible!

(LITAN KUMAR RAY)

TABLE OF CONTENTS

LIST OF FIGURES

LIST OF TABLES

ABBREVIATIONS & NOTATIONS

Abbreviations and notations having common meaning are defined here. Other locally used symbols are defined in the body of the Thesis during their first appearance

ABBREVIATION	DESCRIPTION
@	At The Rate
AIC	Akaike Information Criterion
APHRODITE	Asian Precipitation-Highly Resolved Observational Data Integration Towards Evaluation
AR5	Fifth Assessment Report
CDF/cdf	Cumulative Distribution Function
CGWB	Central Ground Water Board
CLIMAT	Monthly Climatological Data Assembled at Land-Based Meteorological Surface Observation
CRU	Climatic Research Unit
CRU TS 3.21	Climatic Research Unit Time series of 3.21 version
CWC	Central Water Commission
DMI	Dipole Mode Index
DTR	Daily Temperature Range
DWD	Deutscher Wetterdienst
e.g.	exempli gratia (for example)
ENSO	El Niño-Southern Oscillation
GAM	Generalized Additive Model
GAMLSS	Generalized Additive Models for Location, Scale, and Shape parameters
GCM	General Circulation Model
GC-Net	Greenland Climate Network
GHCN	Global Historical Climatology Network
GHCN-v2	Second Version of Global Historical Climatology Network
GMLE	Generalized Maximum Likelihood Estimation
GPCC	Global Precipitation Climatology Centre
GSOD	Global Surface Summary of Day
GU	Gumbel
HadCRUT4	Fourth version of Hadley Centre of the UK Met Office land surface air temperature records compiled by the Climatic Research Unit
i.e.	id est (That is)
IARI	India Agricultural Research Institute
iid	Independent and Identically Distributed

ABBREVIATION	DESCRIPTION
IITM	Indian Institute of Tropical Meteorology
IMD	India Meteorological Department
India-WRIS	Water Resources Information System of India
IOD	Indian Ocean Dipole
IPCC	Intergovernmental Panel on Climate Change
km^2	Square Kilometre
KWH	Kilowatt Hours
m^3	Cubic Meter
m^3/s, cumec	Cubic Meter per Second
MCDW	Monthly Climatic Data for the World
MK	Mann-Kendall
mm	Millimetre
MMK	Modified Mann–Kendall
N	North
NAO	North Atlantic Oscillation
NCA	Narmada Control Authority
NCAR	National Center for Atmospheric Research
NCDC	National Climate Data Center
NCEP	National Centers for Environmental Prediction
ºC	Degree Centigrade
PDF/pdf	Probability Density Function
RACMO2	Regional Climate Model Version 2
RCP	Representative Concentration Pathway
S	South
SOI	Southern Oscillation Index
SST	Sea Surface Temperature
SYNOP	Synoptic Weather Observation Reports
UNFCCC	United Nations Framework Convention on Climate Change
UD	University of Delaware
UK	United Kingdom
VASClimO	Variability Analysis of Surface Climate Observations
W	West
WC	West Coast
WGI	Working Group I
WGII	Working Group II
WMO	World Meteorological Organization
WWR	World Weather Records

CHAPTER 1
INTRODUCTION

1.1 GENERAL ABOUT CLIMATE CHANGE

United Nations Framework Convention on Climate Change (UNFCCC) defines "climate change" as: "a change of climate which is attributed directly or indirectly to human activity that alters the composition of the global atmosphere and which is in addition to natural climate variability observed over comparable time periods".

Human activities have increasingly changed the composition of the atmosphere and the land use. At present, there is strong evidence that the speed and amount of global climate change can be attributed to the combined effect of anthropogenic and natural forcing (IPCC, 2013). According to IPCC (2014), global mean surface (combine land and ocean) temperature increased by 0.85ºC (0.65ºC to 1.06ºC) over the period 1880 to 2012. Available records show that the period for 1983 to 2012 was possibly the warmest 30-year period in Northern Hemisphere (NH) for the last 800 years. The global land surface maximum and minimum temperatures have also increased since 1950. The projected global mean surface temperature increases from 0.9ºC to 1.3ºC over the period of 2016 to 2035 and 0.9ºC to 2.3ºC over the period of 2081 to 2100 with respect to 1850 to 1900. By 2050, all the AR5 representative concentration pathway (RCP) scenarios show an increase of 1.5°C to 2.3°C global warming over 1850 to 1900 period (IPCC, 2014). Globally, the minimum temperature extremes are increasing more rapidly than maximum temperature extremes (Donat and Alexander, 2012; Hansen et al., 2012). It is also reported that since 1950, the frequency of heat wave has increased in large parts of Asia, Australia, and Europe (IPCC, 2014).

Globally, the change in precipitation is very low since 1901. However, an increase in precipitation was found prior to 1951 in the NH mid-latitude land areas. Estimates based on General Circulation Models (GCM) under the RCP8.5 scenario suggest that the annual mean precipitation will possibly increase in the high latitudes and the equatorial Pacific Ocean by the end of this century (IPCC, 2013). The available records show an increase in frequency and intensity of extreme precipitation events in many parts of the world, and both are expected to increase in future as well. There are many other indications of changes in climatic systems such as retreat of glaciers, sea level rise, reduction in snow covers and sea ice thickness etc. The global mean sea level rise is expected to be of the order of 0.52 m to 0.98 m by the year 2100.

Global warming is not only changing the mean climate but also changing the weather extremes (Islam et al., 2014). Due to the global warming, the rainfall and flooding became heavier, hot days became hotter, and droughts became more severe. This intensification of extreme climate will be the most visible impact of global warming in the day-to-day life. The percentage of land area affected by drought is increasing globally since 1950 (Van Der Schrier et al., 2013). However, regionally, flood records reveal strong decadal to temporal variability and non-stationarity in flood frequency over the last few millennia. The magnitude and/or frequency of recent floods are more severe or comparable to the historical floods of various regions of the world (IPCC, 2013).

Global warming may lead to an intensification of the hydrological cycle (Mishra and Singh, 2010), alteration of behaviours of hydrological indicators (Labat et al., 2004), sea level rise (Nicholls and Tol, 2006) etc. Some studies pointed out that the climate change threatens the world's food security, freshwater availability and biodiversity (Vorosmarty et al., 2010; Wheeler and von Braun, 2013). The future global warming may produce different regional effects due to the regional climatology. Climate change may hamper the economic growth of a developing country like India as the country's economy is closely linked to the natural resource base and climate-related sectors like agriculture, water, forestry etc. Global warming may change the quality and distribution of India's natural resources and adversely affect the livelihood of the Indian population. The climatic extremes like heavy rainfall, warmer summer, extended periods without rainfall, etc. are going to increase in the near future (Mittal et al., 2016). Gupta and Deshpande (2004) predicted that due to population growth the per capita availability of water would go down drastically by 2050. Mishra et al. (2013) reported that the yield of rice and wheat might severely reduce due to the climate change. Besides this, the coastal areas of the country are more vulnerable to climate change due to the sea level rise and severe cyclonic activities (Bolch et al., 2012).

1.2 OBJECTIVES OF THE STUDY

The recent changes in climatic conditions pose significant challenges to the developing countries with an agrarian economy. India, the seventh largest country by area in the world, with over 1.2 billion people, is one of the most vulnerable nations to climate change impacts. Despite this fact, very little efforts have been made in the past to study climate change in India. Keeping in mind the above major concerns, a study related to climate change has been taken up with a particular focus on India. For this purpose, the presence of nonstationarity in temperatures and precipitations over India has been investigated. The presence of nonstationarity in the hydrological processes raised questions over the main assumption of stationarity and independence of the classical frequency analysis procedure (Khaliq et al., 2006; Milly et al., 2008). The accuracy of hydrological analysis and design procedure is seriously affected by the non-stationarity in observed data set (Douglas et al., 2000). Therefore, an alternate approach for frequency analysis of rainfall and streamflow series under non-stationary condition is also studied.

In the present study, the efforts have been made in the following directions.

(i) Analysis of recent temperature and rainfall datasets to understand the climate induced changes over parts of India.

(ii) Frequency analysis of extreme rainfall and streamflow series considering both stationarity as well as non-stationarity assumptions.

1.3 ORGANISATION OF THE THESIS

The thesis is divided into six major chapters. The introduction and objectives of the study are presented in Chapter 1.

Chapter 2 describes the studies related to the investigation of stationarity, and in particular, the trend analysis and change point detection of available surface temperature data sets pertaining to India.

The analysis of rainfall patterns over parts of India has been discussed in Chapter 3. The presence of short-term and long-term dependences have been investigated in the station rainfall. The association of rainfall and climate change and climate variability has been evaluated for the station dataset. In recent times, many types of gridded rainfall data with different spatial resolutions have been developed by various agencies, and some of these are freely available in public domain. The effect of the data sources over trend analysis have also been evaluated. The results of these studies are also presented in the chapter.

Chapter 4 presents the details of the frequency analysis of annual maximum rainfall series under stationarity and non-stationarity assumptions over India. Further, the influence of climate indices (i.e. ENSO and Indian dipole mode index), global warming (global average temperature) and local temperature over annual maximum rainfall series is also analysed.

The availability of water in the non-monsoon season is a big concern for India, especially in the water-stressed areas. Therefore, a number of reservoirs have been constructed in various river systems in India. The reservoirs are affecting the natural flow of a river, which means the extreme floods will also be affected by the reservoir regulation strategies. Furthermore, the recent climate variability makes flood more unpredictable. For this reason, the influence of reservoirs and climate variability on frequency analysis of Narmada river floods have been investigated in Chapter 5.

Finally, Chapter 6 presents the conclusions drawn from the study and the scope of further work in the area.

CHAPTER 2
TREND ANALYSIS AND CHANGE POINT DETECTION OF TEMPERATURE DATA OVER INDIA

2.1 GENERAL

Temperature has been widely used as an indicator of global warming. The changes in temperature have serious impacts on the hydrological cycle. A rise in temperature of the globe has been reported in some studies. The rise in temperature leads to an intensification of the hydrological cycle and influences almost all the hydrological processes. Considering the serious impacts of climate change, the analysis of temperature variables has been undertaken by various researchers on local, regional and global scales throughout the world. The Indian subcontinent has also been facing global warming induced changes. The changes in temperature may change the geographical distribution of India’s natural resources regarding quality and quantity. Hence, a study of spatial distribution and magnitude of temperature trends over India has been undertaken in this study.

This chapter deals with the identification of trends in annual and seasonal temperature data over India. The presence of change point in the data set is also investigated. The temperature trends before and after the change point are identified and compared. Lastly, the limitations of the present study have been presented.

2.2 OVERVIEW OF TEMPERATURE VARIABILITY ACROSS INDIA

In India, some studies related to trend analysis have been carried out using the annual and seasonal temperature data for a single station or a group of stations. Pramanik and Jagannathan (1954) studied annual mean maximum and minimum temperature trend over India. They reported that there was no increasing or decreasing trend in the temperature series.

Jagannathan & Parathasarathy (1973) investigated trend over mean annual temperatures for a set of eight Indian stations. The results indicated an increasing trend in the mean annual temperatures of Kolkata, Mumbai, Bangalore and Allahabad, and a decreasing trend at Cochin.

Hingane et al. (1985) analysed trend in temperature over the Indian region using station data. They reported an increasing trend in the mean annual temperatures over the North-East regions of the country. The diurnal asymmetry of temperature trends over India is quite different from that observed over many other parts of the globe, which was first indicated by Srivastava et al. (1992). During the last 100 years, an increasing trend of 0.35℃ for the whole country with a slightly lower increasing trend over southern parts (south of 23°N) and a decreasing trend over most of the northern parts of the country (north of 23°N) was observed.

Rupa Kumar et al. (1994) studied the maximum and minimum temperature trends by using the data of 121 stations for the period of 1901 to 1987. They concluded a country-wide increase of 0.6℃ in mean maximum temperature and 0.10℃ decrease in mean minimum temperature. They also found that the increasing daytime temperature was the reason behind most of the increases in mean surface air temperature over India.

Pant and Kumar (1997) analysed annual and seasonal temperature data for 1881 to 1997 and reported a significant warming trend of 0.57℃ per 100 years over India. They indicated that both the post-monsoon and winter season experienced higher warming. The north-eastern part of India showed a significant negative trend in monsoon temperature while the major part of the country did not show any significant trend.

Sinha Ray and De (2003) found an increasing trend of 0.35℃ for 100 years over extreme temperature events for India. They reported that the extreme maximum and minimum temperature had shown an increasing trend in the south and a decreasing trend in the north.

Arora et al. (2005) analysed mean, maximum and minimum temperature trends using 125 stations distributed over the whole of India for annual, winter, pre-monsoon, monsoon and post-monsoon seasons. They reported that most of the cases showed increasing trend except the mean pre-monsoon, the average monsoon, the average minimum pre-monsoon, and the average minimum monsoon temperatures.

Rao et al. (2005) studied trend using the data of 103 stations data for the period of 1971 to 2000 and reported an increasing trend in the days with critical extreme maximum and minimum temperatures for most of the stations over the peninsular India during March to May.

In the northern part of India, almost 40% of the stations showed an increasing trend in the days with critical extreme maximum temperature while 80% of the stations showed increasing trend in the extremes in night temperatures.

Sen Roy and Balling (2005) analysed trends in maximum and minimum temperatures, Daily Temperature Range (DTR) and cloud cover for the summer season and winter season over India by using Climate Research Unit high-resolution data (1^{o} x 1^{o}) for the period of 1931 to 2002. For both the seasons, it was reported that a significant increasing trend in the maximum and minimum temperatures exists with no statistically significant trend in DTR over entire India.

Rupa Kumar et al. (2006) studied temperature changes over the 21st century for India by generating high-resolution climate change scenario through PRECIS model. They reported an expected increase in future extremes in maximum and minimum temperatures and a faster increase in night temperatures than the day temperatures. Dash and Hunt (2007) analysed maximum and minimum temperatures over India and reported a sharp increase over north India as compared to south India.

Kumari et al. (2007) evaluated the measurements of monthly mean solar radiation reaching surface under all sky conditions for the period of 1981-2004 and they found that the maximum and minimum temperatures have been increasing, though, the solar radiation is decreasing. They concluded that the maximum temperature is increasing slowly from the first decade to second decade while the increase in minimum temperature has been doubled due to the drastic increase in greenhouse gas emissions.

Roy et al. (2007) studied the impact of green revolution on temperature over India. They found that the air temperature is changing due to the intensified irrigation and agricultural activities during the growing season. The increase of maximum temperature and diurnal temperature range is slowed down during the post-GR period due to the introduction of widespread irrigation measures in North Western and North Central India.

Roy (2008) found a direct negative forcing of aerosols during the winter season due to the clear sky, while the prevalence of cloudy and overcast skies during the summer monsoon season resulted in an indirect positive forcing of aerosols with respect to surface temperatures.

They concluded that strongest impact of aerosol on surface temperatures was more for the industrialized and urbanized areas of the subcontinent.

Kothawale et al. (2010a) indicated that the maximum, minimum and mean temperatures all showed increasing trends while minimum temperature increased at a faster rate than the maximum temperature. Kothawale et al. (2010b) analysed pre-monsoon daily temperature extremes over Indian region using station data. They indicated an increasing trend in the frequency of occurrence of hot days and hot nights and a decreasing trend in cold days and cold nights for most of the parts of India. The frequency of occurrence of hot days showed significantly increasing trend over the east coast, west coast and interior peninsula and cold days showed a significant decreasing trend over the western Himalayas and west coast. The frequency of hot nights showed significantly increasing trend for the east coast, west coast, and north-west parts of India. For entire India, the frequency of hot days and nights showed increasing trend and the frequency of cold days and nights showed decreasing trend.

Jain and Kumar (2012) studied temperature trends for 21 river basins in India and reported an increasing trend for mean maximum temperature over most of the stations. Mean minimum temperature showed rising trend at some stations and falling trend at some stations. The annual average temperature showed increasing trend for most of the stations in south, central and western parts and a decreasing trend for some stations in the north and north-eastern India.

Subash and Sikka (2014) analysed trends of temperature and rainfall and its relationship over India. They did not find any direct relationship between increasing rainfall and increasing maximum temperature for the monthly or seasonal pattern over meteorological sub-divisions of India. The maximum temperature increased at a rate of 1.20℃ per 100 years over the west coast. The minimum temperature trend showed a significant increase at a rate of 0.26℃ per 100 years over the India. The annual mean temperature increases are in the order of 0.50℃ per 100 years over India.

Bapuji Rao et al. (2014) studied minimum temperature trends over India for recent decades. They reported that the mean minimum temperature increased at a rate of 0.24℃ per decade. They found that the warming was more in rabi season (October–March) than in kharif season (June–October).

Some regional studies were also carried out over different parts of India. The study by Bhutiyani et al. (2007) using station data for a few stations in North West Himalayan region showed a significant increasing trend for mean, maximum, minimum and diurnal temperature range. They reported that the maximum temperature increased faster than the minimum temperature with a significant increasing trend in diurnal temperature range. Gautam et al. (2009) reported enhanced pre-monsoon warming over Himalayan-Gangetic region from 1979 to 2007.

Subash et al. (2010) investigated observational characteristics for rainfall and temperatures over the central part of northeast India. They reported a significant increasing trend in monsoon maximum temperature, post-monsoon maximum and minimum temperature and decreasing trend in monsoon minimum temperature.

Jhajharia and Singh (2011) analysed trends in temperature, diurnal temperature range, and sunshine duration using eight stations data in north-east India. They observed an increasing trend in the diurnal temperature range at three stations and decreasing trend at three other stations. In the winter and pre-monsoon season, temperature did not show any trend, and an increasing trend was seen in the monsoon and post-monsoon seasons over North East India.

Nayak and Mandal (2012) studied the impact of land-use and land-cover (LULC) changes in the regional variation of temperature trends over Western India using the datasets of 37 years (1973–2009). They found that the Western India is getting warmer by 0.13°C per decade. The change in LULC contributed to the warming over this region by 0.06°C per decade. This increase in temperature over the Western India is due to the reduction of forest area and subsequent increase in the agricultural area.

Jain et al. (2013) analysed rainfall and temperature trends in north-east India. They found an increasing trend in mean maximum temperature and mean minimum temperature for most of the stations with a decreasing trend for some stations in annual average temperature.

The major limitation of most of the previous studies, carried out in India, has been that individual studies have used the data set of a limited number of stations. Besides this, the temperature data used in most of the previous studies are of different lengths (for e.g. Srivastava et al., 1992 used data from 1901 to 1986; Sen Roy and Balling, 2005 used data from 1931 to 2002; Kothawale et al., 2010a used data from 1901 to 2007) and therefore, the results of different temperature trend studies are not directly comparable. Hence, there is a strong need for such studies to be conducted using data of high quality and uniform length from as many stations as possible, so that some useful information could be drawn for different agro-climatic regions of India. Further, earlier studies, have neglected the homogeneity aspect for the analysis of temperature trends over India. The temperature trend analysis may give erroneous results in the presence of shift or break point of any data set. Therefore, in the present study, a comprehensive analysis of the temperature trends over India and breakpoint analysis, using updated data sets, has been taken up. This study will also update the analysis carried out by Arora et al. (2005) using the temperature data up to 2012.

2.3 STUDY AREA AND DATA USED

2.3.1 Study Area

India is the world’s seventh largest country with a geographical area of 3,287,263 km^2. The country has a diverse range of climatic regions. While the tropical climate is experienced in the southern region, the temperate and alpine climate is found in the Himalayan north of the country. The continental plains face severe summer and mild to moderate winters while the coastal areas enjoy a moderate climate with frequent rains. The Himalayan north enjoys mild summer with snowfall in winters. Rainfall occurs mainly during the monsoon season while some regions of the country also receive rainfall in winter due to the north-easterly winds.

India Meteorological Department (IMD) defines four major seasons for the country. The months of January and February are considered as the winter season. During this period, the mean temperature in the country varies from 14°C to 27°C. The pre-monsoon season (summer) begins in March and ends in May. The daily average temperature in the country varies around 30°C to 35°C during this season. The monsoon season is the most significant feature of the Indian climate. The monsoon season, by definition, covers four months from June to September. In the monsoon season, the mean temperature varies from 30°C to 35°C. The post-monsoon season, October to December is a transitional season associated with the north-easterly winds over the Indian subcontinent.

2.3.2 Data Used

The monthly temperature data used in the study were obtained from IMD. After preliminary checking (length of data, data consistency) of the data, the data of only 125 stations out of 212 stations were used in this study (Figure 2.1). These 125 stations are well distributed over India. Out of 125 stations, 83 stations have a common data period of 1941 to 2012. For other stations, the starting and ending years have a mismatch for three to four years. The stations used in the recent study are the same as a previous study conducted by Arora et al. (2005), and hence, a comparison of trends has also been discussed. The annual and seasonal average, maximum, and minimum temperature series were prepared from the monthly data.

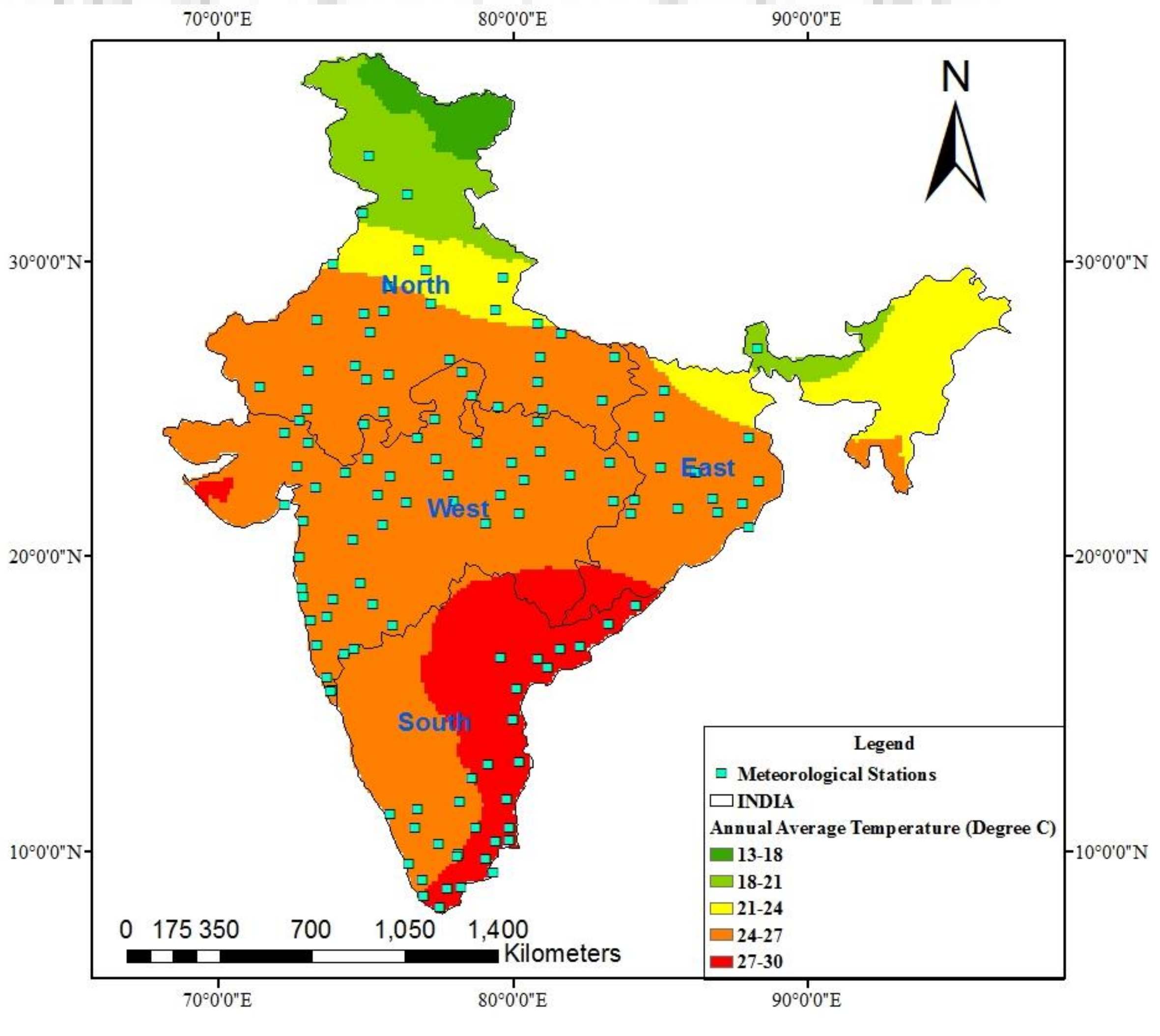

Figure 2.1. Study area and location of meteorological stations used

2.4 METHODOLOGY

The work emphasises on determining the variation of temperature in the Indian context. The methodology starts with the estimation of an average data for India and four of its regions (east, west, north and south) using the arithmetic mean method. Then the temperature anomaly was computed using the average dataset. The Anderson's correlogram test (Anderson, 1942) was performed to check the randomness of the data. The presence of temperature trends in the station data sets was tested using Mann-Kendall (MK) (Mann, 1945; Kendall, 1955) test where autocorrelation was insignificant. Otherwise, the Modified Mann–Kendall (MMK) test was used. The MK or MMK tests was the most useful test for trend estimation in hydrological time series (Jhajharia et al., 2009; Srivastava and Shrivastava, 2011; Kumar et al., 2013; Wagesho et al., 2013; Jena et al., 2014; Mallya et al., 2015). The magnitude of detected trend was computed using Theil and Sen's (Theil, 1950; Sen, 1968)median slope estimator. Thereafter, the homogeneity or the presence of break year in the average dataset was analysed using three tests viz. cumulative deviation test, Standard normal homogeneity test and Wilcoxon Rank-Sum test. In the present study test, statistics were checked at 5% significance level. Finally, the trends of temperature before and after the break years in the average data set were obtained along with temperature trends in data of individual stations. The description of various statistical tests used in this study is given in the following sections.

2.4.1 Trend Detection Methods

2.4.1.1 Anderson's correlogram test

The lag k autocorrelation coefficient for large data sets is estimated as

$$r_k = \frac{\sum_{i=1}^{n-k}(x_i-\bar{x})(x_{i+k}-\bar{x}_{i+k})}{\left[\sum_{i=1}^{n-k}(x_i-\bar{x})^2 \times \sum_{i=1}^{n-k}(x_{i+k}-\bar{x}_{i+k})^2\right]^{1/2}} \tag{2.1}$$

where, $\bar{x}$ and $\bar{x}_{i+k}$ are the sample mean of first (n-k) and last (n-k) terms respectively. The randomness of the data can be checked by t-statistic with (n-2) degree of freedom (Theil 1950 and Sen 1968). Anderson (1942) provides a significance test for autocorrelation coefficient of lag k. The upper and lower bounds β of the autocorrelation coefficient of lag k with α level of significance for n observations is estimated as

$$\beta = -\frac{1}{n-k} \pm Z_{1-\frac{\alpha}{2}}\left(\frac{(n-k-1)^{\frac{1}{2}}}{(n-k)}\right) \tag{2.2}$$

where, $Z_{1-\frac{\alpha}{2}}$ is standard normal variate.

2.4.1.2 Mann-Kendall (MK) test

The Mann-Kendall (Mann, 1945; Kendall, 1955) test is a distribution free, a non-parametric test for the trend estimation of a time series. The MK test statistic is calculated as

$$S = \sum_{i=1}^{n-1} \sum_{j=i+1}^{n} sgn(x_j - x_i) \tag{2.3}$$

where, x_i and x_j are observations j > i, n is the length of data set and the sign function is given by

$$sgn(x_j - x_i) = \begin{cases} 1 & \text{if } (x_j - x_i) > 0 \\ 0 & \text{if } (x_j - x_i) = 0 \\ -1 & \text{if } (x_j - x_i) < 0 \end{cases} \tag{2.4}$$

For independent and identically distributed data, the expected value E(S) and the variance Var(S) are given by

$$E(S) = 0 \tag{2.5}$$

$$Var(S) = \frac{n(n-1)(2n+5)}{18} \tag{2.6}$$

If two or more data values are same, the tie correction is applied, and the sample variance is corrected as

$$Var(S) = \frac{n(n-1)(2n+5) - \sum_{i=1}^{m} t_i(t_i-1)(2t_i+5)}{18} \tag{2.7}$$

where, m is the number of tied groups and t_i is the number of tied elements of extent i. For large dataset ($n \geq 10$), the test static follows normal distribution (Kendall and Stuart, 1968) and the standard normal test statistic is estimated as

$$Z = \begin{cases} \frac{S-1}{\sqrt{Var(S)}} & \text{if } S > 0 \\ 0 & \text{if } S = 0 \\ \frac{S+1}{\sqrt{Var(S)}} & \text{if } S < 0 \end{cases} \quad (2.8)$$

2.4.1.3 Modified Mann-Kendall (MMK) test

The auto-correlated data reduces the chance of significant trend detection in MK test (Yue et al., 2002). To overcome this problem, MMK (Hamed and Rao, 1998; Basistha et al., 2009; Patra et al., 2012) test is applied to the autocorrelated time series. In MMK test, a variance correlation factor n/n_s^* is applied in presence of significant autocorrelations as follows:

$$n/n_s^* = 1 + \frac{2}{n(n-1)(n-2)} \times \sum_{k=1}^{n-1}(n-k)(n-k-1)r_k \quad (2.9)$$

where, n is the number of observations, n_s^* is the effective number of observations to account for autocorrelation in the data. The number of lags can be limited to three for significant autocorrelations (Rao et al., 2004). The corrected variance is then estimated as

$$Var^*(S) = Var(S) \times n/n_s^* \quad (2.10)$$

where, Var(S) is calculated from Equation (2.7), and the rest of the test is same as the MK test.

2.4.1.4 Theil-Sen median slope estimator

Theil-Sen's median slope estimator, Q, (Theil, 1950; Sen, 1968) for n number of data is given by

$$Q = \frac{(x_j - x_i)}{(j-i)} \quad \text{for j > i} \quad (2.11)$$

The Sen's slope, b, is given by

$$b = median\left[\frac{x_j - x_i}{j-i}\right] \quad \text{for j > i} \tag{2.12}$$

where, x_j and x_i are the data values at time j and i (j > i) respectively. The approach provides a robust estimation of trends (Yue et al., 2002).

2.4.2 Homogeneity Test

Three homogeneity tests viz. cumulative deviation test (Buishand, 1982), standard normal homogeneity test (SNHT) and Wilcoxon rank sum test (Bhattacharyya and Johnson, 1977), have been used in this study to check the homogeneity in the datasets.

2.4.2.1 Cumulative deviation test

The homogeneity of a data set can be tested by using cumulative deviations from mean. The test is performed as

$$S_0^* = 0 \tag{2.13}$$

$$S_k^* = \sum_{i=1}^{k}(Y_i - \bar{Y}) \quad k = 1,2,\ldots\ldots n \quad \text{where } S_n^* = 0 \tag{2.14}$$

The rescaled adjusted partial sum S_k^{**} is estimated by dividing the S_k^* by sample standard deviation D_Y.

$$S_k^{**} = S_k^*/D_Y \tag{2.15}$$

The values of S_k^{**} are not influenced by any linear transformation of the data. Then a test static Q is calculated as

$$Q = \max_{0 \le k \le n} |S_k^{**}| \tag{2.16}$$

High value of Q indicates a change in the dataset. For large n, the critical value of Q is checked by using a table of the Kolmogorov-Smirnov goodness-of-fit test statistic.

Another statistic called range, R is also used for testing homogeneity. R is estimated as

$$R = \max_{0 \le k \le n} S_k^{**} - \min_{0 \le k \le n} S_k^{**} \tag{2.17}$$

The high values of range usually indicate the shifts in the mean. Wallis and O'Connell (1973) provide a figure with the percentage point distribution of R.

2.4.2.2 Standard Normal Homogeneity test (SNHT)

The standard normal homogeneity test was developed by Alexanderson (1984, 1986). The test static is estimated as

$$T_{max}^{s} = \max_{1 \le a \le n-1} (T_a^s) = \max_{1 \le a \le n-1} \{a\bar{Z}_1^2 + (n-a)\bar{Z}_2^2\} \tag{2.18}$$

where, $\bar{Z}_1$and $\bar{Z}_2$ are the mean of Z_i series before and after the shift respectively. The value of a, corresponding to this maximum, is when the year is most probable for the break. Two levels of differences before and after the possible break are

$$\bar{q}_1 = \sigma_Q \bar{Z}_1 + \bar{Q} \text{ and } \bar{q}_2 = \sigma_Q \bar{Z}_2 + \bar{Q} \tag{2.19}$$

In the study, simple t-test is used to check the breakpoint (at year A) in time series as

$$t = \frac{\bar{q}_1 - \bar{q}_2}{\sqrt{\frac{\sigma_1^2}{A} + \frac{\sigma_2^2}{n-A}}} \tag{2.20}$$

The critical values are checked from Student's t-table.

2.4.2.3 Wilcoxon Rank-Sum test

For a time-series of size N, N_A and N_B are the number of observations before and after the breakpoint, and N is the sum of N_A and N_B. The observations are given a rank with the smallest value having a rank of 1. The test statistic, W_A, is the sum of the ranks of observations from one of the samples.

$$W_A = sum\ of\ the\ ranks\ for\ observations\ from\ A.$$

when the sample size is greater than 10, the test statistic W_A follows a normal distribution with mean and variance of $E(W_A)$ and $Var(W_A)$ respectively.

$$E(W_A) = \frac{N_A(N_A+N_B+1)}{2} \tag{2.21}$$

$$Var(W_A) = \frac{N_A N_B(N_A+N_B+1)}{12} \tag{2.22}$$

The standardised test static, Z, is calculated as

$$Z = \frac{W_A - E(W_A)}{\sqrt{Var(W_A)}} \tag{2.23}$$

and $Z \sim N(0,1)$.

2.5 RESULTS AND DISCUSSION

The average, maximum and minimum temperature anomalies from annual and the four seasons with reference to their long-term mean of 72 years (1941 to 2012) over India are shown in Figure 2.2 and 2.3 respectively. Annual mean temperature anomalies over four regions (i.e. north, east, west and south) of India are shown in Figures 2.4. The rise or fall of annual and seasonal temperature anomalies represented by a linear trend have also been shown in the Figures 2.2 to 2.4. It can be seen from Figure 2.2, that all the three temperature variables i.e. average, maximum and minimum temperatures over India are showing an increase during 1941 to 2012. Similar results have also been found for the seasonal mean temperatures (Figure 2.3). Figure 2.4 also shows an increasing trend in annual mean temperature anomalies for different-

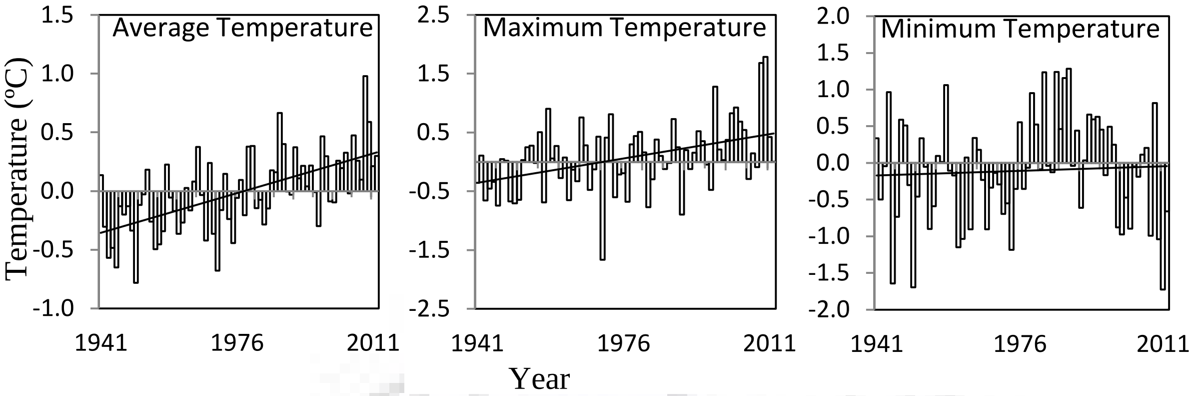

Figure 2.2. Anomalies in annual temperature over entire India

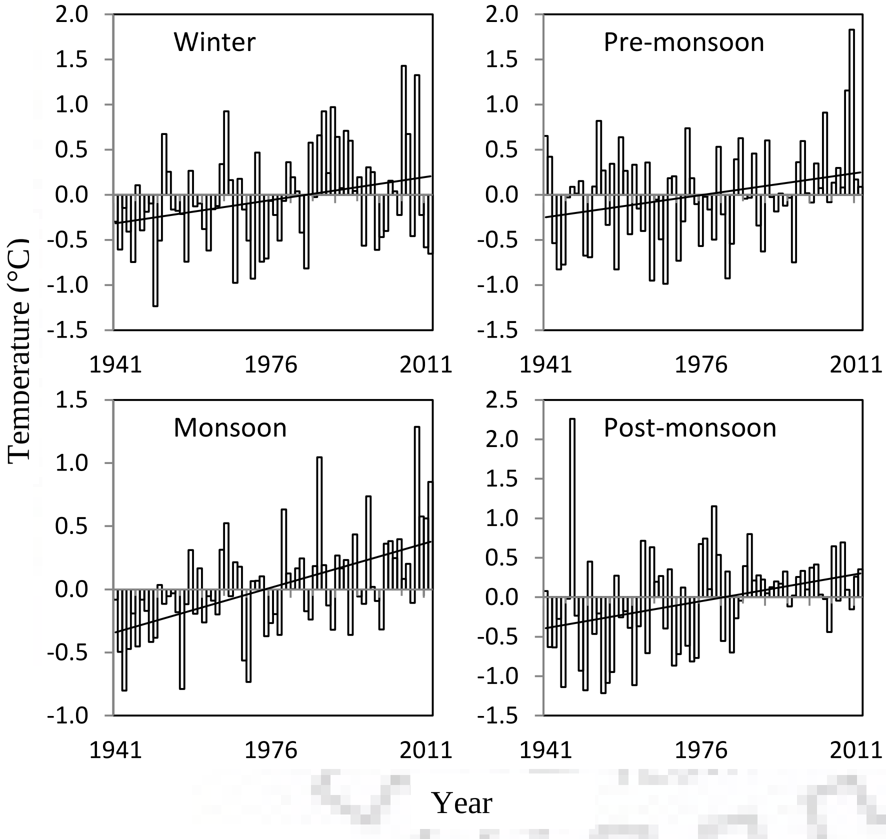

Figure 2.3. Anomalies in seasonal mean temperature over entire India

-regions of India. It may be seen from all the figures that around 1976, there is a change in the temperature anomaly from negative to the positive on all India basis. However, the minimum temperature has not shown the above type of change on all India basis. These results confirm that a change is happening in the annual and seasonal temperature over the country as well as over the regional basis. This poses an immediate and relevant research question that how the change is undergoing over the country. Also, it is important to know that if there is any break in the trend line, which will be helpful for the strategy making for future. To know the answer of these questions, the MK or MMK test was applied for the analysis of trend and three homogeneity tests were applied for break analysis in the temperature data over India.

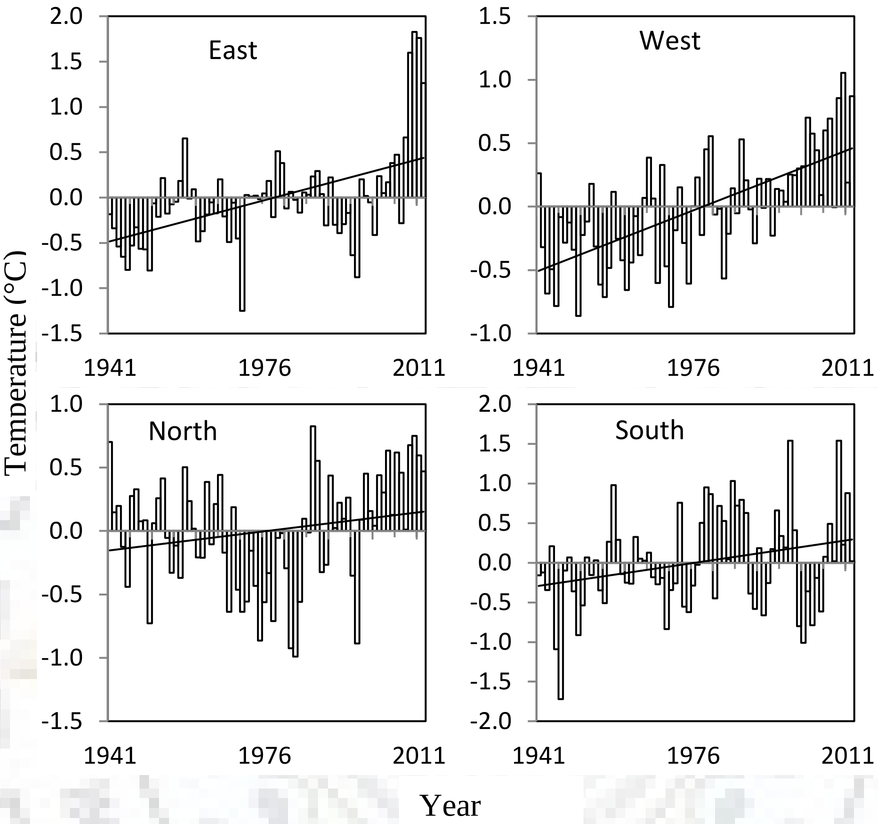

Figure 2.4. Anomalies in annual mean temperature in different regions of India

Results from the study of temperature trends of 125 stations, using MK and MMK tests for average, maximum and minimum temperatures on annual and seasonal (winter, pre-monsoon, monsoon and post-monsoon) basis are given in Table 2.1. The number of stations showing rising and falling trends and the change of rate of temperatures in °C per 100 years is presented in this table. The comparison of trends between recent study (1941-2012) and a previous study by Arora et al. (2005) is also summarised in Table 2.1. For annual average temperature, only 55 stations out of 125 stations show rising trend. The number of stations showing rising trend increased in comparison to the results of Arora et al. (2005). The number of stations showing a falling trend reduced from 17 to 3 in comparison with the observations of Arora et al. (2005). The number of stations with the rising trend decreases from 63 to 37 as compared with the observations of Arora et al. (2005), while the number of stations with falling trend increases from 8 to 11 for annual maximum temperature. For annual minimum temperature, 28 stations showing rising trend while the number of stations showing a falling trend is only 3. The number of stations showing both rising and falling trends decreases with respect to the results of Arora et al. (2005).

The increase in the annual average, maximum and minimum temperature was observed by 0.44℃/100 years, 0.51℃/100 years and 0.19℃/100 years respectively. The rate of rise per 100 years for both the annual average and minimum temperature slightly increased in the recent study as compared to the previous study. However, the rate of rise per 100 years for annual maximum temperature decreases significantly. The increases in annual temperature variables found in the present study are almost similar to that of the other studies conducted by various researchers for the country, though the rates of change differ. A study by Subash and Sikka (2014) observed an increasing trend in annual average and minimum temperature by 0.50℃/100 years and 0.26℃/100 years respectively, which is slightly higher than the recent finding. Bapuji Rao et al. (2014) found an increase in annual minimum temperature by 0.24℃/100 years. The findings are not different from each other and in general, an increasing trend was observed for annual temperatures over India.

The average temperature of all the seasons shows an increase in the number of stations with rising trend, while the number of stations showing falling trend decreases in the present study with respect to the observations of Arora et al. (2005) (Table 2.1). For seasonal maximum temperatures, the number of stations with both rising and falling trend decreases in comparison with the observations of Arora et al. (2005), except in the monsoon season where the number of stations with falling trend increases from 3 to 5. The results are not similar for minimum temperature on a seasonal basis. The number of stations showing rising trend for winter minimum temperature is same (32) with respect to the observations of Arora et al. (2005), while the number of stations showing falling trend decreases from 15 to 7. For pre-monsoon minimum temperature, the number of stations with rising trend increases from 15 to 24 with respect to the observations of Arora et al. (2005), while the number of stations showing falling trend decreases from 42 to 10. Both for monsoon and post-monsoon season, the number of stations show rising as well as falling trend in minimum temperature decreases.

Table 2.1. Comparison of trends between recent study and a previous study by Arora et al. (2005) (number of stations = 125).

Temperature Variables		Number of stations with rising trend			Number of stations with falling trend			Significant trend (%)			Change in °C per 100 years		
		1941-1999	1941-2012	Change	1941-1999	1941-2012	Change	1941-1999	1941-2012	Change	1941-1999	1941-2012	Change
Annual	Average	53	55	+	17	3	-	56	46.4	-	0.42	0.44	+
	Maximum	63	37	-	8	11	+	56	38.4	-	0.92	0.51	-
	Minimum	33	28	-	31	6	-	51	27.2	-	0.09	0.19	+
Winter	Average	39	49	+	19	5	-	46	43.2	-	1.1	0.49	-
	Maximum	48	32	-	17	6	-	52	30.4	-		0.46	
	Minimum	32	32	*	15	7	-	37	31.2	-		0.21	
Pre-monsoon	Average	23	35	+	35	7	-	46	33.6	-	–0.40	0.31	+
	Maximum	42	30	-	18	11	-	48	32.8	-		0.49	
	Minimum	15	24	+	42	10	-	45	27.2	-		0.24	
Monsoon	Average	27	45	+	18	4	-	36	39.2	+		0.27	
	Maximum	47	37	-	3	5	+	40	33.6	-		0.80	
	Minimum	22	16	-	41	8	-	50	19.2	-		-0.05	
Post-monsoon	Average	59	62	+	6	3	-	52	52	*	0.94	0.53	-
	Maximum	73	45	-	4	3	-	61	38.4	-		0.73	
	Minimum	38	35	-	10	3	-	38	30.4	-		0.26	

Note: + = Increase, - = Decrease, *= No change, Blank space represents non-availability of results. The data length of the previous study is 1941 to 1999 and the data length of recent study is 1941 to 2012.

The magnitude of the detected trend for winter and post monsoon average temperature decreases from 1.1ºC/100 years to 0.49ºC/100 years and 0.94ºC/100 years to 0.53ºC/100 years respectively in comparison to the observations of Arora et al. (2005). Only for pre-monsoon average temperature, the magnitude of the detected trend increases from -0.40ºC/100 years to 0.31ºC/100 years. Only the monsoon minimum temperature decreased by -0.05℃/100 years. In the present study, the monsoon maximum temperature shows the highest increase by 0.80℃/100 years. An increasing temperature can create various problems for water resources and agriculture over the country and is given in Annexure 2.1.

2.5.1 Spatial Variability of Temperature Trends during 1941 to 2012 period

The results obtained from trend analysis of annual data are shown in Figure 2.5. The rising trend was observed for the majority of the southern and western region stations, whereas very few stations of the northern and eastern regions show rising trend in annual average temperature. For annual average and maximum temperature, the majority of stations near the coastal regions show rising trend. Similarly, some stations of the upper western region and lower northern region show rising trend in annual minimum temperature. Besides this, few stations of the eastern and northern region show falling trend in annual maximum temperature. However, falling trend does not follow any pattern for average and minimum temperatures. In general, more than 50% stations are showing a non-significant (both rising and falling) trend in average, maximum, and minimum annual temperatures.

The trend analysis results of individual stations for the winter season are depicted in Figure 2.6. The stations showing a rising trend for winter average temperature is well distributed over India. Very few stations over the country show rising trend in winter maximum and minimum temperatures. However, a rising trend for winter maximum temperature was observed for the majority of stations near to the coastal regions. In the winter season, the minimum temperature follows the same pattern as the average temperature. The falling trend does not follow any pattern for winter temperature variables. Both the maximum and minimum temperatures increase at a rate of 0.46℃/100 years and 0.21℃/100 years respectively during the winter season (Table 2.1). During the winter season, the stations with increasing trend are more for minimum temperature than the maximum temperature in the north and west regions of the country. The increase in minimum temperature during the winter season in the lower part of northern India and central India affects the cropping pattern of the Rabi season, which is the-

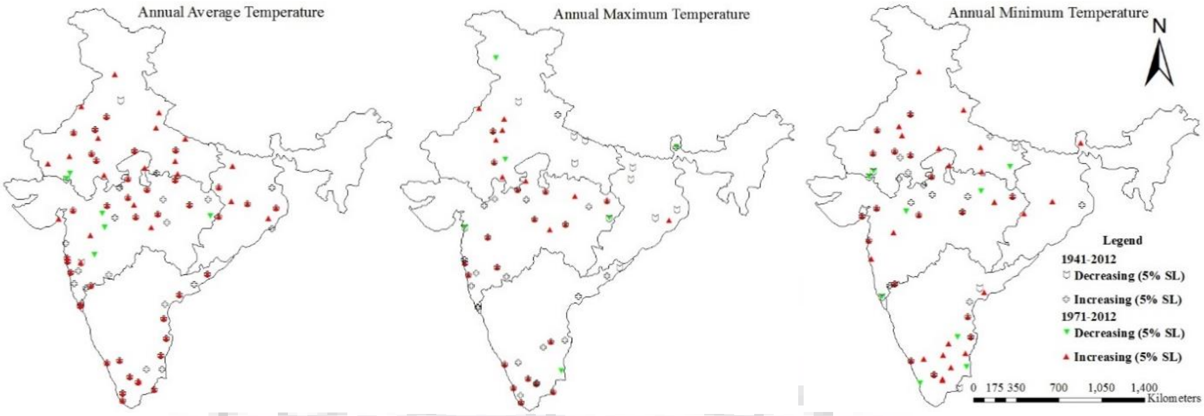

Figure 2.5. Observed trends in annual temperature

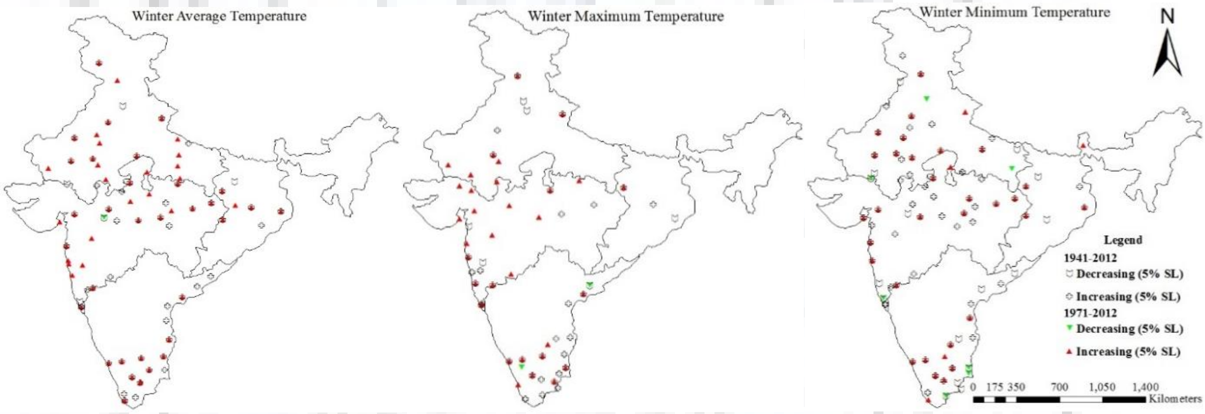

Figure 2.6. Observed trends during the winter season temperature

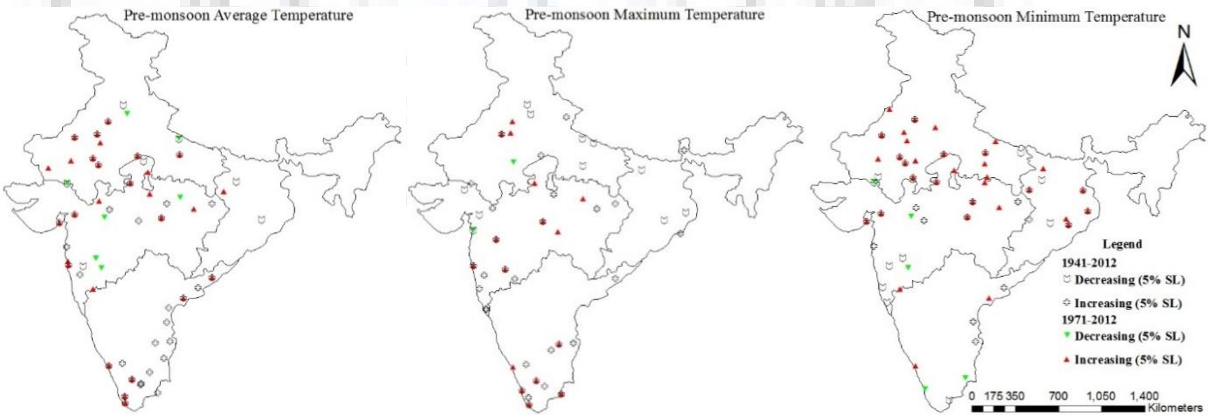

Figure 2.7. Observed trends during the pre-monsoon season temperature

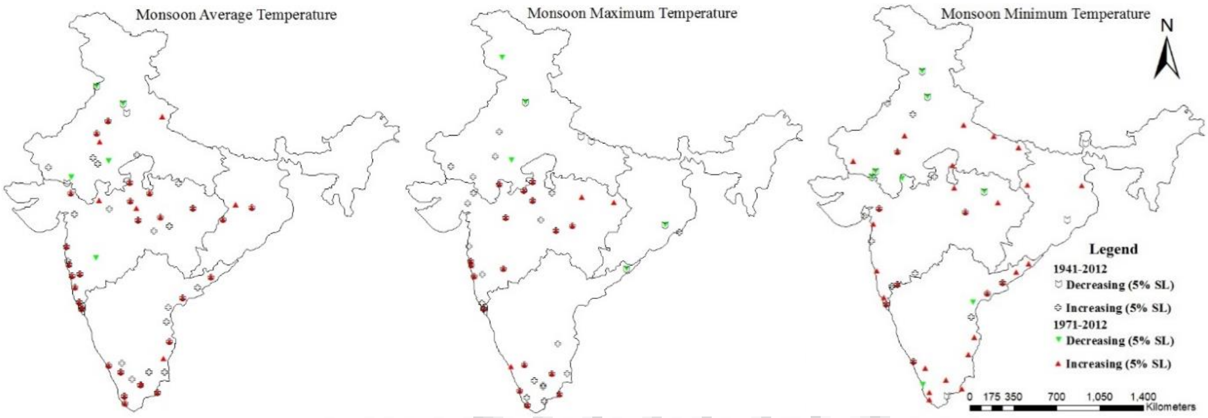

Figure 2.8. Observed trends during the monsoon season temperature

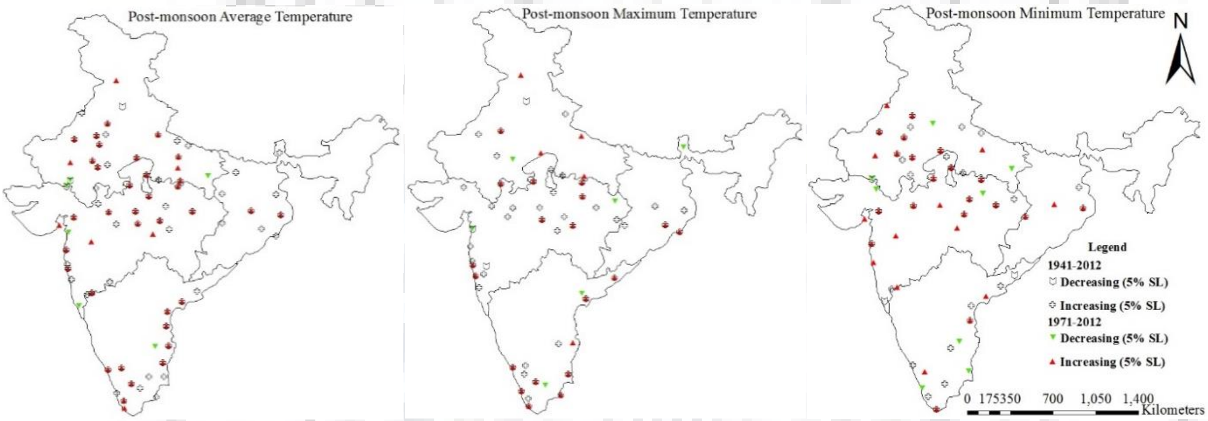

Figure 2.9. Observed trends during the post-monsoon season temperature

-main wheat producing belt of India. Sinha and Swaminathan (1991) reported that an increase of 0.50°C in winter temperature would decrease the wheat production by 0.45 tonne/hectare.

Figure 2.7 show the trend analysis results of individual stations for pre-monsoon season. The majority of the stations with falling trend for pre-monsoon average temperature are located in the coastal parts of western and southern regions. A minimal number of stations show rising trend for pre-monsoon maximum and minimum temperature over the lower portion of the western and southern region. Some of the stations of northern region show rising trend in minimum temperature of pre-monsoon season. The magnitude of detected rising trends for both maximum and minimum temperature is 0.49°C/100 years and 0.24°C/100 years respectively during the pre-monsoon season (Table 2.1). The rise in temperature during the pre-monsoon season will increase the energy consumption for the cooling requirement. During the pre-monsoon season, the temperature is very high for the western and northern regions of the country. Furthermore, most of the water stressed parts during this season are also in the same regions. Hence, a rise in temperature during the pre-monsoon season will worsen the water stress scenario for these regions and affect millions of the poor people living in the region. The increase in winter and pre-monsoon temperature has a severe impact on Himalayan glacier retreat. The Himalayan glaciers annually retreat on an average 2.1 metres (Bahuguna et al., 2014).

The results of trend analysis during the monsoon season are shown in Figure 2.8. The stations showing rising trend for monsoon average and maximum temperature are almost evenly distributed over the southern and western India. Very few stations of the country show rising trend in monsoon minimum temperature. Some stations over the northern and eastern region show falling trend in all the three temperature variables of the monsoon season. The maximum temperature increased by 0.80°C/100 years, while the minimum temperature decreased at a rate of 0.05°C/100 years, during the monsoon season (Table 2.1). The average temperature increased at a rate of 0.27ºC/100 years during the monsoon season. The increase in average temperature during the monsoon season is almost similar to the ones observed by Bapuji Rao et al. (2014) for the period of 1971 to 2009. Monsoon plays a major role in Indian economy by affecting the agricultural production of the country. The rising temperature during this season will increase the evaporation. Bapuji Rao et al. (2012) reported that the crop production would be affected by the increase of evaporation in various parts of India. For the paddy crop, a rise in temperature during the monsoon season linearly reduces the water and nitrogen use efficiencies (Kim et al., 2013).

Figure 2.9 show the trend analysis results of individual stations for the post-monsoon season. The stations showing rising trend in post-monsoon average temperature are well distributed over India. The results are almost similar in the case of maximum temperature for southern and western regions. Very few stations spread over the northern and western regions show rising trend in minimum temperature. No pattern was found for the stations showing falling trend during the post-monsoon season. The post-monsoon average temperature shows the maximum rate of rise (0.80°C/100 years). During the post-monsoon season, both the maximum and minimum temperatures increased by 0.73°C/100 years and 0.26°C/100 years respectively (Table 2.1).

2.5.2 Homogeneity of Annual and Seasonal Temperatures

The data variability can be detected using homogeneity tests. One particular type of non-homogeneity occurring in time series is due to the sudden shifts or jumps of the mean level. In this study, the tests were applied to region wise spatial average series for annual and seasonal data. Three tests namely Cumulative deviation (CD) test, rank sum (RS) test and standard normal homogeneity test (SNHT) were applied to the time series of annual and seasonal temperature variables (average, maximum and minimum) to identify the breakpoints. The break year for a series was selected when at least two out of three tests gave the same year as the result. For few series, all the tests gave different break years. For such series, break years were established by manual inspection of the time series. The break years were also obtained for each station (not presented in the study).

The results obtained from the homogeneity tests for the whole country are summarised in Table 2.2. The break year for annual average temperature was found in the year of 1972 for the country. The results of homogeneity tests show the presence of inhomogeneities in the year 1974 and 1977 for annual maximum and minimum temperature respectively. The results also indicate the presence of inhomogeneity in the seasonal temperatures except for the minimum temperature of winter and monsoon season and maximum temperature for the post-monsoon season.

The results of homogeneity tests for northern, eastern, western and southern regions of India are given in Table 2.3 to 2.6. The break year for annual average temperature was found in the year of 1975 for northern and western regions. However, the break year in annual average temperature was found in 1971 and 1965 for southern and eastern regions respectively. The year 1975 was found as a break year for the average temperature during the winter season in the northern region, and post-monsoon seasons in northern, southern, and western regions. From all the tables, it can be seen that the break year is after the year 1970 for all the annual and seasonal temperatures. The break year before 1970 was observed almost for all the annual and seasonal temperatures for the eastern parts of the India. The year 1964 was found as a break year for the average temperature during monsoon and post-monsoon season whereas the year 1965 and 1979 was found as break years for winter and pre-monsoon seasons respectively.

Table 2.2. Years for which breaks in the temperature series of India as a whole was detected according to the Cumulative deviation (CD) test, Rank sum (RS) test and SNHT.

Temperature Variable		Break Year by CD test	Break Year by RS test	Break Year by SNHT	Year
Annual	Average	1975	1972	1972	**1972**
	Maximum	1975	1974	1974	**1974**
	Minimum	1977	1977	1978	**1977**
Winter	Average	1975	1975	1975	**1975**
	Maximum	1986	1984	1984	**1984**
	Minimum	-	-	-	**-**
Pre-monsoon	Average	1978	1979	1979	**1979**
	Maximum	1971	1971	1971	**1971**
	Minimum	1975	1977	1977	**1977**
Monsoon	Average	1969	1971	1971	**1971**
	Maximum	1969	1972	1971	**1971**
	Minimum	-	-	-	**-**
Post-monsoon	Average	1975	1975	1975	**1975**
	Maximum				
	Minimum	1975	1975	1975	**1975**

Note: Bold characters indicate the assumed breaking year. Empty cells correspond to series without significant breaks.

Table 2.3. Years for which breaks in the temperature series of northern parts of India was detected according to the Cumulative deviation (CD) test, Rank sum (RS) test and SNHT.

Temperature Variable		Break Year by CD test	Break Year by RS test	Break Year by SNHT	Year
Annual	Average	1975	1975	1975	**1975**
	Maximum	-	-	-	**-**
	Minimum	1978	1977	1978	**1978**
Winter	Average	1975	1975	1975	**1975**
	Maximum	-	-	-	**-**
	Minimum	-	-	-	**-**
Pre-monsoon	Average	1979	1979	1979	**1979**
	Maximum	1977	1977	1978	**1977**
	Minimum				
Monsoon	Average	1975	1976	1976	**1976**
	Maximum	1975	1972	1975	**1975**
	Minimum	-	-	-	**-**
Post-monsoon	Average	1975	1975	1975	**1975**
	Maximum	-	-	-	**-**
	Minimum	1975	1975	1975	**1975**

Note: Bold characters indicate the assumed breaking year. Empty cells correspond to series without significant breaks.

The break year for all the annual and seasonal temperature variables was found after the year 1970. Therefore, the trend analysis of temperature data was carried out using the break year as 1970 to get the temperature trends before and after the break year. The occurrence of break years after the year 1970 is most likely linked to the effect of global climate change with the regional changes like land use and land cover changes, intensive cropping, land clearings, industrial development etc. The anthropogenic radiative forcing has increased more rapidly after 1970 than previous records (IPCC, 2013), which is one of the main causes of global warming. However, the possibility of changes in observing patterns and practices, instrument control, surrounding environment of the stations cannot be ruled out for the presence of shift or jump in data. Pielke Sr. et al., (2007) state that an inherent uncertainty can be present in the data sets due to the lack of correctly and consistently sited stations. The cause of this uncertainty should be addressed at the root and any corrections in the data sets should not be performed without correctly quantifying the statistical uncertainties. In the present analysis, the information related to the shifting of station and instrument change were not available. Hence this aspect could not be further verified.

Table 2.4. Years for which breaks in the temperature series of southern parts of India was detected according to the Cumulative deviation (CD) test, Rank sum (RS) test and SNHT.

Temperature Variable		Break Year by CD test	Break Year by RS test	Break Year by SNHT	Year
Annual	Average	1969	1971	1971	**1971**
	Maximum	1971	1971	1971	**1971**
	Minimum	1972	1974	1972	**1972**
Winter	Average	1969	1971	1971	**1971**
	Maximum	-	-	-	-
	Minimum	-	-	-	-
Pre-monsoon	Average	1978	1979	1979	**1979**
	Maximum	1977	1977	1977	**1977**
	Minimum	-	-	-	-
Monsoon	Average	1971	1971	1971	**1971**
	Maximum	1971	1972	1971	**1971**
	Minimum	-	-	-	-
Post-monsoon	Average	1975	1975	1975	**1975**
	Maximum	-	-	-	-
	Minimum	1975	1975	1975	**1975**

Note: Bold characters indicate the assumed breaking year. Empty cells correspond to series without significant breaks.

Table 2.5. Years for which breaks in the temperature series of eastern parts of India was detected according to the Cumulative deviation (CD) test, Rank sum (RS) test and SNHT.

Temperature Variable		Break Year by CD test	Break Year by RS test	Break Year by SNHT	Year
Annual	Average	1964	1965	1965	**1965**
	Maximum	1958	1958	1961	**1958**
	Minimum	1972	1974	1974	**1974**
Winter	Average	1965	1965	1965	**1965**
	Maximum	-	-	-	**-**
	Minimum	-	-	-	**-**
Pre-monsoon	Average	1978	1979	1979	**1979**
	Maximum	1964	1966	1965	**1965**
	Minimum	-	-	-	**-**
Monsoon	Average	1964	1964	1965	**1964**
	Maximum	1964	1964	1964	**1964**
	Minimum	-	-	-	**-**
Post-monsoon	Average	1964	1965	1964	**1964**
	Maximum	-	-	-	**-**
	Minimum	1966	1966	1966	**1966**

Note: Bold characters indicate the assumed breaking year. Empty cells correspond to series without significant breaks.

Table 2.6. Years for which breaks in the temperature series of western parts of India was detected according to the Cumulative deviation (CD) test, Rank sum (RS) test and SNHT.

Temperature Variable		Break Year by CD test	Break Year by RS test	Break Year by SNHT	Year
Annual	Average	1975	1975	1975	**1975**
	Maximum	1978	1977	1977	**1977**
	Minimum	1975	1975	1975	**1975**
Winter	Average	1969	1972	1972	**1972**
	Maximum	-	-	-	**-**
	Minimum	-	-	-	**-**
Pre-monsoon	Average	1978	1979	1979	**1979**
	Maximum	1977	1977	1979	**1977**
	Minimum	-	-	-	**-**
Monsoon	Average	1978	1978	1978	**1978**
	Maximum	1969	1971	1971	**1971**
	Minimum	-	-	-	**-**
Post-monsoon	Average	1975	1975	1975	**1975**
	Maximum	-	-	-	**-**
	Minimum	1975	1975	1975	**1975**

Note: Bold characters indicate the assumed breaking year. Empty cells correspond to series without significant breaks.

2.5.2.1 Results of four typical stations

The analysis of four typical stations namely Bahraich, Pendra, Nagpur and Madras in the northern, eastern, western and southern regions of India has been presented in this section for the demonstration purpose. These stations were selected as they have a complete set of observed time series. The time series plots of annual and seasonal temperature variables (15 in number i.e. average, maximum and minimum temperatures on annual, winter, pre-monsoon, monsoon--and post-monsoon basis) for four stations are shown in Figures 2.10 to 2.13. The straight line depicted the linear trend in the data sets in the figures. The statistical significance of the trend lines was checked at 5% significance level. Figure 2.10 shows that for annual average temperature, the slope of the trend line changes after the year 1971 at Bahraich station. The falling trend changed to a rising trend after the break year for annual maximum and annual minimum temperatures. The rising trend was observed after the break years for all the seasonal temperature variables. However, the absence of break year was also observed for some seasonal temperature variables.

The time series plots of annual and seasonal temperature variables of Pendra station are shown in Figure 2.11. The rising trend was observed for most of the annual and seasonal temperature variables after their respective break years except for the annual minimum and winter minimum temperatures. The falling trend after the break year was found for annual minimum and winter minimum temperatures. The absence of break year was observed for the pre-monsoon average and minimum, monsoon maximum and minimum temperature series. Though a rising trend was observed for all these series except in monsoon minimum temperature, which shows a falling trend.

The results of Nagpur station, located in the western region of India, are shown in Figures 2.12. The falling trend changes to rising trend for annual and seasonal average and maximum temperatures after their respective break years except for the average temperature of pre-monsoon and maximum temperature of winter and post-monsoon season. The average temperature of pre-monsoon and maximum temperature of winter and post-monsoon season shows the absence of break years. The break year is also not observed for the minimum temperature series of annual and all seasons.

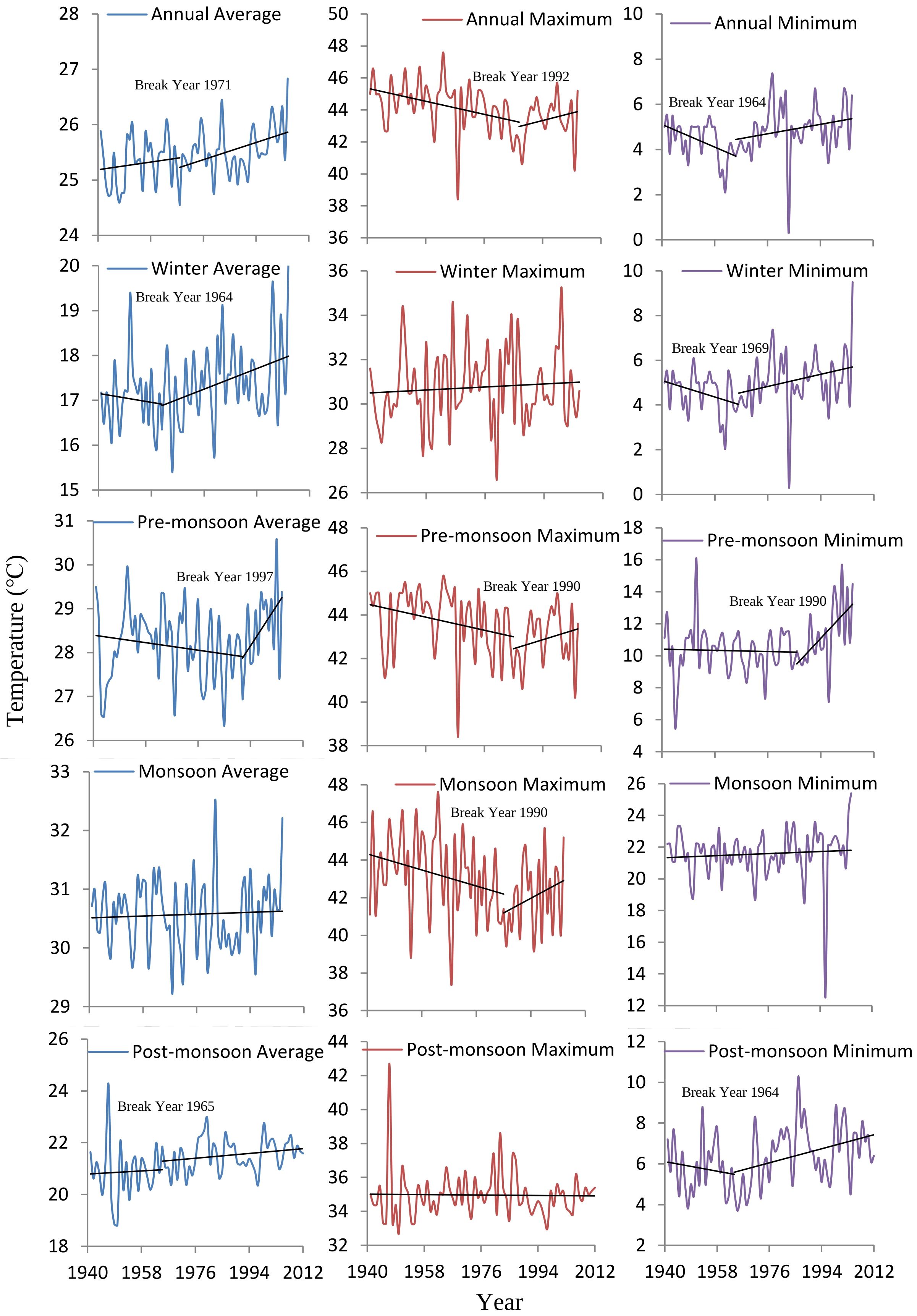

Figure 2.10. Time trends before and after the break year for the Bahraich station over North India

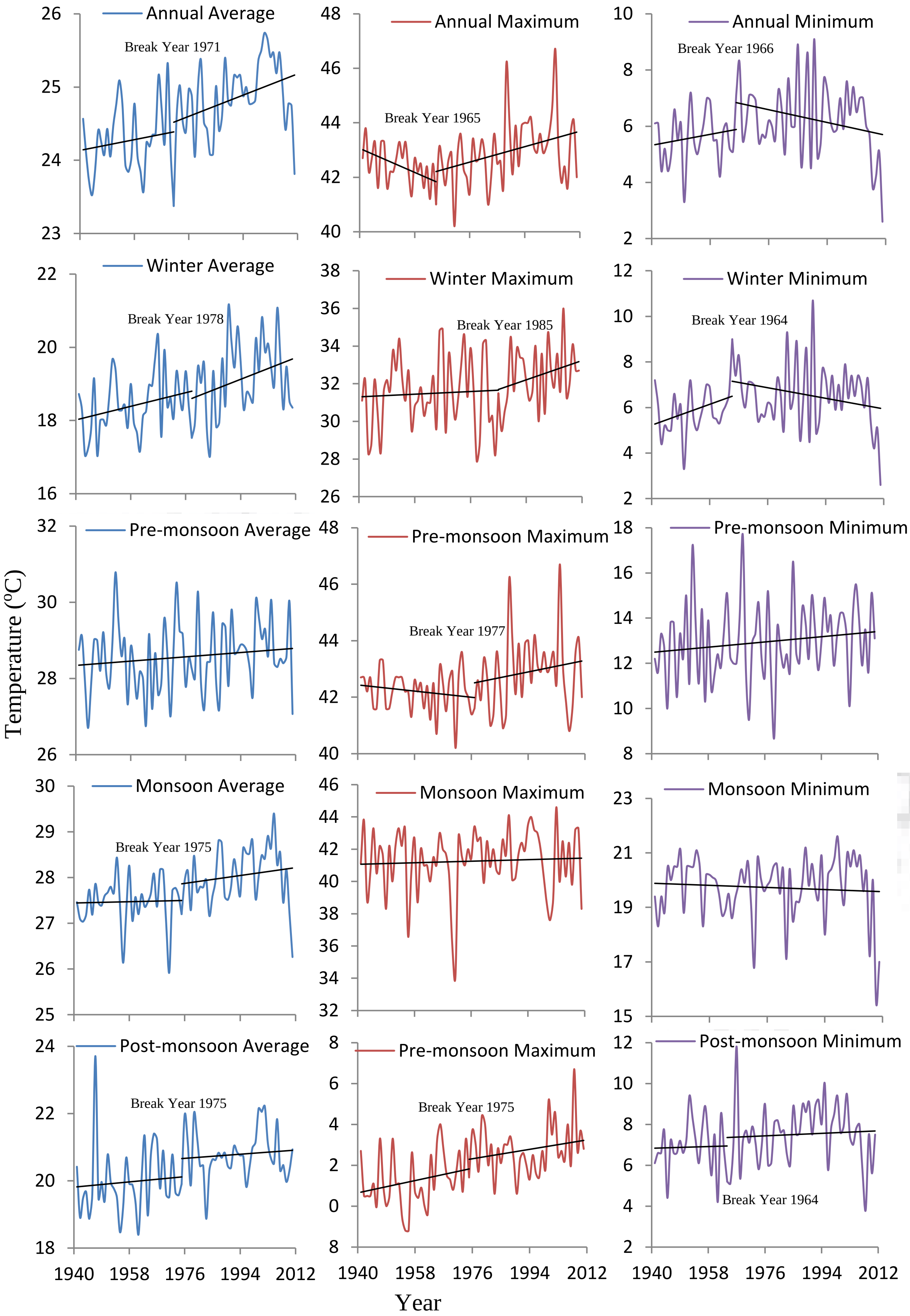

Figure 2.11. Time trends before and after the break year for the Pendra station over East India

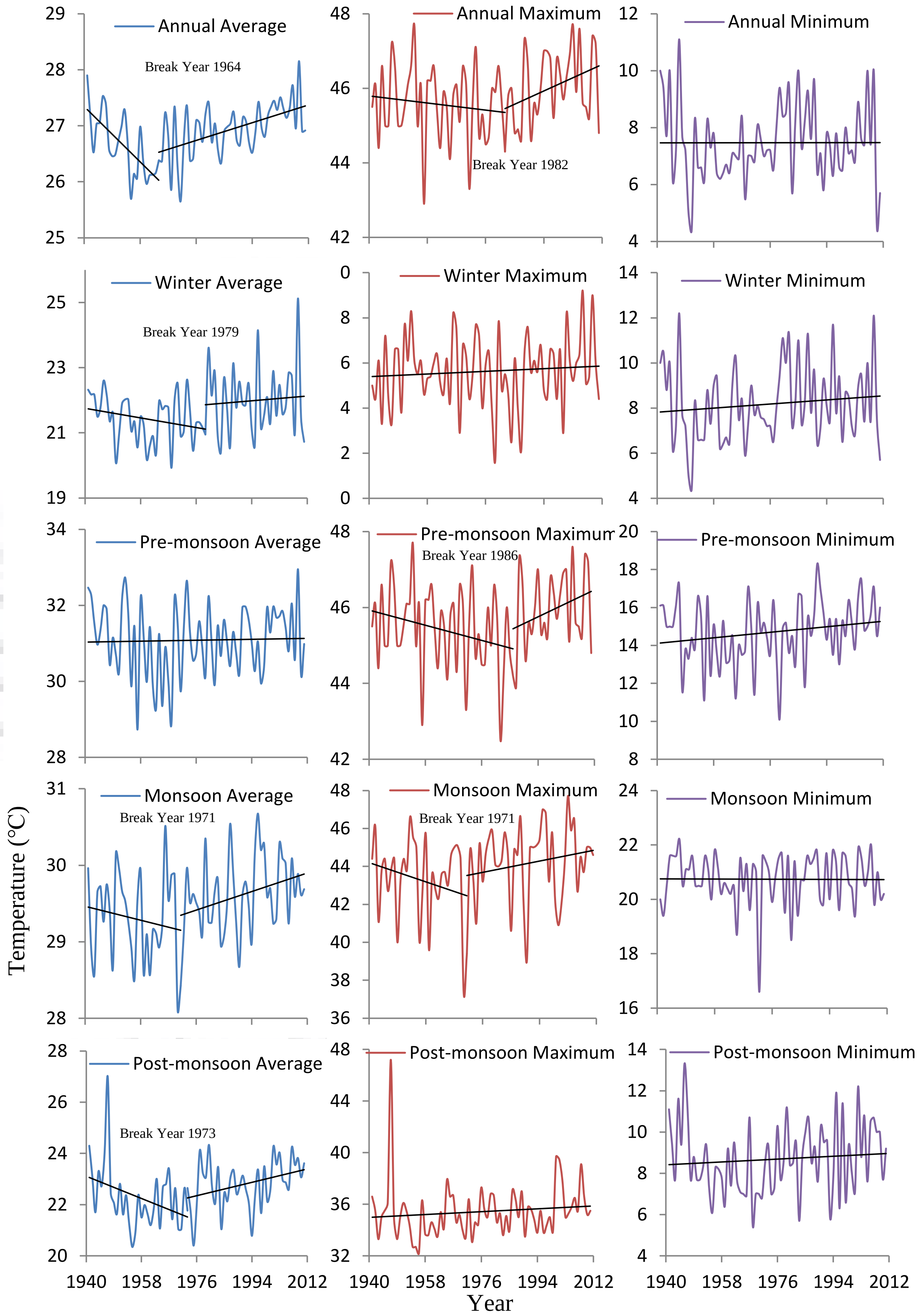

Figure 2.12. Time trends before and after the break year for the Nagpur station over west India

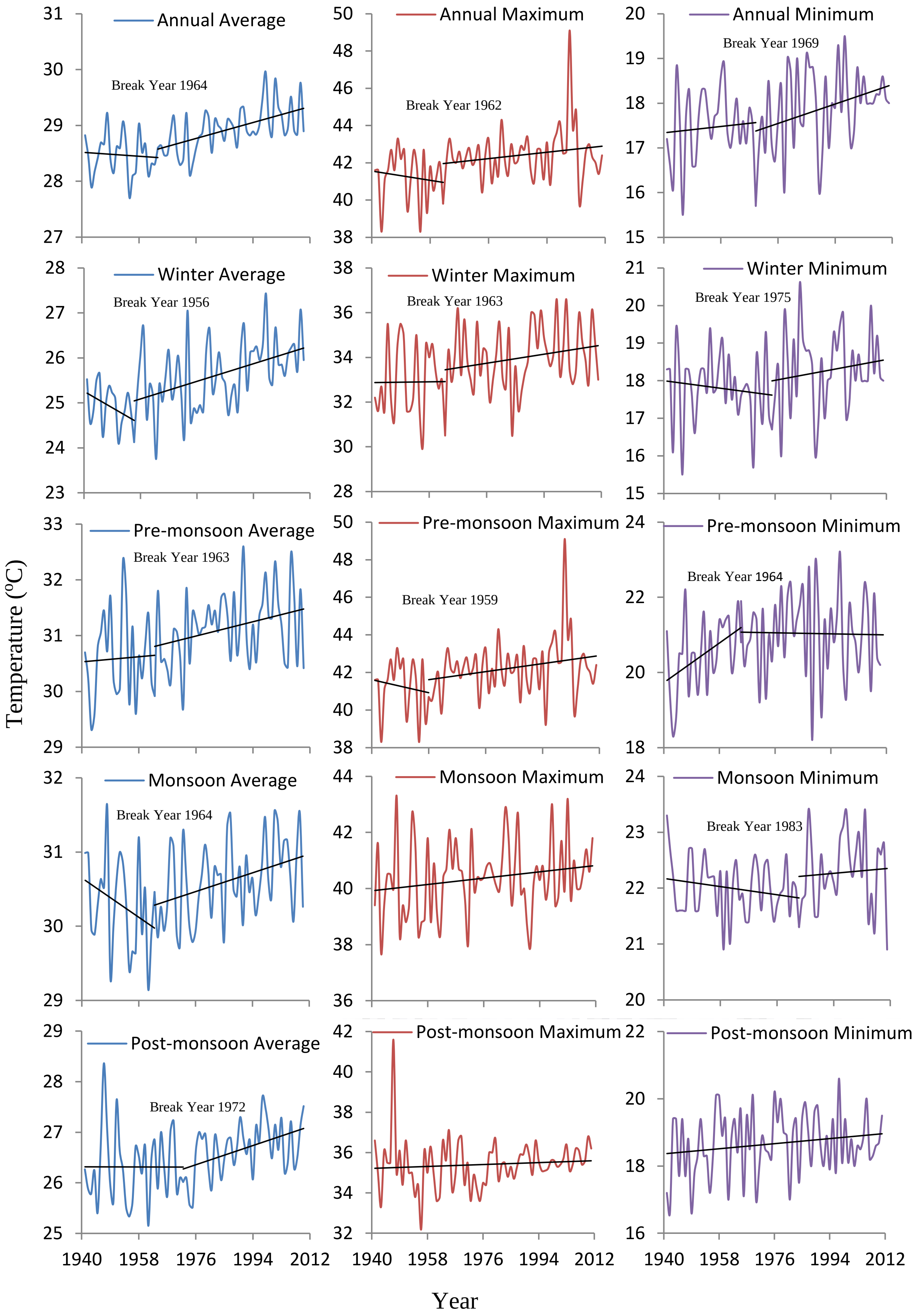

Figure 2.13. Time trends before and after the break year for the Madras station over South India

Figure 2.13 shows the time series plot of annual and seasonal temperatures of Madras station, in the southern region of India. The rising trend was observed after the break year for annual and all seasonal average and maximum temperature series except for the maximum temperature of monsoon and post-monsoon seasons. The break year was absent during the monsoon and post-monsoon maximum temperature and post-monsoon minimum temperature. The rising trend was also found after break year for minimum temperature on an annual basis, winter and monsoon seasons. After the break year, the falling trend was observed only for pre-monsoon minimum temperature. The break year was absent for monsoon maximum and post-monsoon maximum and minimum temperature series.

2.5.3 Trends Before and After Break Point

The significance of trends can be seriously affected by the presence of inhomogeneity or breaks in a time series. To study the recent status of the trends, the trends before and after break year were analysed. The results of trend analysis before and after break year of temperature series for all India and four regions of India are presented in the Tables 2.7 to 2.11. The results indicate more significant rising trend after the break year. The results are in accordance with IPCC (2014), which reported that each of the last three decades from 1983 to 2012 was warmer than the preceding decades. The increase in greenhouse gases into the atmosphere also plays a significant role for rising temperature after 1970.

The annual average and maximum temperature of all India significantly increased after the break year, and the rate of increase are found as 0.11ºC and 0.20ºC per decade (Table 2.7) respectively. These results indicate an increase of temperature extremes. The annual pre-monsoon average and maximum temperatures also significantly increased after break year. The post-monsoon minimum temperature significantly decreased at a rate of 0.13ºC per decade. The results are almost similar for the different regions of India. The annual, pre-monsoon and monsoon average temperature have increased significantly after 1970 for northern and western regions (Table 2.8 and 2.11). The southern region shows a significant increase before the break year whereas no significant increase was found after break year for annual average temperature (Table 2.9). The annual maximum and minimum temperature show a decrease of 0.10ºC and 0.04ºC per decade (Table 2.10) for the eastern part of India. However, the decrease has no statistical significance. Overall, the results before and after break years show increase almost for all the annual and seasonal temperature variables and the increase is more prominent after the break year than before the break year.

Table 2.7. Comparative results of the trend before and after break point for temperature series of India as a whole.

Temperature Variable	Before Break Year		After Break Year	
	MK/MMK (Z statistics)	Change (ºC) per decade	MK/MMK (Z statistics)	Change (ºC) per decade
Annual Average	1.15	0.06	**2.93**	0.11
Annual Maximum	1.63	0.13	**2.30**	0.20
Annual Minimum	-1.06	-0.12	-1.68	-0.35
Winter Average	0.45	0.14	0.15	0.13
Winter Maximum	0.01	0.15	1.07	0.24
Pre-monsoon Average	-0.58	-0.05	**2.40**	0.18
Pre-monsoon Maximum	**3.19**	0.15	**2.19**	0.22
Pre-monsoon Minimum	0.00	0.00	0.56	0.07
Monsoon Average	1.57	0.01	-0.3	-0.02
Monsoon Maximum	0.51	0.14	1.31	0.01
Post-monsoon Average	0.03	0.02	-0.30	-0.01
Post-monsoon Minimum	0.00	0.00	**-2.39**	-0.13

Note: Bold characters indicate the statistically significant trend at 5% significance level.

Table 2.8. Comparative results of the trend before and after break point for temperature series of the northern region of India.

Temperature Variable	Before Break Year		After Break Year	
	MK/MMK (Z statistics)	Change (ºC) per decade	MK/MMK (Z statistics)	Change (ºC) per decade
Annual Average	**-2.64**	-0.19	**2.68**	0.31
Annual Minimum	**-2.41**	-0.40	-0.20	-0.02
Winter Average	0.45	0.11	0.15	0.13
Pre-monsoon Average	-0.58	-0.11	**2.40**	0.24
Pre-monsoon Maximum	0.77	0.05	1.89	0.18
Monsoon Average	**2.10**	0.07	**2.66**	0.27
Monsoon Maximum	0.94	0.14	1.31	-0.02
Post-monsoon Average	0.03	0.04	-0.30	-0.19
Post-monsoon Minimum	0.00	0.02	**-2.39**	-0.10

Note: Bold characters indicate the statistically significant trend at 5% significance level.

Table 2.9. Comparative results of the trend before and after break point for temperature series of the southern region of India.

Temperature Variable	Before Break Year		After Break Year	
	MK/MMK (Z statistics)	Change (^oC) per decade	MK/MMK (Z statistics)	Change (^oC) per decade
Annual Average	**2.19**	0.28	0.02	0.00
Annual Maximum	1.75	0.15	0.48	0.03
Annual Minimum	0.25	0.03	-0.12	-0.02
Winter Average	1.29	0.14	1.00	0.13
Pre-monsoon Average	-0.58	-0.05	**2.40**	0.26
Pre-monsoon Maximum	0.77	0.05	1.89	0.18
Monsoon Average	1.57	0.07	**3.25**	0.27
Monsoon Maximum	0.51	0.01	1.54	0.02
Post-monsoon Average	0.03	-0.14	-0.30	-0.19
Post-monsoon Minimum	0.00	0.09	**-2.39**	-0.07

Note: Bold characters indicate the statistically significant trend at 5% significance level.

Table 2.10. Comparative results of the trend before and after break point for temperature series of the eastern region of India.

Temperature Variable	Before Break Year		After Break Year	
	MK/MMK (Z statistics)	Change (^oC) per decade	MK/MMK (Z statistics)	Change (^oC) per decade
Annual Average	1.44	0.22	1.32	0.12
Annual Maximum	1.36	1.20	-0.99	-0.10
Annual Minimum	**-2.05**	-0.33	-0.39	-0.04
Winter Average	1.38	0.13	0.58	0.10
Pre-monsoon Average	-0.58	-0.24	**2.40**	0.15
Pre-monsoon Maximum	1.00	0.05	1.95	0.18
Monsoon Average	1.81	0.17	**2.46**	0.16
Monsoon Maximum	0.67	0.04	1.31	0.05
Post-monsoon Average	-0.17	-0.21	1.06	0.04
Post-monsoon Minimum	-1.15	-0.10	-0.64	-0.04

Note: Bold characters indicate the statistically significant trend at 5% significance level.

The increasing average temperature in all the seasons will affect the agriculture sector, which provides employment to a majority of the rural community. This community being economically and technologically backwards hence they cannot implement adaptation policies, and therefore this situation will lead to a platitude of socio-economic and scientific challenges. The increasing temperature will trigger increased evapotranspiration, which in turn will increase the irrigation demand. Given the fact that most of India's irrigation projects had been designed before 1970, the growing demand for irrigation shall necessitate revisiting the design and operation of the projects. The increased temperature coupled with an upward mobile population will increase the energy demand (for cooling) thus creating pressure on both natural and economic resources.

Table 2.11. Comparative results of the trend before and after break point for temperature series of the western region of India.

Temperature Variable	Before Break Year		After Break Year	
	MK/MMK (Z statistics)	Change (°C) per decade	MK/MMK (Z statistics)	Change (°C) per decade
Annual Average	0.54	0.03	**2.39**	0.22
Annual Maximum	-0.30	-0.03	0.86	0.15
Annual Minimum	-0.60	-0.10	0.96	0.14
Winter Average	0.79	0.07	0.78	0.12
Pre-monsoon Average	-0.58	-0.05	**2.40**	0.26
Pre-monsoon Maximum	0.77	0.05	1.89	0.18
Monsoon Average	1.60	0.07	**2.13**	0.27
Monsoon Maximum	0.51	0.01	1.54	0.02
Post-monsoon Average	0.03	0.04	-0.30	-0.09
Post-monsoon Minimum	0.00	0.06	**-2.39**	-0.16

Note: Bold characters indicate the statistically significant trend at 5% significance level.

2.5.4 Comparison of Trends between 1941-2012 and 1971-2012

Results from the trend analysis of temperature data are summarised in Table 2.12 for the period of 1971 to 2012. The trend analysis of the station data for 1971 to 2012 is conducted after the break year was found as 1970 for whole India. From Table 2.12 it is observed that for 1971 to 2012 data, the rate of rise has increased for annual average and annual maximum temperature whereas the rate of rise decreased for annual minimum temperature in comparison to the complete data. The results also show that the rate of rise is higher for a shorter length of data as compared to the complete data set though the number of stations showing the rising trend is lesser for a shorter period of average and maximum temperature for annual and seasonal (pre-monsoon, monsoon and post-monsoon) basis. The reverse situation is also found for the minimum temperature of the annual and winter season.

The trend analysis results for the period of 1971 to 2012 are shown in Figures 2.5 to 2.9. Figure 2.5 indicates that the stations with rising trend in annual average temperature for

1971 to 2012 period are well distributed over India. The numbers of stations showing rising trend in annual maximum temperature are very few. Also, the stations are only distributed in the western region of India. The numbers of stations with a rising trend in annual minimum temperature are well spread over India. The number of stations showing falling trend is very few for annual temperature variables. It is visible that the number of stations showing the rising trend has increased to a higher number for the period of 1971 to 2012 as compared to the period of 1941 to 2012 in the eastern and northern region, whereas the number of stations decreased in the western and southern region for annual average temperature. In the case of maximum temperature, the number of stations showing a rising trend has not much changed for either period. The number of stations showing a rising trend for annual minimum temperature is increased for eastern, northern and southern region though the station number has not changed much for the western region.

Table 2.12. Summary of trend analysis results (number of stations = 125)

Temperature Variables		Number of stations with rising trend		Number of stations with falling trend		Change in ºC per Decade	
		1941-2012	1971-2012	1941-2012	1971-2012	1941-2012	1971-2012
Annual	Average	55	59	3	6	0.044	0.114
	Maximum	37	27	11	6	0.051	0.220
	Minimum	28	39	6	9	0.019	-0.049
Winter	Average	49	54	5	1	0.049	0.150
	Maximum	32	33	6	2	0.046	0.220
	Minimum	32	35	7	7	0.021	-0.061
Pre-monsoon	Average	35	28	7	7	0.031	0.159
	Maximum	30	16	11	2	0.049	0.220
	Minimum	24	33	10	5	0.024	0.244
Monsoon	Average	45	35	4	5	0.027	0.122
	Maximum	37	20	5	5	0.080	0.195
	Minimum	16	30	8	8	-0.005	0.061
Post-monsoon	Average	62	41	3	6	0.053	0.098
	Maximum	45	24	3	6	0.073	0.110
	Minimum	35	31	3	8	0.026	-0.041

Figure 2.6 indicated that during the period 1970 to 2012, the number of stations showing rising trend in average temperature of the winter season is well distributed in northern and western regions of India. The stations near the coastal regions of the southern part are also showing rising trend. Very few stations are showing rising trend in northern and western

regions of India though most of the stations near to the coastal regions are showing rising trend in winter maximum temperature. The distribution of the number of stations with rising trend in minimum temperature is almost similar as the average temperature in the winter season. The number of stations showing the rising trend is increased for the period of 1971 to 2012 as compared to the period of 1941 to 2012 in the southern and western region for winter average and maximum temperature.

Figure 2.7 indicated that the number of stations with the rising trend for the average and minimum temperature of the pre-monsoon season, for the period of 1971 to 2012, is very few and are distributed in the northern and upper portion of western regions. For maximum temperature, the number of stations with the rising trend is very few. For pre-monsoon average and minimum temperature, the number of stations increased in comparison to the shorter length data than complete data for the northern region. The number of stations with rising trend for the average and minimum temperature of pre-monsoon season in the western and southern region of India decreased as compared to the 1971 to 2012 data with 1941 to 2012 data.

Figure 2.8 depicted that some stations in the coastal region of India are showing rising trend for average, the maximum and minimum temperature of monsoon season during 1971 to 2012 period. Some stations of the western region also show rising trend in average and maximum temperatures for monsoon season. In monsoon average and maximum temperatures, the number of stations showing the rising trend is lesser for all regions in comparison to the shorter data than complete data. For minimum temperature, the number of stations with rising trend increases during 1971 to 2012 for all regions as compared to 1941 to 2012.

Figure 2.9 shows that the number of stations with the rising trend is well distributed over northern and southern regions for average and minimum temperature in post-monsoon season during the period 1971 to 2012. Very few stations near coastal regions of India show rising trend for all three temperature variables in post-monsoon season. The number of stations showing the rising trend decreased for all regions for the post-monsoon season when compared with 1941 to 2012 data.

2.5.5 Comparison with Trends of Neighbouring Countries

The temperature trends found in the present study are similar to that of the other South Asian countries. Zaman et al. (2013) found a significant increase of 0.00569ºC per year and 0.014498ºC per year for daily mean maximum and mean minimum temperature respectively over Bangladesh for the period of 1949 to 2008. They reported that temperature increased too much higher levels over the last 30 years (1979-2008) than the last 60 years (1949-2008). Hasan and Rahman (2013) analysed monthly temperature data of 63 years (1948-2010) over Bangladesh and reported a rising trend of 0.5ºC/100 years, 1.4ºC/100 years and 0.8ºC/100 years for maximum, minimum and average temperature respectively. The rising trends in maximum, minimum and average temperatures are higher than present analysis. Chandrapala (1997) reported an increase of 0.2°C/year, 0.3°C/year and 0.016°C/year during 1951-2006, 1981-2006 and 1961-1990 period respectively for annual mean temperature over Sri Lanka. It is evident that the rate of change in annual average temperature during 1951 to 2006 period is less compared to the present analysis, but is more for 1981 to 2006 than that of present analysis for the 1970 to 2012 period. Rio et al. (2013) studied 37 weather stations data for 58 years (1952-2009) and found an increase of almost 0.36°C/decade for annual average temperature over Pakistan. They also found an increase of 0.04ºC/year, 0.05ºC/year and 0.016°C/year for the average temperature during winter, pre-monsoon and post-monsoon seasons respectively. The rising trend in annual and seasonal average temperature is lesser than what has been seen in the present analysis. From the above discussion, it can be seen that the trends of increase of temperature across the South Asian countries are almost similar.

2.6 LIMITATIONS OF THE STUDY

The present study has been carried out with a limited number of stations. Also, there is no data sets available for many parts of the study area. For this reason, some errors have been associated with the average data calculations of various parts of India. This errors are calculated and documented in the Table 2.13. It is found that an error in minimum temperature over India is as high as 25%. Hence, the results reported in this study are only indicative and can be improved by adding more number of stations in the analysis.

Table 2.13. Errors associated with trend analysis of temperature over India and four regions of India.

Temperature Variables		Error in %				
		India	Northern India	Eastern India	Western India	Southern India
Annual	Average	1.03	2.47	3.49	0.75	2.14
	Maximum	0.95	2.01	1.55	1.22	2.05
	Minimum	6.77	25.54	11.60	8.17	4.58
Winter	Average	1.96	3.83	4.77	1.81	2.24
	Maximum	1.02	2.61	3.72	0.69	1.65
	Minimum	6.50	22.03	11.24	7.68	4.44
Pre-monsoon	Average	1.02	2.62	3.89	0.67	2.11
	Maximum	0.99	1.87	3.57	1.21	2.09
	Minimum	3.19	6.22	7.27	3.30	3.34
Monsoon	Average	0.94	2.07	2.99	0.94	2.29
	Maximum	1.06	1.77	3.25	1.45	2.27
	Minimum	1.30	3.27	4.00	1.26	2.82
Post-monsoon	Average	1.37	2.68	3.57	1.56	2.21
	Maximum	0.78	1.91	2.47	0.79	1.64
	Minimum	5.59	12.82	9.46	6.88	4.31

2.7 CONCLUSIONS

The present study analysed temperature trends and homogeneity in average, maximum, and minimum temperatures on annual and seasonal basis using the data for the period of 1941 to 2012 of 125 stations distributed over India. The temperature trends showed an increase in all the temperatures except monsoon minimum temperature. Very few stations showed significantly falling trend. The annual average, maximum and minimum temperatures showed an increase of 0.44ºC, 0.51ºC and 0.19ºC per 100 years respectively for whole India.

Homogeneity analysis indicated that the minimum temperature of winter and monsoon season and maximum temperature of post-monsoon seasons were homogeneous in nature. Break years for all the annual and seasonal temperature variables are in between 1970 to 1980. This could be the result of global as well as a local increase of anthropogenic greenhouse gas emission with a significant increase in national and regional agricultural and industrial activities during the same period. The agricultural Green Revolution (GR) over the North and Western states have also changed the temperature over India (Roy et al., 2007). The trend analysis before and after the break year shows more increase in temperature after the break than before. The annual average temperature shows a significant increase (0.11ºC/decade) after the break year for India, though the minimum temperature shows a significant decrease (-0.35ºC/decade). Ramanathan et al. (2001) analysed the effect of aerosol over climate and hydrological cycle. They concluded that the increase in aerosols is directly linked with the change in temperature behaviour over the globe. The results and conclusions drawn from this study have some limitations regarding length and number of stations analysed.

CHAPTER 3

SPATIO-TEMPORAL CHANGE IN RAINFALL DATA OVER PARTS OF INDIA

3.1 GENERAL

The agricultural sector of India is highly dependent on the monsoon. A change in climatic conditions, particularly during monsoon months over the Indian region can significantly affect the agricultural sector and food security of India. Estimation of the rainfall patterns on a regional basis will help in understanding the global impact of climatic systems over the region. The rainfall trends on various spatial scales can provide futuristic scenarios, which are helpful in planning and management of water resources of the region.

This chapter is devoted to the investigation of spatiotemporal trends of rainfall over parts of India. The effect of the resolution of gridded rainfall over the trend analysis is investigated. The coherence between climate indices, global climate change and rainfall is also studied.

3.2 REVIEW OF LITERATURE

A number of studies related to trend analysis of annual and seasonal rainfall in India have been conducted in the past. These studies have used different sets of data (stations as well as gridded) with varied data lengths. These studies have sometimes ended up in contradictory results or results applicable only for a limited region. Prominent studies are reviewed in this section.

Parthasarathy and Dhar (1974) examined rainfall trends and periodicities for annual rainfall of 31 meteorological sub-divisions of India using the data from 1901 to 1960. They observed an increasing trend in the rainfall of central India and some adjoining parts of the peninsula and some small areas of north-west and north-east India. They also found decreasing trends in rainfall over some parts of eastern India.

Mooley and Parthasarathy (1984) studied the fluctuations of monsoon rainfall over India using 306 rainfall series from 1871 to 1978 period. They did not find any significant trends in the all India summer monsoon rainfall.

Pant and Hingane (1988) investigated the rainfall trends over the north-west region of India, using the data of 1901 to 1982. The mean annual and monsoon season rainfall showed a conspicuous increasing trend over most parts of the region.

Rupa Kumar et al. (1992) carried out trend analysis of Indian summer monsoon rainfall using monthly rainfall data of 306 stations for the period of 1871 to 1984. The monsoon rainfall of west coast, north Andhra Pradesh and north-west India showed increasing trend, while the monsoon rainfall of northeast peninsula, northeast India and north-west peninsula showed decreasing trend.

Subbaramayya and Naidu (1992) analysed rainfall trends in monsoon season using the sub-divisional rainfall data for the period of 1871 to 1988. They observed a decreasing trend in the late 19th century and in the 1960s over the central and western Indian sub-divisions. They also concluded that the trends in the 1960s were reversed during the early 1970s for all the regions except the central north Indian sub-divisions.

Kothyari and Singh (1996) studied rainfall trends using seven station data for the period of 1901 to 1989 over the upper, central and lower parts of the Ganga river basin. They found decreasing trends in monsoon rainfall and in the number of rainy days in the second half of the 1960s over the study area.

Ramanathan et al. (2001) studied the effect of aerosols on climate and hydrological cycle. The scattering and absorption of solar radiation is directly increased by these aerosols and also produce brighter clouds. These brighter clouds are less efficient at releasing rainfalls. They stated that the reduction of rainfall during the 20th century is might be due to the increase of pollutions over the East Asia.

Singh and Sontakke (2002) estimated rainfall trends over the Indo-Gangetic Plains for the period of 1829 to 1999. They reported that the monsoon rainfall over the western Indo-Gangetic Plains shows a significant increasing trend (170 mm/100 years) after 1900. In the central Indo-Gangetic Plains, a non-significant decreasing trend (5 mm/100 years) after 1939 was reported. A non-significant decreasing trend (50 mm/100 years) during 1900 to 1984 was also reported for eastern Indo-Gangetic Plains.

Ramanathan et al. (2002) studied the impact of atmospheric brown clouds over South Asian climate and hydrological cycle. They found that an increase in aerosols is directly linked to the decrease in precipitation efficiency. The decrease in monsoon rainfall after 1960 is due to this reason. They concluded that the increase in atmospheric stability and the decrease in rainfall are important aspects of the air pollution impacts on climate.

Niyogi et al. (2007) found that the cloud-radiation feedback and Indian summer monsoon rainfall was affected by the atmospheric aerosols. Due to the large magnitude of aerosol loading, the mesoscale monsoonal characteristics in the Indo-Ganges Basin were significantly influenced by affecting the land–atmosphere interactions and regional coupling.

Pattanaik (2007) analysed monsoon disturbances data for 1941 to 2002 period over 36 meteorological sub-divisions of India. They found a significant decreasing trend in monsoon rainfall over Northwest India and Central India.

Ranade et al. (2008) investigated trends using monthly rainfall data of 316 stations from 1831 to 2006 for the 11 major and 36 minor river basins of India. They did not find the presence of any trend in the starting or ending date, duration and total rainfall for different river basins of India during the hydrological wet season (a continuous period with each of the monthly rainfall more than 50 mm).

Guhathakurta and Rajeevan (2008) analysed rainfall trends using a high-resolution (1º by 1º) gridded monthly data of 36 meteorological subdivisions of India for the period of 1901 to 2003. They found a significant increasing trend in monsoon rainfall for eight sub-divisions and a decreasing trend for three subdivisions.

Basistha et al. (2009) analysed rainfall data of 30 stations from 1901 to 1980 for Indian Himalayas and reported an increasing trend during the 1901 to 1964 period and a decreasing trend for 1965 to 1980 period in the study region.

Douglas et al. (2009) modelled the impact of intensified agriculture and irrigation practices on land-atmospheric interactions and monsoon rainfall over India. They showed that the increase in irrigation indirectly decreases the monsoon rainfall over India. They concluded that the intensification of irrigation practices and agricultural activities could modify the mesoscale convection and the rainfall patterns over the Indian monsoon region.

Ghosh et al. (2009) studied a high-resolution (1º by 1º) gridded rainfall data for 1951 to 2003 period across India. As per the study, the amount of moderate rainfall over some places of central India showed decreasing trend whereas the occurrence of heavy rainfall events showed increasing trend over some places of central India.

Kumar et al. (2010) studied monthly, seasonal and annual rainfall trends using monthly data of 135 years (1871–2005) for 30 sub-divisions of India. They indicated the presence of non-significant trends for monthly, seasonal and annual rainfall across India. However, three sub-divisions showed a significant increasing trend, and one subdivision showed a significant decreasing trend for annual rainfall. In general, the monsoon and annual rainfall decreased, whereas, the winter, pre-monsoon and post-monsoon rainfall increased over India. The results of monthly rainfall analysis indicate a decreasing trend for June, July and September months, whereas the August rainfall showed an increasing trend in India.

Niyogi et al. (2010) analysed the effect of land use change and agricultural intensification on Indian summer monsoon rainfall using the gridded daily rainfall and monthly satellite land surface data sets. They found that the areas of decreasing rainfall coincided with the regions of change in land use due to agricultural intensification. The increase in agricultural intensification reduced the monsoon rainfall over India (mainly over northern and Peninsular India).

Pal and Al-Tabbaa (2011) assessed seasonal rainfall trends over India using the high-resolution (1º by 1º) daily gridded data of 1954 to 2003 period. They reported a presence of increasing trend in the autumn and winter rainfall, and decreasing trend in the spring and monsoon rainfall over India.

Jain and Kumar (2012) provided a good review of rainfall trends for the country-wide scale and concluded that the results of previous studies are not similar and there is no clear and consistent picture of rainfall trends.

Lacombe and McCartney (2013) studied monthly and seasonal cumulative rainfall depth, the number of rainy days and maximum daily rainfall trends over India using the 1°×1°-resolution gridded data for 1951 to 2007 period. They reported a presence of significant increase of rainfall depth in pre-monsoon season for Northeast India with a significant decrease in south-west India. The monsoon rainfall showed decreasing trend in central India with a heterogeneous pattern. Trends in annual rainfall depth and the annual number of rainy days are similar to the results of monsoon rainfall.

Pathak et al. (2014) studied the role of land surface hydrology in regional precipitation and computed recycled precipitation using the NCEP data for 1980 to 2010 period. They found a high precipitation recycling ratio (the ratio of recycled precipitation to total precipitation) for September month and the region of North East India showed maximum recycling ratio. The North Eastern India showed a statistically significant decreasing trend in recycled precipitation.

Subash and Sikka (2014) analysed monthly, seasonal and annual rainfall trends over India using sub-divisional monthly time series for 1904 to 2003 period. A presence of non-significant increasing, as well as decreasing trend, was found in monthly, seasonal and annual rainfall over India. For annual rainfall, 17 meteorological sub-divisions witnessed increasing trend and 13 meteorological sub-divisions witnessed decreasing trend. For the post-monsoon season, a significant increasing trend was found for Marathwada, Telangana and North Interior Karnataka. The monsoon rainfall showed increasing trend for Haryana and Punjab.

Mondal et al. (2015) analysed monthly, seasonal and annual rainfall trends for 141 years (1871–2011) for all the subdivisions and major regions of India. They reported a decreasing trend in annual and monsoon rainfall for the country. The rate of decrease in monsoon rainfall was found very high for Northeast, West Central and Core Monsoon India regions. The increasing trend in monsoon and annual rainfall was observed in the West Central India and peninsular India.

Yaduvanshi and Ranade (2015) studied the effect of global temperature changes on monthly, seasonal and an annual rainfall of seven river basins across eastern Indo-Gangetic plains (EIGP) using area-averaged monthly data (sometimes goes back up to 1829) till 2007. They found that the annual rainfall of all the river basins is not showing any significant long-term trend. A decreasing trend in monsoonal rainfall was found for Brahmani, Sons, Mahanadi and EIGP.

Paul et al. (2016) analysed the effect of land use land cover change on monsoon rainfall over India using the European Center for Medium range Weather Forecast (ECMWF) reanalysis data for 2000 to 2010. They found that the changes in land use pattern have a significant role on rainfall trends. The monsoon rainfall over India is weakening due to the decrease in evapotranspiration resulting from deforestation and warming of Indian Ocean Sea Surface Temperature.

Bera (2017) estimated seasonal and annual rainfall trends over Ganga River Basin using monthly data for 1901 to 2000 period. They analysed the data in district and sub-division level and found a significant decreasing trend in annual rainfall for 39 districts out of 236 districts. A significant decreasing trend in pre-monsoon rainfall was also observed in 54 districts. A significant decreasing trend in annual, pre-monsoon and post-monsoon rainfall was observed for most of the districts under the Kosi, Gandak and Sone sub-basins.

Most of the previous studies have been carried out using the sub-divisional or regional or gridded datasets. Some studies have also been conducted using fewer numbers of station data. Furthermore, the earlier studies have not analysed the short-term and long-term dependence using Indian rainfall datasets. The previous studies have also neglected the association of Indian rainfall with the climate change and climate variability aspect. Therefore, the analysis of Indian rainfall using the data of high quality and the uniform length is highly important. The earlier studies have used various gridded datasets for rainfall trend analysis over India however, none of the previous studies has provided any comparison of the results of analyses of these datasets. The comparison of datasets may provide some differences in the results. Moreover, there is an intense competition for water availability in the inter-state rivers such as Ravi-Beas-Sutlez, Narmada, Mahanadi, Vamsadhara, Tista, etc. In India, water is 'State' subject and always the inter-state rivers are the point of disputes between the associated states. The previous studies have not demonstrated the results state wise. Furthermore, all the states have their different budget allocation and management planning for the water resources separately. Therefore, in the present study, the rainfall has been analysed for different states, which can be used for the planning and management of the water resources of the concerned states on a common database.

3.3 STUDY AREA AND DATA USED

3.3.1 Study Area

In this study, the rainfall data of 15 states of central, east and north India have been analysed. The map of the study area is shown in Figure 3.1. The study area comprises four states of east zone (Bihar, Orissa, Jharkhand and West Bengal), six states of north zone (Jammu and Kashmir, Himachal Pradesh, Punjab, Uttarakhand , Uttar Pradesh and Haryana), two states of west zone (Rajasthan and Gujarat), two states of central zone (Madhya Pradesh and Chhattisgarh) and one state of northeast zone (Sikkim).

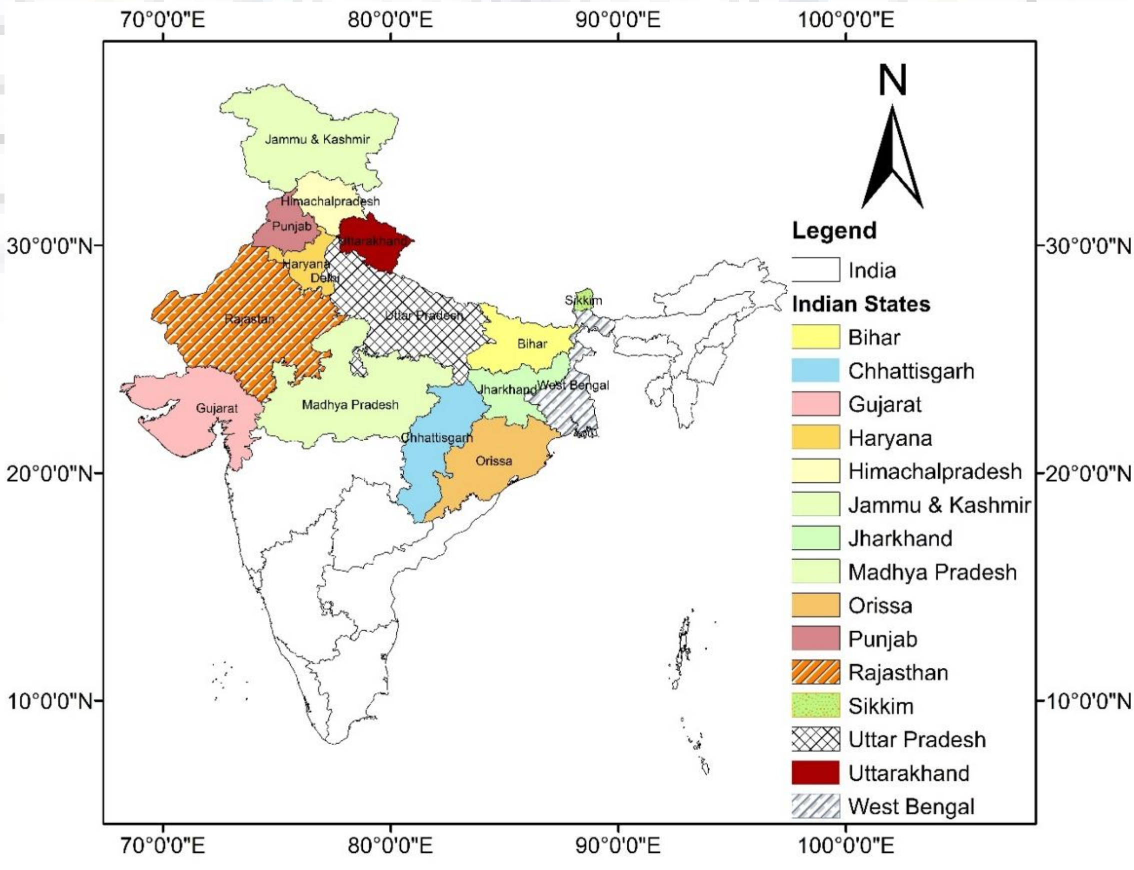

Figure 3.1. Map of the study area used in this study.

3.3.2 Data Used

A summary of different datasets used in this study is given in Table 3.1. In this study, all the datasets are analysed for the same time frame of 1951 to 2007. A brief description of all the datasets used in this study is given in the subsequent sections. Two different types of datasets, i.e. station data and gridded data are used in this study. The station datasets are used for investigation of short and long-term dependence, trends and association of rainfalls with climate change and climate variability indices.

Table 3.1 Summary of gridded rainfall datasets used in this analysis.

Types of Datasets	Temporal resolution	Spatial resolution	Interpolation method	References
Station rainfall	Monthly	Point	No Interpolation	IMD
IMD Gridded	Daily	1º by 1º	Angular Distance Weighting (ADW)	Rajeevan et al. (2008)
APHRODITE	Daily	0.25º by 0.25º	Climatology ratio-based using ShereMap	Yatagai et al. (2012)
CRU	Monthly	0.5º by 0.5º	Climatically-Aided Interpolation	Harris et al. (2014)
GPCC	Monthly	1º by 1º	Climatological anomaly-based using ShereMap	Schneider et al. (2015)
University Of Delaware	Monthly	0.5º by 0.5º	Climatologically-Aided Interpolation	Willmott and Matsuura (2001)

3.3.2.1 Station datasets

The monthly rainfall, number of rainy days and annual maximum rainfall data of 148 stations were collected from India Meteorological Department (Figure 3.2). These stations are well distributed over the study area. Total 79 stations have a common data period of 1951 to 2007. For other stations, the starting and ending years have a mismatch of three to four years. The annual, monsoon and non-monsoon rainfall series and number of rainy days datasets are prepared from the monthly datasets. The numbers of rainfall stations in each of the 15 different states used in this analysis are given in Table 3.2. It may be noted that most of the rainfall stations are concentrated in the four states of Madhya Pradesh, Rajasthan, Uttar Pradesh and West Bengal.

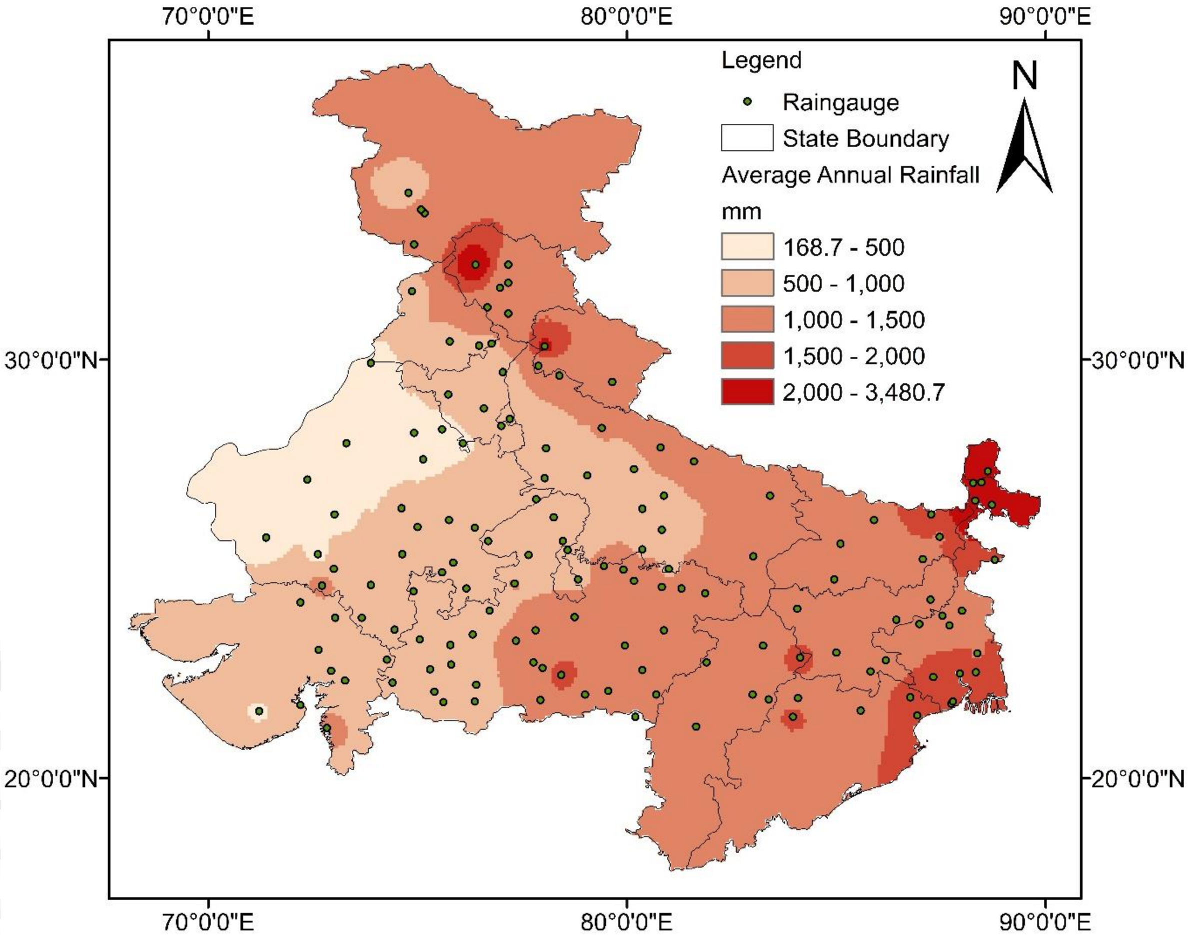

Figure 3.2. Rainfall stations and their distribution over 15 different states used in this analysis

Table 3.2 Number of rainfall stations in various states used in this analysis.

States Name	Name of Zones	Number of rainfall stations
Bihar	East Zone of India	6
Orissa	East Zone of India	5
Jharkhand	East Zone of India	6
West Bengal	East Zone of India	15
Jammu and Kashmir	North Zone of India	4
Himachal Pradesh	North Zone of India	6
Punjab	North Zone of India	3
Uttarakhand	North Zone of India	3
Uttar Pradesh	North Zone of India	16
Haryana	North Zone of India	7
Rajasthan	West Zone of India	23
Gujarat	West Zone of India	9
Madhya Pradesh	Central Zone of India	38
Chhattisgarh	Central Zone of India	6
Sikkim	North East Zone of India	1

3.3.2.2 Climate indices and Global Average Temperature

Two climate indices, namely, NINO3.4 Sea Surface Temperature (SST) anomaly (as ENSO-index) and Indian Ocean Dipole (IOD) mode index have been used in this study to see the influence of these indices over station rainfall. These indices represent the climate variability on a larger scale. Various studies in pasts have used the SST anomalies (Zhang et al., 2010; Kellner and Niyogi, 2015; Khan et al., 2017). The data of NINO3.4 (5N-5S 170W-120W) monthly SST anomalies from 1951 to 2000 mean are extracted from http://www.esrl.noaa.gov/psd/gcos_wgsp/Timeseries/Nino34/. ENSO is a large-scale ocean-atmosphere phenomenon resulting from the natural internal variability of climate. For many parts of the globe, the regional climatic pattern varies due to the phenomenon mentioned above. In general, ENSO pattern varies within two states, i.e., El Niño, which represents the warmer phase of the ENSO cycle and La Niña, which represents the cooling phase of the ENSO cycle. However, the ENSO region with near average temperature is known as ENSO neutral. Kenyon and Hegerl (2010) found the strongest influence of ENSO index on extreme precipitation in the winter season. Zhang et al. (2010) reported that the average SST anomalies over the NINO3.4 region provide similar results as found by using average SOI over the winter season. In the Indian context, the researchers have mostly used the NINO3.4 SST anomalies as an ENSO-index for extreme rainfall events (Gershunov et al. 2001; Maity and Kumar, 2006 and 2008; Revadekar and Kulkarni, 2008; Mondal and Mujumdar, 2015). Therefore, NINO3.4 SST anomalies have also been used as an ENSO-index for the present study.

Many researchers have found a relationship between IOD index and Indian monsoon rainfall (Saji et al., 1999; Ashok et al., 2003; Kulkarni et al., 2007; Surendran et al., 2015). The Indian Ocean Dipole mode index (IOD) datasets are taken from http://www.jamstec.go.jp/frsgc/research/d1/iod/iod/dipole_mode_index.html. IOD is a large-scale coupled ocean-atmosphere phenomenon in the Indian Ocean. The IOD is defined as the SST gradient difference between the tropical western Indian Ocean (50ºE-70ºE and 10ºS-10ºN) and the tropical south eastern Indian Ocean (90ºE-110ºE and 10ºS-equator). This gradient is named as Indian Ocean Dipole (IOD) mode index. Saji et al. (1999) studied the relationship between summer monsoon rainfall of India and IOD. They reported that there is no clear evidence of IOD influence over Indian summer monsoon rainfall. However, Ashok et al. (2003)

reported that the IOD played a vital role as a modulator for Indian monsoon rainfall. Kulkarni et al. (2007) suggested that the summer monsoon rainfall had more influence over IOD than the opposite. Surendran et al. (2015) reported a higher influence of ENSO index than IOD over Indian summer monsoon rainfall. Based on the above literature review, the study of the association of rainfall with of NINO and IOD indices were done.

The Global Average Temperature (GAT) is used to see the effect of human-induced climate change (Hegerl et al., 2007) on the station rainfall. The relationship between extreme rainfalls and global temperature is well established (Trenberth et al., 2003; Simmons et al., 2010; Westra et al., 2013). Global warming increases the specific humidity across the globe. Fowler and Wilby (2010) used GAT to compute the detection times for gridded extreme precipitations in the UK. On the basis of the above studies, the association of rainfall and GAT is taken up for analysis. The monthly observed HadCRUT4 land surface air global average temperature (GAT) anomalies with respect to 1961 to 1990 mean have been extracted from http://www.metoffice.gov.uk /hadobs/ hadcrut4/.

3.3.2.3 IMD 1º by 1º daily gridded rainfall

IMD has created a 1º by 1º daily gridded rainfall data for the entire country (Rajeevan et al., 2008). The daily gridded rainfall dataset have been developed from point data. The stations with 70% data of total data length are only selected for minimising the heterogeneity. Therefore, the gridded dataset have been created using 1384 numbers of stations. Before using the station dataset for interpolation, a multi-stage quality control procedure has been carried out. The gridded dataset have been developed using the interpolation technique proposed by Shepard (1968). More details of the interpolation technique used to prepare the dataset are given by Shepard (1968) and Rajeevan et al. (2005). The 1º by 1º gridded dataset have been compared with a previously developed gridded dataset by Rajeevan et al. (2006) and was reported to be of similar quality.

3.3.2.4 APHRODITE 0.25º by 0.25º daily gridded rainfall

The Asian Precipitation-Highly Resolved Observational Data Integration Towards Evaluation (APHRODITE) project has developed a high-resolution (0.25º by 0.25º) daily gridded precipitation datasets for Asia (Yatagai et al., 2012). These datasets are available for 1951 to

2007 period. The gridded datasets have been developed using more than 2500 rainfall stations over India and can be downloaded from http://www.chikyu.ac.jp/precip/. The quality of the station datasets was checked by three steps, i.e., 1) checking the initial errors (like wrong date, shifted columns), 2) information of the location of a rain gauge and 3) eliminating erroneous station data. As a first step, the climatology of different stations was interpolated. Then a ratio of daily precipitation to daily climatology was created using the angular distance weighting interpolation method and ShereMap (Willmott et al., 1985). The daily precipitation was finally calculated by multiplying the daily climatology with the daily ratio (Yatagai et al., 2012).

3.3.2.5 CRU 0.5º by 0.5º monthly gridded rainfall

The Climate Research Unit (CRU) has developed high-resolution monthly datasets for a number of climatic variables (Harris et al., 2014). In the present analysis, 0.5º by 0.5º monthly gridded rainfall data, i.e., CRU TS 3.21 version is used. The datasets are available for 1901 to 2012 period. These datasets were developed from the station observations over the globe. The main data sources of CRU are Jones and Moberg (2003), the Global Historical Climatology Network GHCN-v2 (Peterson and Vose, 1997), monthly climate bulletins (CLIMAT), Monthly Climatic Data for the World (MCDW) and World Weather Records (WWR) decadal data publication. The total number of stations for developing the gridded dataset varies with time (like 7075 stations for rainfall in 2000). The homogeneity of the dataset is not checked. The Climate Anomaly Method (CAM), (Peterson et al., 1998) was used for developing the CRU TS datasets. The anomaly time series was prepared for each of the stations from the 1961 to 1990 mean. For interpolation, an angular distance-weighted (ADW) method was used. However, the thin-plate splines interpolation method was used for 1961 to 1990 climatological reference data (New et al., 1999). The final rainfall values were calculated by multiplying the gridded percentage anomalies with the climatology, divided by 100 and adding the climatology (Harris et al., 2014).

3.3.2.6 GPCC 1º by 1º monthly gridded rainfall

Global Precipitation Climatology Centre (GPCC) is operated by German Weather Service DWD (Deutscher Wetterdienst, Germany) and supported by the World Meteorological Organization (WMO). The main objective of GPCC is to collect, archive global precipitation data and develop high-resolution gridded data products for the end users (Rudolf et al., 1994).

The data sources of GPCC are synoptic weather observation reports (SYNOP) and climatic mean (1951-2000) monthly precipitation totals calculated from more than 97,000 stations globally. GPCC provides four data products, which are the first-guess product, monitoring product, full data reanalysis product and VASClimO 50-Year Data Set. In this analysis, only the full data reanalysis product is used. This reanalysis product is based on all stations available in the GPCC database supplying data for the individual month. The reanalysis product version 7 (GPCC-V7) is available for the period of 1901 to 2013. The number of stations used for analysis varies with time (like 11,000 stations in 1901 to more than 51,000 stations in 1986). The datasets have been developed using anomalies from the climatological normal for each station. The anomalies are then interpolated by applying SPHEREMAP. The interpolation technique was done by a spherical adaptation (Willmott et al., 1985) of Shepard's empirical weighting scheme (Shepard, 1968).

3.3.2.7 UDel. 0.5º by 0.5º monthly gridded rainfall

The University of Delaware (UD) precipitation dataset is a monthly high resolution (0.5º by 0.5º) gridded data developed from station data (Willmott and Matsuura, 2001). The dataset is available for the period of 1900 to 2014 and can be freely downloaded from http://www.esrl.noaa.gov/psd/. The station datasets are compiled from various sources. These sources are the Global Historical Climatology Network (GHCN2), GC-Net data (Steffen et al., 1996), National Center for Atmospheric Research (NCAR) daily India data, Global Surface Summary of Day (GSOD) (NCDC), Station climatologies from Legates and Willmott (1990) etc. The datasets were developed from the observations of about 4,100 to 22,000 stations globally. A Climatologically aided interpolation (CAI) (Willmott and Robeson, 1995) method was used to calculate the monthly values. The traditional interpolation (Shepard, 1968; Willmott et al., 1985) was then used to get the gridded difference values from monthly station differences. Finally, each gridded difference value is added to the climatology at the corresponding set of grid points. The spatial interpolation errors are minimised using a station-by-station cross-validation method (Willmott and Matsuura, 1995).

3.3.3 Preliminary Data Analysis

The available raw data may have some errors, which can degrade the quality of the actual results by adding uncertainty to it. Therefore, a preliminary analysis of the datasets used in this study has been conducted using the single station and multi station time series plots and filling of data gaps by the help of normal ratio method.

3.4 METHODOLOGY

The variability of rainfall is measured by calculating the coefficient of variation (CV) for the station and gridded datasets. Then, the randomness of the rainfall was checked by using Autocorrelation test. For the station rainfall, the short-term and long-term dependence are measured by using Von Neumann ratio test and Hurst phenomenon respectively. For both the station and gridded rainfall trend estimation, the Mann-Kendall (MK) test/Modified Mann-Kendall (MMK) test is used for the non-random/random datasets. Theil-Sen's median slope estimator is used to measure the change in rainfall during the analysis period. The relationship between station rainfall with climate change and climate variability is analysed by the Spearman's rank correlation coefficient. The statistical tests mentioned in this analysis are well documented in the literature. However, a brief description is given in the subsequent sections for completeness sake.

3.4.1 Coefficient of Variation (CV)

The coefficient of variation (CV) is the ratio of standard deviation to the mean (in this analysis mean of 1951 to 2007 period) of a dataset. It is the standardised measure of variability or dispersion of a variable. The higher value of CV means a greater dispersion in the variable. The CV has been used by various researchers for the analysis of rainfalls (Mishra and Chatterjee, 2009; Tanarhte et al., 2012; Wasko et al., 2016).

3.4.2 Autocorrelation Test

Autocorrelation is the correlation between the past and future values of the same time series. It is also called "serial correlation" or "lagged correlation". The hydrological processes are many times auto-correlated. For example, the streamflow of a day may impart correlation to successive daily flows of the stream. The autocorrelation function can be used to detect the randomness of a time series and thereby, identifying the suitable time series model. The significance of first order autocorrelation coefficient for an independent and identically distributed (iid) data set can be analysed by Anderson's correlogram test (Anderson 1942). The mathematical background of the test is given in section 2.4.1.1. In hydrology, the lag-one correlation coefficient is vital for the strongest dependence of past values to the most recent past. The higher order lag correlation coefficient is only used when the lag-one correlation coefficient cannot adequately describe the effect of serial correlation. A plot of the serial correlation coefficient is used to detect randomness and stationarity of a time series (McCuen, 2003). The presence of significant autocorrelation in a time series causes further trend estimation (Hamed and Rao, 1998; Yue et al., 2002).

3.4.3 Short Term and Long Term Dependence

The analysis of short-term and long-term dependences in time series have been started long back and provide information about the time evaluation of a natural process. Chow (1964) mentioned that the hydrological processes are possibly dependent to an extent. Therefore, the possibility of these dependences should always be examined. These dependences could be for short time interval (interannual variability) as well as for long time interval (more than a year). The analysis of dependences is made by using various statistical tests such as autocorrelation test (Yevjevich, 1971), Von Neumann ratio test (Madansky, 1988), cumulative periodogram test (Box and Jenkins, 1970), rank difference test (Meacham, 1968) etc. In this analysis, the Von Neumann ratio test (Madansky, 1988) is used for measuring short-term dependence. The long-term dependence in time series analysis was first statistically measured by Hurst (1951). The Hurst coefficient is widely used for the analysis of long-term dependence (Wallis and O'connel, 1973; Boes and Salas, 1978; Lye and Lin, 1994; Rao and Bhattacharya, 1999; Koutsoyiannis, 2003, Otache et al., 2008, Wagesho et al., 2012).

3.4.3.1 Von Neumann ratio test

It is a parametric test applied for checking of the short-term dependence of time series. The length of time series for implementing the test is generally thirty. The test statistics "V" for a time series X(t) of length N is calculated (von Neumann, 1941; Bratels, 1982) as:

$$V = \frac{\sum_{t=1}^{N}(X_{t+1}-X_t)^2}{\sum_{t=1}^{N}(X_t-\bar{X})^2} \qquad (3.1)$$

where $\bar{X}$ is the mean of the time series. If the time series is independent, the test statistics "V" follows normal distribution with a mean and variance of 2 and $4(N-2)/(N^2-1)$ respectively. The standardized test statistic, C, can be calculated as:

$$C = \frac{V-2}{\sqrt{\frac{4(N-2)}{(N^2-1)}}} \tag{3.2}$$

If the value $|C| > Z_{1-\frac{\alpha}{2}}$ (α *is significance level*), the null hypothesis of independent is rejected.

3.4.3.2 Hurst coefficient

The Hurst coefficient is used to measure the long-term dependences from a time series. The Hurst coefficient is estimated by Hurst's 'H', which is easy to assess. The Hurst's H (Hurst, 1951) is calculated as:

$$H = \frac{\log(\frac{R}{S})}{\log(\frac{n}{2})} \tag{3.3}$$

where R is the range of cumulative departure from the mean of a time series, S is the standard deviation of a time series, and n is the length of time series. R is calculated as:

$$R = \max(\sum_{i=1}^{n}(X_i - \bar{X})) - \min(\sum_{i=1}^{n}(X_i - \bar{X})) \tag{3.4}$$

The value of H lies in between 0 and 1. In general, the value of H more than 0.5, implies a presence of long-term dependence in the time series. However, the significance of the calculated Hurt's H should always be tested. In this analysis, the significance of Hurst's H is tested using a chart of empirical percentage points developed by Lye and Lin (1994).

3.4.4 Trend Tests and Changes in Rainfall

The estimation of trends in hydroclimatic time series started long back. A number of studies with temperature data (Arora et al., 2005, Jhajharia and Singh, 2011), rainfall data (Subash and

Sikka, 2014; Mondal et al., 2015), evapotransporation data (Bandyopadhyay et al., 2009; Anabalón and Sharma, 2017), and stream flow data (Wagesho et al., 2012; Ajami et al., 2017) have been conducted using both the parametric and non-parametric methods for trend estimation. In general, the parametric tests are more powerful than the non-parametric tests. However, the parametric tests require independent and normally distributed data sets (Jhajharia et al., 2009), which is not always the case in actual hydrological observations. The non-parametric tests, on the other hand, are a distribution free test and can be used with outliers also.

The most widely used non-parametric trend test in hydrological fields is Mann-Kendall Test (Mann, 1945; Kendall, 1955). It is developed for two groups of observations using a rank correlation test proposed by Kendall (1955). The null hypothesis of the test is that the observations are independent and randomly ordered, which means, the observations are free from any trends and autocorrelations. Many times, however, the actual hydrological observations are auto-correlated in nature. The presence of autocorrelation in observed dataset affects the estimated trends (Hamed and Rao, 1998; Serrano et al., 1999; Yue et al., 2002, 2003; Cunderlik and Burn, 2004; Novotny and Stefan, 2007). Therefore, the Modified Mann-Kendall (Hamed and Rao, 1998) test is applied for auto-correlated data. Details of statistical background of Mann-Kendall test and Modified Mann-Kendall test are given in the sub-sections 2.4.1.2 and 2.4.1.3 respectively.

The analysis of trends will always not provide statistically significant results. However, both the statistically significant and non-significant trends may have the practical interest and vice versa (Yue and Hashino, 2003). Radziejewski and Kundzewicz (2004) mentioned that the presence of non-significant trends in a time series might be due to the change in climatic systems. Therefore, the variation of rainfall during the study period is estimated by approximating it with a linear trend. The magnitude of the trend present in the rainfall dataset is assessed by Theil and Sen's median slope estimator. The Theil and Sen's median slope estimator is mostly used by the researchers to analyse the magnitude of the detected trend in a time series (Subash et al., 2011). The details of these statistical tests are given in the subsection 2.4.1.4 of the previous chapter.

3.4.5 Spearman's Rank Correlation Coefficient

Spearman's correlation coefficient is a rank-based non-parametric test introduced by Spearman (1904). It is used to identify and measure the strength of a monotonic relationship between two sets of data. The rank correlation coefficient, r_s, can be calculated as:

$$r_s = 1 - \frac{6\sum_{i=1}^{n} d_i^2}{n(n^2-1)} \tag{3.5}$$

where n is the length of observations in both of the datasets, d_i is the ranked difference between i^{th} observations for the two sets of data. The range of the r_s value is from -1 to 1. The significance of the calculated r_s is tested by the p-value using the student's t-test as:

$$t = \frac{r_s}{\sqrt{\frac{1-r_s^2}{n-2}}} \tag{3.6}$$

with $n-2$ degrees of freedom.

3.5 RESULTS AND DISCUSSION

Annual average rainfall values show a wide variation in the study area with annual values ranging from 3481 mm (in the Himalayan Mountain) to 169 mm (in the western part of India). The average annual rainfall during 1951 to 2007 for the study area is shown in Figure 3.3(a). The figure indicates that the states of the eastern part of India and the Himalayan region of northern part of India get very high annual average rainfall (more than 1300 mm/year). The annual average rainfall of Rajasthan and Gujarat states are very low, and almost all parts of these two states receive less than 750 mm annual rainfall during the analysis period. The variability of annual rainfall is shown in Figure 3.3(b). The coefficient of variation indicates a higher value of 83 in the western parts of the study area to a lower value of 13 in the mountain area. The rainfall variability is also low in the states of the eastern part of India and the Himalayan region of northern part of India with a CV ranging from 13 to 30. The western region, mainly two states, i.e., Rajasthan and Gujarat show a greater variability in annual rainfall with a CV ranging from 30 to 83.

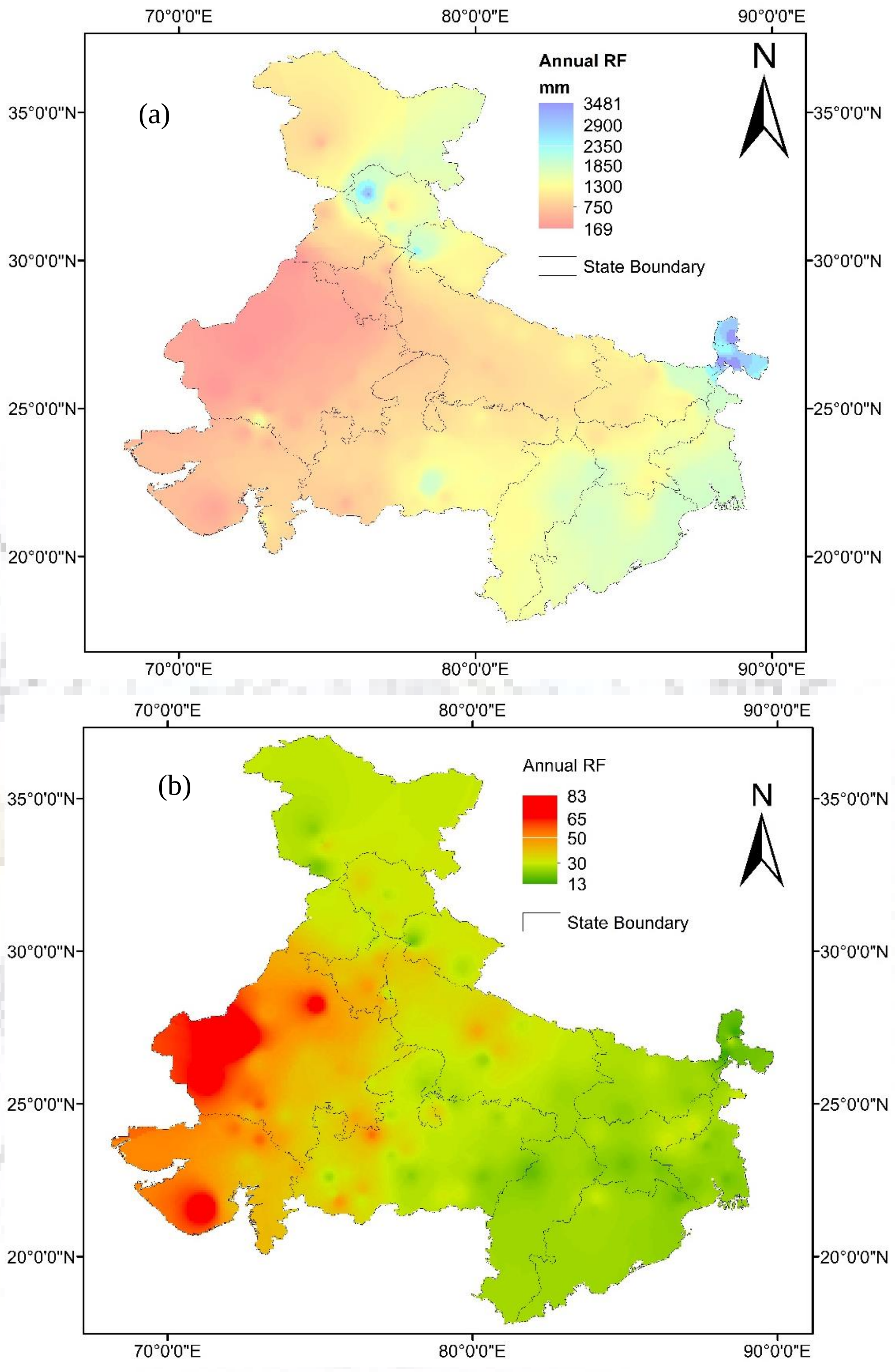

Figure 3.3. Annual average rainfall and its variation in the study area during 1951 to 2007. a) Total annual, b) Coefficient of variation (CV)

3.5.1 Autocorrelation in Station Data

The lag-one autocorrelation effect is assessed in this analysis with the help of Anderson's approach. The results with significant lag one autocorrelation coefficient in different states are given in Table 3.3. The results show that out of 148 stations, only 20 stations (13.51%) have significant lag one autocorrelation effect in annual rainfall. The results are almost similar for the rainfall of monsoon (11.48% stations with significant lag one autocorrelation coefficient) and non-monsoon seasons (14.86% stations with significant lag one autocorrelation coefficient). However, the annual maximum rainfall shows lesser effect of autocorrelation (4.73% stations with significant lag one autocorrelation coefficient). The autocorrelations of annual and seasonal number of rainy days also show the similar type of results. The details of percentage of stations in different states are given in Table 3.3.

Table 3.3 Percentage of stations with significant lag one autocorrelation coefficient**,** at 5% significance level in different states.

State	Total Station	ARF	MRF	NMRF	AMRF	ARD	MRD	NMRD
Bihar	6	0	16.67	16.67	0	0	33.33	16.67
Orissa	5	0	0	20	20	0	0	0
Jharkhand	6	0	0	0	16.67	0	0	0
West Bengal	15	6.67	6.67	0	0	33.33	40	0
Jammu & Kashmir	4	25	0	75	0	75	25	50
Himachal Pradesh	6	33.33	0	16.67	0	50	33.33	16.67
Punjab	3	66.67	33.33	66.67	0	0	0	66.67
Uttarakhand	3	0	33.33	0	0	0	0	0
Uttar Pradesh	16	12.5	12.5	25	12.50	0	0	6.25
Haryana	7	42.86	14.29	14.29	0	14.29	14.29	14.29
Rajasthan	23	17.39	21.74	17.39	4.35	26.09	21.74	13.04
Gujarat	9	11.11	11.11	22.22	11.11	11.11	0	33.33
Madhya Pradesh	38	10.53	10.53	7.89	2.63	13.16	13.16	7.89
Chhattisgarh	6	0	0	0	0	0	0	16.67
Sikkim	1	0	0	0	0	100	100	0
Total	148	13.51	11.48	14.86	4.73	16.89	15.54	12.16

ARF = total annual rainfall, MRF = total monsoon rainfall, NMRF = total non-monsoon rainfall, AMRF = annual maximum rainfall, ARD = number of rainy day in a year, MRD = number of rainy day in monsoon season, NMRD = number of rainy day in the non-monsoon season.

The state wise results show that the percentage of stations with significant lag-one autocorrelation in annual and seasonal rainfall series is lesser for the states with the higher number of stations (Madhya Pradesh, Rajasthan, Uttar Pradesh, and West Bengal). The result is similar to the analysis of rainy day series. The correlogram is also computed for all the series. For this, the autocorrelation coefficient is calculated up to the n/4 lags. The Anderson's correlogram test is used to estimate the upper and lower confidence limits of the correlogram. The correlograms of three stations having significant autocorrelations are presented in Figure 3.4. These correlograms show that the serial dependence for the annual and seasonal series are higher for the first two lag and approaching near to zero at high lags. The lag-one autocorrelation coefficient is not showing any spatial pattern over the study area.

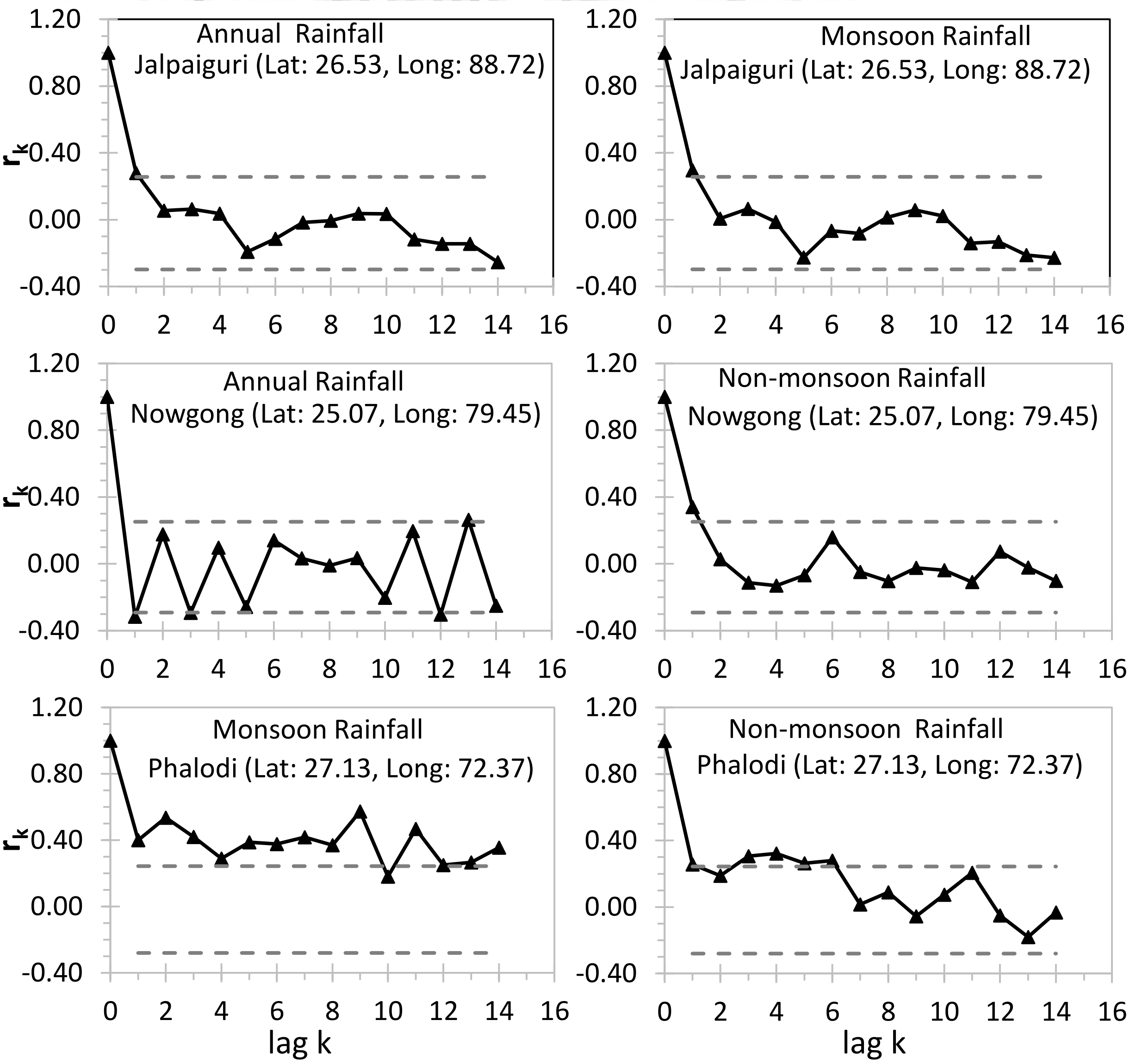

Figure 3.4. Correlogram of three representative stations with significant autocorrelations for annual and seasonal rainfall

3.5.2 Time Dependence in Station Data

In this analysis, the short and long-term dependences are measured using Von Neumann ratio test and Hurst coefficient respectively. The results of Von Neumann ratio test for annual and seasonal rainfall and the number of rainy days of 148 stations in different states are given in Table 3.4. The results show low percentage of stations with short-term dependence in seasonal, annual and annual maximum rainfall series. The result is similar to the analysis of the annual and seasonal number of rainy days. However, the percentage is slightly increased for the analysis of the number of rainy days.

Table 3.4 Percentage of stations with significant short-term dependence at 5% significance level in different states.

State	Total Station	ARF	MRF	NMRF	AMRF	ARD	MRD	NMRD
Bihar	6	0	16.67	16.67	0	16.67	33.33	16.67
Orissa	5	0	0	20	0	0	0	0
Jharkhand	6	0	0	16.67	16.67	0	16.67	0
West Bengal	15	0	6.67	6.67	6.67	20	33.33	6.67
Jammu & Kashmir	4	50	0	25	0	50	0	50
Himachal Pradesh	6	33.33	0	33.33	33.33	50	16.67	33.33
Punjab	3	33.33	33.33	0	0	0	0	33.33
Uttarakhand	3	0	33	33	0	0	0	0
Uttar Pradesh	16	12.50	12.50	18.75	18.75	0	0	6.25
Haryana	7	42.86	42.86	14.29	0	0	0	14.29
Rajasthan	23	8.70	4.35	17.39	13.04	30.43	21.74	26.09
Gujarat	9	0	0	11.11	11.11	0	0	44.44
Madhya Pradesh	38	13.16	10.53	7.89	7.89	18.42	13.16	26.32
Chhattisgarh	6	16.67	0	16.67	0	16.67	0	16.67
Sikkim	1	0	0	0	0	0	100	0
Total	148	12.16	9.46	14.20	9.46	16.22	13.51	20.27

ARF = total annual rainfall, MRF = total monsoon rainfall, NMRF = total non-monsoon rainfall, AMRF = annual maximum rainfall, ARD = number of rainy day in a year, MRD = number of rainy day in monsoon season, NMRD = number of rainy day in the non-monsoon season.

The states with higher number of stations (like Madhya Pradesh, Rajasthan, Uttar Pradesh and West Bengal) show lesser percentage of stations with significant short-term dependence. Only three states (Himachal Pradesh, Haryana and Punjab) are showing some higher percentage of stations with short-term dependence. However, those states account for very less number of stations in this analysis. There is no spatial pattern for the stations showing significant short-term dependence in annual and seasonal rainfall (Figure 3.5). However, the stations of Rajasthan and some nearby states are mainly showing significant short-term-

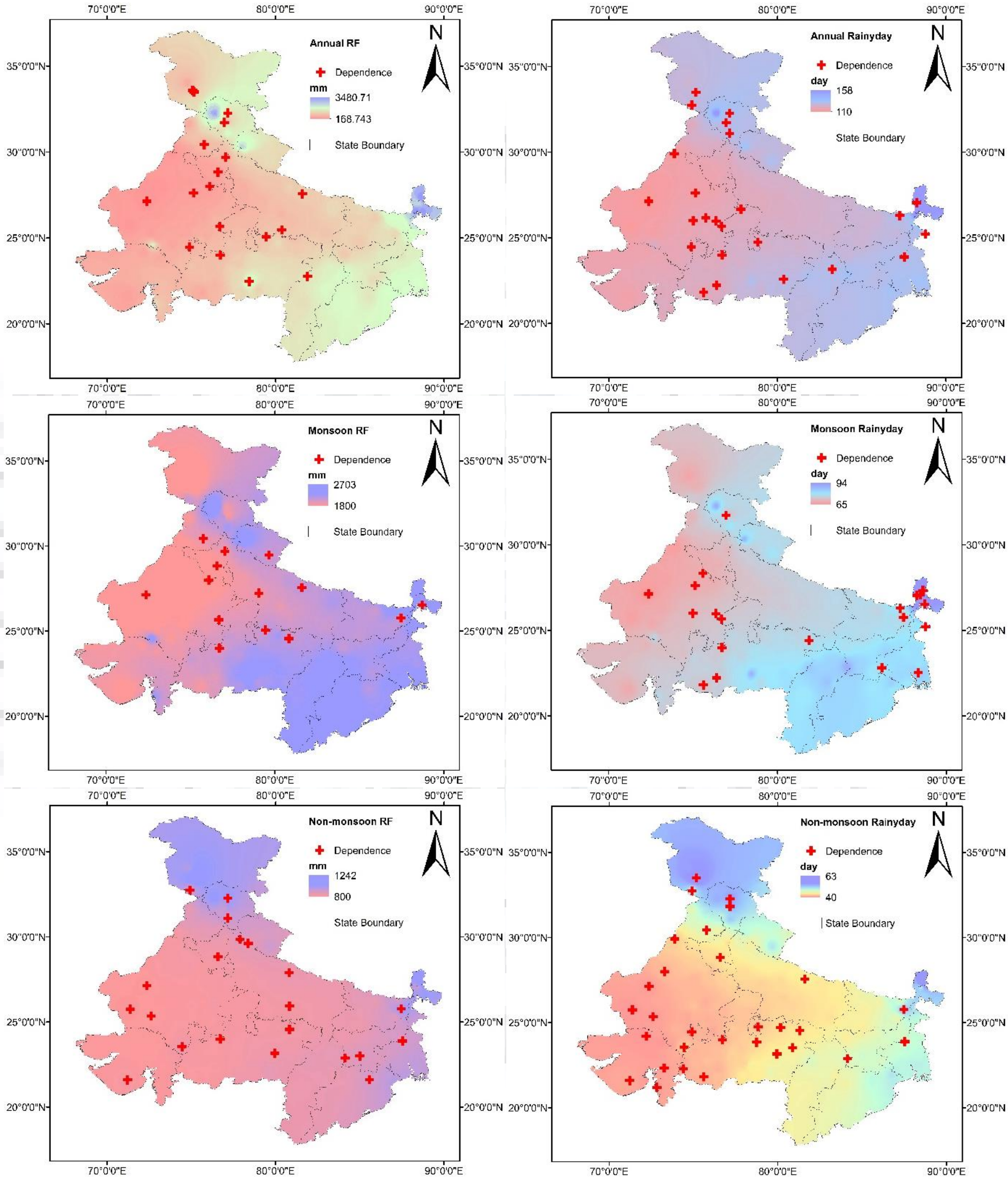

Figure 3.5. Stations with significant short-term dependence in different states for annual and seasonal rainfall and rainy day series

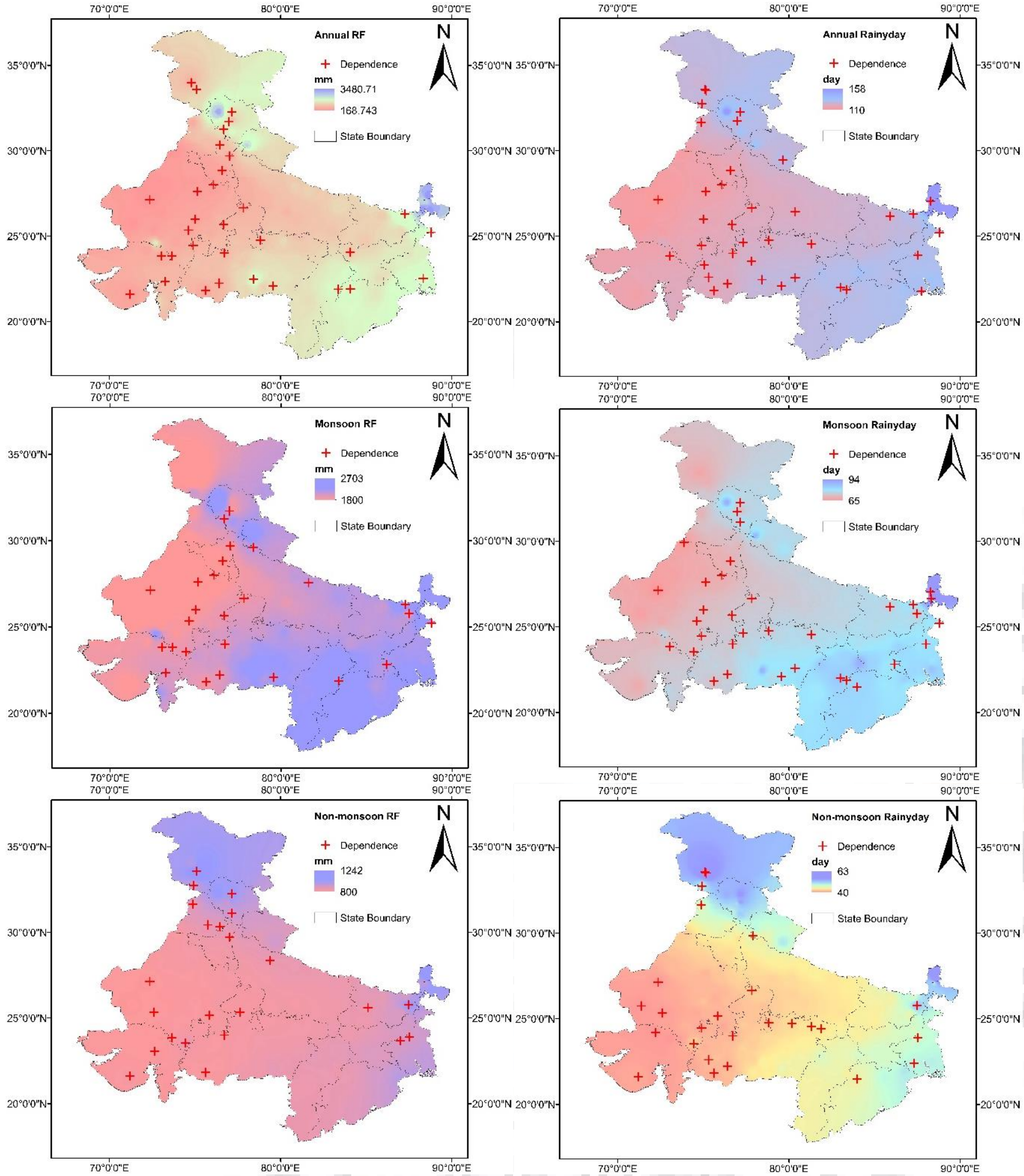

Figure 3.6. Stations with significant long-term dependence in various states for annual and seasonal rainfall and rainy day series

-dependence for annual and monsoon season rainfall and rainy day series. For rainy day series, the stations near to the Himalayas are also showing significant short-term dependence. The stations showing significant short-term dependence in rainfall and rainy day series of the non-monsoon season are distributed over the study area. The stations showing short-term dependence for rainfall variables are mainly from the low rainfall area. These stations have more variability and the effect of local climatic variables will be more prominent in these stations. Hence, there is a need to revisit the hydraulic designs based on stationarity assumption in these areas. Detailed discussion on this aspect has been done in Chapter 4 and 5.

The Hurst coefficient is used to measure the long-term dependence in annual and seasonal rainfall and rainy day series. The results of long-term dependence on annual and seasonal rainfall and the number of rainy days of 148 stations in different states are given in Table 3.5. The significant long-term dependence is available in less than 25% of stations in annual and seasonal rainfall as well as number of rainy day series. The significant long-term dependence is more in the states, like, Madhya Pradesh, Rajasthan, Punjab and Himachal Pradesh. For annual and monsoon rainfall, the spatial distribution shows that the stations with long-term dependences are in straight line from northern states to the western states (Figure 3.6). Similar results have been obtained for the annual and monsoon season rainy day series. However, in rainy day series, some stations from Madhya Pradesh are also showing significant-

Table 3.5 Percentage of stations with significant long-term dependence at 5% significance level in different states.

State	Total Station	ARF	MRF	NMRF	AMRF	ARD	MRD	NMRD
Bihar	6	16.67	33.33	33.33	0	33.33	50	16.67
Orissa	5	20	0	0	20	0	20	20
Jharkhand	6	16.67	16.67	0	0	0	16.67	0
West Bengal	15	13.33	6.67	13.33	0	26.67	26.67	13.33
Jammu & Kashmir	4	50	0	50	0	75	0	75
Himachal Pradesh	6	50	33.33	33.33	16.67	33.33	50	0
Punjab	3	33.33	0	100	33.33	33.33	0	33.33
Uttarakhand	3	0	0	0	0	33.33	0	33.33
Uttar Pradesh	16	0	12.50	6.25	12.50	6.25	0	0
Haryana	7	42.86	42.86	14.29	28.57	28.57	28.57	0
Rajasthan	23	26.09	30.43	21.74	4.35	17.39	30.43	26.09
Gujarat	9	33.33	22.22	22.22	11.11	11.11	11.11	22.22
Madhya Pradesh	38	21.05	13.16	7.89	2.63	36.84	26.32	23.68
Chhattisgarh	6	16.67	16.67	0	0	33.33	33.33	0
Sikkim	1	0	0	0	0	0	0	0
Total	148	21.62	17.57	15.54	6.76	25.00	22.97	17.57

ARF = total annual rainfall, MRF = total monsoon rainfall, NMRF = total non-monsoon rainfall, AMRF = annual maximum rainfall, ARD = number of rainy day in a year, MRD = number of rainy day in monsoon season, NMRD = number of rainy day in the non-monsoon season.

-long-term dependence. For non-monsoon rainfall and rainy day series, the stations near to the western states are mainly showing long-term dependence. Koutsoyiannis (2003) stated that the long-term dependence might be found in regional scales. The present analysis also show the similar results. However, IPCC does not recognise the presence of long-term dependence in the presence of climate change. Therefore, those stations with long-term dependence will not be considerably affected by the change in the climatic conditions. Hence, these stations can be modelled by using the long-term variations present in them.

3.5.3 Evaluation of Trends in Station Data

The summary of trend analysis for 148 stations distributed over 15 different states is given in Table 3.6. The results indicate that less than 30% of stations only are showing a significant trend (increasing or decreasing) for all the rainfall and rainy day variables. The change in magnitude of all the rainfall and rainy day variables is analysed during the 1951 to 2007 period. For the change analysis, the magnitude of the trend is estimated by using the Theil and Sen's median slope estimator. The station wise trend analysis results and change of magnitude for all the rainfall and rainy day variables are depicted in Figure 3.7 to 3.10.

Trend analysis of annual rainfall indicates that only 22.97% of stations are showing a significant trend (increasing and decreasing) over the study area, whereas, only 27.03% of stations are showing a significant trend (increasing and decreasing) in the number of rainy days in a year. The state wise results indicate that the highest percent of stations showing significant trend are in the West Bengal state for annual rainfall, while for the number of rainy days, both Jharkhand and Chattisgarh states have a maximum percent of stations with the significant trend. For both the rainfall and rainy day analysis, the significant trend is not observed for some states. The station wise trend analysis result with the magnitude of change during the analysis period for both rainfall and number of rainy day in annual basis are depicted in Figure 3.7. The significant increasing trend is observed for only 6 stations, while 28 number of stations show a significant decreasing trend in annual rainfall over the study area during the analysis period. Most of the stations showing significant increasing trend are in West Bengal, while the stations showing significant decreasing trend are mainly distributed over Madhya Pradesh and Rajasthan states. The change in magnitude of annual rainfall provides a better picture of the study area. It is observed that most of the study area shows up to 200 mm of a decrease in annual rainfall during the analysis period. Most parts of Himachal Pradesh and Uttarakhand and some parts of Madhya Pradesh, Rajasthan, Uttar Pradesh and Jammu and Kashmir are showing a decrease of 400 mm or more than that in annual rainfall. However, parts of West Bengal with adjacent areas of the state and parts of Gujarat state are showing an increase of annual rainfall up to 200 mm and more during the analysis period.

The trend analysis of the number of rainy days on an annual basis indicated that only 3 stations of three different states are showing a significant increase, while, 37 stations are showing a significant decrease in the number of rainy days during the analysis period. Those stations showing significant decreasing trend are from mainly Madhya Pradesh, Rajasthan and Uttar Pradesh. However, very few stations of some other states are also indicating a significant decreasing trend in the number of rainy days. Most of the study area observed up to 10 days decrease in the number of rainy days for a year during the analysis period. Some parts distributed over the study area also observed more than 10 days decrease of rainy days in a year, while some other parts in different states observed an increase of up to 10 rainy days in a year. It was observed from the results that large parts of the study area indicated a decrease in annual rainfall and number of rainy days. The decreasing rainfall is going to affect the water availability of the region. The decreasing number of the rainy days means the intensity of the rainfall is going to increase or the amount of rainfall going to decrease. Both the situations are going to create water shortage over some parts of the study area. It can be seen that in Rajasthan state (<750 mm of mean annual rainfall for the most part of the state), where the shortage of water is the main concern, a decrease of rainfall up to 200 mm can worsen the situation. In addition, most parts of the northern India shows decreasing trend in annual rainfall and number of rainy days can trigger the problem of available drinking water in the mega cities of this area.

Trend analysis of rainfall and number of rainy days in monsoon season indicated that only 22.30% and 27.70% of stations have significant trend respectively. The station wise results show that nearly 30% stations are having a significant trend in rainfall for most of the states. However, the stations of six states are not showing any significant trend in monsoon rainfall. Nearly, 50% stations of Bihar and Chattisgarh states are showing a significant trend in the number of rainy days. More than 30% stations of some other states are also showing a significant trend in the number of rainy days. All the stations of three states are showing a non-significant trend in the number of rainy days. However, very few number of stations are available for trend analysis from those states. The station wise results of trend analysis, change-

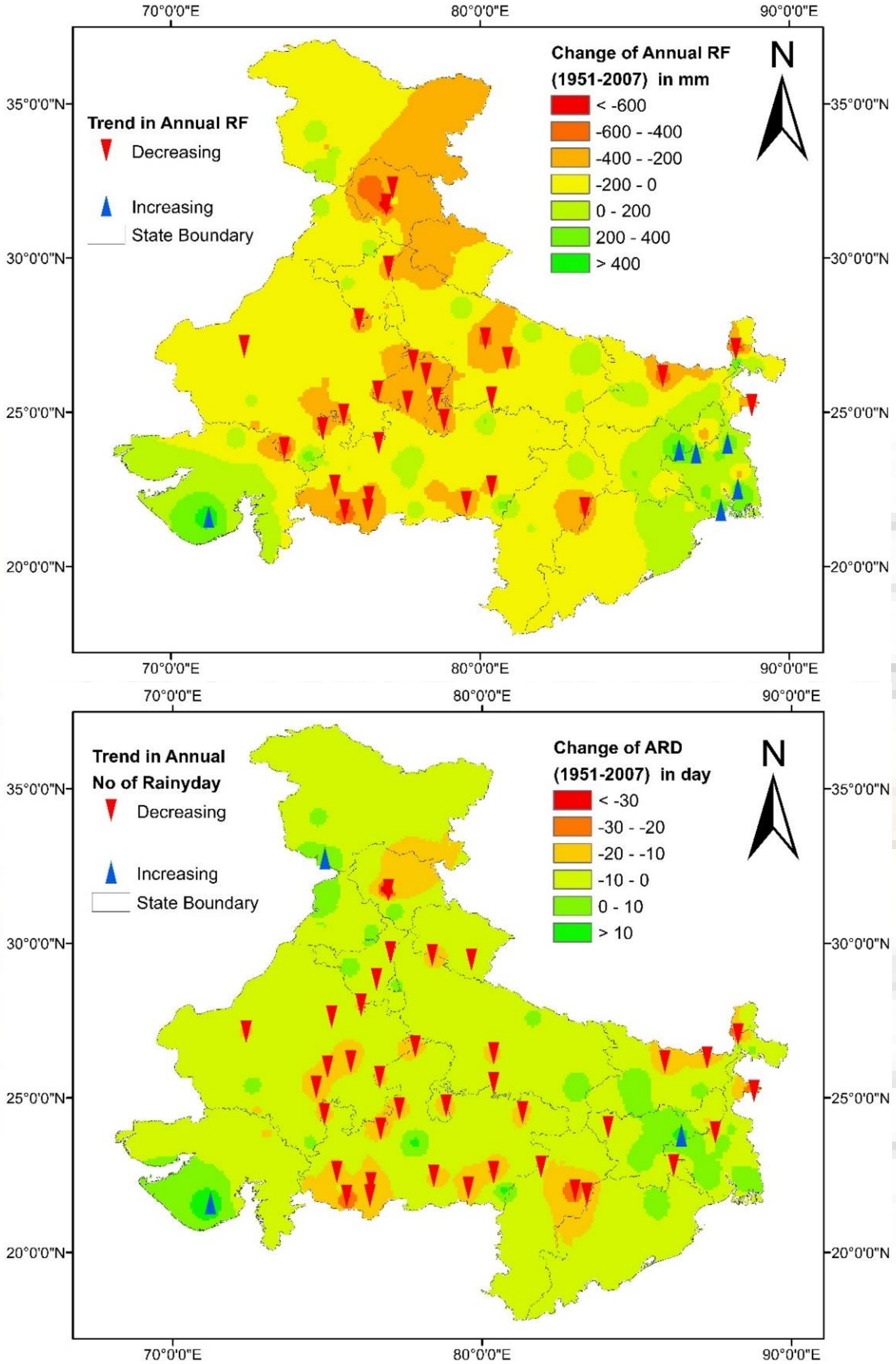

Figure 3.7. Observed trend and change in annual rainfall amount and number of rainy days in a year during the 1951-2007 period

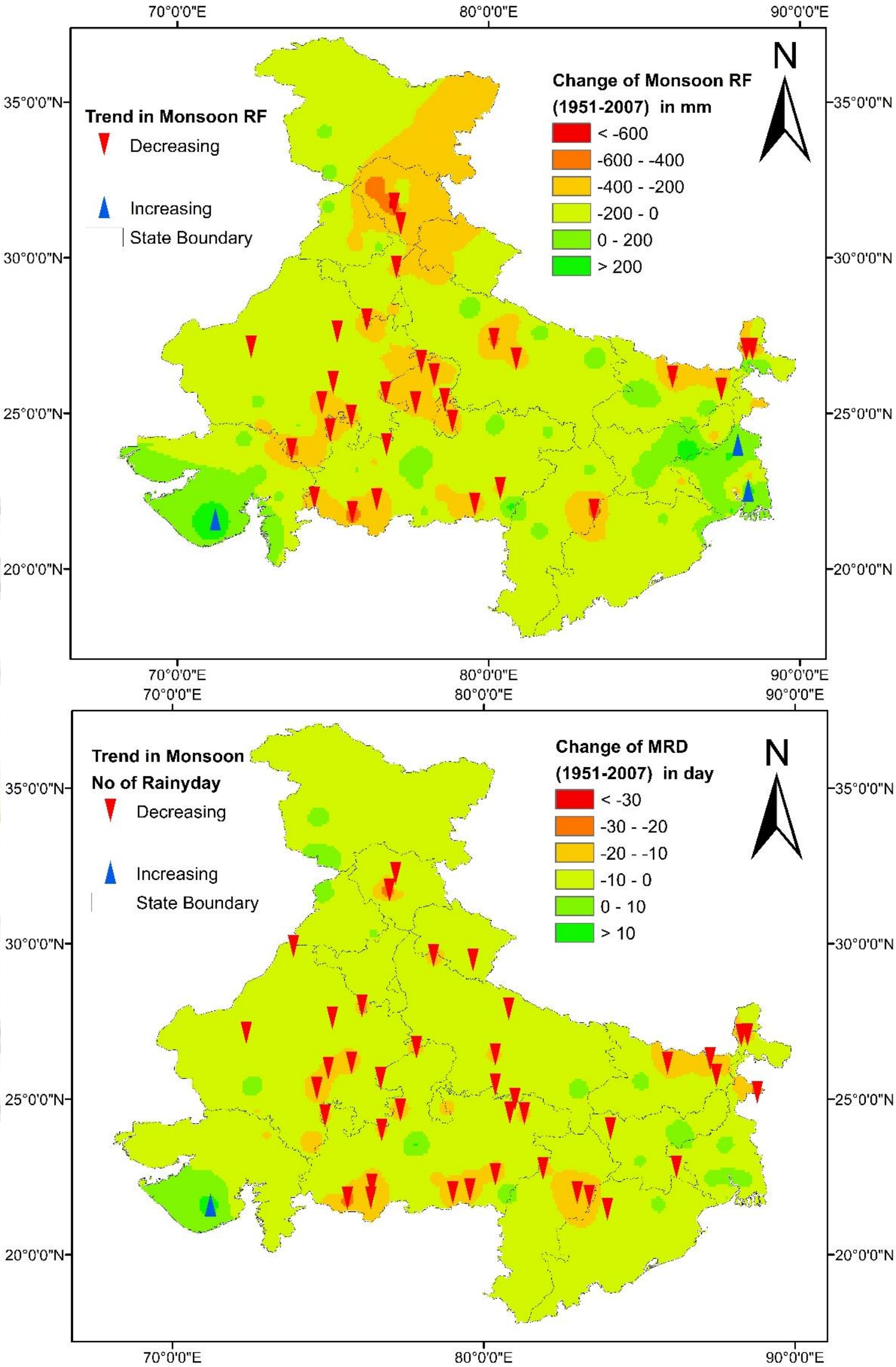

Figure 3.8. Observed trend and change in monsoon rainfall amount and number of rainy days in the monsoon season during the 1951-2007 period

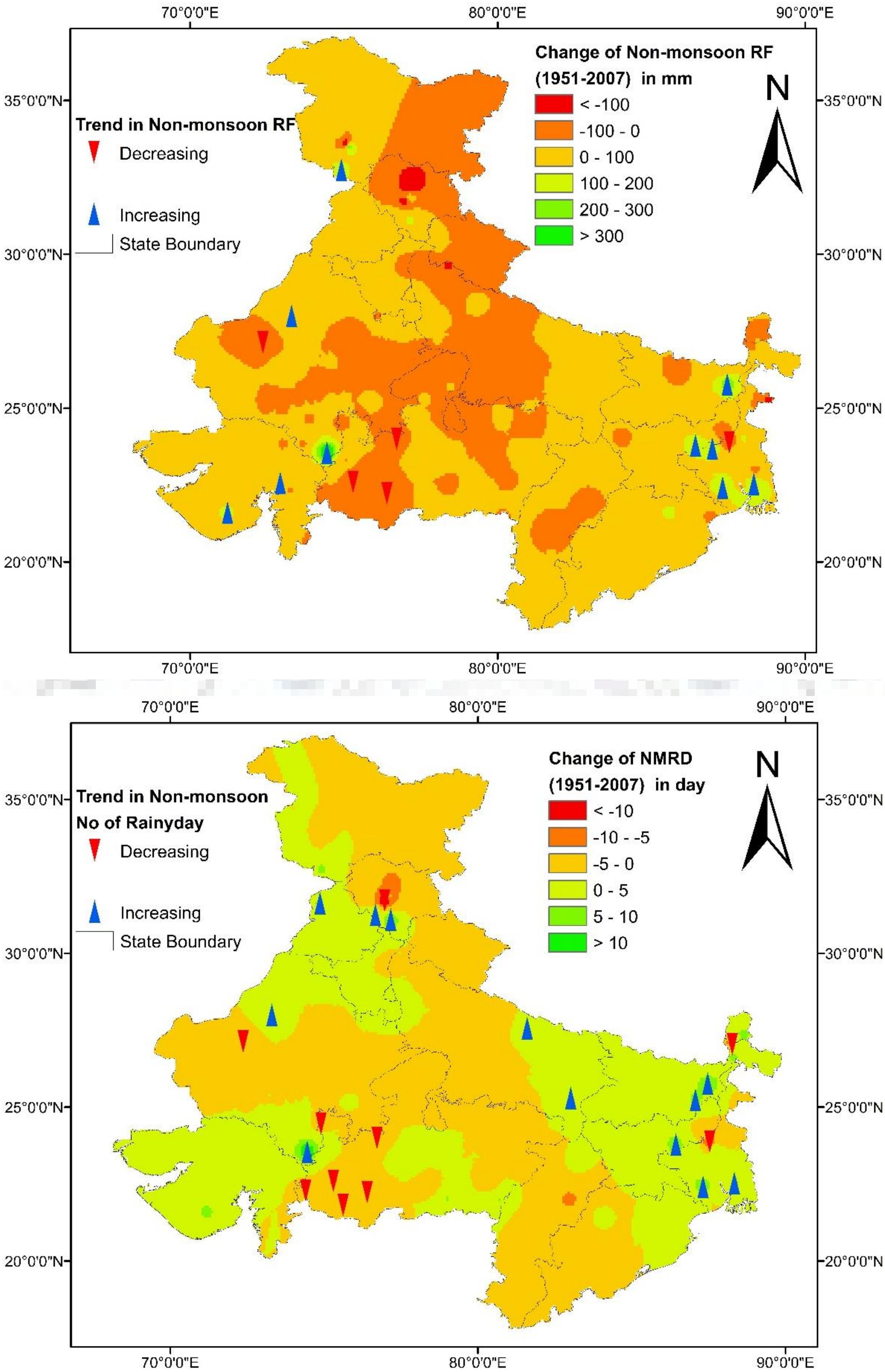

Figure 3.9. Observed trend and change in non-monsoon rainfall amount and number of rainy days in the non-monsoon season during the 1951-2007 period

Table 3.6 Summary of the percentage of stations with significant trends (both increasing and decreasing) at 5% significance level in different states.

State	Total Station	ARF	MRF	NMRF	AMRF	ARD	MRD	NMRD
Bihar	6	16.67	33.33	16.67	0	33.33	50	33.33
Orissa	5	0	0	0	0	0	20	0
Jharkhand	6	16.67	0	16.67	0	50	33.33	16.67
West Bengal	15	40	26.67	26.67	13.33	20	20	26.67
Jammu & Kashmir	4	0	0	25	0	25	0	0
Himachal Pradesh	6	33.33	33.33	0	0	16.67	33.33	50
Punjab	3	0	0	0	0	0	0	33.33
Uttarakhand	3	0	0	0	0	33.33	33.33	0
Uttar Pradesh	16	25	18.75	0	18.75	18.75	31.25	12.5
Haryana	7	28.57	28.57	0	14.29	42.86	14.29	0
Rajasthan	23	17.39	30.43	13.04	8.70	26.09	30.43	13.04
Gujarat	9	11.11	11.11	22.22	22.22	11.11	11.11	0
Madhya Pradesh	38	31.58	28.95	7.89	7.89	34.21	31.58	15.79
Chhattisgarh	6	16.67	16.67	0	16.67	50	50	0
Sikkim	1	0	0	0	0	0	0	0
Total	148	22.97	22.30	10.13	9.46	27.03	27.70	14.86

ARF = total annual rainfall, MRF = total monsoon rainfall, NMRF = total non-monsoon rainfall, AMRF = annual maximum rainfall, ARD = number of rainy day in a year, MRD = number of rainy day in monsoon season, NMRD = number of rainy day in the non-monsoon season.

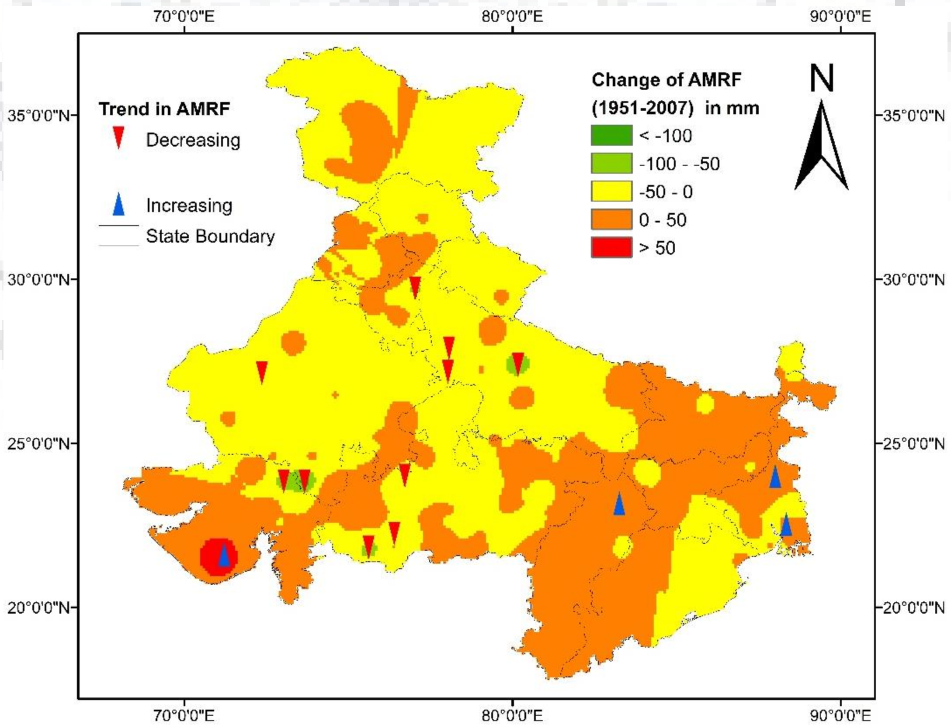

Figure 3.10. Observed trend and change in annual maximum rainfall during 1951-2007 period

-of magnitude in rainfall and number of rainy days for monsoon season during the analysis period is shown in Figure 3.8. It can be observed from the figure that only two stations of West Bengal show a significant increasing monsoon rainfall trend and one station of Gujarat shows a significant increasing trend in both rainfall and number of rainy days. A significant decreasing trend is observed for 30 stations and 40 stations in rainfall and rainy day respectively for the study area. The stations showing a decreasing trend in monsoon rainfall are mostly from Madhya Pradesh and Rajasthan, whereas, the stations showing a decreasing trend in the number of rainy days are distributed over the study area. Most part of the study area shows up to 200 mm of a decrease in monsoon rainfall with up to 10 days decrease in the number of rainy days. The increase in monsoon rainfall and decrease of more than 200 mm rainfall is similar to the pattern of increase and decrease for annual rainfall. The monsoon season is most important for the livelihood of this region. The monsoon season rainfalls are the main contributor of water for most parts of the country's arable land. Therefore, monsoon rainfall is a key element of the Indian economy, and a decrease in monsoon rainfall over most of the study area may reduce the growth of Indian economy. The number of rainy days is also decreasing over most parts of the study area, which may increase the intensity of monsoon rainfall. The regions near to West Bengal may face the similar situation as the rainfall amount increases with the number of rainy days decrease in monsoon season. The decrease in the number of rainy days in monsoon season can cause some day early or delay sowing for the crops and change the agricultural productions, which will surely affect the livelihood of the farmers of this region.

In non-monsoon season, the significant trend is observed for less than 15% stations over the study area for both rainfall and number of rainy days. No stations of eight different states are showing any significant trend in rainfall, while the stations in seven different states are showing same results as of rainfall for the number of rainy days. The state wise results indicated that the maximum percent of stations showing a significant trend in rainfall are from West Bengal state. For the number of rainy days, the highest percent of stations from the Himachal Pradesh is showing a significant trend. The station wise results of trend analysis and change of magnitude during the analysis period for rainfall and number of rainy days in a non-monsoon season is depicted in Figure 3.9. It can be observed that only 10 stations are showing a significant increasing trend, while only 5 stations are showing a significant decreasing trend in rainfall of the non-monsoon season. Four stations from West Bengal, two stations from Gujarat and one station each from Bihar and Jammu and Kashmir states are showing the significant increasing trend in rainfall. Two stations from Madhya Pradesh and one station from each West Bengal and Rajasthan are indicating a significant decreasing trend in rainfall.

The results of trend analysis of the number of rainy days for the non-monsoon season show only 12 stations with significant increasing trend and only 10 stations with significant decreasing trend. Most of the stations with significant decreasing trend are from the Madhya Pradesh and Rajasthan. For the number of rainy days, 10 stations are showing a significant increasing trend from northern and eastern India. Most parts of the study area experience an increase up to 100 mm, while some parts of northern, western and central India show a decrease up to 100 mm of rainfall in non-monsoon season during the analysis period. An increase or decrease of rainfall more than 100 mm is also observed for some other parts of the study area. For the number of rainy days in the non-monsoon season, an increase of up to 5 days is observed for the most part of the eastern and western India with some parts of northern and central India. A decrease of up to 5 rainy days is also observed over most part of the study area. The parts of study area showing increasing rainfall will be benefited in the non-monsoon season. However, the areas showing decreasing non-monsoon rainfall are likely to face water shortage during the non-monsoon season, and this problem will increase further for those regions.

The trend analysis results of station rainfall from different states show that only 9.46% of stations having a significant trend in annual maximum rainfall over the study area. No stations from eight different states are showing any significant trend in annual maximum rainfall. The station wise results of trend analysis and change detection in annual maximum rainfall during the 1951 to 2007 period are shown in Figure 3.10. The results show only 4 stations (from the remaining seven states) with the significant increasing trend and 10 stations with the significant decreasing trend over the study area. Most of the eastern India, Chattisgarh and Gujarat states are subjected to an increase of 0 to 50 mm annual maximum rainfall. Very few parts of other states are subjected to an increase of annual maximum rainfall of 0 to 50 mm. Most parts of northern India, Rajasthan, Madhya Pradesh and Sikkim states are subjected to a decrease of up to 50 mm annual maximum rainfall. An increase or decrease of more than 50 mm annual maximum rainfall is also observed in very small parts of the study area. The intensity of rainfall over the eastern India is already very high, and the increasing intensity may worsen the situation. Also, the increase of annual maximum rainfall intensity may increase the occurrence of flash flood like situation over most parts of the study area.

3.5.4 Association of Climate Change and Climate Variability to Rainfall

The relationship between rainfall and climate change is not much discussed in the Indian context. However, globally the relationship between rainfall and climate change is well established (Trenberth et al., 2003; Hegerl et al., 2007; Fowler and Wilby, 2010; Westra et al., 2013). In India, only Mondal and Mujumdar (2015) used global average temperature (GAT) as a climate change indicator to see the effect of climate change on extreme rainfall. In the present analysis statistical correlation between GAT and annual, monsoon and annual maximum rainfall is established. Also, the correlation between rainfall and two climate index, i.e., NINO3.4 SST anomaly and IOD index, is analysed.

The monsoon rainfall is the main contributor of annual rainfall over India, and therefore, the annual and monsoon average value of the GAT and climate indices are correlated with the annual, monsoon and annual maximum rainfall series. For the last three decade, the positive values of GAT and IOD indices are more frequently encountered (Figure 3.11 and 3.13). However, the NINO 3.4 SST anomaly shows the almost same number of positive and negative signals over the analysis period (Figure 3.12). The significant correlation between annual rainfall with the annual and monsoon GAT, IOD and NINO SST anomaly is shown in Figure 3.14. The figure indicates that presence of significant correlation between annual rainfalls with-

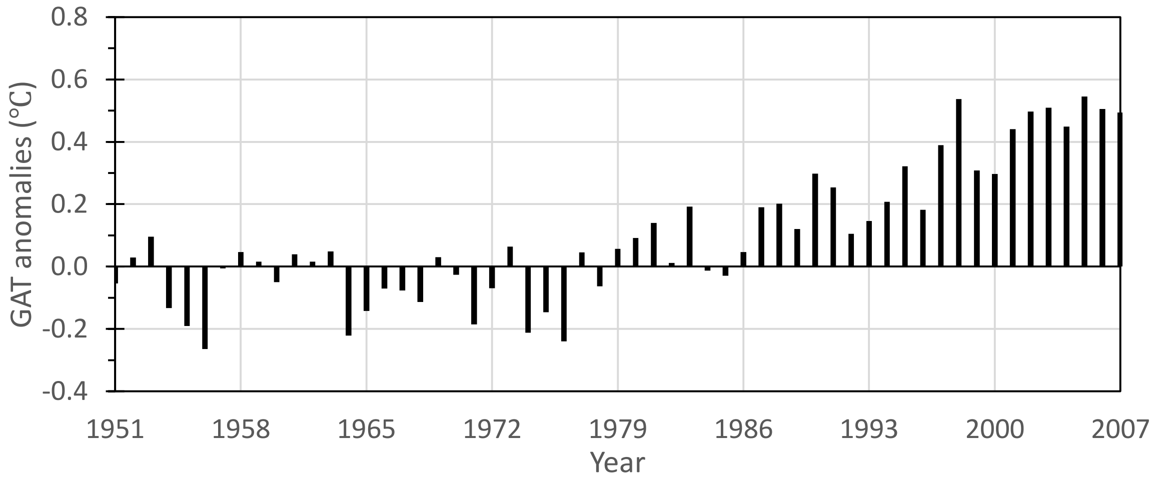

Figure 3.11. Annual HadCRUT4 land surface air global average temperature (GAT) anomaly with respect to the mean of 1961 to 1990

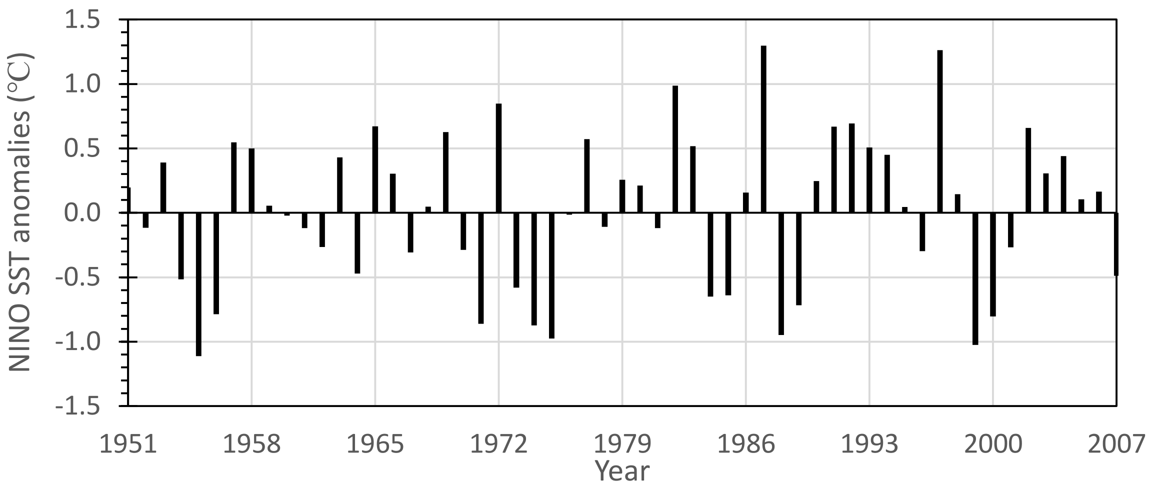

Figure 3.12. Annual Average NINO 3.4 sea surface temperature (SST) anomaly with respect to the mean of 1951 to 2000

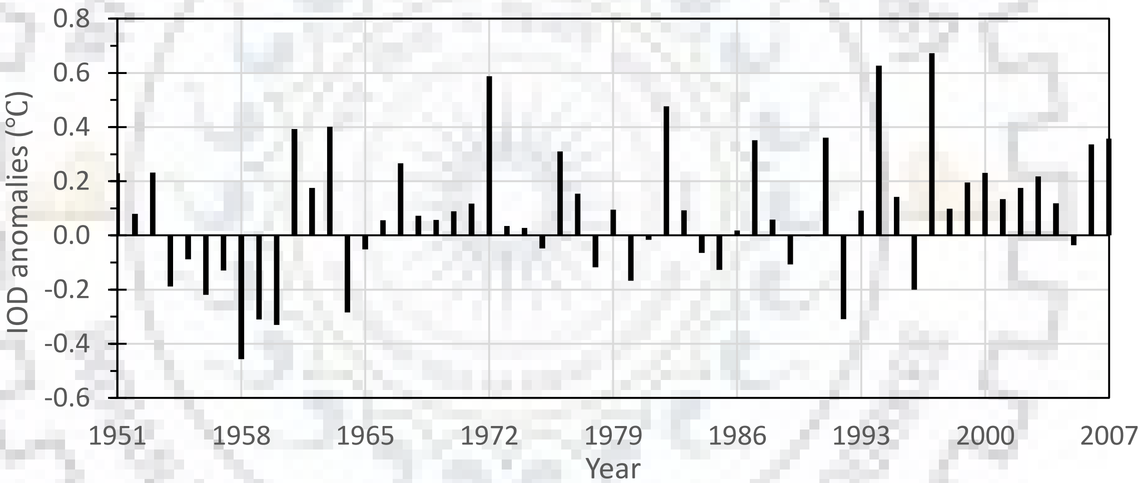

Figure 3.13. Annual Average Indian Ocean Dipole (IOD) mode index

-GAT, IOD and NINO is very less in northern India. Only, 27 stations show a significant correlation between annual rainfall and GAT, while the significant correlation between annual rainfall and NINO is observed in 16 stations over the study area. Mainly the stations of Rajasthan and Madhya Pradesh states are showing a significant correlation between annual rainfall with GAT and NINO SST anomaly. Some stations from eastern India are also showing the significant correlation between annual rainfall with GAT and NINO SST anomaly.

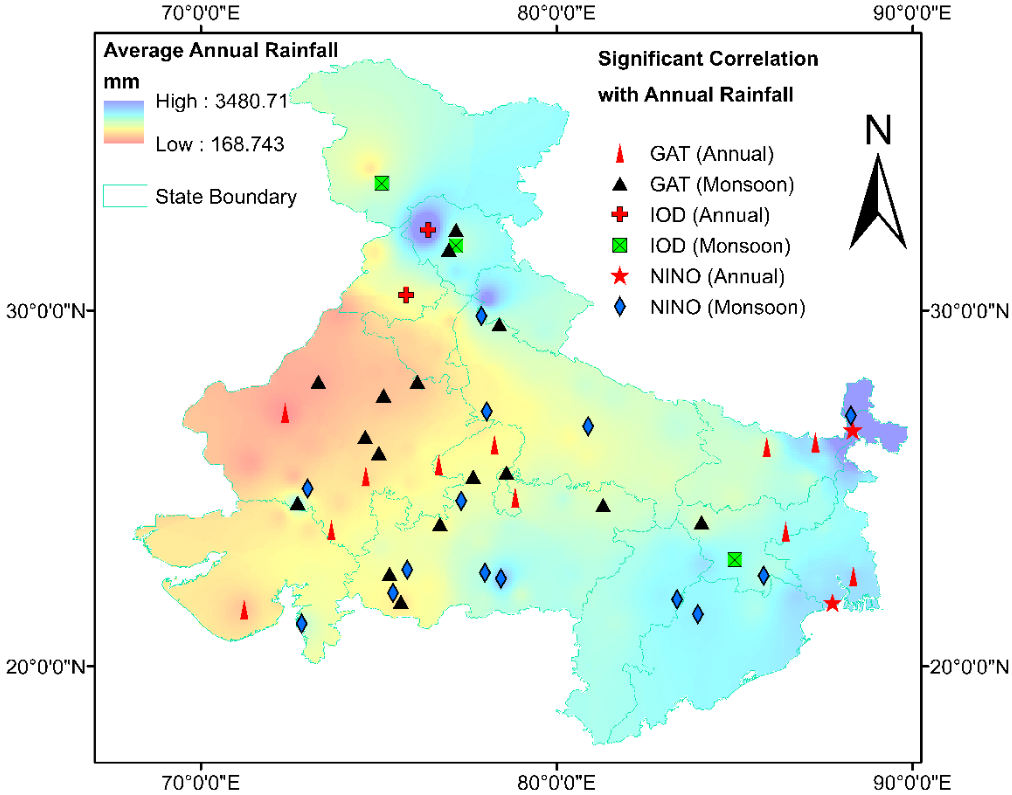

Figure 3.14. Significant correlation of annual rainfall with global average temperature (GAT), Indian Ocean Dipole (IOD) and NINO SST anomalies

The significant correlation between monsoon rainfall with the annual and monsoon GAT, IOD and NINO SST anomaly is shown in Figure 3.15. The association of monsoon rainfall with climate change is observed in 25 stations, while 23 stations show a significant positive correlation of monsoon rainfall with climate variability over the study area. Only two stations are showing a significant correlation between monsoon season rainfalls with IOD. The significant correlation between monsoon season rainfall with both the GAT and NINO SST anomaly is observed in 46 stations. Out of the 46 stations, 10 and 16 stations are from Rajasthan and Madhya Pradesh respectively. Mixed response is observed in stations of eastern and northern India.

The significant correlation between annual maximum rainfall with the annual and monsoon GAT, IOD and NINO SST anomaly is shown in Figure 3.16. Only 32 stations out of 148 stations show a significant correlation between annual maximum rainfall with the GAT, IOD and NINO SST anomalies over the study area. The significant correlation of annual maximum-

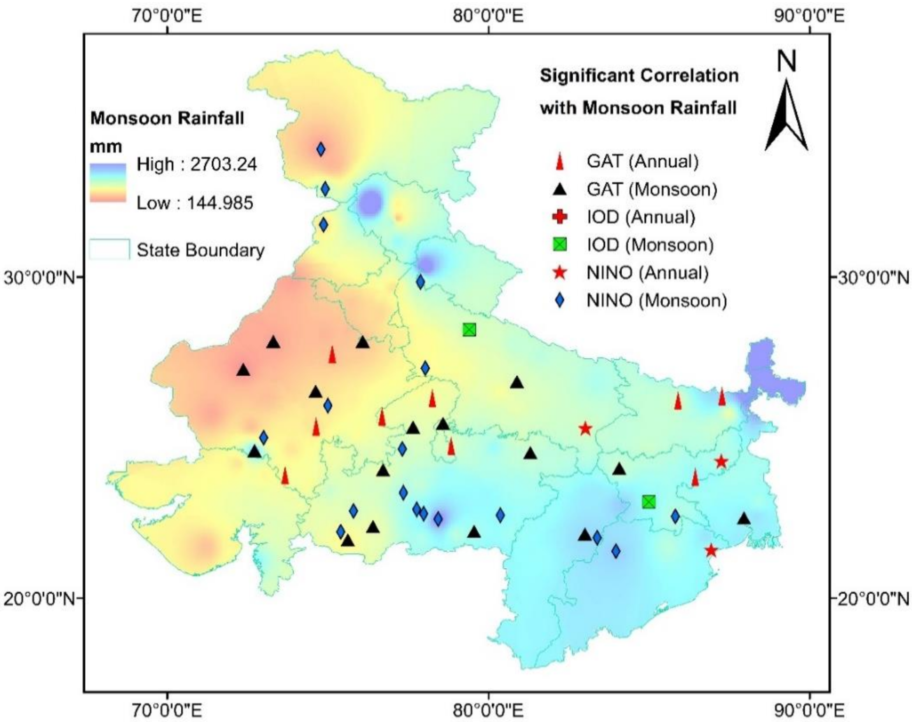

Figure 3.15. Significant correlation of monsoon rainfall with global average temperature (GAT), Indian Ocean Dipole (IOD) and NINO SST anomalies

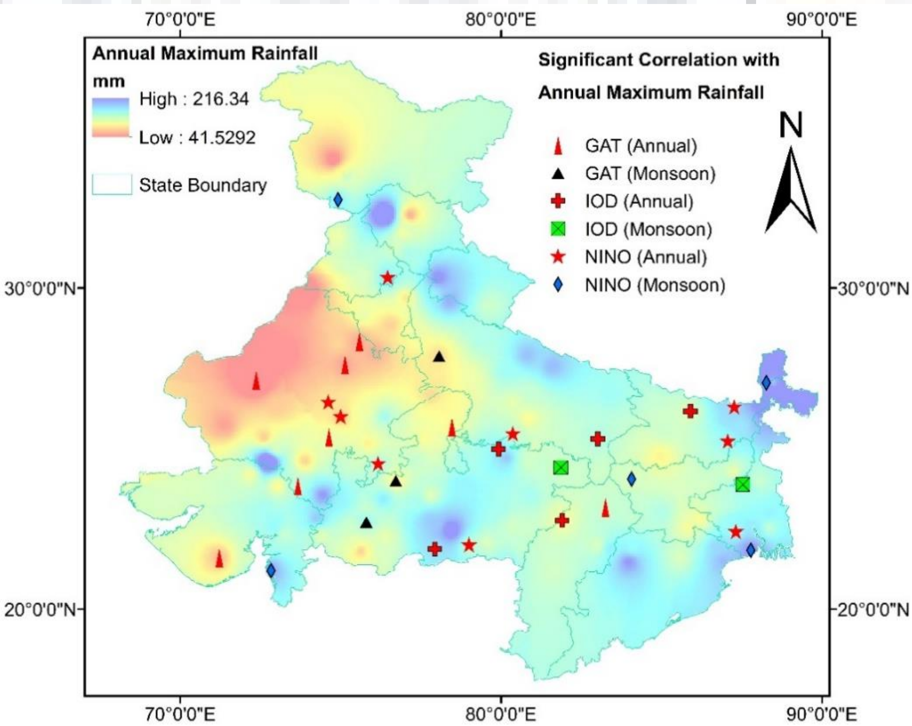

Figure 3.16. Significant correlation of annual maximum rainfall with global average temperature (GAT), Indian Ocean Dipole (IOD) and NINO SST anomalies

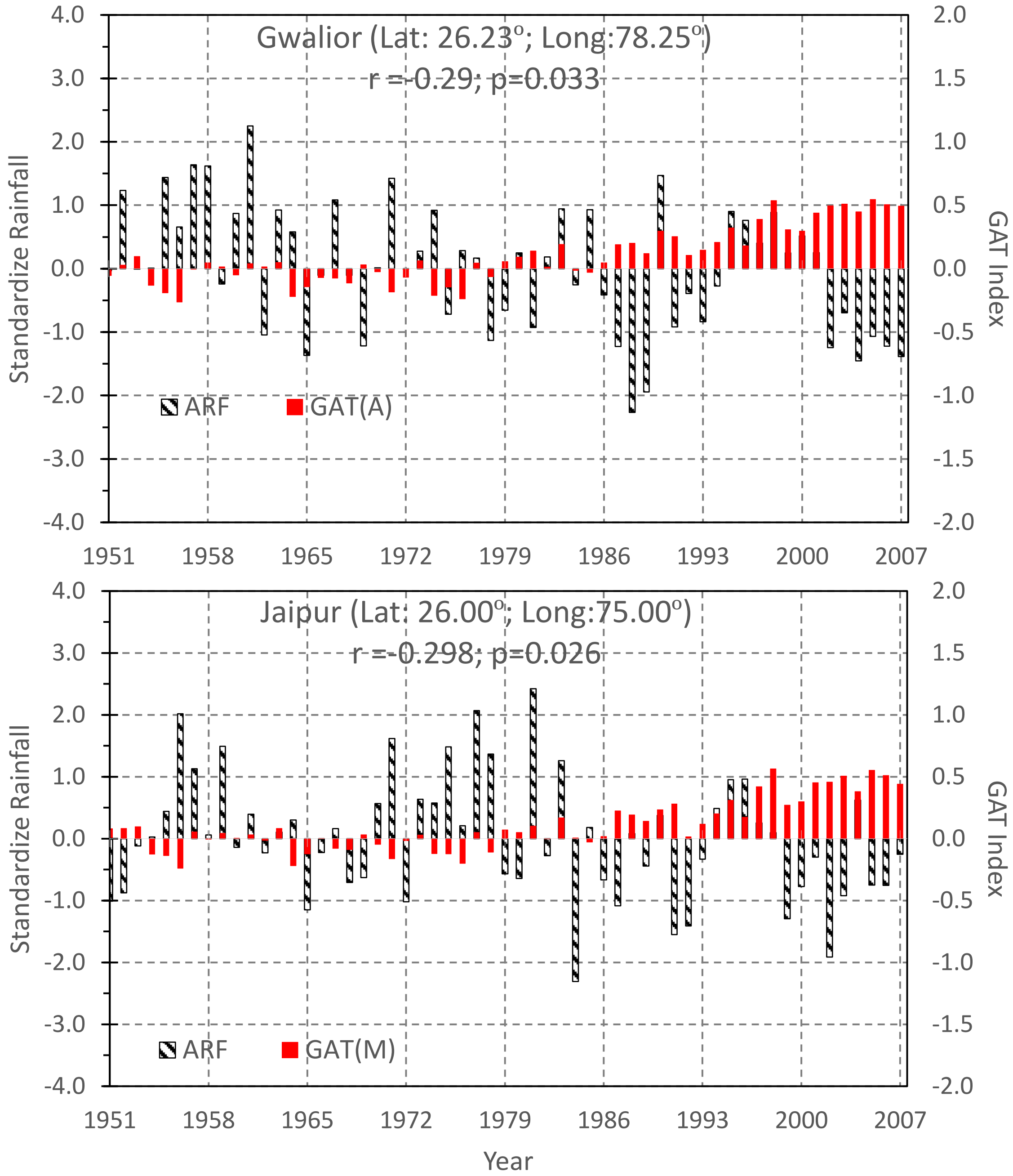

Figure 3.17. Standardised annual rainfall and global average temperature based on 1961 to 1990 mean at Gwalior and Jaipur stations. The latitude and longitude, correlation coefficient (r) and probability value (p at 5% significance level) of both the stations are given in the figure. The ARF, GAT(A) and GAT(M) represents annual rainfall series, GAT value in annual basis and GAT value in monsoon season respectively

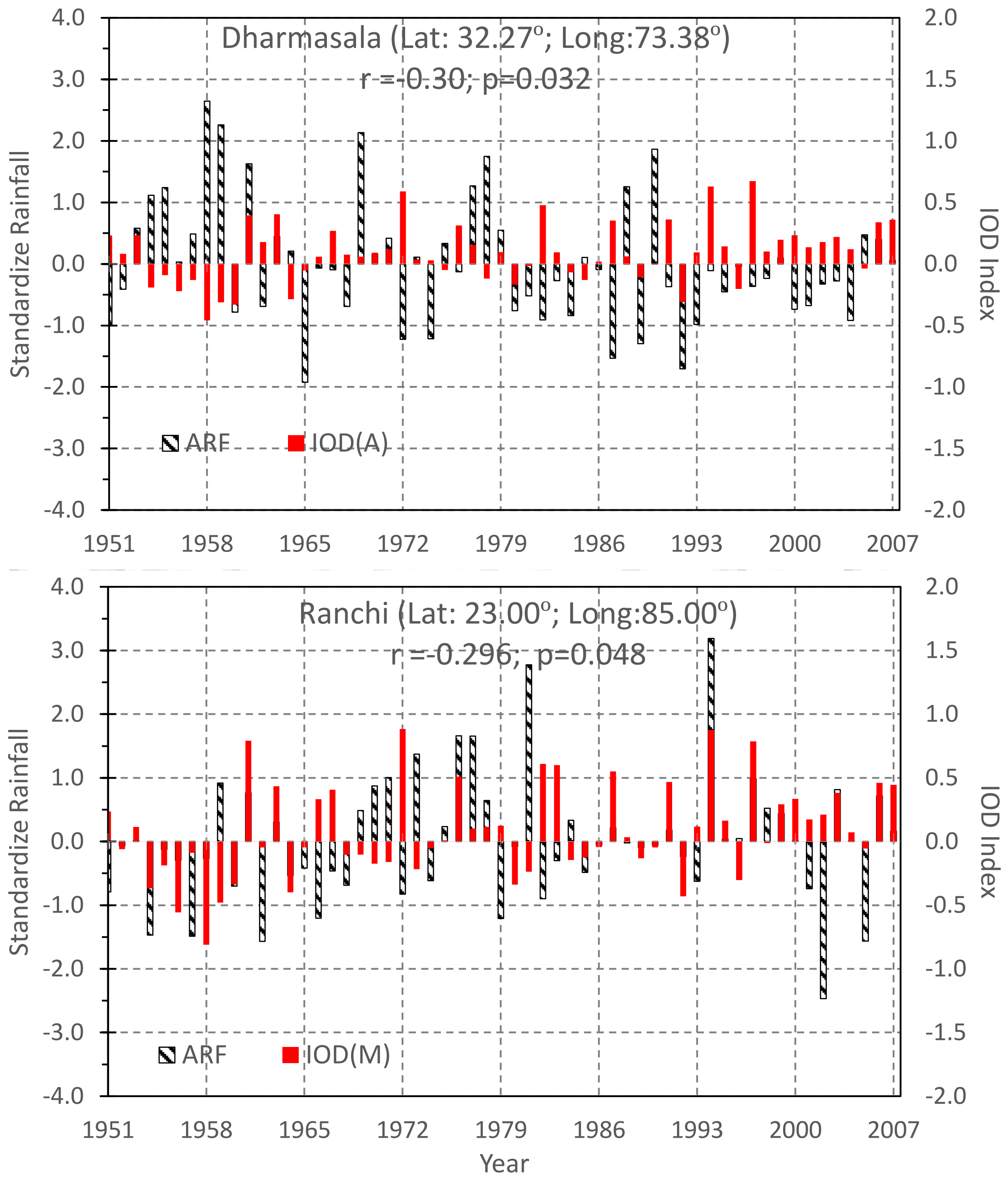

Figure 3.18. Standardised annual rainfall and Indian Ocean Dipoles (IOD) at Dharmasala and Ranchi stations. The latitude and longitude, correlation coefficient (r) and probability value (p at 5% significance level) of both the stations are given in the figure. The ARF, IOD(A) and IOD(M) represents annual rainfall series, IOD value in annual and IOD value in monsoon season respectively

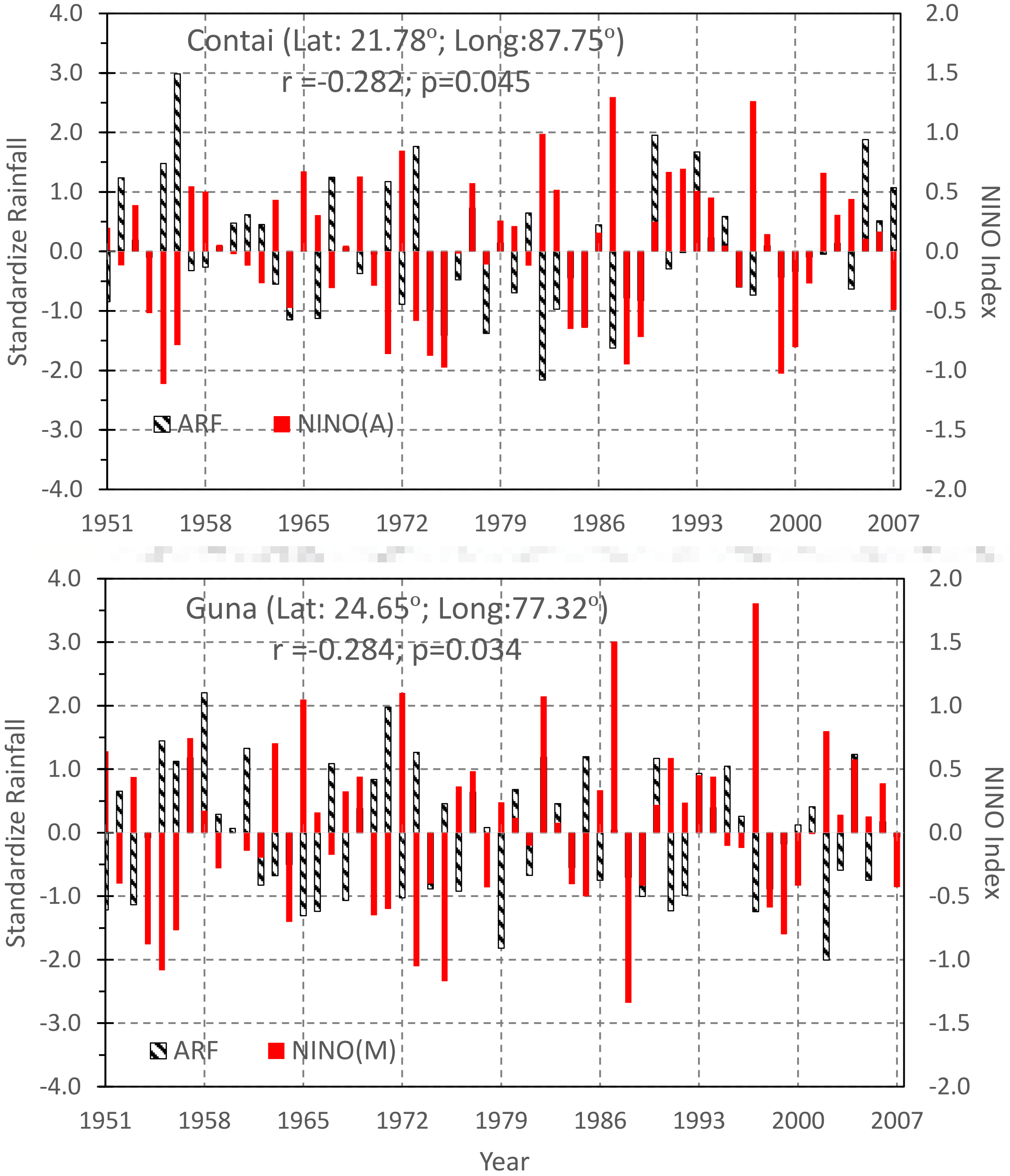

Figure 3.19. Standardised annual rainfall and NINO3.4 SST anomaly based on 1951 to 2000 mean at Contai and Guna stations. The latitude and longitude, correlation coefficient (r) and probability value (p at 5% significance level) of both the stations are given in the figure. The ARF, NINO(A) and NINO(M) represents annual rainfall series, NINO value in annual and NINOIOD value in monsoon season respectively

-rainfall to the IOD index is observed in only 6 stations. The climate change and annual maximum rainfall are closely associated in 11 stations. The annual maximum rainfall of 15 stations is significantly correlated with the NINO3.4 SST anomaly. There is no spatial pattern observed. However, the stations near to the Rajasthan and Madhya Pradesh are mainly showing a significant correlation between annual maximum rainfall with the climate change and climate variability indices. The results indicated that the climate change and climate variability is closely associated with the station rainfall over the study area.

The exact relationship between station rainfall with the GAT, IOD and NINO SST anomalies are shown in Figure 3.17 to 3.19 respectively. The figures show that for all the six different stations, annual rainfall is negatively correlated with the GAT, IOD and NINO SST anomalies. Except for some years, the extremely dry years are characterised by positive values of GAT, IOD and NINO SST anomalies. However, the extreme wet years always cannot be interpreted by negative anomalies of the GAT, IOD and NINO SSTs. Therefore, low values of correlation coefficient are obtained for wet years.

3.5.5 Effect of Data Source in Trend Analysis

Globally, a number of gridded monthly and daily rainfall data sets exist. In the present analysis, five different gridded data sets are compared. Out of five, two gridded datasets, i.e., IMD (1º by 1º) and APHRODITE (0.25º by 0.25º) are available on a daily basis and rest three gridded data sets, i.e., CRU, GPCC and UD are available on monthly basis. Therefore, the trends are compared for only annual and seasonal rainfall of the five gridded datasets.

3.5.5.1 Comparison of multi-dataset for annual rainfall

The annual average rainfall estimated over the period of 1951 to 2007 from different gridded datasets are shown in Figure 3.20 (a) to (e). All the datasets show the similar pattern with the highest annual average rainfall over the eastern India and the lowest annual average rainfall in the western India. However, there is a large difference in the range of average annual rainfall from different datasets. The maximum value of average annual rainfall is almost similar (near to 3500 mm) from three gridded data sets, i.e., APHRODITE, GPCC and IMD. However, the CRU datasets provide very less value (almost 2700 mm) from the other three datasets. The maximum value obtained from UD dataset is very high (almost 4500 mm) as compared to the other datasets. The minimum value is almost same (near to 100 mm) for APHRODITE, CRU-

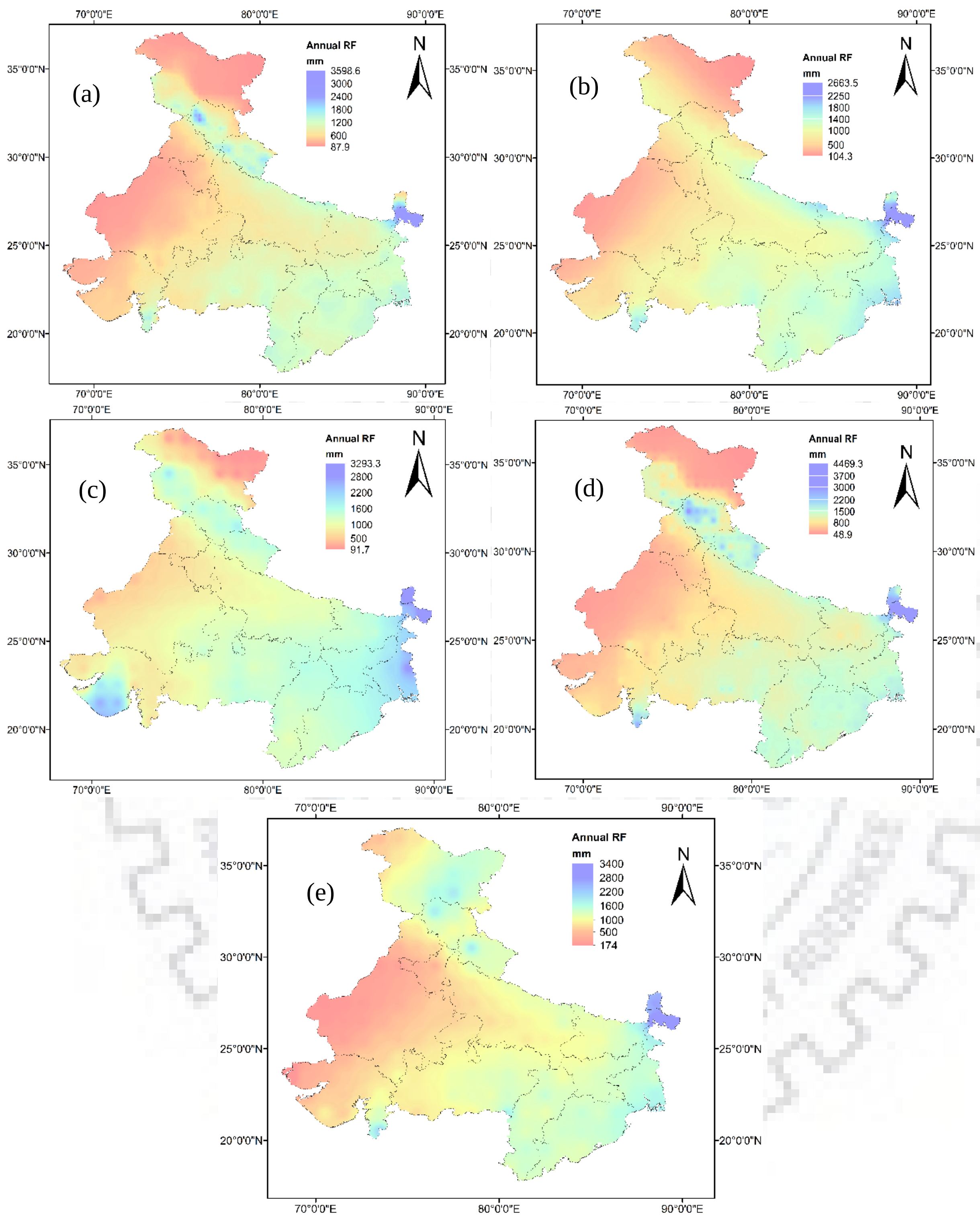

Figure 3.20. Average annual rainfall over the study area during 1951 to 2007 period from (a) APHRODITE, (b) CRU, (c) GPCC, (d) UD and (e) IMD gridded datasets

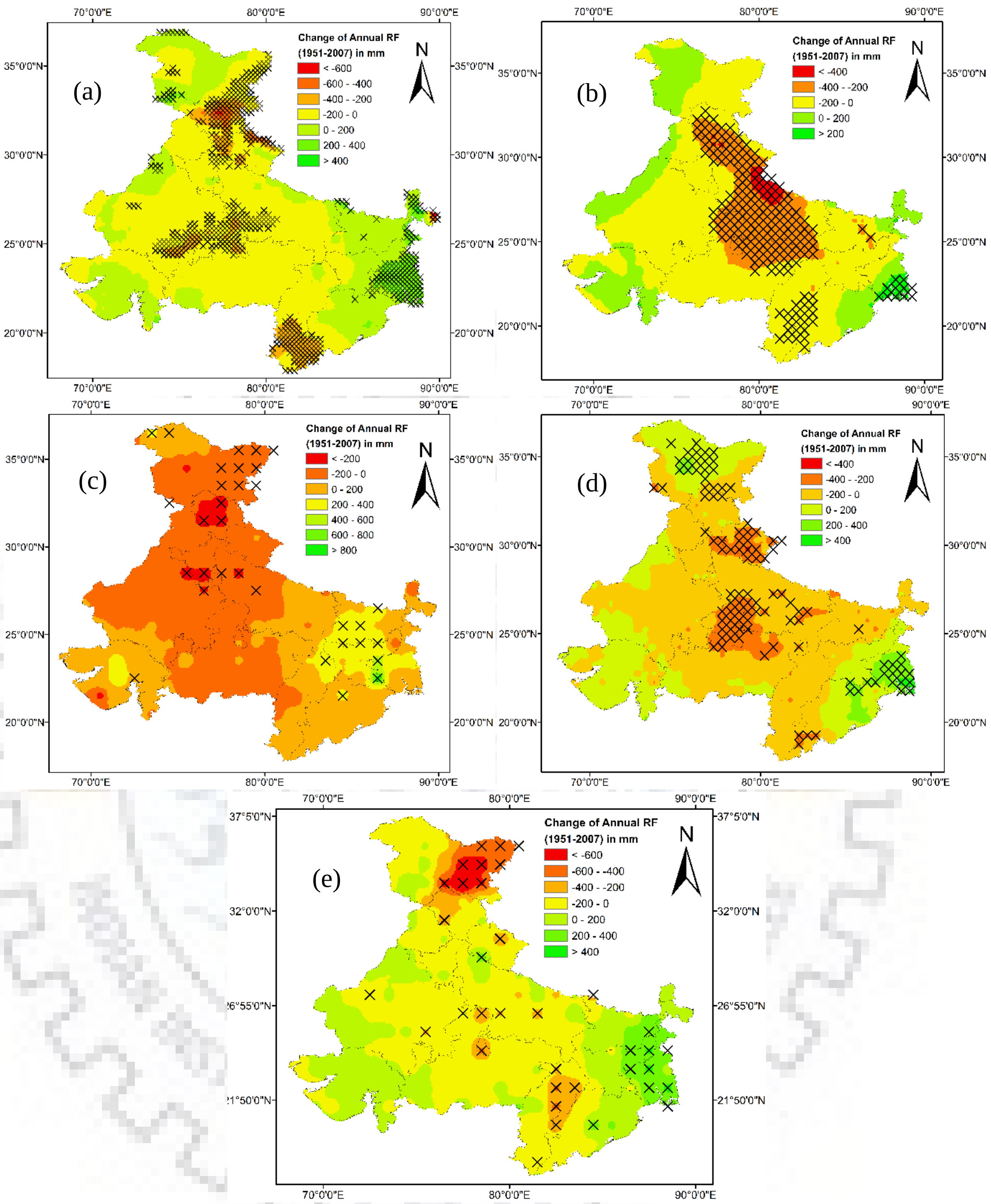

Figure 3.21. Trends in annual rainfall over the study area during 1951 to 2007 period from (a) APHRODITE, (b) CRU, (c) GPCC, (d) UD and (e) IMD gridded datasets

-and GPCC gridded datasets. The minimum value obtained from IMD dataset is very high (174 mm), while the value obtained from UD dataset is very low (49 mm). Except for IMD dataset, other four gridded rainfalls show very low average annual rainfall over the upper parts of

Jammu and Kashmir state, which is due to the non-availability of station data in this region for all four gridded datasets. The average annual rainfall from GPCC dataset in Saurashtra region shows a very high value, which may be due to low station density over the area in the dataset. However, other gridded datasets are showing lower values of average annual rainfall over the Saurashtra region.

Trends in annual rainfall during the 1951 to 2007 period from different gridded dataset are shown in Figure 3.21. The trends in annual rainfall from all the datasets are not similar. However, except GPCC dataset, all other data sets are indicating a significant increasing trend in the lower parts of West Bengal state. Mainly, the significant decreasing trends are not in a similar pattern for all the datasets. A significant decreasing trend is observed in some parts of Rajasthan state by APHRODITE dataset, which is not the case for other four datasets. The CRU dataset is not showing any significant decreasing trend in Jammu and Kashmir State. However, all other data sets are indicating a significant decreasing trend in Jammu and Kashmir State. The CRU dataset is also indicating a presence of significant decreasing trend over the entire Uttar Pradesh state, while other datasets are showing it only for very small parts of the state. Almost all the datasets are showing a similar change in annual rainfall (-200 mm to 0 mm) during the analysis period over most parts of the study area. A similar type of increase of annual rainfall (0 to 200 mm) is also observed for all the dataset, and the spatial pattern of increase is also same. However, the range of increase or decrease in annual rainfall is not similar for all the datasets. The APHRODITE and IMD datasets are showing an almost similar range of increase and decrease for annual rainfall, while the CRU and UD datasets are also showing a similar range of increase and decrease for annual rainfall. The maximum increase is observed more than 400 mm of annual rainfall from APHRODITE, IMD, and UD datasets, while CRU and GPCC dataset showing an increase of more than 200 mm and 800 mm respectively. The maximum decrease is observed lesser than -600 mm from both APHRODITE and IMD datasets, while it is lesser than -400 mm from both CRU and UD datasets. The GPCC data set only shows less than of -200 mm decrease in annual rainfall during the analysis period.

3.5.5.2 Comparison of multi-dataset for monsoon rainfall

The average rainfall in monsoon season over the study area is estimated for the 1951 to 2007 period from different datasets. The same is shown in Figure 3.22 (a) to (e). The range of average monsoon rainfall is not same for all the datasets. The spatial pattern is similar as found for the annual rainfall and also among the datasets. The maximum and minimum value of almost 3500 mm and 25 mm rainfall are obtained from UD datasets. The maximum value is nearly similar (close to 2600 mm) for APHRODITE, GPCC and IMD gridded datasets. The CRU dataset provides the lesser value of the maximum (almost 2100 mm). The minimum value of the average monsoon rainfall is also not similar for the datasets. The highest value of the minimum average monsoon rainfall among the five datasets is 152 mm and is obtained from IMD dataset. The minimum value of more than 100 mm is also obtained from CRU dataset. Other three datasets are providing the very less minimum value of the average rainfall, and this may be due to lesser density of rainfall stations in the gridded datasets. The GPCC data provides higher values for the Saurashtra region of Gujarat state, which may also be due to lower station density in GPCC dataset over the area. Except for the IMD dataset, all the four datasets interpreted very less average monsoon rainfall over the Jammu and Kashmir state, which is not the actual scenario.

Trends and change of magnitude during the 1951 to 2007 period over the study area is estimated from different gridded rainfall datasets in monsoon season and are shown in Figure 3.23. The spatial pattern of the estimated significant trend is not similar for different datasets. In Jammu and Kashmir State, the IMD and GPCC datasets show significant decreasing trends, while other datasets are not showing any significant trend. A significant increasing trend is obtained in lower parts of the West Bengal state from APHRODITE, UD and IMD datasets. However, other two datasets are not showing any significant trend over the region. The IMD, GPCC and UD datasets are showing a very less significant decreasing trend in the Rajasthan and Uttar Pradesh states. The results are not same for other two datasets. The APHRODITE dataset is indicating a more significant decreasing trend in Rajasthan state and less in Uttar Pradesh state, while the CRU dataset provides more significant decreasing trend in Uttar Pradesh state and no significant trend in Rajasthan state. All the four datasets show a significant decreasing trend in the Uttarakhand and Himachal Pradesh states, except GPCC dataset, which provides significant decreasing trend over only the Himachal Pradesh state. A significant decreasing trend is also found in the lower parts of Orissa and Chhattisgarh states from APHRODITE, CRU and UD datasets, while other two datasets are not showing any significant trend over the region.

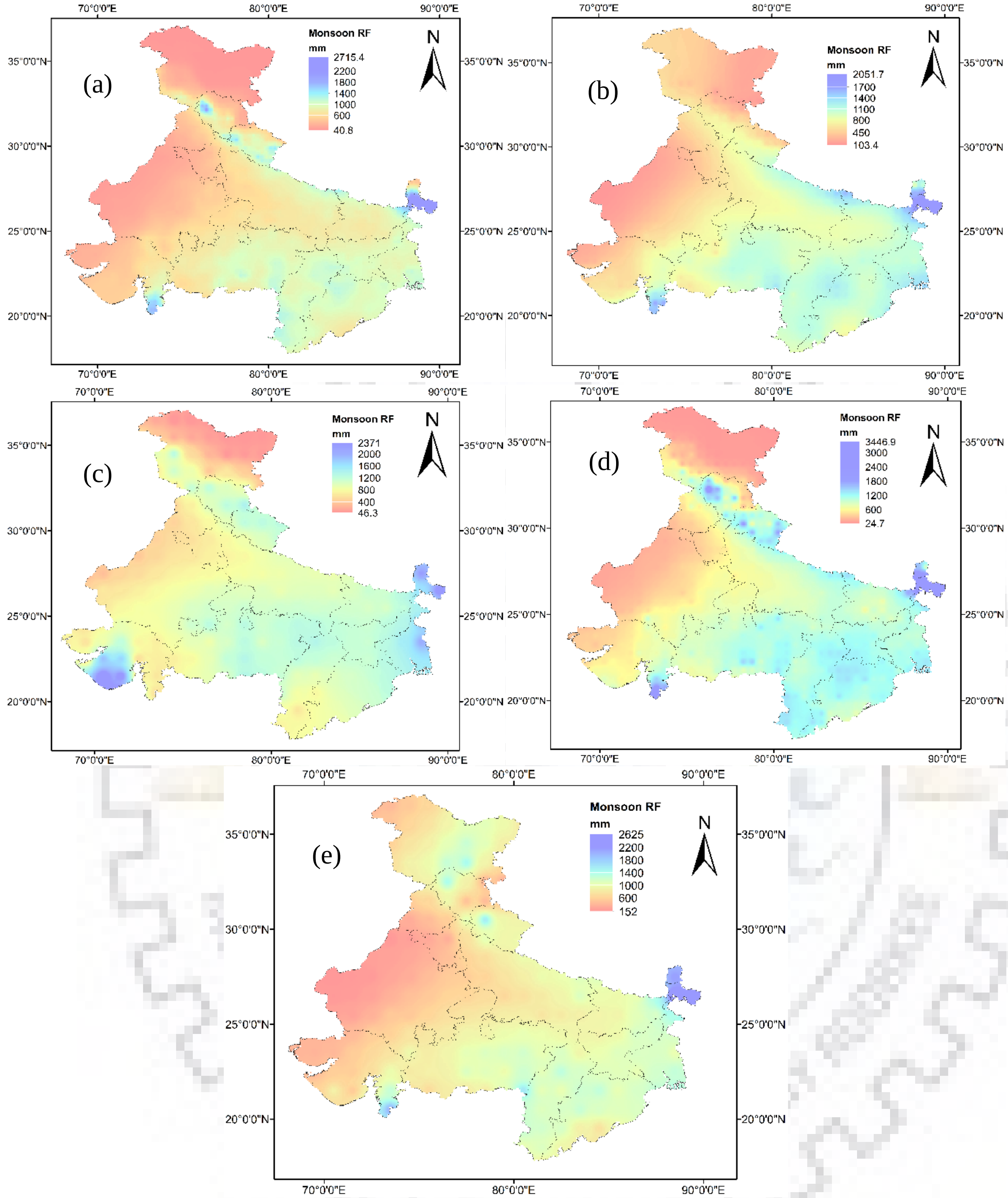

Figure 3.22. Average rainfall in monsoon season over the study area during 1951 to 2007 period from (a) APHRODITE, (b) CRU, (c) GPCC, (d) UD and (e) IMD gridded datasets

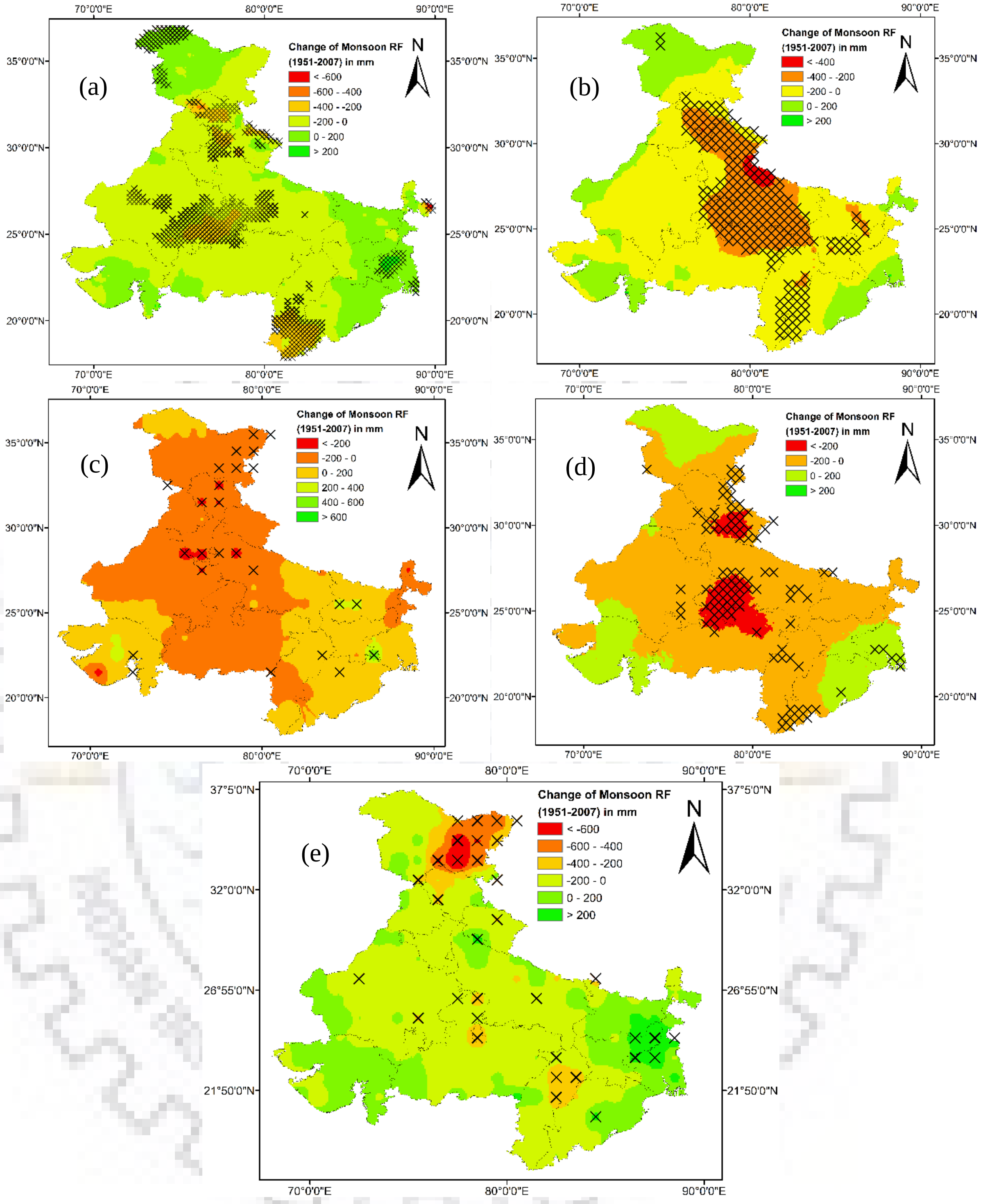

Figure 3.23. Trends in monsoon rainfall over the study area during 1951 to 2007 period from (a) APHRODITE, (b) CRU, (c) GPCC, (d) UD and (e) IMD gridded datasets

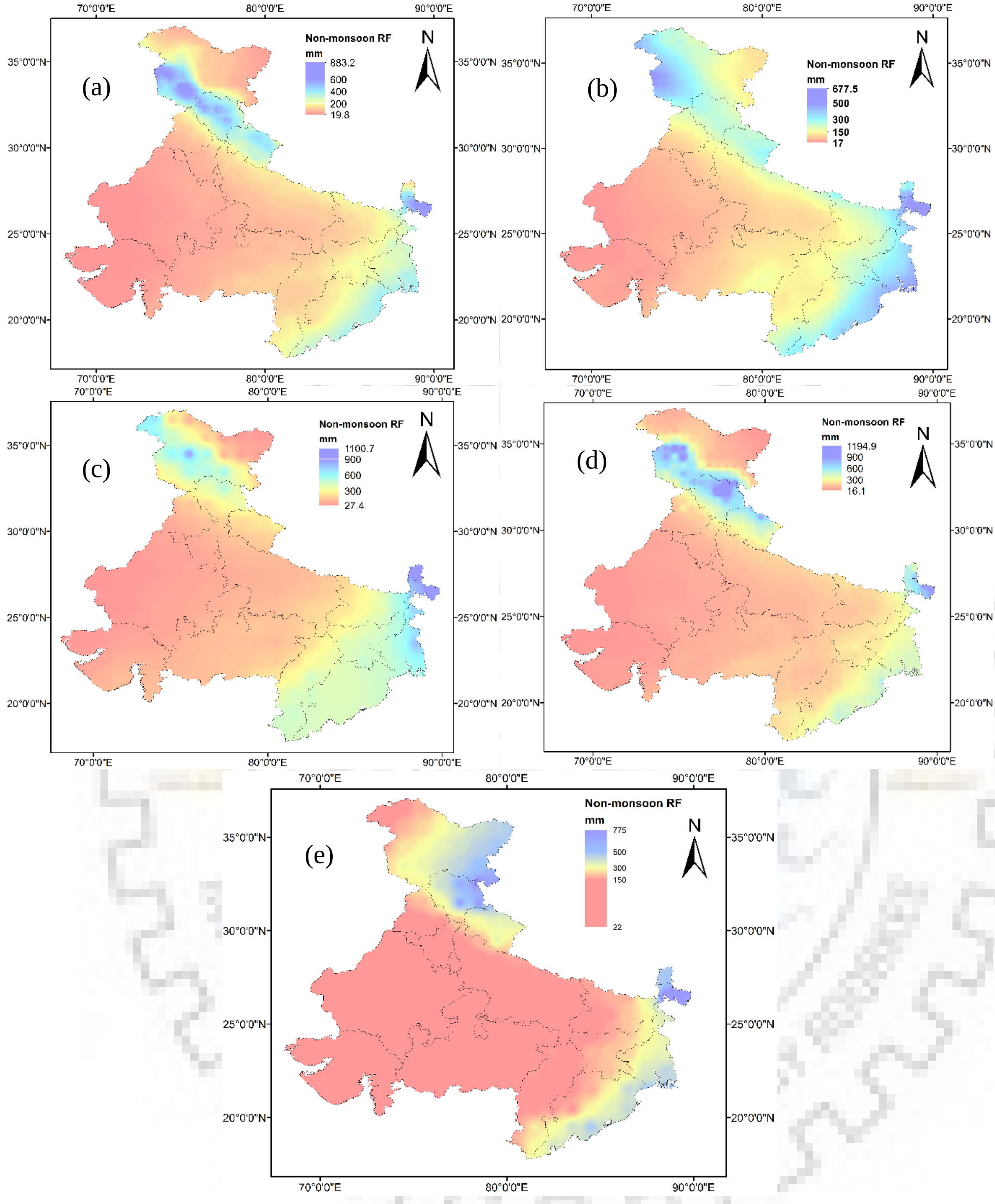

Figure 3.24. Average rainfall in non-monsoon season over the study area during 1951 to 2007 period from (a) APHRODITE, (b) CRU, (c) GPCC, (d) UD and (e) IMD gridded datasets

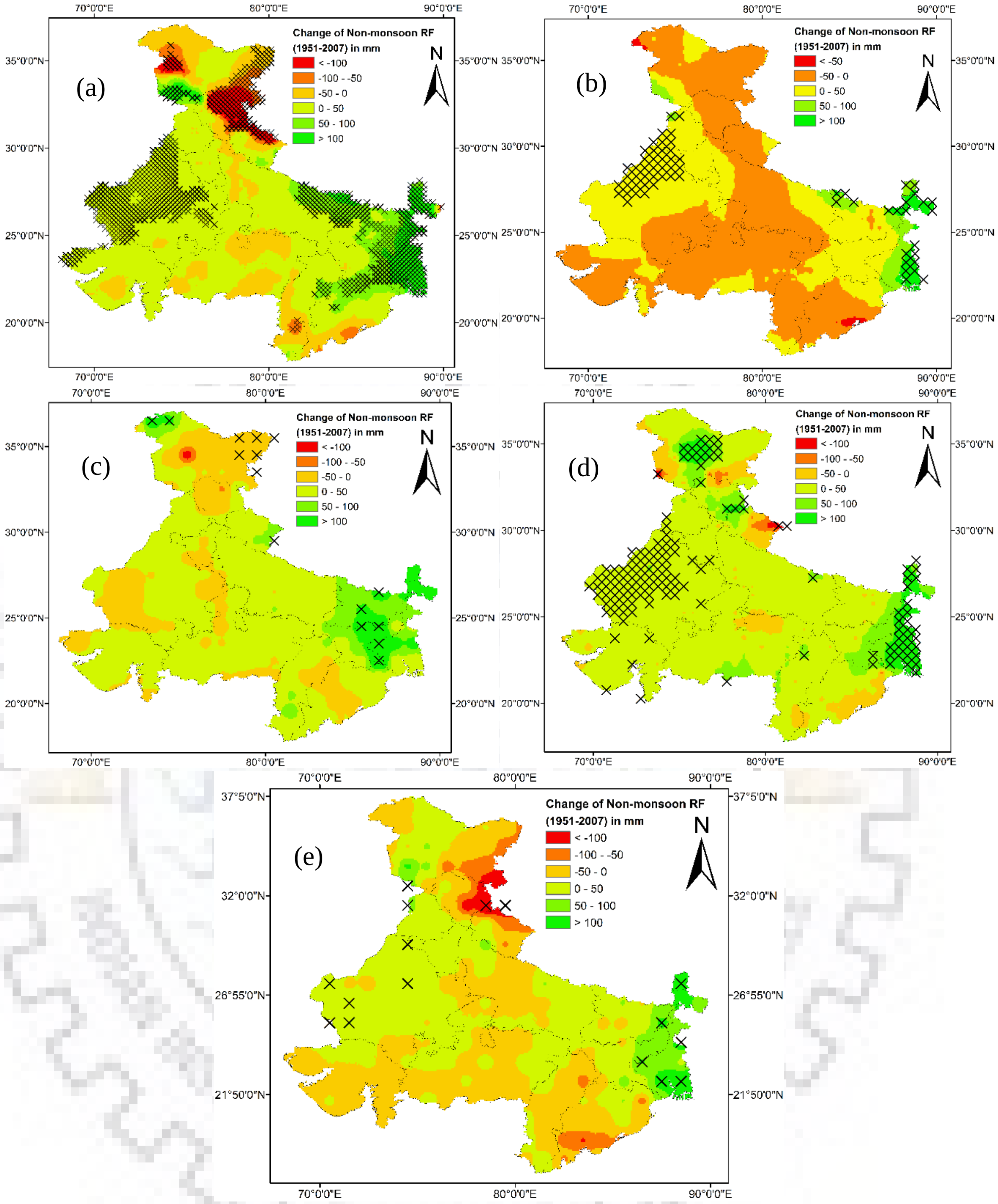

Figure 3.25. Trends in non-monsoon rainfall over the study area during 1951 to 2007 period from (a) APHRODITE, (b) CRU, (c) GPCC, (d) UD and (e) IMD gridded datasets

The estimation of change in magnitude of monsoon rainfall during the analysis period is almost similar to most parts of the study area for all the gridded datasets. However, some regional differences are observed from different datasets. Most parts of the study area show decreasing monsoon rainfall of 0 to 200 mm during 1951 to 2000 period by all the datasets. In addition, an increase of 0 to 200 mm or more than that is obtained by all the datasets over most parts of the eastern region. Though the increase or decrease in monsoon rainfall is similar for most parts of the study area by all the datasets, the range of change in magnitude of monsoon rainfall is obtained different from different datasets. The highest decrease of more than 600 mm rainfall is obtained from both the APHRODITE and IMD datasets, while the GPCC dataset finds the largest increase of more than 600 mm rainfall. Except for GPCC, all the other datasets are showing a maximum increase of only more than 200 mm rainfall. The maximum decrease or increase in monsoon rainfall though observed only for very small patches over the study area.

3.5.5.3 Comparison of multi-dataset for non-monsoon rainfall

The average rainfall in non-monsoon season is estimated for the 1951 to 2007 period from different datasets over the study area and is shown in Figure 3.24. Following the similar pattern of annual and monsoon rainfall, the eastern India is getting the more rainfall during the non-monsoon season. For the most part of the study area, the spatial pattern of average non-monsoon rainfall is similar for all the gridded datasets. The only difference is observed in the upper parts of the Jammu and Kashmir state, where the east parts have high average rainfall by IMD dataset. Other four datasets show high average rainfall in the west part of the Jammu and Kashmir state.

Results of trend analysis and estimation of change in magnitude of non-monsoon rainfall during 1951 to 2007 period from different gridded datasets are depicted in Figure 3.25 (a) to (e). A significant increasing trend is observed over the eastern and western India from all the gridded datasets. However, no similarity is observed for significant decreasing trend obtained from all the gridded datasets. The IMD and APHRODITE datasets are showing a significant decreasing trend in Himachal Pradesh and Uttarakhand states, while UD data shows a significant decreasing trend in only Uttarakhand state and other two datasets are not showing any significant trend. The significant decreasing trend is also observed in some parts of Jammu and Kashmir State by only GPCC and APHRODITE datasets. The GPCC dataset is also not showing any significant increasing trend over the Rajasthan state, while other datasets have shown a significant increasing trend in the region.

All the datasets observed an increase of 0 to 50 mm of non-monsoon rainfall over most parts of the eastern India. All the datasets show more than 50 mm rainfall increase during the 1951 to 2007 period over the West Bengal state. Most parts of the study area also observed an increase of 0 to 50 mm rainfall by all the datasets, except CRU and IMD datasets, which shows almost same parts of the study area is also observed a decrease of up to 50 mm of non-monsoon rainfall. Other three datasets are showing up to 50 mm decrease in rainfall over a very small portion of the study area. However, a decrease more than 100 mm rainfall is observed by the APHRODITE and IMD datasets for some parts of Himachal Pradesh and Jammu and Kashmir states. All the annual and seasonal results show some dissimilarity for different datasets. However, for most of the cases, the CRU and GPCC datasets are not providing results similar to the other datasets for trend analysis. These results indicated that a conclusion drawn from the rainfall trend analysis results might be biased if only one gridded dataset is used.

3.6 CONCLUSIONS

Analysis of rainfall and number of rainy days on annual and seasonal basis in recent climatic conditions is crucial to understand the climate-induced changes and to suggest proper water resources planning and management strategies for the future. Trends in rainfall and number of rainy days on annual and seasonal basis from 148 station dataset over parts of India are evaluated. The correlation between annual and monsoon rainfall and annual maximum rainfall with the GAT (to see the effect of climate change), IOD and NINO SST anomalies are examined to see the interrelationship of these variables with rainfall. Furthermore, the effect of gridded data source over the trend analysis is also investigated using five different resolution datasets.

The results of this analysis show that the most part of the study area exhibit a decrease in rainfall for annual and monsoon seasons during the analysis period. A significant decreasing trend in rainfall and number of rainy days is found mainly in the stations of Madhya Pradesh and Rajasthan on annual and monsoon season basis. An increasing trend in monsoon and annual rainfall was mainly found in the lower part of West Bengal. Few stations exhibit a significant trend in rainfall and number of rainy days for the non-monsoon season over the study area. The annual and seasonal number of rainy days have also decreased. The results of decreasing trend are in good agreement with most of the researcher's findings (Pattanaik, 2007; Ghosh et al., 2009; Lacombe and McCartney, 2013; Mondal et al., 2015) over the study area.

Almost one-third station rainfalls are significantly correlated with the climate change and climate variability indices over the study area. The significant correlation between rainfall series and GAT are found for a maximum number of stations among the other variables for the study area. However, the correlation between rainfall and IOD is insignificant. It confirms the finding of Saji et al. (1999), that the relationship between IOD and the variability of Indian summer monsoon rainfall is not clear. These results also show that the global climate change is one of the major factor for the change of Indian summer monsoon rainfall. The future rainfall can be predicted using the results of the stations with good correlations.

Trends in multi-datasets of gridded rainfall almost follow a similar pattern for most part of the study area. However, for some parts, the results are also different for these gridded datasets. The results of multi-datasets of gridded rainfall can be tabulated for a particular region and the interferences can be drawn based on results shown by majority of the gridded datasets. Further study may investigate the effect of multi-gridded datasets for more climate change concerns using the extreme indices, like, maximum 1-day rainfall, the number of consecutive wet days, rainfall over a threshold value, etc.

The findings of this study have multitudinous implication over Indian water resources. Due to the decrease of annual rainfall and number of rainy days over most part of study area, all the states will require more research oriented management strategies for the available water resources. The results indicated that most of the states would have more pressure on their water resources due to the decreasing rainfall. Therefore, these results will be very useful for the proper planning and management of water resources and found allocation at state level and country level.

CHAPTER 4
NON-STATIONARY FREQUENCY ANALYSIS OF EXTREME RAINFALL EVENTS ACROSS INDIA

4.1 GENERAL

The rapid changes in the climatic conditions influence the overall environment as well as the daily activities of human life (Kurane, 2010). Intergovernmental Panel on Climate Change (IPCC) stated, "Climate change, whether driven by natural or human forcing, can lead to changes in the likelihood of the occurrence or strength of extreme weather and climate events or both" " (Climate Change 2013: The Physical Science Basis, IPCC). In recent times, researchers have found that a change in the characteristics of the hydrological cycle is due to global warming or increasing temperature (Vinvent et al., 2007; Zhang et al., 2013). These changes in extreme events may induce non-stationarity in the process. However, the classical frequency analysis is based on the assumptions of stationarity and independence. In a changing climate, the stationarity assumption may not provide good results, and more advanced methods are required for the non-stationary processes. Furthermore, the accuracy of hydrological analysis and design procedure is severely affected by non-stationarity in the observed data set (Douglas et al., 2000). In recent past, a number of researchers, worldwide, have worked on the methods of carrying out frequency analysis under non-stationary condition.

This chapter addresses the issue of non-stationarity using station rainfall data covering most parts of India. The influence of climate indices (i.e. NINO3.4 SST anomaly and Indian Ocean Dipole mode index), global warming (in the form of Global Average Temperature), and local temperature over non-stationary annual maximum rainfall series has also been investigated. The non-stationary frequency analysis of extreme rainfall is carried out using Generalized Additive Models for Location, Scale, and Shape parameters (GAMLSS) model.

4.2 STATIONARITY AND NON-STATIONARITY

In order to carry out non-stationary frequency analysis, one should have clear understanding of stationarity and its counterpart. Stationarity is often misunderstood and wrongly related with the property of observed dataset. Stationarity is not, infact, related to the observed data. Rather, it is a property of an underlying stochastic process. Kendall et al. (1983) define it as: for a given observed data $t_1, \dots, t_l$, the joint statistical distribution of $X(t_1), \dots, X(t_\ell)$ is the same as the joint statistical distribution of $(Xt_{1+\tau}), \dots, X(t_{\ell+\tau})$ for all ℓ and τ . This is a very strict definition of stationary, i.e., all moments (means, variances, etc.) of all degrees of a process are same irrespective of their positions. However, a weaker definition of stationary i.e., the second order or weak stationary is mostly used. In a weak stationary series, mean and covariance are constant, i.e., identical across time. In general, the researchers have used second order stationarity for real world practices.

Non-stationary can simply be defined as a process that is not stationary, where the distribution parameters are not constant and vary with time. All the natural systems are necessarily non-stationary. WMO (Lins, 2012) note on stationarity and non-stationarity ends up with the following statement:

*"**Although it is important to recognize that nonstationarity exists as a characteristic of the natural world, it is also important to acknowledge that all of the variations that have been recorded in the observed and historical records of hydroclimatic processes can be represented with stationary stochastic models. In conclusion, there are two critical points to remember from this note:***

- ***Stationarity ≠ static***
- ***Nonstationarity ≠ change (or trend)**"*

Therefore, the natural processes should be analysed by the best model, which can be stationary or non-stationary.

4.3 FREQUENCY ANALYSIS IN THE CONTEXT OF NON-STATIONARITY

The traditional flood frequency analysis is based on the assumption of stationarity and independence. However, Milly et al. (2008, 2015) argued that stationarity is no more valid for hydrological extremes due to climate change and anthropogenic changes. Under non-stationarity, the sample parameters may not be representative of population parameters. This necessitates the need of consideration of non-stationarity in flood frequency analysis. Moreover, several studies have been conducted in the past for analysing the changing patterns of extreme rainfall in India. Almost all the studies have indicated significant changes, mostly on rising side (Rakhecha and Somanthe, 1994; Joshi and Rajeevan, 2006; Goswami et al., 2006;

Rajeevan et al., 2008; Pattanaik and Rajeevan, 2010; Kishtawal et al., 2010; Ghosh et al., 2011). Goswami et al. (2006) reported a significant increasing trend in the frequency and the magnitude of extreme rain events over central India. Most of the previous studies have reported that the increase of heavy rainfall events over India is due to the urbanisation (Ghosh et al., 2011; Kishtawal et al., 2010; Vittal et al., 2013; Shastri et al., 2014). However, all the previous studies have indicated a change in extreme rainfall after 1950 and reported some possible reasons such as climate change, urbanisation, changes in population density, etc. These changes may alter the hydrological processes and induce non-stationarity in extreme rainfall events (Singh et al., 2016). Therefore, in this section a detailed review of significant contributions made by various researchers in the field of non-stationary frequency analysis of extreme rainfall and flood events have been presented.

In the previous studies, different methods have been used by researchers for carrying out the frequency analysis of non-stationary data sets (Salas et al., 2012). Most of the researchers have used the frequency analysis under non-stationary conditions considering the trend component of time series in the past (Olsen et al., 1998; Strupczewski et al., 2001; He et al., 2006; Leclerc and Ouarda, 2007; Delgado et al., 2010; Cheng et al., 2014). In recent times, a number of researchers have incorporated different covariates (linear or non-linear dependence) as an external predictor of the frequency analysis model (Katz et al., 2002; Gilroy and McCuen, 2012; López and Francés, 2013; Tramblay et al., 2013; Mondal and Mujumdar, 2015; Zhang et al., 2015). It has been established that the use of external covariates such as climate indices over time provides a better model fit. Khaliq et al. (2006) provide a brief review of non-stationary frequency analysis methods prior to 2006.

Olsen et al. (1998) developed a non-stationary model using extreme value distribution for estimating the probability of flooding in the Mississippi river basin. As per the authors, the probability of failure can be modelled by Extreme Value Type I distribution function in the presence of a known trend in the variable.

Strupczewski et al. (2001) studied at-site non-stationary flood frequency analysis using the maximum likelihood method. They used both the annual maximum and partial duration series with the presence of trend. They found that the hydraulic design under non-stationarity was a direct result of environmental change. They concluded that the results of GCMs at the present stage of development might not be the climate change scenarios.

Strupczewski et al. (2001) carried out non-stationary at-site flood frequency analysis for 39 flow series of Polish rivers. They reported that more than 50% flow series were non-stationary. Lognormal and Pearson type III distributions were found to be the best fitting distributions for most of the flow series.

Cunderlink and Burn (2003) applied second order non-stationary pooled flood frequency analysis to the homogeneous catchments of British Columbia Mountains Climate region. They generated 50 years of data using GEV distribution assuming different trend scenarios. Bias of 7% in location parameter and 15% in scale parameter of the distribution were found. It was concluded that the presence of non-stationarity in a flood series might seriously bias the quantile estimation.

Kiem et al. (2003) studied multi-decadal variability of flood risk using the inter-decadal Pacific Oscillation (IPO) index. They found that the flood risk was elevated due to the IPO modulation of ENSO events. The flood risk on multi-decadal timescales was both reducing and elevating by the dual modulation of ENSO processes. They finally concluded that the natural climate variability should include for the quantification of hydrological variability.

He et al. (2006) carried out non-stationary flood frequency analysis of 10 gauging stations of Southern Germany using Gumbel and LP3 distributions. The consideration of non-stationarity in flood frequency analysis is not only necessary but also is a feasible option. However, the non-stationarity should only be included in design practices after the assessment of uncertainty.

El Adlouni et al. (2007) developed generalized maximum likelihood estimation method (GML) for the nonstationary generalized extreme value model. They have used the developed technique for non-stationary frequency analysis of annual maximum precipitation at the Randsburg station in California. Southern Index Oscillation was used as covariate for the non-stationary model. The recommended that the nonstationary GEV model could be used as an efficient tool to take into consideration the dependencies between extreme value random variables or the temporal evolution of the climate. For design problem, time should be used as covariate. The climate indices should be used as covariates for management practices.

Leclerc and Ouarda (2007) examined the feasibility of the regional flood frequency analysis using nonstationary GEV1 model utilizing the data of 29 gauging stations located in south eastern Canada and north eastern United States. They reported that non-stationary multiple regression models could efficiently estimate the regional flood quantiles and non-consideration of trend component may lead to serious under or over estimation of flood quantiles.

Laio et al. (2009) examined the correctness of recent developed different model selection criteria for the identification of probability distribution for extreme events, when the available samples were small and the parent distribution was highly asymmetric. They reported that those recent developed criteria were very effective when the parent is a two-parameter distribution for small samples. The extrapolation of results of flood frequency analysis should done by selecting two parameter distributions even though the parent is a three-parameter distribution.

Sugahara et al. (2009) analysed the frequency of non-stationary extreme values (EVs) of daily rainfall (1933–2005) in the city of Sao Paulo, Brazil. They used peaks-over-threshold (POT) and Generalized Pareto Distribution (GPD) approach for non-stationary frequency analysis. They reported that the model with the positive linear trend in the scale parameter shows a better result.

Villarini et al. (2009) applied GAMLSS model for carrying out flood frequency analysis of annual peak records of the urban drainage basin of Charlotte, North Carolina considering Gumbel, Weibull, Gamma, and Lognormal distribution functions. They reported that the GAMLSS model could incorporate covariates related to urbanization, changing climate and is very much able to describe the variability in the mean and variance of annual peak discharge value. However, the model should be used very cautiously for the prediction of flood quantiles in the presence of cubic splines or other smoothing techniques within the model. They concluded that a very good understanding of physical processes related to climate change and other anthropogenic changes is needed for the modelling of non-stationary flood frequency analysis.

Cancelliere et al. (2010) investigated the sampling properties of precipitation frequency estimates for non-stationary series which mainly affected by the trend. They concluded that the knowledge of sampling properties of extreme precipitation was important when the sample showed nonstationary characteristics in the form of the trend.

Stedinger and Griffis (2010) proposed the use of time dependent parameters for accounting the time variability in flood risk assessment. They used ENSO indices to see the effect of climate variability on flood risk assessment in United States. They suggested that the flood trends can be projected using the climate indices.

Vogel (2010) developed a simple statistical model, which could mimic observed trends and the frequency of floods in a nonstationary world. They used a number of anthropogenic processes including changes in land use, climate and water use for modelling non-stationary floods. They proposed a decadal flood magnification factors and recurrence reduction factors for nonstationary floods.

Ouarda and El-Adlouni (2011) analysed annual maximum rainfall (AMR) using Bayesian approach and Generalised Maximum Likelihood Estimation (GMLE) method for non-stationary frequency analysis.

Gilroy and McCuen (2012) developed a method for non-stationary flood frequency analysis and applied it on Little Patuxent River at Guilford, Maryland. The 100-year flood quantile was found to be 30.2% higher due to nonstationarity for the design year of 2100.

Lopez and Franes (2013) used GAMLSS model for non-stationary frequency analysis of annual maximum flood records of 20 continental Spanish rivers. They reported that the first approach, which applied time varying non-stationarity, provide a hint of nonstationarity in the flood regime. The second approach, in which the parameters of the distributions were modelled as a function of climate indices and a reservoir index (RI), highlight the important role of inter-annual variability in low-frequency climate forcing. They concluded that the inclusion of the external covariates improved the predictive performance of the non-stationary model.

Tramblay et al. (2013) used a non-stationary POT model with climatic covariates for analysing heavy rainfall events in southern France. They used Poisson distribution for the occurrence and a generalised Pareto distribution for the magnitude of the heavy rainfall events and reported that the non-stationary model provided better results than the stationary model.

Roth et al. (2014) predicted extreme rainfall events using a non-stationary POT model for the Netherlands and north-western Germany. They analysed two different simulations of RACMO2 Regional Climate Model (RCM) for the period 1950–2100 and found that the regional approach performed better than the at-site approaches. Both the simulations of RACMO2 showed a significant increase in extreme precipitation over the study area for summer and winter seasons.

Machado et al. (2015) analysed 400 years flood records of the Tagus river in Central Spain under stationary and nonstationary conditions using GAMLSS model. They used North Atlantic Oscillation (NAO) indices, and reservoir index (RI) as external covariates. They reported that the non-stationary model using NAO and RI as external covariates could correctly reflect the internal climatic variability in the occurrence of floods.

Mondal and Mujumdar (2015) used POT approach to model finer resolution (1º by 1º) gridded extreme rainfall. They analysed the intensity, duration, and frequency of rainfall by non-stationary distributions using ENSO-index, GAT and local gridded temperature as external covariates. They reported that the intensity and frequency of extreme rainfall show non-stationarity at a large number of gridded locations due to the local changes in temperatures.

Singh et al. (2015) developed a framework for stationary and non-stationary flood frequency analysis under changing climate. They found non-stationarity in the gauging sites, which have significant trend. The occurrence of flood extremes were more accurately predicted by higher order non-stationarity than the lower order non-stationarity.

Vittal et al. (2015) analysed at-site flood frequency analysis for multivariate datasets using both parametric and non-parametric approaches. They have used 110 years of data from Allegheny River at Salamanca, New York, USA. They found the nonparametric Gaussian kernel as best estimator for both the univariate and multivariate case. The nonparametric method should be considered during any at-site flood frequency analysis to provide the broadest choices for best estimation of the flood return periods.

Zhang et al. (2015) carried out flood frequency analysis of six sites of East River basin in China using GAMLSS model. They used both the stationary and non-stationary flood frequency analysis method and found that the stationary model could not describe the changing behaviour of floods. The non-stationary model with climate indices and reservoir index performed better than the stationary model.

Sherly et al. (2016) examined both parametric and non-parametric approaches for multivariate rainfall datasets of Mumbai. They have suggested the use of a new semiparametric model approach, which can evaluate all possible combinations of the parametric-nonparametric marginal without restrictions.

Singh et al. (2016) used Generalized Additive Model for Location, Scale and Shape model for non-stationary frequency analysis of extreme summer monsoon rainfall events over India. They analysed the gridded daily rainfall data (mm/d) with a 1° resolution from 1901 to 2004. They found significant non-stationarity in the extreme rainfall events. The urbanizing/developing-urban areas (transitioning from rural to urban) were more prone towards the non-stationarity than the completely urbanized or rural areas. They concluded that the urbanization plays a major role in introducing nonstationarity in Indian summer monsoon rainfall extremes.

Singh et al. (2016) studied non-stationary multivariate frequency analysis using 104 years 1º by 1º gridded rainfall data over India. They have used GAMLSS model for all the non-stationarity analysis. They found significant differences in the stationary and nonstationary bivariate return periods for the urbanizing grids than the urbanized and rural grids. The non-stationarity characteristics of precipitation datasets have been identified by using comprehensive multivariate analysis.

The review of literature clearly establishes the need for frequency analysis assuming non-stationarity in the extreme events, to take care of the influence of climate and anthropogenic changes in the extremes. Therefore, in the present study, the frequency analysis have been carried out assuming non-stationarity.

4.4 DATA USED IN THE STUDY

The details of annual maximum rainfall data analysed in this study are given in this section. This section also provides the details of climatic indices and other covariates used in this study.

4.4.1 Annual Maximum Rainfall Data

Annual maximum rainfall (AMR) data for more than 3000 stations across India were collected from India Meteorological Department (IMD). Most of these stations had data of 10 to 20 years only, and many of the stations did not have continuous data. For this analysis, the stations having continuous data for the period of 1931 to 2000 were identified in order to have a common data length. Only 239 stations out of 3000 stations fulfilled this requirement. The data for these stations were thoroughly checked for their quality by the single station and multi-station time series plots. The location of these stations is shown in Figure 4.1. This figure also-

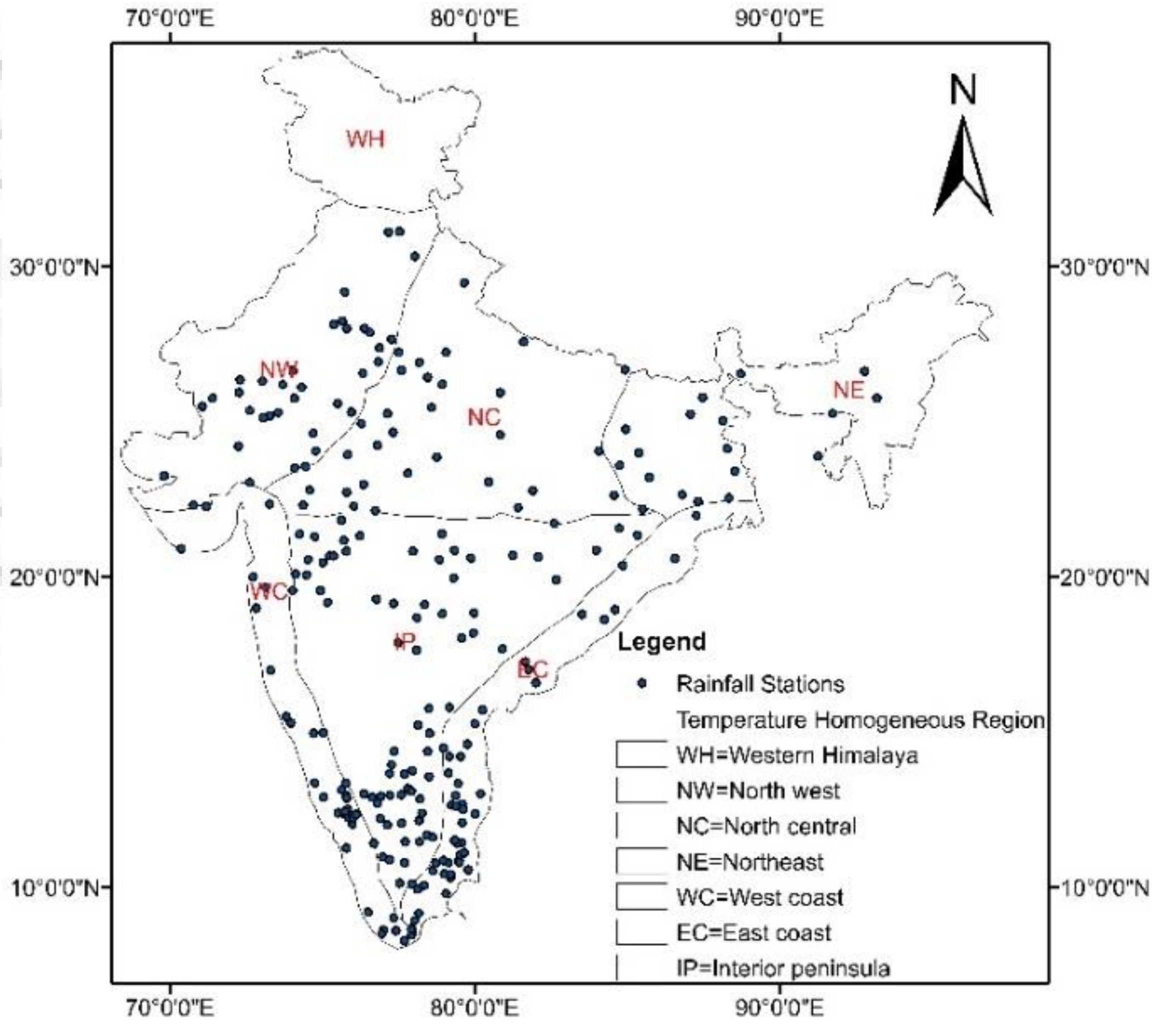

Figure 4.1. Location of rainfall stations under 7 temperature homogeneous regions over India

-shows different temperature homogeneous regions of India, derived by Indian Institute of Tropical Meteorology (IITM). These temperature homogeneous regions have been used in order to link the changes in station rainfall of each region with the local temperature of the same region. The numbers of stations in different regions are given in Table 4.1. The details of the regional temperature data and the homogeneous regions are documented in Kothawale and Rupa kumar (2005). Western Himalayan region remained unrepresented in this analysis as none of the station of this region could qualify the requirement of the length of data.

Table 4.1 Number of rainfall stations in various temperature homogeneous regions.

Temperature Homogeneous Regions	Number of Stations
Interior Peninsula (IP)	70
North West (NW)	35
North Central (NC)	33
North East (NE)	17
West Coast (WC)	38
East Coast (EC)	46
Western Himalaya (WH)	0

4.4.2 Covariates Used in the Study

Two climate indices namely, NINO3.4 SST anomaly (as ENSO-index) and Indian Ocean Dipole (IOD) index, Global Average Temperature (GAT) and Regional Average Temperature (RAT) have been used in this study as covariates. ENSO and IOD indices represent the climatic variability on a larger scale. NINO3.4 SST anomalies from 1951 to 2000 mean were extracted from http://www.esrl.noaa.gov/psd/gcos_wgsp/Timeseries/ Nino34/. In the Indian context, the researchers have mostly used the NINO3.4 SST anomalies as an ENSO-index for extreme rainfall events (Gershunov et al. 2001; Maity and Nagesh Kumar, 2006, 2008; Revadekar and Kulkarni, 2008; Mondal and Mujumdar, 2015). Therefore, NINO3.4 SST anomalies have also been used as an ENSO-index for the present study. More details about the ENSO indices are given in the previous chapter. The IOD index data are taken from http://www.jamstec.go.jp/frsgc/research/d1/iod/e/iod/about_iod.html. Many researchers have found a relationship between IOD index and Indian monsoon rainfall (Ashok et al., 2003; Kulkarni et al., 2006; Surendran et al., 2015). Therefore, the NINO and IOD indices as covariates for annual maximum rainfall series is considered in the present analysis.

The monthly observed HadCRUT4 land surface air GAT anomalies with respect to 1961 to 1990 mean have been extracted from http:// www.metoffice.gov.uk /hadobs/ hadcrut4/. The details of GAT and the justification of its use is as a covariate for Indian rainfall is well established in the previous chapter. Trenberth (2011, 2012) mentioned that the global warming and local temperatures might affect the rainfall differently. Therefore, the RAT of seven homogeneous regions has also been used to see the effect of regional temperatures on AMR data of individual stations. The homogeneous monthly surface temperature data from 1901-2007 have been extracted from http://www.tropmet.res.in/static_page.php?page_id=54.

4.5 METHODOLOGY

For the analysis of non-stationary series, a modelling framework, in which the selected distribution parameters can vary with explanatory variable(s), is required. The GAMLSS modelling framework proposed by Rigby and Stasinopoulos (2005) has been used in the present study. This model provides a flexible modelling framework for the analysis of stationary as well as non-stationary series. The details of GAMLSS model are shown in Annexure 4.1. All the statistical analysis for stationary and non-stationary conditions have been computed in GAMLSS model.

As a first step, the presence of trend was tested using Mann-Kendall (MK) test at 5% significance level. Theil-Sen median slope estimator was used for estimating slope to determine the change in the magnitude of annual maximum rainfall during the study period. The analysis for stationary as well as nonstationary cases was performed irrespective of the results of Mann-Kendall test, in the light of the closing remarks about stationarity and non-stationarity in WMO (Lins, 2001).

4.5.1 Frequency Analysis under Stationary Assumption

For frequency analysis of AMR series of 239 stations under the stationary assumption, five continuous distribution functions, namely, Gumbel (GU), Lognormal (LOGNO), Gamma (GA), Generalized Gamma (GG), and Logistic (LO) were used. The details of these distribution functions are given in Table 4.2. The goodness of fit was tested using the worm plots, residual moments (mean, variance, skewness, and kurtosis), Filliben Correlation Coefficient (FCC), and Akaike Information Criterion (AIC) (Akaike, 1974) for selecting the best fit distributions.

Worm Plot: It is a de-trended form of qq-plot (quantile plot), which provides the difference between the empirical and theoretical values (shown in the vertical axis) from the theoretical values (shown in the horizontal axis). The data points appear like a worm-shaped string. The shape of the worm provides information about the difference of assumed distribution from the original. A different pattern of worm plots indicated different interceptions about the residual moments (like mean, variance etc.). More details about the worm plot are presented by van Buuren and Fredriks (2001).

Filliben Correlation Coefficient (FCC): The test of Probability Plot Correlation Coefficient (PPCC) is developed by Filliben (1975). This correlation coefficient is actually used in GAMLSS model as FCC. The test is known as one of the powerful measures of goodness of fit. In GAMLSS, FCC is used to examine the normality of residuals. The test is also developed for checking the hypothesis of normality. However, the test can also be used for non-normal distributions (Vogel, 1986; Vogel and Kroll, 1989; Vogel and McMartin, 1991; Heo et al., 2008). The FCC is calculated as:

$$FCC = \frac{\sum_{i=1}^{n}(X_i - \bar{X})(M_i - \bar{M})}{\sqrt{\sum_{i=1}^{n}(X_i - \bar{X})^2 \sum_{i=1}^{n}(M_i - \bar{M})^2}} \tag{4.1}$$

where, X_i and M_i are the observed and fitted quantiles respectively, $\bar{X}$ and $\bar{M}$ are the mean values of X_i and M_i, and n is the sample size.

Akaike Information Criterion (AIC): AIC is a criterion for model selection (for nested statistical models). It was developed from information theory by Akaike (1974). It is an estimate of the mean log-likelihood and measures the relative quality of the nested statistical models. It does not test null hypothesis for model selection, and thus, the quality of a selected model cannot be assured by AIC in a complete sense. AIC cannot provide any warning, even though all the candidate models fit poorly. It can be estimated as:

$$AIC = (-2)\log(maximul\ likelihood) + 2(number\ of\ indipedently\ adjusted\ parameters\ within\ the\ model) \tag{4.2}$$

Table 4.2 Summary of the distribution functions used in this study.

Distributions	Probability density function (PDF)	Cumulative distribution function (CDF)	Distribution Moments
Gumbel	$f_Y(y\|\theta_1,\theta_2) = \frac{1}{\theta_2}\exp\left\{-\left(\frac{y-\theta_1}{\theta_2}\right) - \exp\left[-\frac{y-\theta_1}{\theta_2}\right]\right\}$ $-\infty < y < \infty, -\infty < \theta_1 < \infty, \theta_2 > 0$	$F(y) = 1 - \exp^{-\exp\frac{y-\theta_1}{\theta_2}}$	$E[Y] = \theta_1 + y\theta_2$ $\cong \theta_1 + 0.57722\theta_2$ $Var[Y] = \frac{\pi^2{\theta_2}^2}{6} \cong 1.64493{\theta_2}^2$
Lognormal	$f_Y(y\|\theta_1,\theta_2) = \frac{1}{\sqrt{2\pi\theta_2^2}}\frac{1}{y}\exp\left\{-\frac{[\log(y)-\theta_1]]^2}{2\theta_2^2}\right\}$ $y > 0, \theta_1 > 0, \theta_2 > 0$	$F(y) = \Phi\left(\frac{\log(y)-\theta_1}{\theta_2}\right)$ Φ is the distribution function of the standard normal distribution	$E[Y] = \omega^{1/2}e^{\theta_1}$ $Var[Y] = \omega(\omega-1)e^{2\theta_1}$ Where $\omega = \exp(\theta_2^2)$
Gamma	$f_Y(y\|\theta_1,\theta_2) = \frac{1}{(\theta_2^2\theta_1)^{1/\theta_2^2}}\frac{y^{\frac{1}{\theta_2^2}-1}e^{-y/(\theta_2^2\theta_1)}}{\Gamma(1/\theta_2^2)}$ $y > 0, \theta_1 > 0, \theta_2 > 0$	$F(y) = \frac{\gamma\left(\frac{1}{\theta_2^2}, y/(\theta_2^2\theta_1)\right)}{\Gamma(1/\theta_2^2)}$ $\gamma(.,..)$ is incomplete gamma function	$E[Y] = \theta_1$ $Var[Y] = \theta_2^2\theta_1^2$
Generalized Gamma	$f_Y(y\|\theta_1,\theta_2) = \frac{\|\theta_1\|y^{\theta_1\theta_3-1}}{\Gamma(\theta_3)\theta_2^{\theta_1\theta_3}}\exp\left\{-\left(\frac{y}{\theta_2}\right)^{\theta_1}\right\}$ $y > 0, -\infty < \theta_1 < \infty, \theta_2 > 0, \theta_3 > 0$	$F(y) = \frac{\gamma\left(\theta_3, \left(\frac{y}{\theta_2}\right)^{\theta_1}\right)}{\Gamma(\theta_3)}$ $\gamma(.,..)$ is incomplete gamma function	$E[Y] = \ln\theta_1 + \frac{\ln\theta_2 - \ln\theta_3}{\theta_3}$ $Var[Y] = \frac{1}{\sqrt{\theta_2\theta_3}}$
Logistic	$f_Y(y\|\theta_1,\theta_2) = \frac{\exp\left[-\left(\frac{y-\theta_1}{\theta_2}\right)\right]}{\theta_2\left\{1+\exp\left[-\left(\frac{y-\theta_1}{\theta_2}\right)\right]\right\}^2}$ $-\infty < y < \infty, -\infty < \theta_1 < \infty, \theta_2 > 0$	$F(y) = \left[1 + exp\left\{-\left(\frac{y-\theta_1}{\theta_2}\right)\right\}\right]^{-1}$	$E[Y] = \theta_1$ $Var[Y] = \frac{\pi^2{\theta_2}^2}{3}$

4.5.2 Frequency Analysis under Non-stationary Assumption

In non-stationary analysis, five explanatory variables, namely time, GAT, RAT, NINO, and IOD have been used as covariates. The Pearson's correlation coefficient was used to check the correlation between AMR series with the covariates (except time) used in this analysis. Then the GAMLSS model is used for the statistical calculations under the non-stationary assumption. The same five distribution functions have been used for the stationary as well as non-stationary frequency analysis of AMR series. All the covariates used in this study are also used in different combinations. In addition to the stationary case, six different non-stationary cases have also been considered. The details of these models are given in Table 4.3. The covariates are varied with the distribution parameters using the link functions. The link functions for all five distributions used in this study are given in Table 4.4. A cubic spline smoothing technique, which allows an additional modelling flexibility, is used to model the dependence of distribution parameters on the explanatory variables. The selection of best model and distribution function is similar as used for the stationary case.

After the selection of best non-stationary model, the T-year return period quantiles for stationary and non-stationary assumptions have been estimated for an exceedance probability of 0.02 (i.e. return period of 50 years). The T-year return level can be estimated as:

$$F_T\left(r_p(T)\right) = 1 - p \tag{4.3}$$

where, F_T is distribution function, $r_p(T)$ is return level changes with year T, p is the exceedance probability. In the end, the results of stationary and non-stationary models are compared.

Table 4.3 Details of the models analysed in this study.

S.N.	Models	Model of non-stationary series where the distribution parameters can vary with
1	Model 1	TIME
2	Model 2	GAT
3	Model 3	RAT
4	Model 4	IOD
5	Model 5	NINO
6	Model 6	IOD and NINO

Table 4.4 Distributions with their different link functions for the non-stationary condition.

S.N.	Distributions	Link functions		
		θ_1	θ_2	θ_3
1	Gumbel	Identity	Log	-
2	Lognormal	Identity	Log	-
3	Gamma	Log	Log	-
4	Generalized Gamma	Log	Log	Identity
5	Logistic	Log	Identity	-

4.6 RESULTS AND DISCUSSION

The results and discussion are presented in three sub-sections. The first sub-section presents the results and discussions on trend identification using MK test, changes in AMR during the study period using Theil and Sen's slope test and correlation of AMR with different covariates. The second sub-section presents the detailed analysis of AMR series of Amritur station using GAMLSS model for stationary and non-stationary cases. This is followed by results of non-stationary frequency analysis of AMR series for the entire country. In this study, the non-stationary frequency analysis of extreme rainfall data of 239 stations spread over India has been carried out. The relationship between urbanisation and increase of extreme rainfall events have also been studied for the investigation of possible causes of non-stationarity.

4.6.1 Trend Analysis, Change Detection, and Correlation Studies

Non-parametric MK test and Theil-Sen median slope estimator are applied to the AMR series of all the 239 stations. The results of MK test are given in Annexure 4.2. As per MK test results, only 65 stations are showing a presence of significant trend at 5% significance level. However, the results of MK test are not required for the frequency analysis under the non-stationary assumption. The median slope of the trend line is also estimated using Theil-Sen median slope estimator for all the 239 stations. The median slope of the trend line is used for the calculation of the change in magnitude of AMR series during the study period. These results are also given in the Annexure 4.2. The spatial pattern of change in magnitude of AMR series is depicted in Figure 4.2. The results indicate that the magnitude of AMR series during the study period of 1931 to 2000 changed from -1.20 mm/year to 1.80 mm/year. A decreasing trend is observed in the central and western parts of India whereas the increasing trend is observed in the north eastern and some part of northern, southern, and western parts of India. The results clearly indicate that the AMR is changed over the year and the changing pattern is also not similar to the whole India. Therefore, non-stationary frequency analysis of the AMR series is carried out using five different covariates.

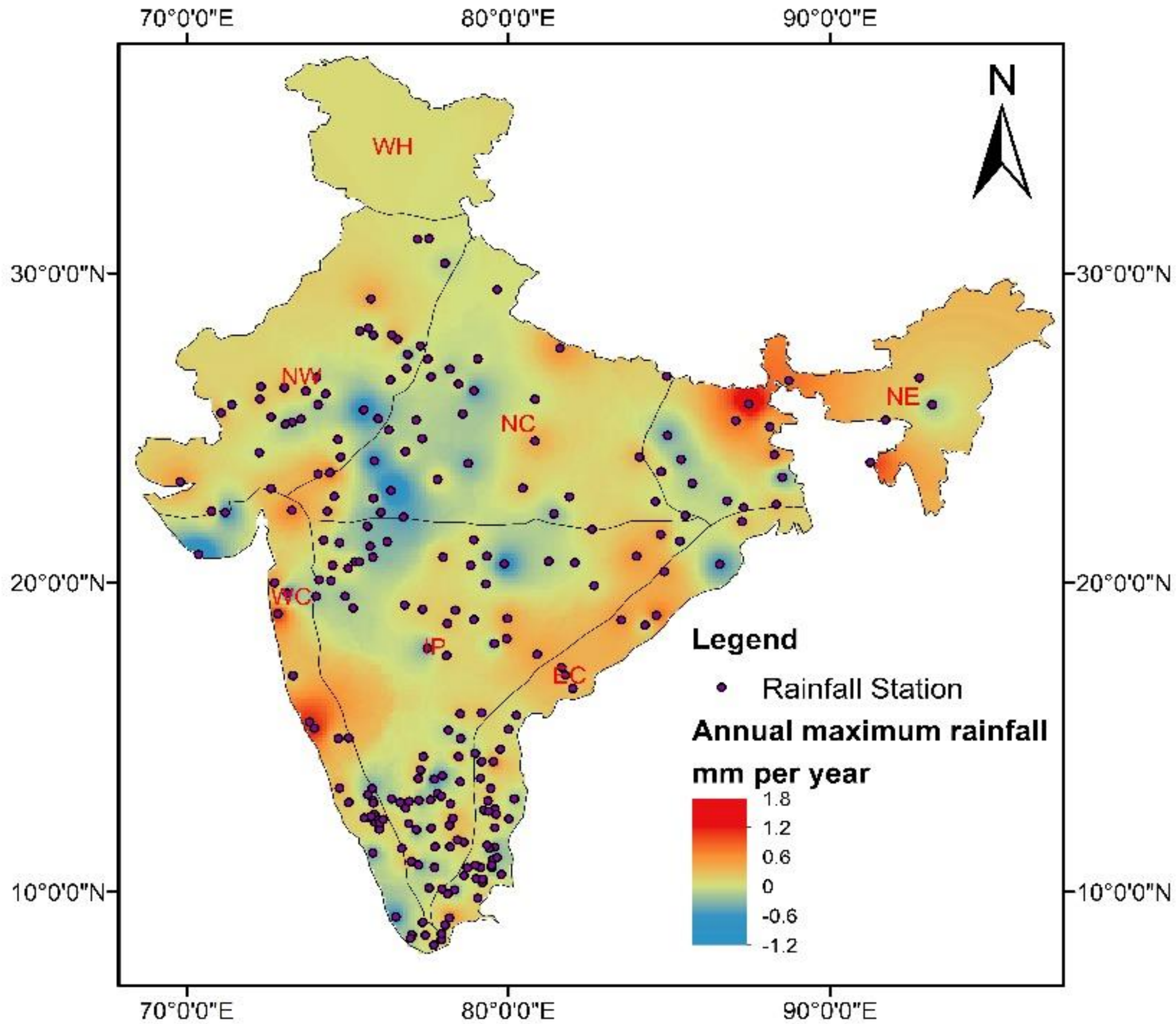

Figure 4.2. Presence of trends (mm/year) in annual maximum rainfall events

The correlation of AMR series with the four covariates (except time) is analysed. The correlation coefficient values for all the stations are given in the Annexure 4.3. The spatial pattern of significant correlation is shown in Figure 4.3. A significant correlation between AMR series and GAT anomalies of monsoon month have been found in some stations of southern and eastern India (Figure 4.3(a)). Similar results as found in the case of GAT were observed for RAT (Figure 4.3(b)). The number of stations with significant correlations are comparable. The stations with a significant correlation between AMR series and RAT are well distributed over India. Very less number of stations show a significant correlation between AMR series and IOD anomalies over India (Figure 4.3(c)). Similar kind of result was found for NINO (Figure 4.3(d)). The number of stations showing a significant correlation between AMR series with GAT and RAT are the maximum among the other anomalies.

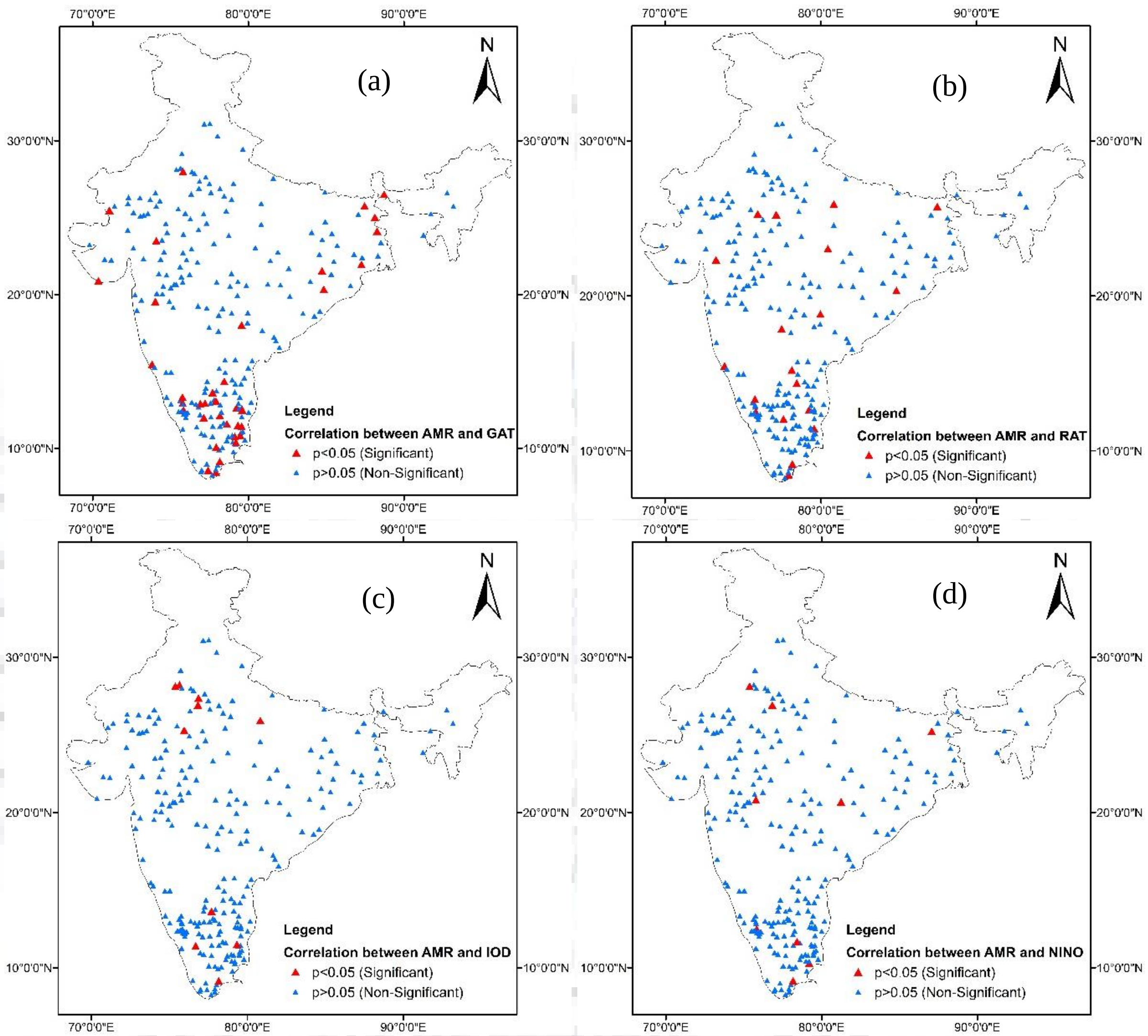

Figure 4.3. Correlation between annual maximum rainfall (AMR) and four covariates data and $p < 0.05$ indicates significant correlations. (a) Correlation between AMR and global average surface air temperature (GAT), (b) Correlation between AMR and regional monsoon monthly mean temperature (RAT), (c) Correlation between AMR and Indian Ocean Dipoles (IOD), (d) Correlation between AMR and NINO anomalies

4.6.2 Application of GAMLSS Model for AMR Series of Amritur Station

The GAMLSS model is used for the frequency analysis of AMR series of 239 stations (Figure 4.1) across India, for the period of 1931 to 2000. The AMR series of each station was analysed using stationary and six different non-stationary models (Table 4.3). For all the models, five different distributions (Table 4.2) were also used. The model fitting for all the models was evaluated using the worm plots, residual moments, and Filliben coefficients (Filliben, 1975).

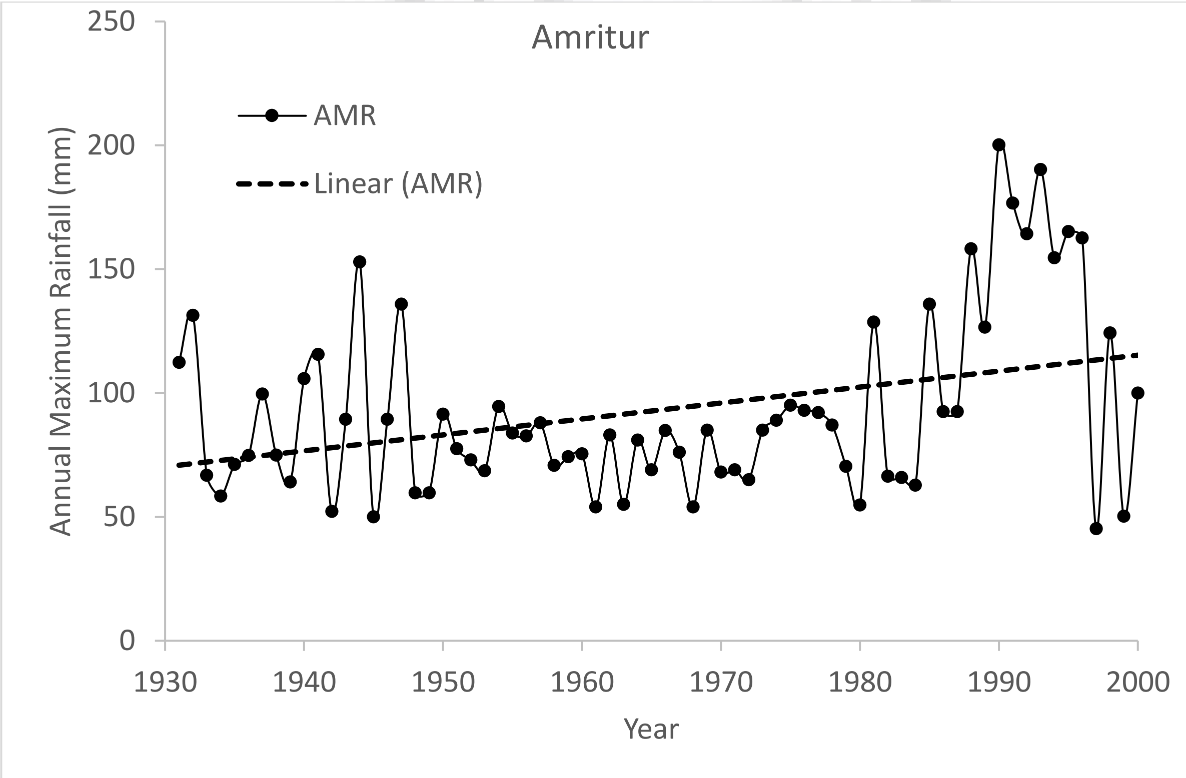

Figure 4.4. Annual maximum rainfall series of Amritur station. The dotted line shows the linear trend in the series

The detail application of GAMLSS model for non-stationary frequency analysis of Amritur station, which is located in the southern India, are presented in this section. The latitude and longitude of the station are 12.92º N and 76.92º E respectively. The AMR series of Amritur station is shown in Figure 4.4. This series has an increasing trend and is shown by a dotted line in the figure. The Mann-Kendall test has confirmed the presence of a significant increasing trend in the AMR series of the station. The AIC value, a summary of residual moments and Filliben coefficients (Filliben, 1975) for all five distribution functions of the stationary model are given in Table 4.5. The Generalised Gamma distribution shows the lowest AIC value and is fitted well for the stationary model of the station. The worm plot of the stationary model is-

Table 4.5 AIC values, distribution parameters, a summary of residual moments and Filliben correlation coefficients for different distributions of the Stationary model.

Distribution functions	AIC value	θ_1	Std. Error	θ_2	Std. Error	Mean	Var	C_s	C_k	FCC
Gumbel	683.79	77.21	3.14	3.22	0.10	0.01	1.11	0.48	2.42	0.98
Lognormal	683.65	84.47	0.04	-1.03	0.08	0.00	1.01	0.50	2.46	0.98
Gamma	688.86	84.53	0.04	-1.02	0.08	-0.00	1.01	0.72	2.70	0.97
Generalized Gamma	**680.86**	84.33	0.07	-1.16	0.12	-0.00	1.01	0.03	2.37	**0.99**
Logistic	703.39	87.71	4.06	2.98	0.10	0.11	1.03	0.91	2.81	0.95

Std. Error = Standard Error, Var = Variance, C_s = Coefficient of Skewness, C_k = Coefficient of Kurtosis, FCC = Filliben correlation coefficient

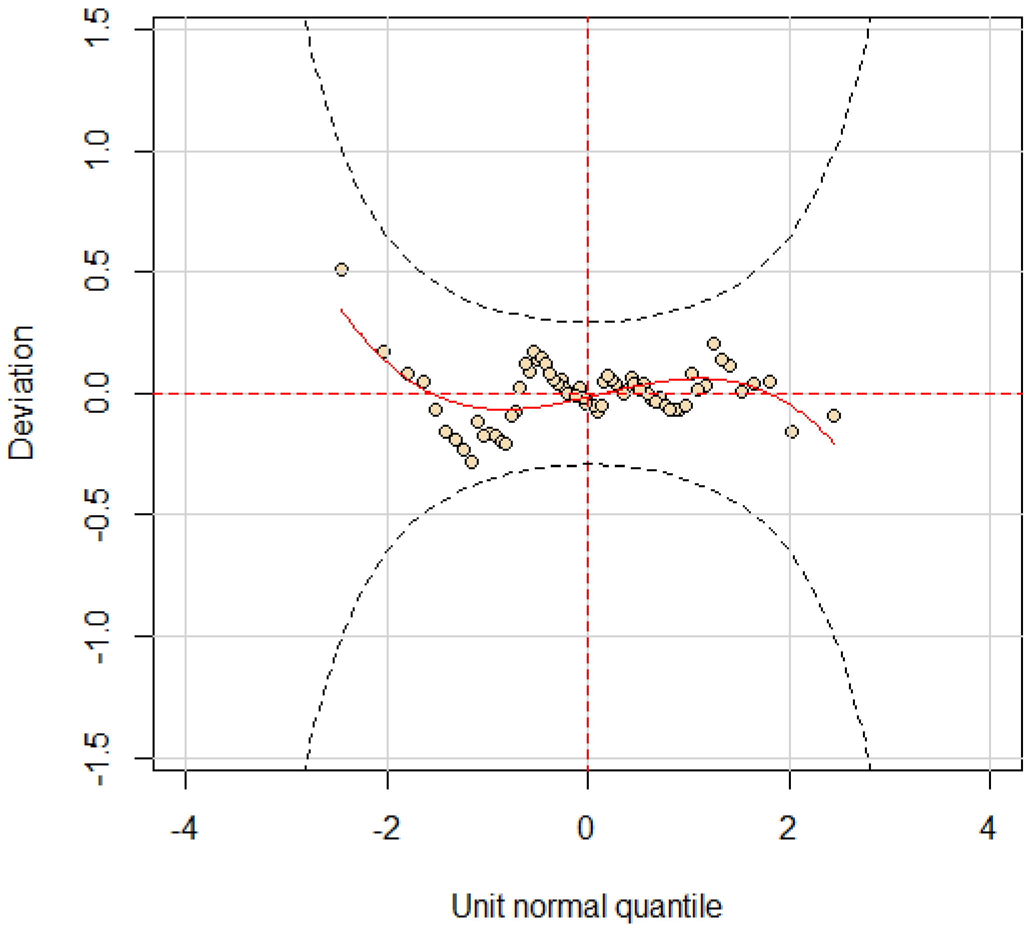

Figure 4.5. Worm plots of residuals for annual maximum rainfall series of the stationary model. The 95% confidence interval is shown by the two black dotted lines

-given in Figure 4.5. It can be observed from the worm plot that, the standard residuals are inside the upper and lower limit (shown by dotted lines), which is indicative of no discrepancy in model fitting. For stationary model, i.e., with Generalised Gamma distribution, the mean and variance values are close to 0 and 1, indicating a significant normality in residuals. Furthermore, the Filliben correlation coefficients (FCC) are more than 0.972 (critical value for Filliben coefficient is 0.972 for a sample size of 70), implies that the residuals followed normality. The θ_1(related to mean) and θ_2(related to variance) parameters of the stationary model are 4.33 and -1.16 respectively. The standard error of estimating θ_1 and θ_2 parameters are 0.07 and 0.12 respectively.

The six different non-stationary models have also been used for all the five distribution functions. The AIC value, fitted distributions, parameters with their different link functions and the selected explanatory variables for all the non-stationary models used in this study are given in Table 4.6. The summary of residual moments and Filliben correlation coefficients for all the non-stationary models are also provided in the table. The AIC value is lowest for Model 1, i.e., the non-stationary model, whose distribution parameters can vary with time or the trend component of the AMR series. The Gumbel distribution is best fitted for the non-stationary model. The worm plot of residuals for the best fitted non-stationary model (Model 1) is shown-

Table 4.6 AIC values, fitted distribution, and dependences of fitted models with covariates, a summary of residual moments and Filliben correlation coefficients for different non-stationary models.

Models	Distribution functions	AIC value	θ_1	θ_2	Mean	Var	FCC
Model 1	Gumbel	**661.680**	(t)	(t)	0.003	1.012	**0.986**
Model 2	Lognormal	663.359	(GAT)	(GAT)	-0.001	1.014	0.990
Model 3	Generalised Gamma	682.223	(RAT)	(RAT)	-0.012	1.001	0.992
Model 4	Generalised Gamma	681.928	(IOD)	ct	0.000	1.012	0.992
Model 5	Generalised Gamma	682.411	(NINO)	ct	0.001	1.013	0.992
Model 6	Generalised Gamma	683.064	(IOD+ NINO)	ct	0.001	1.012	0.993

Note: Var = Variance, FCC = Filliben correlation coefficient, (.) denotes linear function as link function, ct denotes a constant parameter.

-in Figure 4.6. The figure indicates that all the standard residuals of Model 1 are within the boundary limit, which is indicative of no discrepancy in model fitting. The boundary limit (upper and lower limit) is shown by dotted lines, which is actually the 95% confidence limit. For Model 1, the residual moments (mean and variance), and FCC values indicating a significant normality in residuals. All the model selecting criterion shows the very good result, and therefore, the Model 1 is chosen for the AMR series of Amritur station.

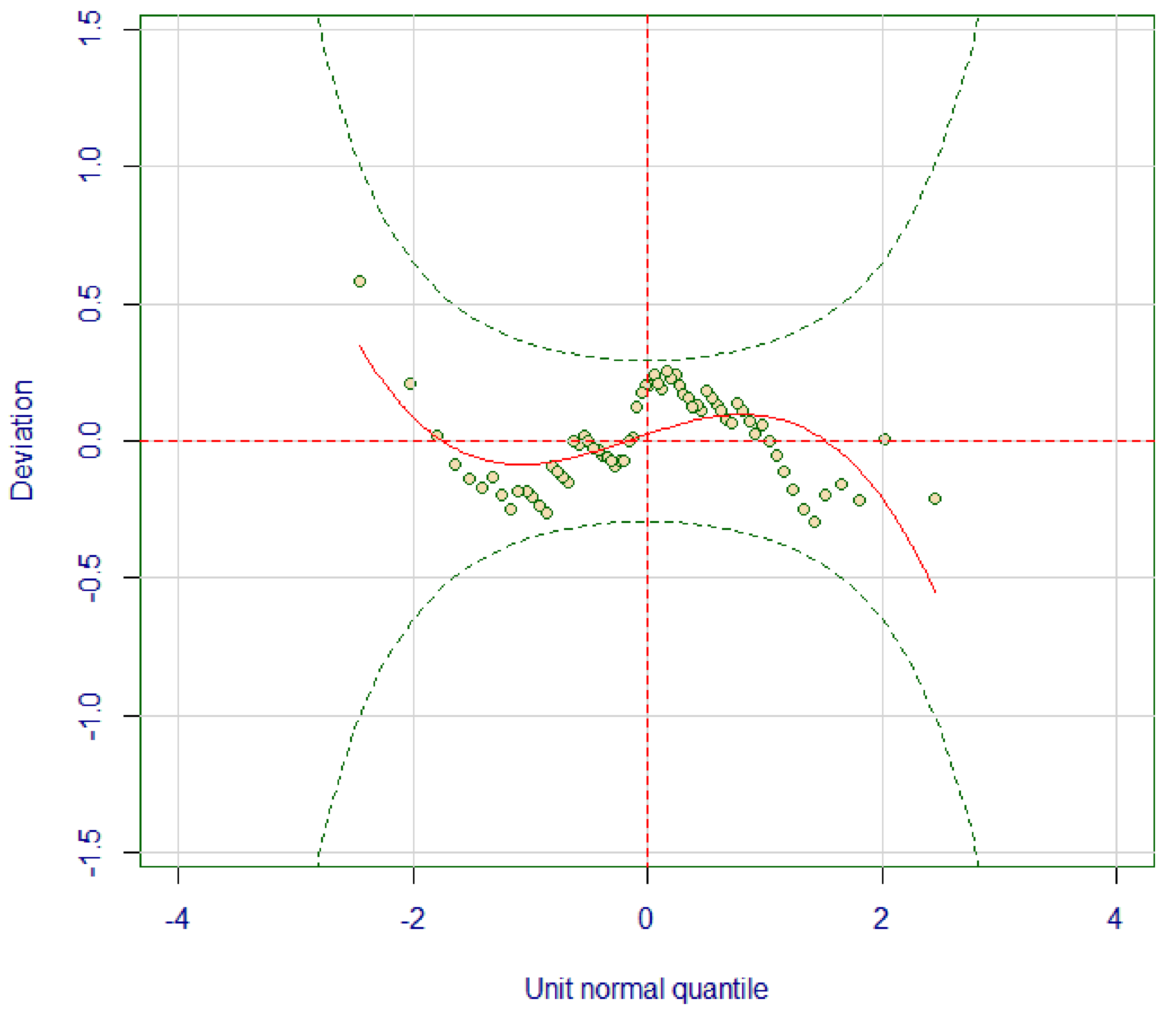

Figure 4.6. Worm plots of residuals for AMR series of the best fitted non-stationary model (Model 1). The 95% confidence interval is shown by the two black dotted lines

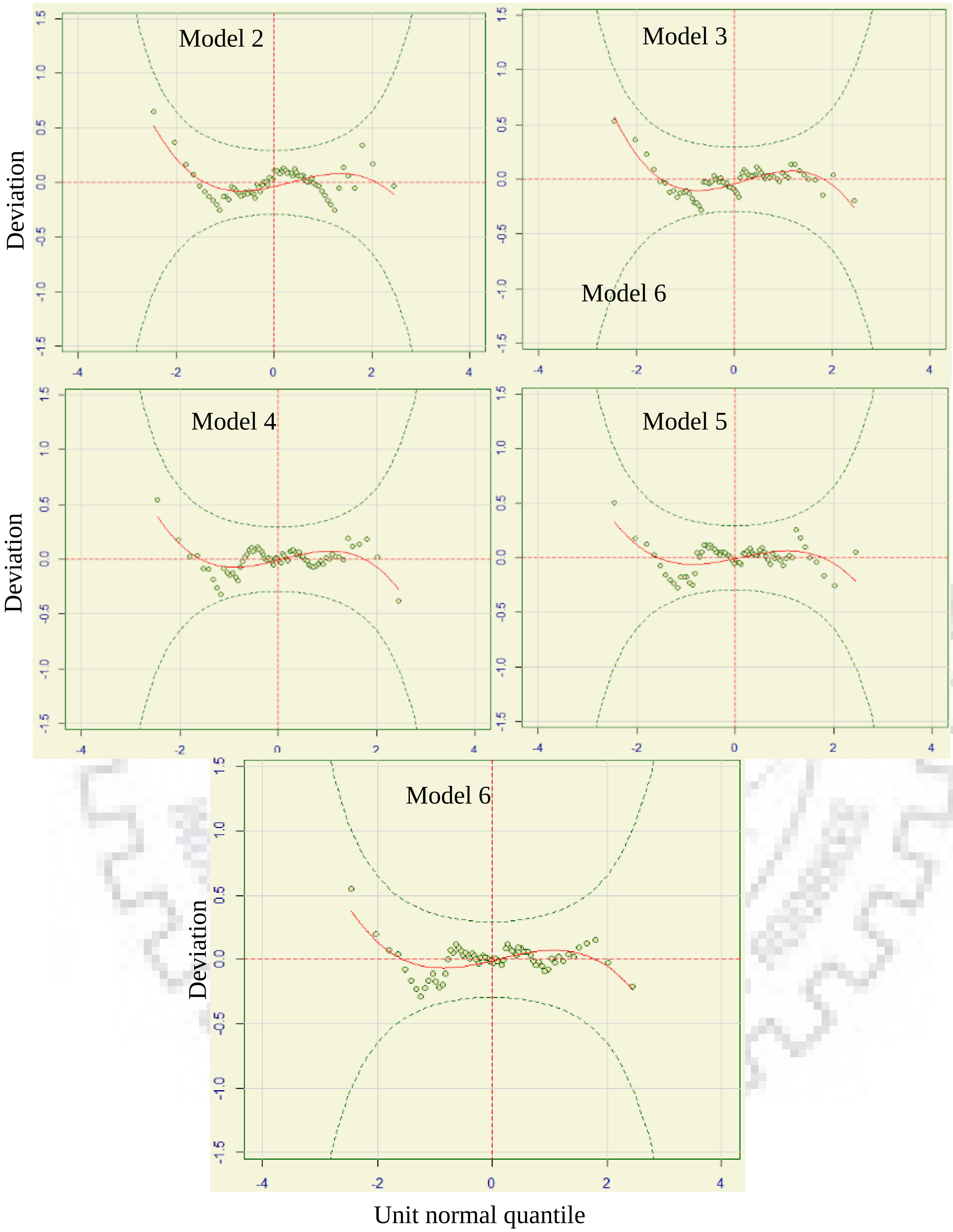

Figure 4.7. Worm plots of residuals for annual maximum rainfall series of all models. The 95% confidence interval is shown by the two black dotted lines

The AIC values of all the non-stationary models (Table 4.6) show that at least 2 models (Model 1 and 2) have lower AIC value than the stationary model for the AMR series of Amritur station. The residual moments for the model 2 have also followed normality. The worm plots of residuals for all the non-stationary models (except Model 1) are shown in Figure 4.7. The figure also shows no discrepancy of standard residuals (within confidence limit) for all the five models. The goodness of fit test for all these models confirms that these models can be used as a non-stationary model for the AMR series of Amritur station. The Model 2, which used GAT as a covariate is also a possible option for the non-stationary frequency analysis of AMR series of Amritur station. The Model 2 provides the lowest AIC value among all other non-stationary models, which uses physical covariates except time. However, in this study, the Model 1 is used for the frequency analysis of AMR series of Amritur station under the non-stationary assumption. The results of Model 2 is also given in the subsequent sections for the comparison purpose of two type of non-stationary models, one which only used the trend component of a dataset, and the other used physical covariates.

4.6.2.1 Comparison of stationary and non-stationary model results

The results of the frequency analysis of AMR series for 50-years return period (0.02% probability of exceedance) by Model 0, 1 and 2 are shown in Figure 4.8. The 50 years return level rainfall is constant for the entire time period based on the results of Model 0. The result of Model 1 shows an increasing tendency of annual maximum rainfall. The 50-years return level rainfall is overestimated by the stationary model (Model 0) as compared to time varying non-stationary model (Model 1) before 1988. The situation is completely altered after 1991. However, an overestimation of AMR values is observed by Model 1 as compared to Model 2 from 1953 to 1979. Furthermore, the frequency analysis of AMR series by Model 1 provides a maximum value of 237.42 mm in 2000 and a minimum value of 85.55 mm in 1931. It can be seen from the Figure 4.4 that the AMR series is following an increasing tendency. The results of model 1 is clearly following the same pattern of the original AMR series.

The results of Model 2 provide a maximum value of 547.37 mm in 1998 and a minimum value of 101.99 mm in 1933. These values show that the return level values from a non-stationary frequency analysis may change intensely if the results were compared with stationary return level values (196.22 mm). Moreover, Figure 4.8 shows that the return levels of AMR series estimated by Model 2 can produce the impact of global warming and also provide a better estimation. But, the results of Model 0 is underestimated or overestimated and can give deceptive results for any design practices. Generally, it is well accepted that the climate change or global warming due to anthropogenic activity intensify the hydrological processes (Allen and Ingram, 2002) and the concept of stationarity in frequency analysis became questionable. The use of stationary model under non-stationary condition may over or underestimate the return level values and provide misleading information. Further, the results of the non-stationary model may suddenly change from year to year. Therefore, under the non-stationary condition "return period" loses its meaning and need to redefine it (Salas and Obeysekera, 2013, 2014; Zhang et al., 2015).

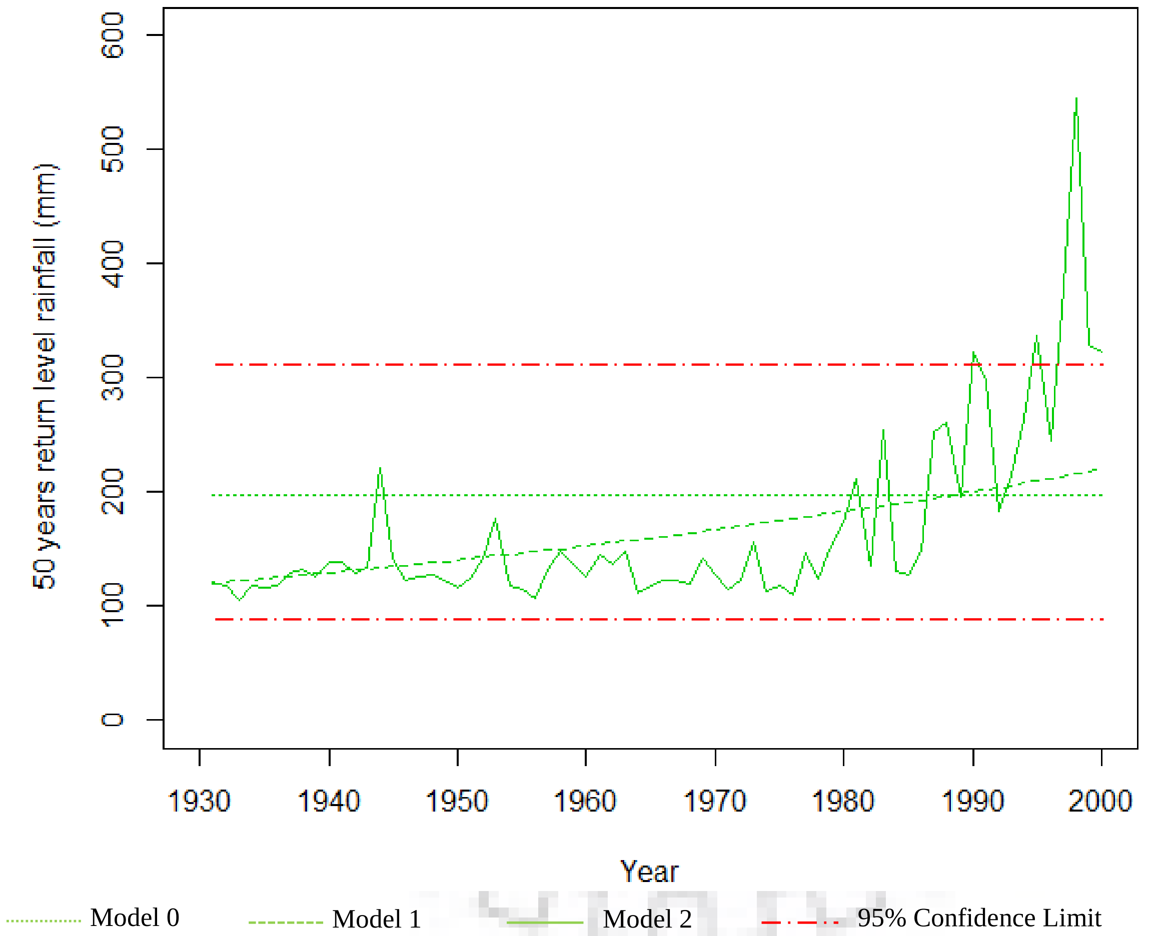

Figure 4.8. Estimated 50-year return level annual maximum precipitation for 1931 to 2000 period, using Model 0, 1 and 2

4.6.2.2 Predictions using non-stationary model

Two models, i.e., Model 1 and 2 were used to predict the frequency of rainfall for the non-stationary condition. In these two models, a relationship between distribution parameters with time and GAT was developed and used as a predictive model. Four different time periods were used for calibration and prediction of 2.5th, median (50th) and 97.5th percentiles of AMR series. The predictive performance of Model 1 is shown in Figure 4.9. The residuals of Model 1 for four different time periods (used for calibration and prediction) were summarised in Table 4.7 to see the goodness of fit of the model. The results of residuals show that the normal distribution was followed by Model 1 for all four different time periods. Out of four different time periods, at first, the 1931 to 1970 period was used for calibration purpose and 1971 to 2000 period as a predictive model. From Figure 4.9, it can be seen that the calibration model can capture the changes in AMR series. The prediction up to 1980 is almost accurate, and after this period, the model followed the same decreasing tendency of the observations from 1945 to 1980. For the second period, the 1931 to 1980 period is used as calibration model and performed well for this period. The prediction is made for 1981 to 2010, and the predictive model performs similarly to the previous one. The results were almost similar to the previous one for 1931 to 1990 time periods. However, the predictions for the 1991 to 2010 time periods generate very high value. The calibration model used for the period of 1991 to 2000 is the best model out of the four time periods. This model can almost capture all the changes in AMR series. The prediction values for 2001 to 2010 is not also very high and can be used for the future.

Table 4.7 Summary of residual moments and Filliben correlation coefficients for a model with time as a covariate. Four columns refer to four different periods used for model fitting.

Residuals	1931-1970	1931-1980	1931-1990	1931-2000
Mean	-0.01	0.01	0.04	0.00
Variance	1.04	1.01	0.95	1.01
Skewness	-0.34	-0.42	-0.39	-0.27
Kurtosis	1.97	2.26	2.45	2.73
Filliben correlation coefficient	0.98	0.98	0.99	0.99

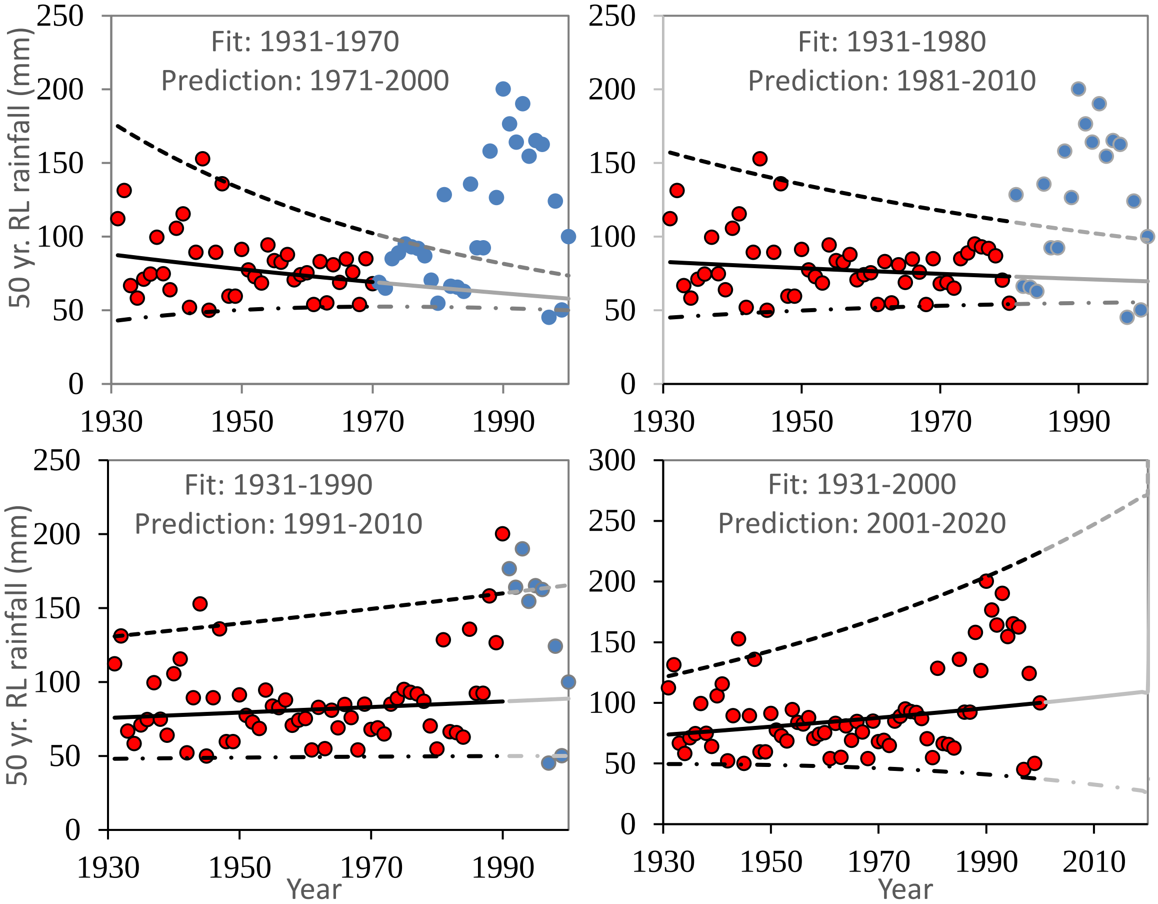

Figure 4.9. Non-stationary frequency analysis of AMR series of Amritur station with Model 1. Red points, black dashed and continuous lines are indicating fitted model performance and blue points, grey dashed and continuous lines are indicating predictive model performance (RL denotes return level)

The predictive performance of Model 2 shows that the model can capture the ups and downs of AMR values (Figure 4.10). The residuals of Model 2 for four different time periods (used for calibration and prediction) were summarised in Table 4.8 to see the goodness of fit of the models. Table 4.10 indicated that the residuals of all four models followed normality, which suggests no discrepancy of model fitting. Figure 4.10 shows that the results of the calibrating model for three different time periods i.e. 1931 to 1970, 1931 to 1980 and 1931 to 1990 can reasonably capture all the fluctuations of AMR series at Amritur station. The predictive performance of Model 2 for those three different time periods can also capture the fluctuations of AMR series. The prediction using the calibration model for 1931 to 2000 follows the same upward tendency of observed rainfall series. The results are indicating the difficulties of any non-stationary model for prediction beyond the range of observed values used for model fitting. However, to use any predictive model, the non-stationary model should be fitted very carefully.

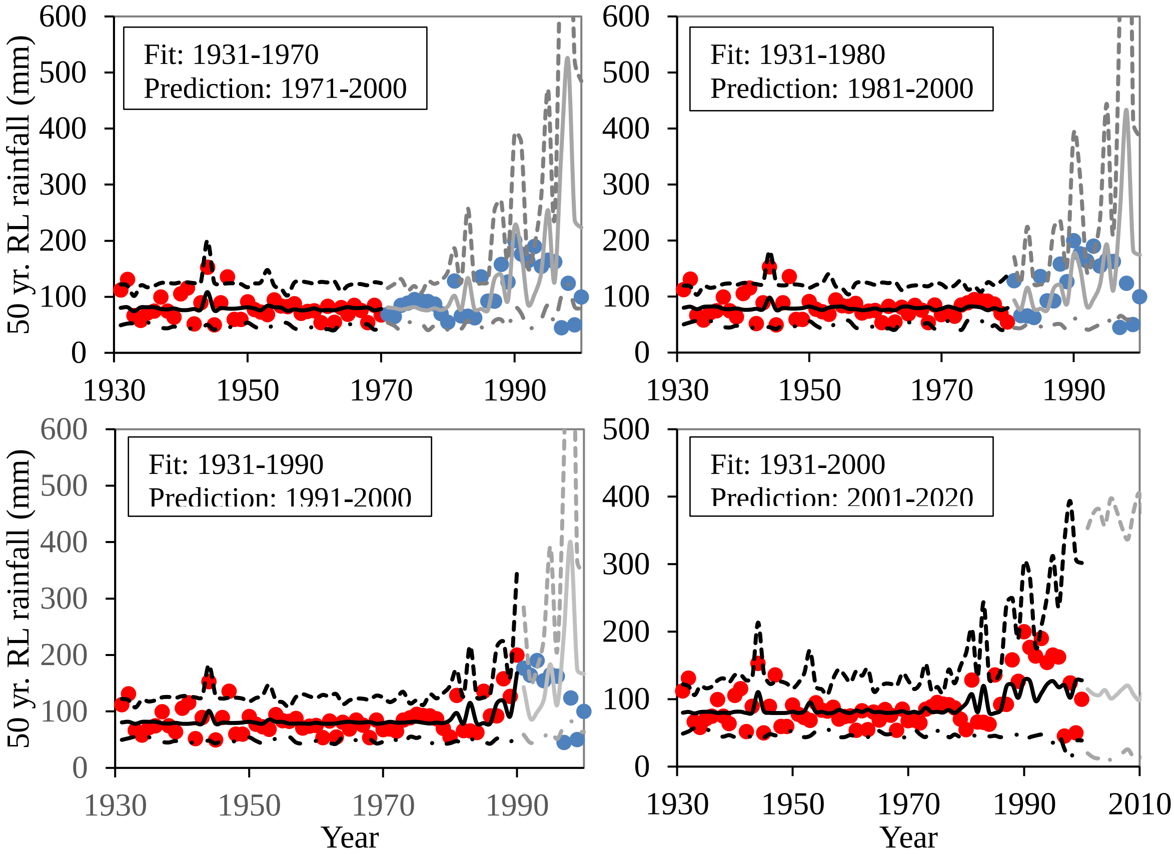

Figure 4.10. Non-stationary frequency analysis of AMR series of Amritur station with Model 2. Red points, black dashed and continuous lines are indicating fitted model performance and blue points, grey dashed and continuous lines are indicating predictive model performance (RL denotes return level)

Table 4.8 Summary of residual moments and Filliben correlation coefficients for a model with GAT as a covariate. Four columns refer to four different periods used for model fitting.

Residuals	1931-1970	1931-1980	1931-1990	1931-2000
Mean	0.00	0.00	0.00	0.00
Variance	1.03	1.02	1.02	1.01
Skewness	0.49	0.44	0.41	0.32
Kurtosis	2.77	2.84	2.69	2.55
Filliben correlation coefficient	0.99	0.99	0.99	0.99

4.6.3 Frequency Analysis Results of AMR Series across India

The number of stations showing the best-fitted distribution for stationary and non-stationary analysis of all the 239 stations under different temperature homogeneous regions of India are summarised in Table 4.9. From Table 4.9, it can be seen that for both the stationary and non-stationary cases the Gumbel, Lognormal and Generalized Gamma distributions fit well to most of the stations. The results show that for the stationary case, the lognormal distribution is fits well for the maximum number of stations of Interior Peninsula (IP), East Coast (EC), West Coast (WC), and North West (NW) regions of India. The Gumbel distribution fits well for most of the stations of North Central (NC) region of India. The same patterns as found for stationary case are also observed for non-stationary case.

Table 4.9 Selected distribution functions for frequency analysis of annual maximum rainfall of different temperature homogeneous regions of India.

Distributions	Stationary Condition							Non-stationary Condition						
	IP	EC	WC	NC	NW	NE	Total	IP	EC	WC	NC	NW	NE	Total
Gumbel	14	3	8	12	5	4	46	21	4	12	13	6	2	58
Lognormal	25	24	22	10	20	3	104	26	21	18	9	20	2	96
Gamma	9	5	3	2	3	1	23	8	7	4	2	4	2	27
Generalised Gamma	21	14	4	9	7	6	61	15	14	3	9	4	8	53
Logistic	1	-	1	-	-	3	5	-	-	1	-	1	3	5

The results of non-stationarity in AMR series across India due to various covariates are shown in Figure 4.11. It can be observed that the selected covariate or the combination of a covariates vary from one station to another station. The large spatial variability of monsoon rainfall over India is the main reason behind this. The rainfall series, which indicated non-stationarity due to GAT, RAT and time as covariates are distributed over India and no spatial pattern is observed. However, the physical covariate IOD shows non-stationarity mostly over the stations of central and eastern India. The NINO and combination of IOD and NINO as covariates show non-stationarity in AMR series of southern and coastal regions of India. It is very much interesting to see that the climate variability indices (except IOD as single covariate) are influencing over the southern and coastal regions. These results confirm that the effect of climate indices are more prominent in the stations closer to the sea.

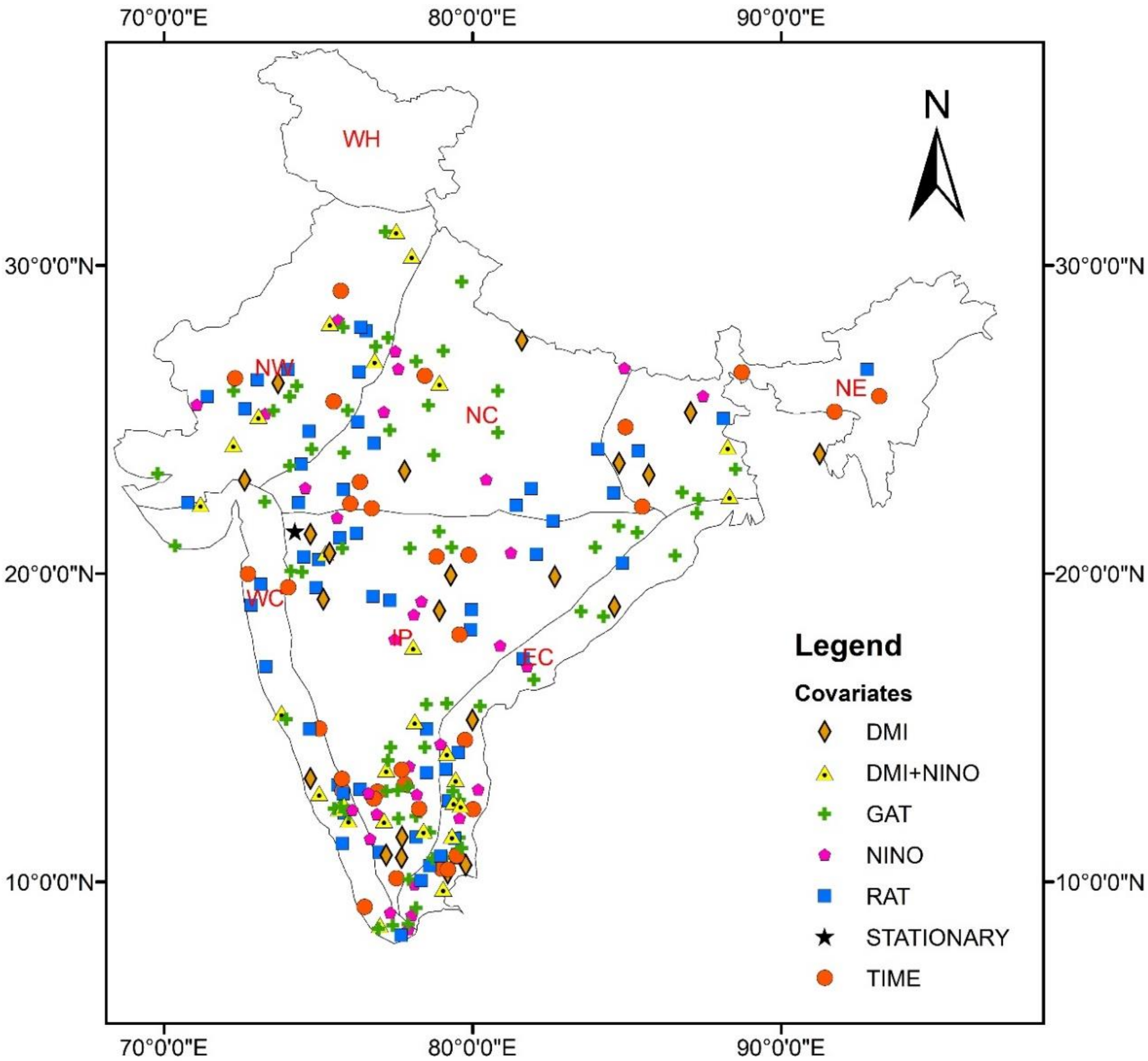

Figure 4.11. Station-wise best statistical models due to the covariates for frequency analysis of annual maximum rainfall series across India

The percentage of stations showing non-stationarity in AMR series of different temperature homogeneous regions across India, due to the selected models, is given in Table 4.10. For IP region, Model 2 is selected for the maximum number of stations. In this region, Model 3 is also used for more than 20% of AMR series. Similar kind of results of IP region is found for EC and WC regions with Model 2 as the most useful non-stationary model. The Model 3 is also used for more than 20% of AMR series for both the EC and WC regions. For NC regions of India, Model 3 is used for the maximum number of stations. In NC region, Model 2 is the second highest useful non-stationary model. Both the non-stationary models, i.e. Model 2 and Model 3 are used for more than 25% stations in NW region. The Model 1 and Model 4 are used for the maximum number of stations (23.5%) in NE region of India. In this region, Model 2 and Model 3 are also used for more than 15 % of AMR series. The Model 2 and 3, which uses GAT and RAT as covariates, are most selected non-stationary model in an overall for the country. Therefore, the changes in temperature had some notable influence for non-stationary frequency analysis of AMR series across India.

Table 4.10 Selected models for non-stationary frequency analysis of annual maximum rainfall over different temperature regions of India.

Non-stationary for various Models	% of Station showing non-stationary						
	IP	EC	WC	NC	NW	NE	India
Model 1	13.0	10.9	18.4	15.2	8.6	23.5	14.9
Model 2	29.0	32.6	26.3	27.3	34.3	17.6	27.9
Model 3	21.7	21.7	23.7	30.3	25.7	17.6	23.5
Model 4	13.0	8.7	2.6	6.1	5.7	23.5	9.9
Model 5	14.5	13.0	10.5	18.2	8.6	5.9	11.8
Model 6	8.7	13.0	18.4	3.0	17.1	11.8	12

The station-wise results show that the selected statistical models incorporated the trends in AMR characteristics due to nature of observed changes in the used combination of covariates. Also, periodicities or non-linear variations in the covariates are automatically incorporated into the model in terms of the covariates. The return level of AMR series estimated by the non-stationary model will thus have the same type of variability as the selected covariates. A change in the estimated rainfall quantiles of AMR is observed for almost all the stations across India due to non-stationarity. The spatial pattern of change in the 50-year rainfall quantiles of AMR series for all the stations is shown in Figure 4.12. Due to the linear variation in non-stationary rainfall quantiles, the maximum value is taken for the calculation of increase or decrease in estimated non-stationary 50-year rainfall quantile from stationary 50-year return level rainfall. Only 4 out of 239 stations are showing a change of less than or equal to 0% in 50-year return level of AMR series across India. Most of the stations across India are showing a change of 0 to 50% whereas one station in NW region showing an increase of more than 200% in 50-year return level. However, no spatial pattern is observed for more than 50% increase in 50-year return level AMR across India.

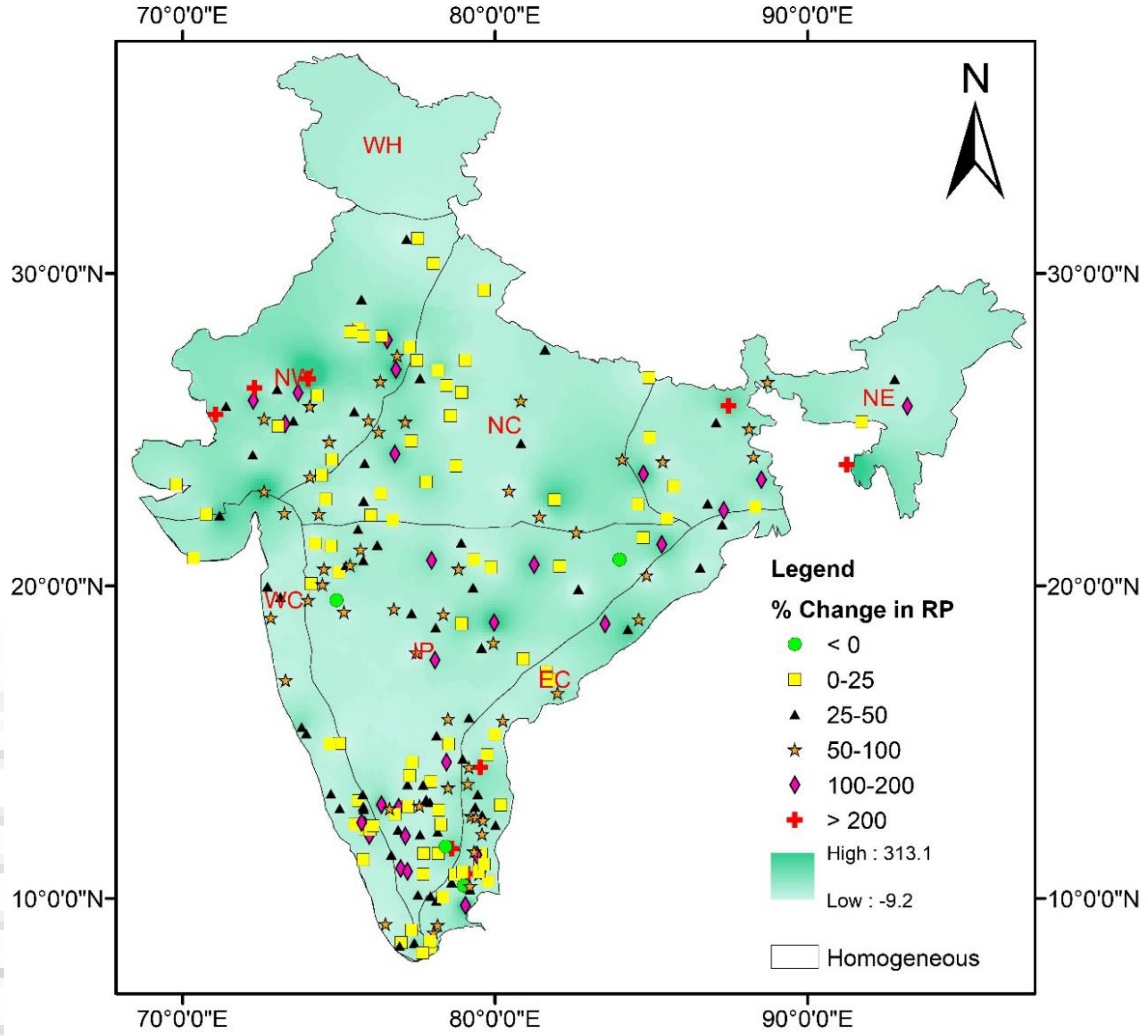

Figure 4.12. Changes in 50-year return level annual maximum rainfall due to non-stationary frequency analysis. The maximum return level given by the best fitted non-stationary models are taken for calculating the change

4.6.4 Causes of Non-stationarity

The results of non-stationary frequency analysis show a significant change in the rainfall quantiles over the country. However, the causes of this non-stationarity in the AMR series across India have not been discussed. The previous studies related to changes in extreme rainfalls showed that the climate change, the natural variability of climatic system, urbanisation, increase of aerosols etc. are the main reasons behind the change. Therefore, in this analysis the results of non-stationarity have been merged in four different classes. These are the non-stationarity due to the trend in the AMR series, non-stationarity due to climate change, non-stationarity due to local temperature change and non-stationarity due to natural climate variability. These classes are based on the use of covariates by different models. The model used time as covariate is classified as non-stationarity due to the trend. The changes of global average temperature can be significantly describe the climatic change (discussed earlier), and therefore, the model used GAT as covariate is classified as non-stationarity due to climate change. Similarly, the non-stationarity due to local temperature change are those models, which uses RAT as covariate. The models used IOD, NION and both IOD and NINO as covariates are demarcated as non-stationarity due to natural climate variability. The results are shown in Figure 4.13. It can be observed that stations showing non-stationarity due to natural climate variability is the highest in numbers (more than 30%). However, the effect of global temperature change is also felt for the AMR series over India. The local temperature change is another reason for the non-stationarity in AMR series. The effect of global and regional temperature change, i.e. mostly on the rising site is observed on the annual maximum rainfall of India.

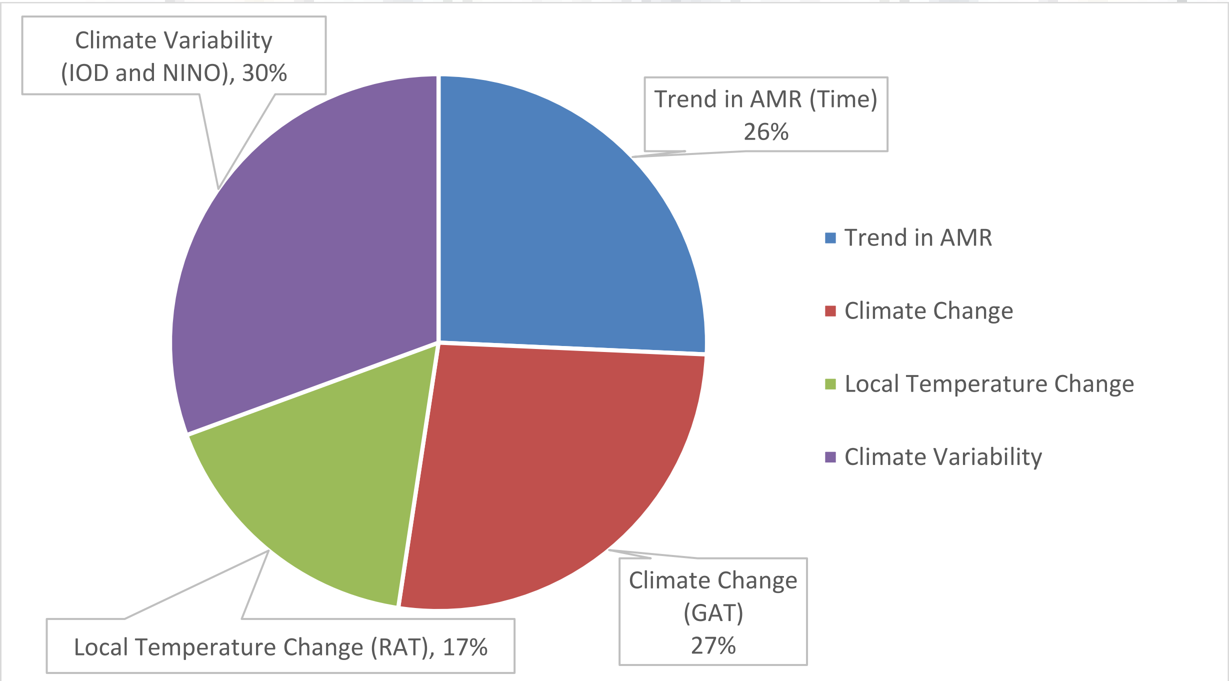

Figure 4.13. Percentage of stations showing non-stationarity due to various reasons in annual maximum rainfall across India

4.6.5 Effect of urbanisation on Non-stationarity

The results of non-stationary analysis show that the changes in temperature (GAT and RAT) is significantly affect the AMR series over India. The role of urbanisation in the changes of extreme rainfall over India has also been studied by a number of researchers. The study by Singh et al. (2016) shows that the extreme rainfall become non-stationary due to rapid urbanisation. Niyogi et al. (2010) reported that in the context of fine-resolution spatial changes, urbanization might affect the patterns and extremes of regional rainfall through urban roughness, urban heat island, modified winds over urban area, and aerosols. This evidence provides sufficient connectivity between urbanization and non-stationarity in the rainfall extremes. Therefore, the role of urbanisation in non-stationarity of AMR station data over India was also investigated in this study.

To understand the role of urbanisation in non-stationarity, the results analysed for this study are divided into three classes. These classes are divided based on population density data (based on 2000-2001 census data). Based on population density data, the stations are divided into urbanised, urbanising and rural areas. The urbanised areas are mainly covered by the cities with population density more than $1000/km^2$. The areas with population density in between $200/km^2$ to $1000/km^2$ are demarcated as urbanising area. The rural areas are those with less than $200/km^2$ population density. The results are summarised in Table 4.11. The results clearly indicated that the stations under urbanised and urbanising areas are more likely to follow non-stationarity than the stations of rural areas. This may be because in the urbanising areas the process of urbanisation is continuing. In India, the process of urbanisation is still continuing in the urbanised areas. For this reason, the stations under urbanised category show 100% non-stationarity. The stations of rural areas are showing some typical change from stationarity to non-stationarity. This may be due to the change of land use and land cover pattern with the intensifying agricultural activities over the rural areas. The results clearly indicate that for non-stationarity analysis the extent of urbanisation and the changes in land use land cover due to increasing agricultural activity should be considered.

Table 4.11 Comparison of stationary and non-stationary results under each category of classes.

Class	Stationary		Non-stationary	
	No. of station	% of station	No. of station	% of station
Urbanised	-	-	15	100
Urbanising	6	5	117	95
Rural	28	28	73	72

4.7 CONCLUSIONS

The frequency analysis of the AMR series of 239 stations spread across India, with each having data length of 70 years (1931 to 2000) is carried out under stationary and non-stationary conditions respectively using GAMLSS statistical modelling framework. GAMLSS is a useful statistical tool for modelling extreme hydro-meteorological variables under non-stationary condition (Villarini et al., 2009). The dependence of the distribution parameter under non-stationary condition was modelled by explanatory covariates i.e. time, GAT, RAT, and climate indices.

The results of non-stationary frequency analysis of annual maximum rainfall over the country show that the GAMLSS model can be used for the non-stationary frequency analysis. The results indicated that due to non-stationarity in annual maximum rainfall, the rainfall quantiles are mostly increasing over the country. The storage and other structures over the country are based on the stationary design values and might be need to revisit those design values in the context of non-stationarity. The reason of the non-stationarity in AMR series over India was also investigated. It was found that the increase in extreme rainfall is mainly due to the combined effect of climate change (increasing global average temperature), climate variability (NINO and IOD indices used in the analysis) and local temperature change (increasing or decreasing regional average temperature) over India. The results also show that the recent increase in temperature (GAT and RAT) at global and regional scales has a major impact on AMR series over India. The IOD and NINO, i.e. climate variability indices have a significant influence on the stations of coastal region. The categorisation of the stations under urbanised, urbanisation and rural areas also indicated the influence of urbanisation and intensification of agricultural activities on non-stationarity of the extreme rainfall over India. However, this aspect of urbanisation and intensification of agricultural activities in urban and rural areas need further investigation.

CHAPTER 5
NON-STATIONARY FLOOD FREQUENCY ANALYSIS OF NARMADA RIVER BASIN, INDIA

5.1 GENERAL

Global warming has become a major concern for the world in recent times. According to the Intergovernmental Panel on Climate Change (IPCC), the observed global warming is mainly due to the human activities, since the mid-20th century. The anthropological activities like increasing urbanisation and construction of storage structures in the rivers are changing the streamflow regimes (Mittal et al., 2016) and consequently introducing non-stationarity in flood records (Villarini et al., 2009; Zhang et al., 2009; Lopez and Frances, 2013). In Narmada river basin, a number of water storage structures have been constructed to provide water during the non-monsoon season. Many researchers (Gosain et al., 2006; Gupta et al., 2011) have reported that the Narmada river basin will face water-stressed conditions due to climate change. The combined effect of storage structures and climate change will trigger non-stationarity in extreme floods in Narmada river basin. Hence, there is a need to consider this aspect in flood quantile estimation.

This chapter presents the non-stationary flood frequency analysis of Narmada river at 6 gauging sites using NINO3.4 SST anomaly, Indian Ocean Dipole Mode Index (IOD), Global average temperature (GAT), and reservoir index (RI) as covariates. The GAMLSS model is used for carrying out flood frequency analysis.

5.2 STUDY AREA AND DATA USED

5.2.1 Study Area

The Narmada river, one of the seven most holy rivers of India, originates from the Amarkantak plateau of Madhya Pradesh, flows through the states of Madhya Pradesh, Maharashtra and Gujarat and finally meets the Gulf of Khambhat. It is the fifth longest river of the Indian subcontinent. The length of the river is 1312 km and it covers a basin area of 98,796 km^2 (Figure

5.1). The major part of the basin, i.e. almost 57%, is agricultural land. The development of the water resources of the basin started in 1980, when Government of India formed an administrative authority called Narmada Control Authority (NCA). A number of storage reservoirs, 274 till 2010, have been constructed in the river basin. These reservoirs are used -

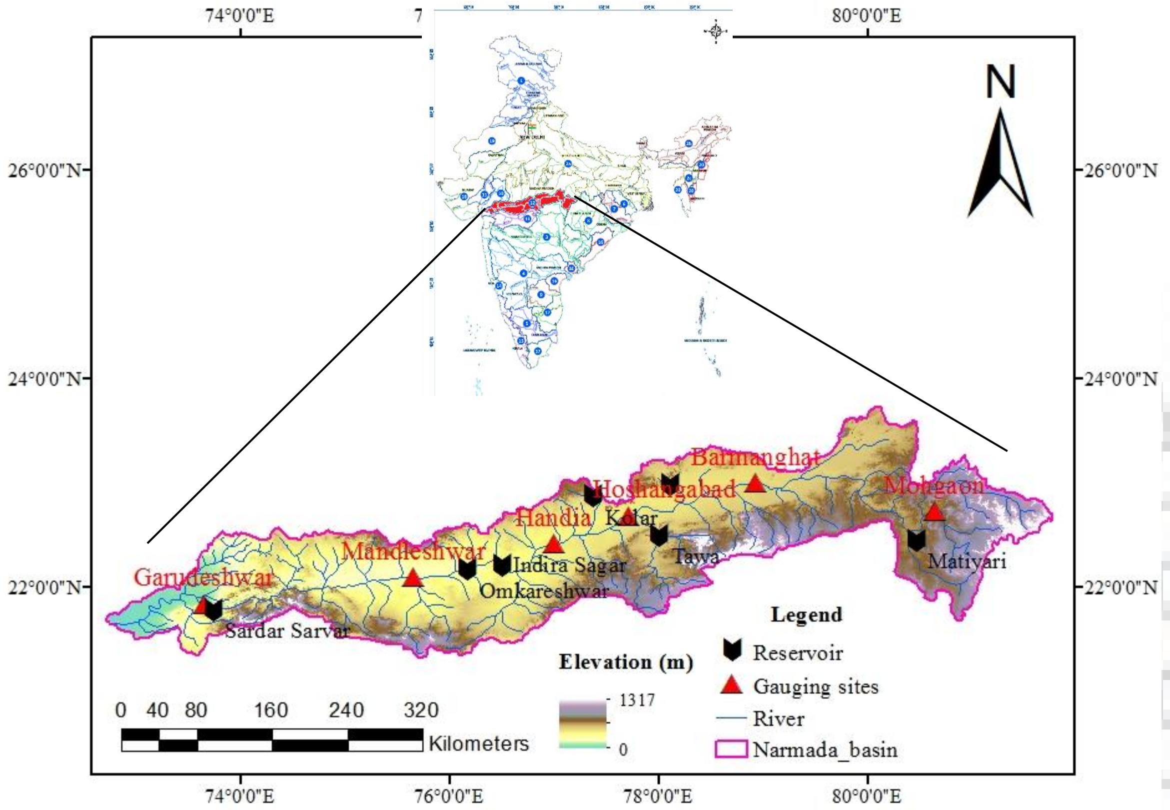

Figure 5.1. Locations of the Narmada River basin, hydrological stations and storage reservoirs

Table 5.1 Details of seven water reservoirs in the Narmada river basin.

Name	Year of Completion	Latitude (Degree)	Longitude (Degree)	Drainage Area (km^2)	Total storage capacity (10^6 m^3)
Matiyari	1986	22.46	80.46	158.75	56.8
Barna	1977	22.99	78.10	1176	539
Tawa	1978	22.50	78.00	6000	2312
Kolar	1990	22.89	77.37	508	270
Indira sagar	2006	22.21	76.49	61642	12200
Omkareshwar	2007	22.18	76.16	64880	987
Sardar sarvar	1979	21.79	73.74	87000	9500

-for a variety of purposes such as water supply for drinking, irrigation, and hydropower generation. Seven major reservoirs of the basin, namely Matiyari, Barna, Tawa, Kolar, Indira sagar, Omkareshwar and Sardar sarvar, have a total storage capacity of 2.58×10^{10} m^3. The details of these reservoirs are given in Table 5.1 and these reservoirs are shown in Figure 5.1.

5.2.2 Data Used

The daily discharge data of six gauging stations (Fig. 5.1 and Table 5.2) were downloaded from Water Resources Information System of India (http://www.india-wris.nrsc.gov.in/wris.html). The stations are uniformly distributed over the basin. There are major reservoirs in the upstream of 5 gauging stations. One station namely, Mohgaon, is in the natural regime. Table 5.2 provides the main characteristics of the gauging stations. The quality of the data is ensured by Central Water Commission (CWC) before its release.

Table 5.2 Main characteristics of six gauging stations used in this study.

Name	Latitude (Degree)	Longitude (Degree)	Start and end year of data	Drainage Area (km2)	Annual Average stream flow (m3/s)	Coefficient of Variation
Mohgaon	22.76	80.62	1978-2012	3919	72.15	3.75
Barmanghat	23.03	79.02	1972-2012	26453	381.40	2.62
Hosangabad	22.76	77.73	1973-2012	44548	692.55	2.65
Handia	22.49	76.99	1978-2012	54027	784.02	2.43
Mandleshwar	22.17	75.66	1971-2012	72809	1812.19	2.54
Garudeshwar	21.89	73.65	1972-2012	87892	945.20	2.74

Two climate indices, namely, NINO3.4 Sea Surface Temperature (SST) anomaly and Indian Ocean Dipole Mode Index (IOD) have been used in this study. These indices are used to examine the impact of climate variability on the flood frequency estimates. The impact of these two climate indices over Indian rainfall changes have also been explained by Berkelhammer et al. (2013), Surendran et al. (2015), Mondal and Mujumdar (2015). The data of NINO3.4 (5N-5S; 170W-120W) monthly SST anomalies from 1951 to 2000 mean were extracted from http://www.esrl.noaa.gov/psd/gcos_wgsp/Timeseries/Nino34/. The monthly Indian Ocean Dipole Mode Index (IOD) datasets were taken from http://www.jamstec.go.jp/frsgc/research/d1/iod/iod/dipole_mode_index.html. The global average temperature (GAT) is also used as a covariate in this study. GAT is used to see the effect of human-induced climate change (Hegerl et al., 2007). The monthly observed HadCRUT4 land surface air GAT anomalies with respect to 1961 to 1990 mean have been extracted from http://www.metoffice.gov.uk /hadobs/ hadcrut4/.

5.3 METHODOLOGY

5.3.1 Reservoir Index (RI)

In order to study the impact of reservoir regulation on river floods, a dimensionless reservoir index (RI) was used in this study. The RI index is proposed by Lopez and Franes (2013) as:

$$RI = \sum_{i=1}^{N} \left(\frac{A_i}{A_T}\right) \times \left(\frac{C_i}{C_T}\right) \quad (5.1)$$

where, N is the number of reservoirs upstream of the gauging station, A_i is catchment area of each reservoir, A_T is catchment area at the gauging station, C_i is the total storage capacity of each reservoir, and C_T is mean annual runoff at the gauge station. Lopez and Franes (2013) suggested a threshold value of 0.25 to determine whether the reservoir induced alteration is low or high.

5.3.2 Frequency Analysis under Non-stationarity

Flood frequency analysis under non-stationary condition requires a modelling framework, in which the selected distribution parameters can vary with time or can be considered as a function of explanatory variables. In this study, GAMLSS model (Rigby and Stasinopoulos, 2005) has been used for carrying out non-stationary frequency analysis. The observed annual maximum discharges follow a parametric distribution function in GAMLSS modelling framework. Four distribution functions, namely, Gumbel, Weibull, Gamma, and Lognormal have been used in the present study. These distributions have been used widely in streamflow modelling (El Adlouni et al., 2008; Villarini et al., 2009).

The parameters of the selected distributions were considered to be stationary as well as non-stationary using time (t), NINO4.3 SST, IOD, GAT, and RI as covariates. This resulted in the following five types of models:

(i) Model with stationary parameters, named as Model 0;

(ii) Time varying non-stationary model, named as Model 1;

(iii) Non-stationary model with climate indices (NINO4.3 SST, and IOD) dependent parameters, named as Model 2;

(iv) Non-stationary model with parameters varying with GAT, named as Model 3;

(v) Non-stationary model with parameters varying with RI, named as Model 4.

Akaike Information Criterion (AIC) (Akaike, 1974) was used to select the best fitting distribution function. The worm plot (de-trended form of a qq-plot, which highlights the departure from normality) was used to check the goodness of fit of the distributions. However, in the absence of goodness of fit statistics, normality and independence of the residuals, as recommended by Rigby and Stasinopoulos (2005), was also checked for the model selection. All the computations were performed in R based GAMLSS model.

5.4 RESULTS AND DISCUSSION

The association of the annual maximum discharges of all the six stations with four covariates are checked using the Spearman's rank correlation coefficient. The significance of the correlation is also investigated. The correlation coefficients for six different sites are given in Table 5.3. It can be observed from the table that the relationship of annual maximum discharge with NINO, IOD, and GAT are not statistically significant for any of the stations. The correlations of annual maximum discharge with RI for all the stations are statistically significant except in the Handia station, which clearly shows the regulation effect of water reservoirs over flood generation processes in Narmada river basin. Two climate indices at a time were used for correlating the distribution parameters. The correlation between annual maximum discharge and GAT is higher than the relationship with climate indices for all the stations except in Mohgaon station. These results are further used for the GAMLSS modelling exercise.

Table 5.3 Correlation of annual maximum discharge in six sites with RI, GAT, NINO, and IOD indices.

Stations	RI	GAT	NINO	IOD
Mohgaon	-	0.046	0.050	0.120
Barmanghat	**-0.489**	-0.275	-0.102	0.149
Hoshangabad	**-0.592**	-0.293	-0.107	0.067
Handia	-0.199	-0.266	0.164	0.109
Mandleshwar	**-0.348**	-0.294	-0.079	-0.058
Garudeshwar	**-0.493**	-0.278	-0.142	-0.158

Bold values represent the significant correlation at 5% significance level

5.4.1 Implementation of GAMLSS Model

The annual maximum discharge series (AMS) of six gauging stations were analysed for frequency analysis of stationary and non-stationary conditions using GAMLSS for five different models as explained in previous section. Table 5.4 provides the details of the five models fitted for all the six gauging stations.

In the first step the stationary model, i.e. Model 0 is setup for Mohgaon station. For stationary model, the lognormal distribution fits well to the AMS of Mohgaon site. The value of two parameters is given in Table 5.4. The Model 1, i.e., time varying nonstationary model is then applied to the flood series of Mohgaon station. The Lognormal distribution is also suited best for the Model 1. For the flood series of Mohgaon station, the cubic spline model is applied for both the θ_1 (related to mean) and θ_2 (related to standard deviation) parameters. Similarly, for Model 2, which analyses the effect of climate variability, the lognormal distribution is best suited. In this case, the θ_1 parameter is linearly varying with the external covariate NINO and IOD, while the θ_2 parameter is varying non-linearly (using cubic spline smoothing technique) with the external covariate NINO and IOD. Likewise, for Model 3, which shows the effect of climate change, also the lognormal distribution is suited best. The θ_1 parameter is linearly varying with the external covariate GAT, while the θ_2 parameter is constant. The station Mohgaon is in the upper most portion of the Narmada river basin, and in the upstream of the gauging station no storage reservoir is constructed till date. Therefore, the Model 4, which consider RI as an external covariate, was not applied for the Mohgaon station. Using the similar procedure all the five models are set up for each of the other stations. The best fitting distribution function was selected for each of the five different models based on AIC value, normality of the residuals and worm plots. Then the AIC value of all the five models was calculated. Finally, the best model for a station was selected on the basis of minimum AIC value.

The AIC values for all the models are tabulated in Table 5.5. It can be observed from the Table 5.5, that the Model 2 is giving the minimum AIC value for three stations, namely Mohgaon, Handia, and Mandleshwar. The AIC value is minimum for other three stations, namely Barmanghat, Hoshangabad, and Garudeshwar for the Model 4. The suitability of the -

Table 5.4 Summary of all five models using Physical Covariates and the type of dependence between the selected covariates with distribution parameters.

Model	Variables	Mohgaon	Barmanghat	Hoshangabad	Handia	Mandleshwar	Garudeshwar
Model 0	Fitted Distribution	Lognormal	Weibull	Gamma	Weibull	Weibull	Weibull
	θ_1	7.39	9008.73	11798.05	15614.18	22091.93	22212.02
	θ_2	1.26	6043.88	5902.80	9555.25	14228.98	15118.77
Model 1	Fitted Distribution	Lognormal	Weibull	Weibull	Gamma	Weibull	Weibull
	θ_1	cs(t)	t	t	t	cs(t)	cs(t)
	θ_2	cs(t)	ct	ct	t	ct	ct
Model 2	Fitted Distribution	Lognormal	Weibull	Lognormal	Weibull	Weibull	Weibull
	θ_1	NINO+IOD	cs(NINO)	cs(NINO)	cs(NINO+IOD)	cs(IOD)	cs(IOD)
	θ_2	cs(NINO+IOD)	ct	NINO+IOD	cs(NINO+IOD)	IOD	IOD
Model 3	Fitted Distribution	Lognormal	Weibull	Weibull	Weibull	Weibull	Weibull
	θ_1	GAT	GAT	GAT	GAT	GAT	cs(GAT)
	θ_2	ct	GAT	ct	ct	ct	ct
Model 4	Fitted Distribution	-	Gamma	Gumbel	Gamma	Weibull	Weibull
	θ_1	-	RI	cs(RI)	cs(RI)	RI	cs(RI)
	θ_2	-	cs(RI)	cs(RI)	ct	ct	RI

cs(.) indicates the dependence via cubic splines; without cs(.) denotes linear dependence; and ct refers to a constant parameter.

-models was further checked using the normality of the residuals and the worm plots. The summary of all the residual moment's and the Filliben correlation coefficients for the stationary, time varying non-stationary and best suited non-stationary models are given in Table 5.6. The worm plot of all the stations except for Handia station, for three type of models are shown in Figure 5.2.

In this study, Model 2 is selected as best model for Mohgaon, Handia, and Mandleshwar stations, while the Model 4 is selected as best model for Barmanghat, Hoshangabad, and Garudeshwar stations. The flood regimes of those three stations are heavily influenced by the upstream reservoirs, and therefore, the model which includes the effect of reservoir index is selected. Although, the Mandleshwar station shows a very high value of RI than the Barmanghat station, thereafter, the Model 4 is not best suited for the Mandleshwar station. The reservoirs completed in the upstream of the Mandleshwar station after 2005. Therefore, the data length from 2005 to 2012 is not sufficient to draw any concrete conclusions regarding reservoir index. This type of situation can be avoided by using a new model, which can take care of both the influence of climate variability and reservoir. In this study, the main aim is to select the best type of covariate for each of the gauging stations, and hence, no model is generated, which can take care of the influence of more than one external covariate. However, Model 2 shows the combined effect of NINO3.4 SST anomaly and IOD index. Those two indices are combinedly used to see the influence of climate variability on the floods of Narmada basin.

Table 5.5 AIC values for the five different models analysed in each of the stations.

AIC	Mohgaon	Barmanghat	Hoshangabad	Handia	Mandleshwar	Garudeshwar
Model 0	643.91	817.00	819.71	710.01	901.81	896.24
Model 1	635.35	812.93	815.42	707.79	896.22	889.18
Model 2	**625.18**	816.46	804.85	**689.05**	**895.83**	893.54
Model 3	645.74	817.46	817.50	710.53	900.43	895.09
Model 4	-	**802.69**	**788.02**	700.45	897.06	**877.61**

"-" denotes non availability of covariates for the station. Bold numbers indicate the minimum AIC values.

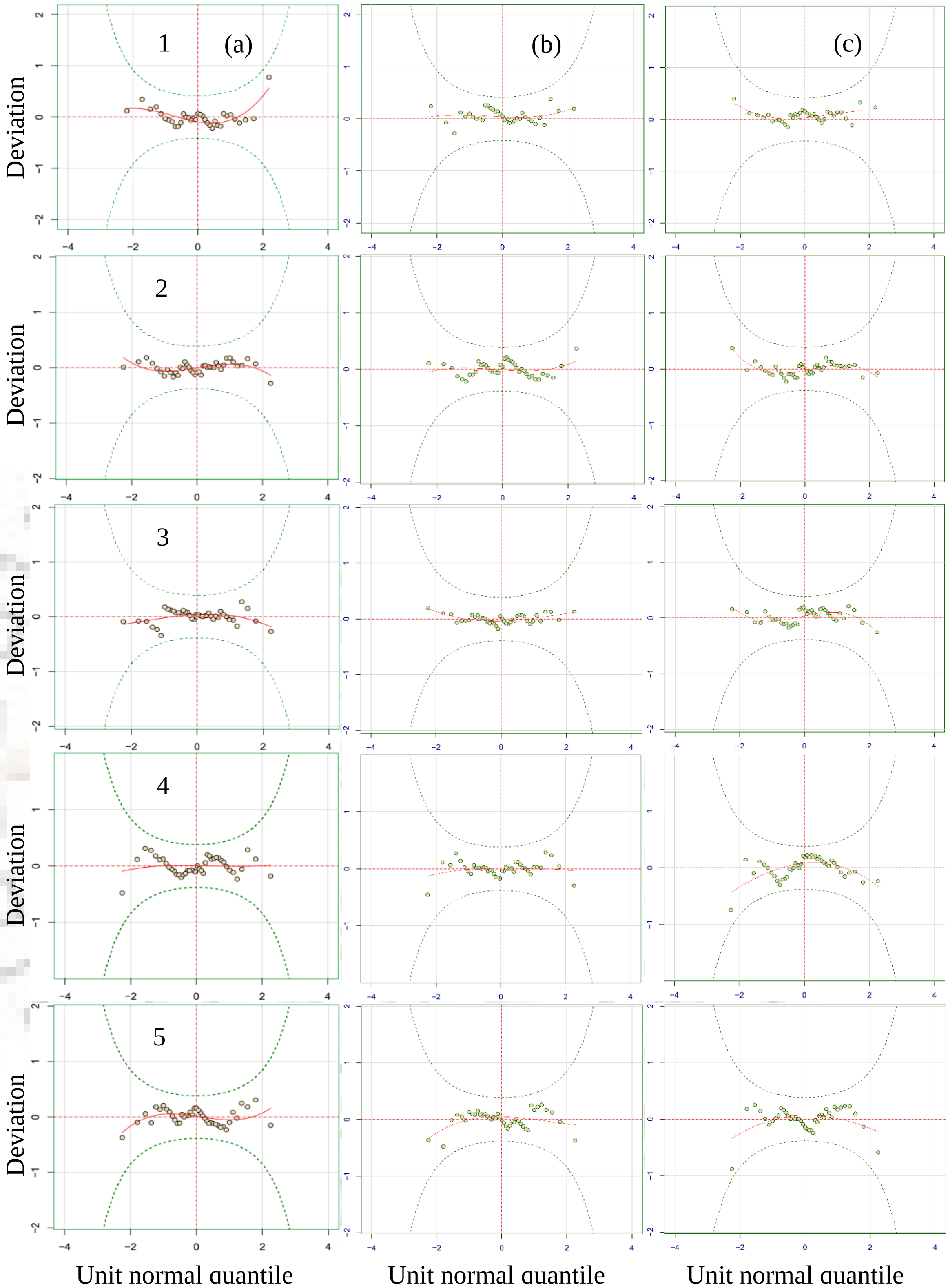

Figure 5.2. The worm plots of residuals from three models (i.e., (a) stationary, (b) time varying non-stationary and (c) best fitted non-stationary) of annual maximum discharge. The dotted lines denote 95% confidence limit. The five rows of sub-plots are the results of (1) Mohgaon, (2) Barmanghat, (3) Hoshangabad, (4) Mandleshwar, and (5) Garudeshwar stations.

Table 5.6 Summary of residuals moment's and computed Filliben coefficients for stationary, time varying non-stationary and best fitted non-stationary models.

Types of models	Stations	Mean	Variance	Skewness	Kurtosis	Filliben coefficient
Stationary	Mohgaon	-0.000	1.029	0.052	3.417	0.984
	Barmanghat	-0.003	1.023	0.035	2.268	0.995
	Hoshangabad	0.001	1.026	-0.186	2.553	0.993
	Handia	-0.003	1.030	0.034	2.288	0.992
	Mandleshwar	-0.000	1.033	-0.078	2.836	0.988
	Garudeshwar	0.001	1.032	-0.068	3.066	0.990
Time varying non-stationary	Mohgaon	0.055	1.026	0.079	2.713	0.992
	Barmanghat	0.000	1.017	0.077	2.822	0.992
	Hoshangabad	0.001	0.999	0.177	2.515	0.997
	Handia	-0.002	1.028	-0.092	2.245	0.995
	Mandleshwar	-0.001	1.038	-0.102	2.812	0.992
	Garudeshwar	-0.002	1.063	-0.237	2.906	0.988
Best fitted non-stationary	Mohgaon	0.074	1.024	0.019	2.424	0.994
	Barmanghat	-0.003	1.004	0.010	2.145	0.994
	Hoshangabad	0.024	1.020	-0.049	2.138	0.993
	Handia	0.017	1.044	-0.021	2.159	0.992
	Mandleshwar	-0.007	1.106	-0.045	2.842	0.984
	Garudeshwar	-0.001	1.076	-0.037	3.298	0.979

For Mohgaon station, θ_1 (related to mean) parameter of Model 2 linearly varies with NINO and IOD, while the θ_2 (related to standard deviation) parameter of Model 2 is non-linearly (cubic spline, cs) vary with NINO and IOD. For Handia station, both the parameters of Model 2 are non-linearly vary with NINO and IOD. The results of Model 2 for Madleshwar shows that the θ_1 parameter is non-linearly vary with IOD and the θ_2 parameter linearly varies with IOD. For Barmanghat station, in which Model 4 is selected, the θ_1 parameter is linearly vary, while the θ_2 parameter is non-linearly vary with RI. In Hoshangabad, both the distribution parameter non-linearly vary with RI. However, in Garudeshwar station, the dependence of both the parameters with RI is opposite of the dependence found in Barmanghat station.

It can be observed from Table 5.6 that for three models (Model 0, Model 1, and best fitted model) the residuals follow normality for all the gauging stations. The Filliben coefficient value is also higher than 0.973 (critical value for a sample size of 42 obtained from Filliben, 1975) for all the models and for all the gauging stations. Figure 5.2 also shows that for all the stations, the standard residual values are within the range of 95% confidence limits for all the models. However, the worm plot of residuals for Handia station is not shown in Figure 5.2.

This further clarifies the selection procedure of the best suited model for each of the gauging stations. The selected model is then used to see the performance of best fitted models for all the gauging stations.

5.4.2 Performance of Non-stationary Models

The results of time varying non-stationary and best fitted non-stationary models for all six gauging stations are shown in Figure 5.3. The observed values, 2.5th, median (50th), and 97.5th percentiles were plotted in the figure. The results of non-stationary model for Mohgaon station is depicted in Figure 5.3 (a). The figure shows that the 2.5th, median, and 97.5th percentile values are correctly model all the values of the annual maximum series by both the non-stationary models. Generally, both the model followed a decreasing tendency after 1990. Thereafter, both increasing and decreasing tendency is also observed. However, the time varying non-stationary model cannot capture the abrupt changes in annual maximum discharge series. The best fitted non-stationary model (for Mohgaon the climate variability model) almost perfectly captures the abrupt changes in annual maximum discharge series.

The results of non-stationary models are depicted in Figure 5.3 (b) for the Barmanghat station. The 2.5th, median percentiles are almost correctly modelled the lower values of the annual maximum discharge series by both times varying (Model 1) and best fitted (Model 4, taken care the reservoir regulation problems) nonstationary models. However, the 97.5th percentiles cannot model the higher value in 1999 by the Model 1, whereas, this is not the case for Model 4, which modelled all the values. The percentiles of Model 1 followed a decreasing tendency from the start, while, after 1988, no decreasing tendency is followed by Model 4. Also the abrupt changes in flood series cannot be captured by the Model 1. Figure 5.3 (c) shows the results of non-stationary models in the Hoshangabad station. Similar results as obtained for Barmanghat station is observed for the Hoshangabad station. For the Hoshangabad station both the non-stationary models follow a decreasing tendency from the start by the 97.5th percentile.

The results of non-stationary models for the Handia station are shown in Figure 5.3 (d). In this case, the best fitted non-stationary model is Model 2. For the Handia station also, both the 2.5th and median percentiles are almost correctly modelled the lower values of the annual maximum discharge series by both time varying (Model 1) and best fitted (Model 4, taken care-

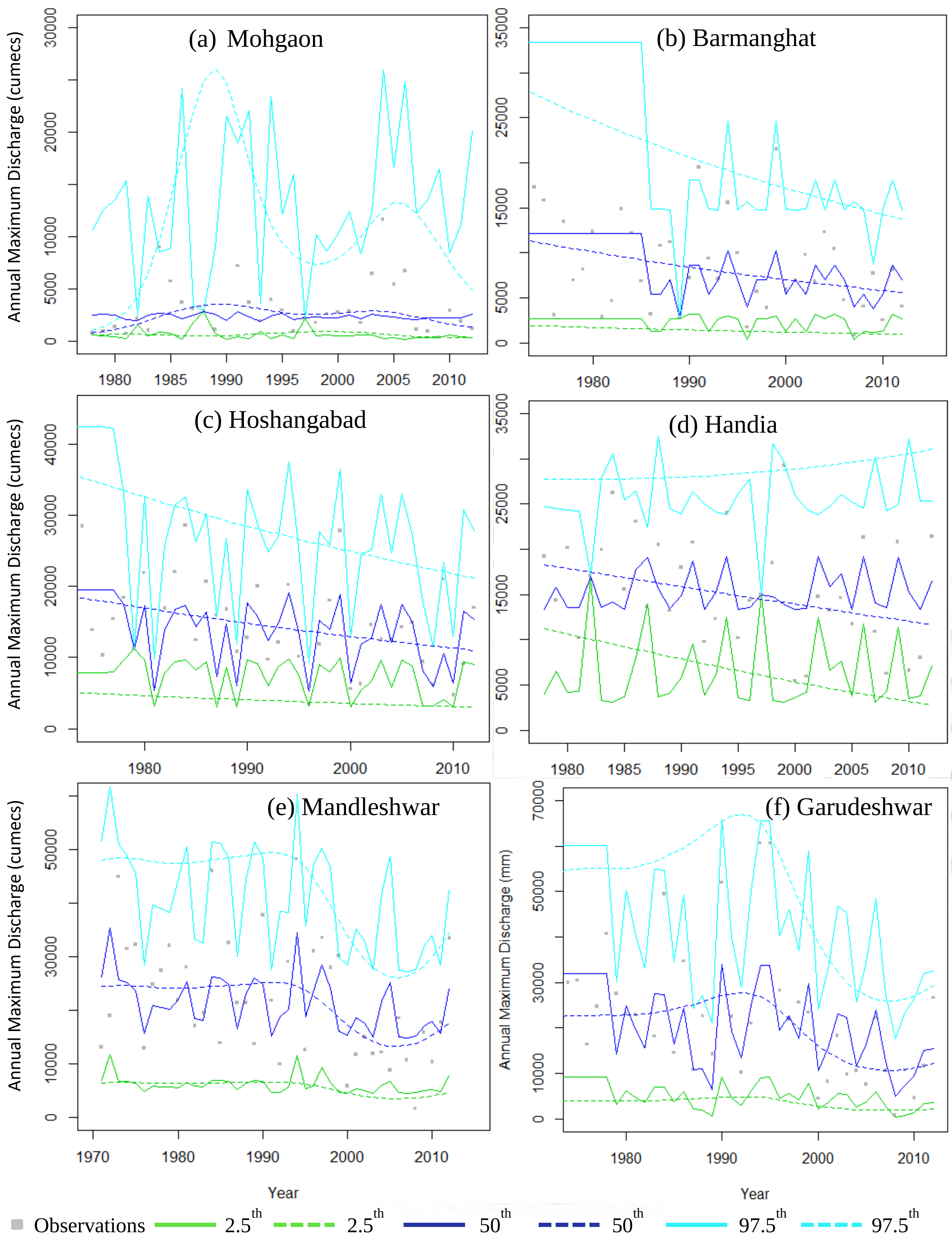

Figure 5.3. Changes in the 2.5th, median (50th), and 97.5th percentile values estimated by time varying non-stationary and best fitted non-stationary models. The dotted lines are results of time varying non-stationary model, and the smooth lines are the results of best fitted non-stationary model

-the reservoir regulation problems) nonstationary models. Similar results as obtained for Barmanghat station is observed for the Handia station for the 97.5th percentile. However, the results of both the models by the 97.5th percentiles show an increasing tendency for the Handia station. For the Handia station, the time varying non-stationary model follow a decreasing tendency by both the 2.5th and median percentiles, while an increasing tendency was observed by the 97.5th percentile by the same model.

Figure 5.3 (e) and (f) show the results of time varying non-stationary and best fitted non-stationary models for Mandleshwar and Garudeshwar stations respectively. Both the figures show that all three percentiles are capturing the general tendency of the flood series for each of the stations. For both the stations, a decreasing tendency is observed in between 1992 to 2007. For Mandleshwar station, the best fitted non-stationary model is Model 2, while it is Model 4 for Garudeshwar station. For both the stations, the abrupt changes in annual maximum discharges are captured by the respective percentiles of both the best fitted non-stationary models. All the non-stationary model results show that the models perfectly capture the general tendency of the annual maximum discharge series, which implies that the non-stationary models fitted for all the stations are reliable and performed expectedly.

5.4.3 Comparison of Flood Quantile Estimates by Stationary and Non-stationary Models

The design flood quantiles for 50 years return period is estimated by stationary, time varying non-stationary and best fitted non-stationary models for all the six gauging stations, and is depicted in Figure 5.4 (a) to (f). The figure indicates that the design flood quantiles estimated by the stationary model is constant for the entire analysis time period and cannot reflects the temporal changes of flood discharges due to the influence of climate change or climate variability and human interferences. The flood quantiles estimated for 25, 50, and 100 years return period by stationary, time varying non-stationary, and best fitted non-stationary model is given in Table 5.7.

The results of time varying non-stationary model for Mohgaon station indicate that the flood discharge is decreasing for 1978 to 1988 period, thereafter increasing up to 2005, and then decreasing for the period of 2005 to the end of the analysis year, i.e. 2012. The results of stationary model are underestimated in comparison to the results of time varying non-stationary model for 1985 to 1992 period and the results are reverse for the remaining period of analysis.

The design flood quantiles estimated by best fitted non-stationary model capture the changing feature of the actual flood process of Mohgaon station. The best fitted non-stationary model results in four time sudden increase in estimated design flood quantiles. The flood quantile estimated by stationary model for 50 years return period is 21892.5 m^3/sec, while the maximum quantile value estimated by time varying and best fitted non-stationary models are 39956.7 m^3/sec and 43047.5 m^3/sec respectively. The minimum quantile value estimated by both the non-stationary models are lesser than the stationary model and the values are 1093.5 m^3/sec and 2248.6 m^3/sec. The results indicated that the best fitted non-stationary model provides the maximum flood quantile value compared to the stationary and time varying non-stationary models.

The flood quantiles estimated by time varying non-stationary model for both the Barmanghat and Hoshangabad stations are following a decreasing tendency. The flood quantiles are underestimated by stationary model than the time varying non-stationary model up to 1988 for Barmanghat station and up to 1982 for Hoshangabad station. For both the stations, the results are completely different after the respective times. The estimated flood quantiles by the best fitted non-stationary model provide maximum value at the start of the analysis, when the RI value is 0 for both the stations. Thereafter, some sudden shifts in flood quantiles are also observed by the best fitted non-stationary model for both the stations. For both the stations, the maximum flood quantile value is estimated by the best fitted non-stationary models irrespective of return periods (Table 5.7).

The flood quantiles estimated by time varying non-stationary model for Handia station followed an increasing tendency. The flood quantiles are always underestimated by the stationary model compare to the time varying non-stationary model. The best fitted non-stationary model results show the effect of climate variability in the flood process of Handia station. The maximum value of flood quantiles estimated by the best fitted non-stationary model for both 25 and 50 years return period, while the result is maximum by time varying non-stationary model for 100 years return period (Table 5.7).

The time varying non-stationary model for Mandleshwar station provides higher flood quantile values than the stationary model up to 1994, and thereafter, the results are completely different. Similarly more sudden increase in flood quantiles is observed up to 1994 by the -

Table 5.7 Flood quantile estimation for 25, 50, and 100 years return periods from Stationary, time varying non-stationary and best fitted non-stationary (Minimum and Maximum).

Stations	Return Period (Year)	Stationary Quantiles (Cumecs)			Time Varying Non-stationary Quantiles (Cumecs)		Best Fitted Non-stationary Quantiles (Cumecs)	
		95% upper confidence limit	Quantiles	95% lower confidence limit	Maximum	Minimum	Maximum	Minimum
Mohgaon	25	24162.9	15121.8	10332.8	26533.8	1022.4	26387.6	2236.8
	50	38354.6	21892.5	12973.3	39956.7	1093.5	43047.5	2248.6
	100	58824.7	30626.3	15124.2	57922.3	1159.9	67096.4	2257.8
Barmanghat	25	27183.3	20645.1	14106.9	27695.4	13317.2	32000.0	2806.4
	50	33441.3	23760.9	14080.5	31576.1	15174.9	37826.5	2819.5
	100	40442.4	26851.2	13260.0	35374.5	17018.6	44005.1	2829.4
Hoshangabad	25	36059.3	29335.3	22611.3	33985.2	20195.4	39395.2	8799.1
	50	42094.3	32729.3	23364.3	36598.4	21771.8	44280.7	9645.2
	100	48307.8	35829.1	23350.4	38865.7	23107.6	48849.2	10458.3
Handia	25	31259.2	27054.1	22849.0	30123.2	27313.5	31859.3	15000.4
	50	34510.2	29052.6	23594.9	34608.8	29270.1	34856.8	15000.4
	100	37637.6	30769.3	23901.0	38815.9	30964.2	37470.7	15000.4
Mandleshwar	25	56358.2	45234.2	34110.2	48336.8	25446.7	60521.6	26692.3
	50	66425.6	50750.9	35076.2	53293.9	28056.7	65582.3	29131.4
	100	77126.6	56004.8	34883.0	57940.1	30502.8	70249.1	31395.6
Garudeshwar	25	87430.4	53898.1	40643.5	63732.8	24613.9	63435.9	16389.5
	50	113895.9	63622.3	43972.2	73005.9	28195.4	70213.7	19892.8
	100	145176.1	73753.2	45937.8	82397.4	31822.3	76862.3	23640.6

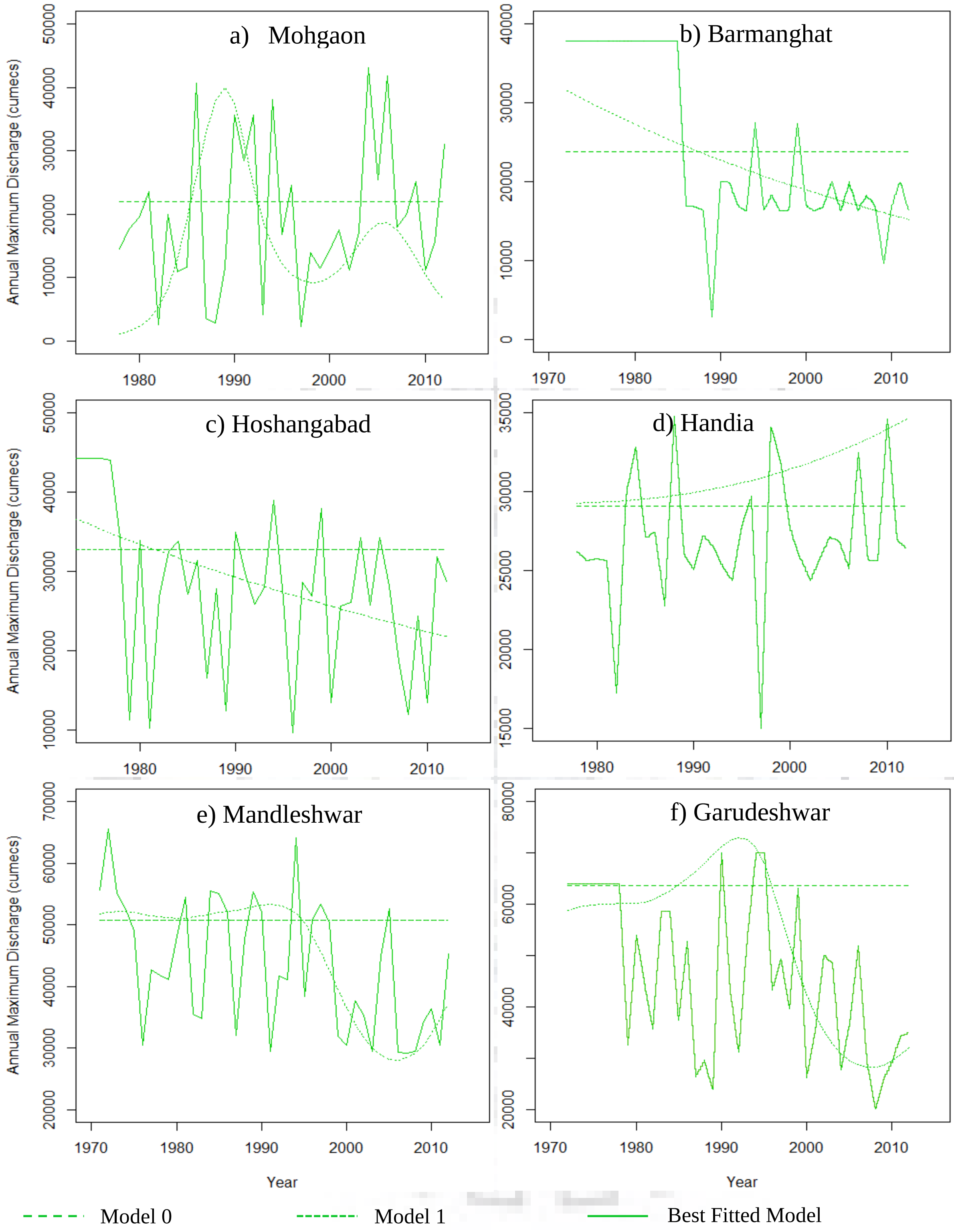

Figure 5.4. Estimated flood quantiles for 50 year return period by stationary, time varying non-stationary and best fitted non-stationary models

-best fitted non-stationary model. For Mandleshwar station the highest value of estimated flood quantile is estimated by the best fitted non-stationary model irrespective of the return periods.

The flood quantile is over estimated by the stationary model than both the non-stationary models for the Garudeshwar station for most of the analysis time period. Only two sudden increase more than the stationary quantiles is observed in 1990 and 1993 by the best fitted non-stationary model. However, the flood quantiles estimated by stationary model is underestimated than by the time varying non-stationary model for the 1986 to 1993 period. The highest flood quantile value is always estimated by the time varying non-stationary model for the Garudeshwar station. Generally, the results of the best fitted non-stationary model show an abrupt behaviour similar to the observed dataset. However, in all the stations the non-stationary model shows a decreasing tendency except Mohgaon and Handia stations. The decreasing tendency is mainly observed after the construction of reservoirs for all the stations. Therefore, the influence of reservoir should always consider for the flood frequency analysis. The design flood quantiles of a non-stationary process will always be over- or under-estimated for flood frequency analysis by a stationary model. Besides, the results of frequency analysis by a non-stationary model may show dramatic changes with time, while a stationary model will always provide a constant value.

5.4.4 Prediction Using Non-stationary Model

The frequency analysis of floods from three stations (Mohgaon, Handia, and Mandleshwar) are showing non-stationarity due climate variability and other three stations (Barmanghat, Hoshangabad, and Garudeshwar) are showing non-stationarity due to RI. The non-stationary models are then prepared using both the climate variability indices and RI as external covariates. These non-stationary models are than used to predict the design flood quantiles. For prediction purpose, the annual maximum discharge of up to 2004 is used to calibrating the best fitted non-stationary model for all the stations. The calibrated model is then used to predict the annual maximum discharge of 2005-2012 in terms of 2.5th, median, and 97.5th percentiles. The prediction of 2.5th, median, and 97.5th percentiles using best fitted non-stationary models for all the stations are depicted in Figure 5.5. The predicted non-stationary model is capable of capturing the fluctuation of actual flood process for their respective stations. The 97.5th and 2.5th percentiles estimated by the non-stationary model is almost correctly modelled the flood values. Therefore, it can be said that the non-stationary model includes the effect of climate variability or the influence of reservoir index, performs well for the flood frequency analysis, and can also be used to correctly predict the flood values for the Narmada river basin.

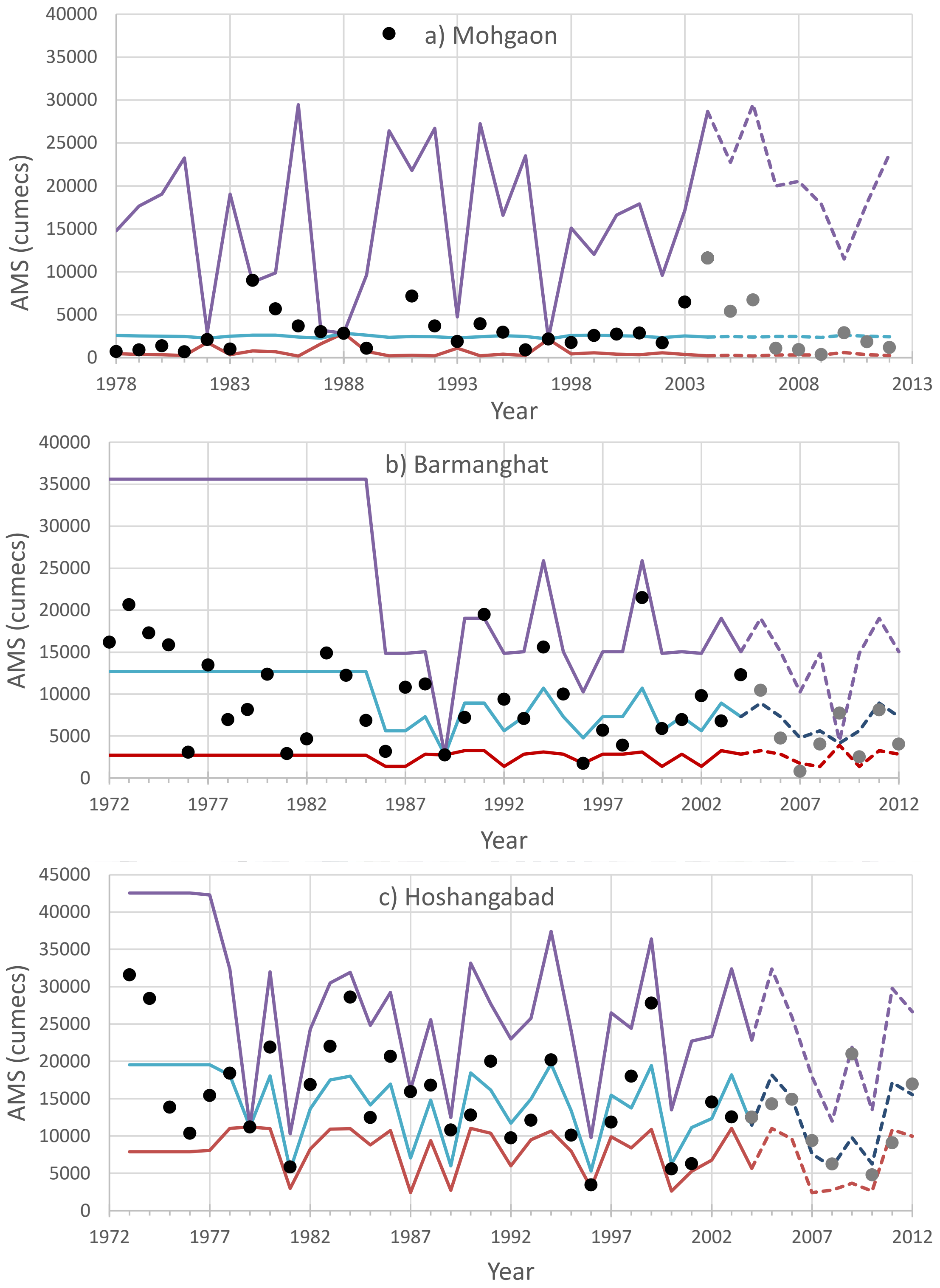

Figure 5.5. Prediction of annual maximum discharge series by the best fitted non-stationary model for all the stations of Narmada river basin. The observed annual maximum discharge of up to 2004 are used to model fitting (black data points and solid lines). The prediction of annual maximum discharge from 2005 to 2012 is made using the fitted model (dotted lines). The gray data points are observed data not used for modelling (used as referenced data)

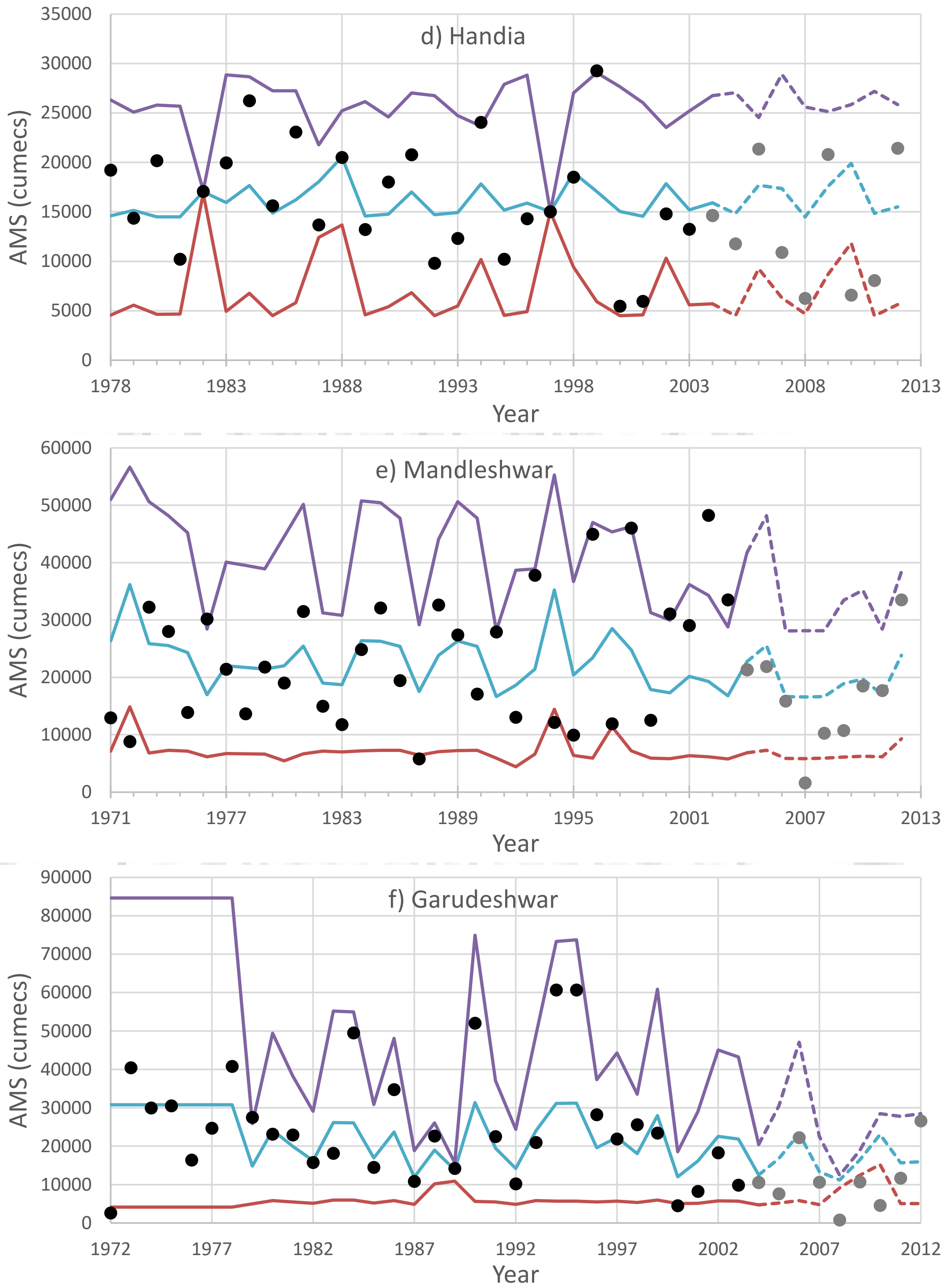

Figure 5.5. Cont'd

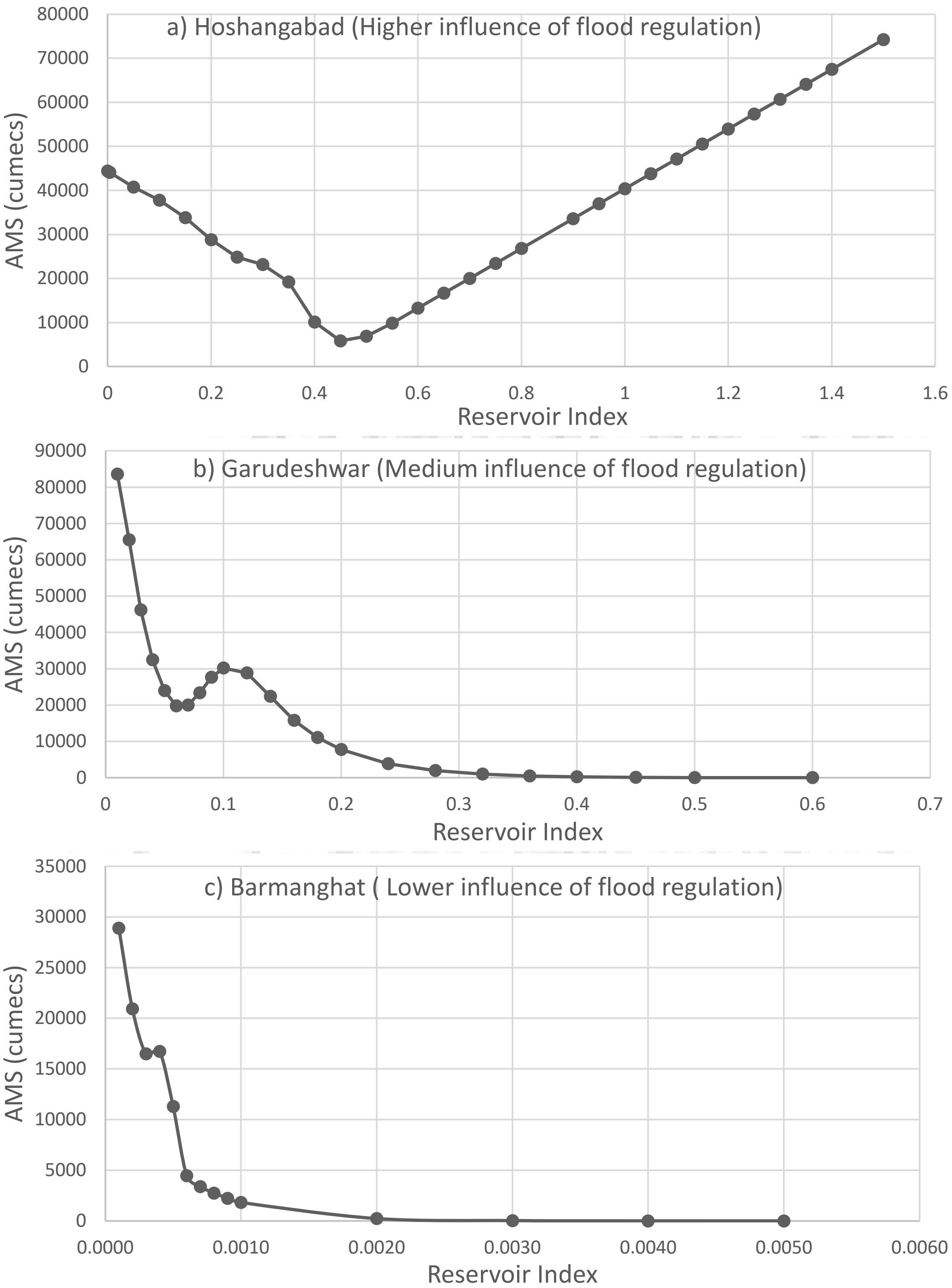

Figure 5.6. Predicted Design flood quantiles (50 years return period) from a non-stationary model for three stations. From the three stations, first station is showing higher influence of reservoir, second is showing medium influence of reservoir, and the third is show lower influence of reservoir in flood quantile prediction

The design flood quantiles for 50 years return period estimated by non-stationary model, which includes reservoir as an external covariate, is shown in Figure 5.6. Three figures, i.e., Figure 5.6 (a) to (c) are depicted, out of which the first one is for Hoshangabad station, the second one is for Garudeshwar station, and the last one is for Barmanghat station. The Hoshangabad stations show a high influence of the constructed reservoir in the upstream of the station. For other two stations, the Garudeshwar shows a medium influence, while Barmanghat shows a very low influence of the constructed reservoir in the upstream of both the stations. The reservoir index is used beyond the range of the actual value obtained by the observed data for non-stationary modelling of all three stations. The design flood quantiles for 50 years return period showing the decreasing tendency for RI values up to 0.45 for the Hoshangabad station. Thereafter the design flood value is increased with the RI value. The design flood quantiles of 50 years return period estimated by non-stationary model for the station with medium influence of reservoir, i.e., Garudeshwar shows a decreasing tendency for the lower and higher values of RI. The maximum flood quantile value is obtained as 84000 m3/sec for a RI value of zero and then continuous decrease up to the RI value of 0.06. Thereafter a very small increase in design flood values are observed for RI values up to 0.1 and beyond this range the design flood value continuously decreasing. Almost similar result is observed for the Barmanghat station, in which the influence of reservoir is very less. For Barmanghat station, the maximum design flood value is obtained as 30000 m3/sec for a zero value of RI and then it is continuously decreasing with the increasing RI values. These results can be very useful for the design of various structures like, bridges, reservoirs etc. in the downstream of the already constructed reservoirs. Therefore, the influence of big reservoirs or small water holding structures on changing the flood flows should always be considered.

5.5 CONCLUSIONS

Frequency analysis of annual maximum discharge of six stations from Narmada river basin of India has been carried out under stationary and non-stationary assumptions. The GAMLSS model is used for the statistical analysis. The study highlights the importance of application of anthropogenic activities for non-stationary flood frequency analysis. For Hoshangabad station, more influence of reservoir in annual maximum discharge is established as compared to the other stations. The changes in streamflow in Narmada river basin are also influenced by the natural climate variability.

This analysis clearly shows non-stationarity in the annual maximum discharge of the Narmada river basin. On the basis of these results, it is clear that the non-stationarity arises in the flood processes of the Narmada river basin due to the human interventions. The changes in climatic conditions also introduce non-stationarity in the flood processes of the basin. Therefore, the frequency analysis of flood processes (which are heavily influenced by human activities) should be conducted using the non-stationary model, which can take care of the influence of reservoirs, climate change and other human activities etc.

CHAPTER 6

CONCLUSIONS AND SCOPE FOR FURTHER WORK

6.1 GENERAL

In the present work, an attempt has been made to investigate the climate related changes in hydro-climatic variables over parts of India. In recent decades, the climate change is more prominently visible on hydo-climatic variables. Therefore, the studies on spatio-temporal variation of temperature and rainfall have been taken up in the present analysis. The changes in climatic conditions has also been reported to alter the intensity and frequency of extreme rainfall and flood events. Hence, the frequency analysis of annual maximum rainfall and discharge data under stationary and non-stationary assumptions has also been attempted.

The following aspects have been examined in the present study:

(i) The analysis of temperature datasets cover entire India. Trend and homogeneity in annual and seasonal temperature data of 125 stations for 1941 to 2012 period have been investigated. The Mann-Kendall trend detection test, Theil and Sen's trend slope estimator, Cumulative deviation test, Standard normal homogeneity test and Wilcoxon Rank-Sum test are used for identification of trends and homogeneity in the datasets.

(ii) The spatio-temporal changes in rainfall series are investigated using 148 station observations covering 15 different states of northern, western, central, eastern and nort-eastern region of India. The Von Neumann ratio, Hurst's coefficient, Mann-Kendall trend and Spearman's rank correlation tests are used for identification of short-term dependence, long-term dependence, trends and the correlation between rainfall with climate change and climate variability indices.

(iii) The non-stationary frequency analysis of annual maximum rainfall from 139 stations have been carried out using GAMLSS model. The effect of climate change (global average temperature, GAT), climate variability (NINO and IOD) and local temperature change (RAT) over non-stationarity have been studied.

(iv) The non-stationary flood frequency analysis have been carried out for annual maximum discharge data of six gauging stations. The effect of natural climate variability (NINO and IOD) and anthropogenic climate change (GAT) over the annual maximum discharge of

Narmada basin has been examined. The influence of reservoir construction over non-stationarity has also been investigated in this analysis.

6.2 MAJOR FINDINGS OF THE STUDY

The major findings of the study are summarised under the following two categories.

(i) Spatio-Temporal Changes in Temperature and Rainfall over Parts of India

(ii) Frequency Analysis of Rainfall and Streamflow under Stationary and Non-stationary Conditions

(i) Spatio-Temporal Changes in Temperature and Rainfall over Parts of India

The annual average, maximum and minimum temperatures showed an increase of 0.44ºC, 0.51ºC and 0.19ºC per 100 years respectively for whole India. The results indicated that the rate of increase of maximum temperature slowed down while the rate of increase of minimum temperature accelerated in comparison to the previous studies. An increase in average temperature is observed for all the seasons and for all the regions. The monsoon maximum temperature depicts a maximum increase at the rate of 0.80ºC/100 years. Therefore, these results may have multitudinous effect over Indian agricultural activities. An increasing temperature may affect the production of food grains, change the showing and harvesting time of principle crops, increasing the power requirement for increasing irrigation demand, etc. The results indicated a non-significant increasing trend for more than 50% stations. However, for climate change studies, the magnitude of change is important and not the number of stations with significant trend (IPCC 2001). Hence. As per IPCC recommendations, it can be concluded that the temperature trends are showing climate change signals.

The homogeneity analysis shows break years around 1972, 1974 and 1977 for the annual average, maximum and minimum temperatures respectively for India. The analysis of homogeneity for all the temperature variables show a break year around 1970s. The magnitude of trend in all annual and seasonal temperature variables changed significantly after the break year. This may be due to the heavy industrialisation in post independence era. The result is in consonance with the IPCC AR5 (2013) report, which stated that the anthropogenic activities have a direct effect on climatic variables.

Rainfall is one of the most important factors of Indian economy. The estimation of spatio-temporal trends of rainfall on a regional basis will help in understanding the global impact of climatic systems over the region. The results indicated that only one-fourth of the station rainfall and rainy day datasets exhibit short-term and long-term dependences on annual and seasonal basis. However, some stations of Gujarat, Rajasthan, Panjab, Madhya Pradesh and Himachal Pradesh show long-term dependence in rainfall and number of rainy day series. Those stations are in a straight line, which is in agreement with the finding of Koutsoyiannis (2003) that the long-term dependence may found in regional basis. However, there are contradictory views in International community regarding the concept of long-term dependence.

Few numbers of station showed a significant increasing or decreasing trend for all the rainfall and number of rainy day series. However, most parts of the study area exhibit a decrease of 0 to 200 mm rainfall during the 1951 to 2007 period in annual and monsoon season. Some parts of Jammu and Kashmir, Himachal Pradesh, Uttarakhand, Uttar Pradesh, Rajasthan and Madhya Pradesh are showing a decrease of up to 400 mm of rainfall. In non-monsoon season, the decrease is 0 to 100 mm. These numbers are quite high and the consequences over the states may be severe. The study area selected in this analysis is also the main pulse-growing region of India. Furthermore, these states have high dependence on agriculture due to huge population with low-income. Therefore, a decrease in rainfall will have multitudinous impact on the peoples related to agricultural activities. The number of rainy days on annual and seasonal basis also show a decrease of up to 10 days during the analysis period. Trends in multi-datasets of gridded rainfall also follow the similar pattern. The CRU and GPCC gridded datasets in general do not follow the spatial patterns shown by other gridded datasets. Therefore, before using the gridded data sets, it is necessary to crosscheck the gridded data with the available observed data.

(ii) Frequency Analysis of Rainfall and Streamflow under Stationary and Non-stationary Conditions

Frequency analysis of annual maximum rainfall (AMR) data across India and the streamflow series of Narmada river basin has been carried out considering both stationarity and non-stationarity assumptions using GAMLSS model. The annual maximum rainfall datasets of 239 stations, which are well distributed across India are used to see the effect of climate change (global average temperature, GAT), climate variability (NINO and IOD) and local temperature change (RAT) on rainfall quantiles of 25, 50 and 100 years return periods. The results indicated that the GAMLSS model could be used for non-stationarity analysis. The results of frequency analysis show that the Gumbel, Lognormal and Generalised Gamma are the most useful distributions for the non-stationarity case. The results indicated that in 80% of stations the non-stationarity models performed better than stationary models. It is found that due to the incorporation of non-stationarity in frequency analysis, the design rainfall quantiles are increasing across India. Therefore, it is important to revisit the design rainfall quantiles and use the revised quantiles for future design.

The results indicated that non-stationarity in AMR series across India are related to the increasing global and regional temperature and changes in natural climatic variability (NINO and IOD indices). It is found that in 44% of stations, the non-stationarity is directly attributed to the increasing temperature (GAT and RAT), and in 30% of stations the non-stationarity can be attributed to the change in natural climate variability. For the remaining 26% of stations, the non-stationarity can be attributed to the trend presence in the AMR series itself. The results also show that no stations under urbanised category and only 10% of stations under urbanising category follow stationarity. For rural area, more than 30% stations are follow stationarity. However, further investigation regarding non-stationarity and its causes are required.

Frequency analysis of annual maximum discharge of six stations of Narmada river basin of India is carried out under stationary and non-stationary conditions using external covariates, like, GAT, NINO, IOD and reservoir index (RI). The results exhibit that in comparison with the non-stationary model; the stationary model either overestimates or underestimates the design flood quantiles. The non-stationary model can also capture the effect of natural variability of any flood process. The results of non-stationary model confirm that the climate variability and construction of reservoirs have a sublime effect on flood process of Narmada river basin. The non-stationarity in annual maximum discharge is mainly due to the influence of reservoirs for three out of six stations, while other three stations are showing non-stationarity due to the effect of natural climate variability across the Narmada river basin. The results highlighted the importance of model based non-stationarity analysis for flood frequency estimates.

6.3 LIMITATIONS OF THE STUDY

The limitations of the present study are given below:

(i) The study of homogeneity and trend analysis of temperature across India has been conducted using only 125 stations. The spatial pattern of the stations is not well distributed across the country as well. The number of stations is also not adequate for the analysis across the country. The analysis period should also be more for accurate assessment of the regional characteristics.

(ii) In the study of spatio-temporal changes in rainfall and number of rainy days, the data of only 148 stations have been used. This may not be sufficient for the entire study area. Only few stations (14) are available in the Himalayan region, which is also not sufficient for representing the entire Himalayan region. Further, a larger length of the database is required for assessing long-term regional rainfall patterns.

(iii) Lack of availability of gridded daily data and inadequacy of data length (1951 to 2007) posed restrictions on the gridded data analysis.

(iv) The flood frequency analysis of Narmada river basin under stationary and non-stationary assumptions has been carried out using only six stations having data length of less than 50 years. This may not be adequate for the non-stationary analysis.

6.4 SCOPE FOR FURTHER WORK

Based on the above limitations and related literature review, the following future studies are proposed:

(i) The results of temperature change across India can be used to study the implications on agriculture and water resources for the different regions. Further, the number different of climatic variables in the scenario of changing climate may also be studied in detail.

(ii) The causes and effects of spatial rainfall variability and temporal change may be looked into.

(iii) IPCC stated that the extremes are more affected by the changes in climatic systems, and therefore more extreme variables (not only the annual maxima) should be analysed. The analysis of other indices related to climate change study, like the coldest daily maximum temperature, the coldest daily minimum temperature, the warmest daily maximum temperature, the warmest daily minimum temperature, etc. should also be studied.

(iv) The effect of grid resolution over trend analysis using multi-gridded dataset can be performed. Further, the reanalysis data (like NCEP) can also be used for this purpose.

(v) The analysis of spatio-temporal change of temperature and rainfall variables can be done by obtaining a data denial exercise to see the importance of the stations in terms of the conclusions/trends/patterns reached.

(vi) The multivariate aspects of non-stationary frequency analysis should be carried out to explore the linkages between non-stationarity and anthropogenic activities.

(vii) The results of non-stationary flood frequency analysis can be used confidently after analysing larger data sets. The effect of more physical covariates like the seasonal occurrence of Southern Synoptic Pattern, Southern Oscillation Index (SOI), Mediterranean Oscillation Index (MOI), North Atlantic Oscillation (NAO) indices should be analysed on flood process.

Research studies are never complete, and every analysis opens up areas for further research. The same has happened with the present piece of research work also. However, due to the limitation of time, the results of the research had to be compiled and presented to the scientific community for future use.

REFERENCES

Ajami, H., Sharma, A., Band, L.E., Evans, J.P., Tuteja, N.K., Amirthanathan, G.E., Bari, M.A., 2017. On the non-stationarity of hydrological response in anthropogenically unaffected catchments: An Australian perspective. Hydrol. Earth Syst. Sci. 21, 281–294. doi:10.5194/hess-21-281-2017

Akaike, H., 1974. A New Look at the Statistical Model Identification. IEEE Trans. Automat. Contr. 19, 716–723. doi:10.1109/TAC.1974.1100705

Alexandersson, H., 1984. A Homogeneity Test Based on Ratios and Applied to Precipitation Series. Report 79, Department of Meteorology. Uppsala, 55 pp.

Alexandersson, H., 1986. A homogeneity test applied to precipitation data. Journal of Climatology 6(6), 661–675.

Allen, M.R., Ingram, W.J., 2002. Constraints on future changes in climate and the hydrologic cycle. Nature 419, 224–32.

Anabalón, A., Sharma, A., 2017. On the divergence of potential and actual evapotranspiration trends: An assessment across alternate global datasets. Earth's Futur. 5, doi:10.1002/2016EF000499

Anderson, R.L., 1942. Distribution of the Serial Correlation Coefficient. Ann. Math. Stat. 13, 1–13.

Arora, M., Goel, N.K., Singh, P., 2005. Evaluation of temperature trends over India / Evaluation de tendances de température en Inde. Hydrol. Sci. J. 50. doi:10.1623/hysj.50.1.81.56330

Ashok, K., Guan, Z., Yamagata, T., 2003. A Look at the Relationship between the ENSO and the Indian Ocean Dipole. J. Meteorol. Soc. Japan 81, 41–56. doi:10.2151/jmsj.81.41

Bahadur, J., 1999. The Himalayan Environment (eds Dash, S.K. and Bahadur, J.). New Age International (P) Ltd. New Delhi. Pp. 258-268.

Bahuguna, I.M., Rathore, B.P., Brahmbhatt, R., Sharma, M., Dhar, S., Randhawa, S.S., Kumar, K., Romshoo, S., Shah, R.D., Ganjoo, R.K., Ajai, 2014. Are the Himalayan glaciers retreating? Curr. Sci. 106, 1008–1013.

Bandyopadhyay, A., Bhadra, A., Raghuwanshi, N.S., Singh, R., 2009. Temporal Trends in Estimates of Reference Evapotranspiration over India. J. Hydrol. Eng. 14, 508–515. doi:10.1061/(ASCE)HE.1943-5584.0000006

Bapuji Rao, B., Sandeep, V.M., Rao, V.U.M., Rao, A.V.M.S., 2012. Climatic change and crop water requirements : An assessment for future climates. J. Agromet. 14, 125–129.

Bapuji Rao, B., Santhibhushan Chowdary, P., Sandeep, V.M., Rao, V.U.M., Venkateswarlu, B., 2014. Rising minimum temperature trends over India in recent decades: Implications for agricultural production. Glob. Planet. Change 117, 1–8. doi:10.1016/j.gloplacha.2014.03.001

Bartels, R., 1982. The Rank Version of von Neumann's Ratio Test for Randomness. J. Am. Stat. Assoc. 77, 40–46.

Basistha, A., Arya, D.S., Goel, N.K., 2009. Analysis of historical changes in rainfall in the Indian Himalayas. Int. J. Climatol. 29, 555–572.

Bera, S., 2017. Trend Analysis of Rainfall in Ganga Basin , India during 1901-2000. Am. J. Clim. Chang. 6, 116–131. doi:10.4236/ajcc.2017.61007

Berkelhammer, M., Sinha, A., Mudelsee, M., Cheng, H., Yoshimura, K., Biswas, J., 2013. On the low frequency component of the ENSO-Indian monsoon relationship; a paired proxy perspective. Clim. Past 9, 3103–3123. doi:10.5194/cpd-9-3103-2013

Bhattacharya, S., Sharma, C., Dhiman, R.C., Mitra, A.P., 2006. Climate change and malaria in India. Curr. Sci. 90, 369–375.

Bhattacharyya, G.K., Johnson, R.A., 1977. Statistical Concepts and Methods. Volume 106 of Wiley Series in Probability and Statistics. Wiley.

Bhutiyani, M.R., Kale, V.S., Pawar, N.J., 2007. Long-term trends in maximum, minimum and mean annual air temperatures across the Northwestern Himalaya during the twentieth century. Clim. Change 85, 159–177.

Bisht, D.S., Chatterjee, C., Raghuwanshi, N.S., Sridhar, V., 2017b. An analysis of precipitation climatology over Indian urban agglomeration. Theor. Appl. Climatol. 1–16. doi:10.1007/s00704-017-2200-z

Bisht, D.S., Chatterjee, C., Raghuwanshi, N.S., Sridhar, V., 2017a. Spatio-temporal trends of rainfall across Indian river basins. Theor. Appl. Climatol. 1–18. doi:10.1007/s00704-017-2095-8

Boes, D.C., Salas, J.D., 1978. Nonstationarity of the mean and the hurst Phenomenon. Water Resour. Res. 14, 135–143. doi:10.1029/WR014i001p00135

Bolch, T., Kulkarni, A., Kaab, A., Huggel, C., Paul, F., Cogley, J.G., Frey, H., Kargel, J.S., Fujita, K., Scheel, M., Bajracharya, S., Stoffel, M., 2012. The State and Fate of Himalayan Glaciers. Science (80). 336, 310–314.

Box, G.E.P., Jenkins, G.M., 1970. Time Series Analysis Forecasting and Control. Holden Day, San Francisco.

Buishand, T.A., 1982. Some methods for testing the homogeneity of rainfall records. J. Hydrol. 58, 11–27. doi:10.1016/0022-1694(82)90066-X

Cancelliere, A., Bonaccorso, B., Rossi, G., 2010. Effect of trends on the estimation of extreme precipitation quantiles. Hydrologydays.Colostate.Edu 27–36.

Chandrapala, L., 1997. Comparison of areal precipitation of Sri Lanka on district basis during the period 1931–60 and 1961–90. In Procd. Nat. Symp. Clim. Chng., Colombo, Sri Lanka.

Cheng, L., AghaKouchak, A., Gilleland, E., Katz, R.W., 2014. Non-stationary extreme value analysis in a changing climate. Clim. Change 127, 353–369. doi:10.1007/s10584-014-1254-5

Chow, V.T., 1964. Handbook of Applied Hydrology. McGraw-Hill: New York

Cunderlik, J.M., Burn, D.H., 2003. Non-stationary pooled flood frequency analysis. J. Hydrol. 276, 210–223. doi:10.1016/S0022-1694(03)00062-3

Cunderlik, J.M., Burn, D.H., 2004. Linkages between regional trends in monthly maximum flows and selected climatic variables. J. Hydrol. Eng. 9, 246–256.

Dash, S.K., Hunt, J.C.R., 2007. Variability of climate change in India. Curr. Sci. 93(6), 782–788.

Delgado, J.M., Apel, H., Merz, B., 2010. Flood trends and variability in the Mekong river. Hydrol. Earth Syst. Sci. 14, 407–418.

Ding, H., Li, Y., Ni, S., Ma, G., Shi, Z., Zhao, G., Yan, L., Yan, Z., 2014. Increased sediment discharge driven by heavy rainfall after Wenchuan earthquake: A case study in the upper reaches of the Min River, Sichuan, China. Quat. Int. 333, 122–129. doi:10.1016/j.quaint.2014.01.019

Donat, M.G., Alexander, L.V., 2012. The shifting probability distribution of global daytime and night-time temperatures. Geophys. Res. Lett. 39, 1–5. doi:10.1029/2012GL052459

Douglas, E.M., Beltrán-przekurat, A., Niyogi, D., Sr, R.A.P., Vörösmarty, C.J., 2009. The impact of agricultural intensi fi cation and irrigation on land – atmosphere interactions and Indian monsoon precipitation — A mesoscale modeling perspective. Glob. Planet. Change 67, 117–128. doi:10.1016/j.gloplacha.2008.12.00

Douglas, E.M., Vogel, R.M., Kroll, C.N., 2000. Trends in floods and low flows in the United States: Impact of spatial correlation. J. Hydrol. 240, 90–105. doi:10.1016/S0022-1694(00)00336-X

El Adlouni, S., Bobée, B., Ouarda, T.B.M.J., 2008. On the tails of extreme event distributions in hydrology. J. Hydrol. 355, 16–33. doi:10.1016/j.jhydrol.2008.02.011

El Adlouni, S., Ouarda, T.B.M.J., Zhang, X., Roy, R., Bobée, B., 2007. Generalized maximum likelihood estimators for the nonstationary generalized extreme value model. Water Resour. Res. 43, 1–13. doi:10.1029/2005WR004545

Filliben, J.J., 1975. The Probability Plot Correlation Coefficient Test for Normality.

Fowler, H.J., Wilby, R.L., 2010. Detecting changes in seasonal precipitation extremes using regional climate model projections: Implications for managing fluvial flood risk. Water Resour. Res. 46, 1-17. doi:10.1029/2008WR007636

Gautam, R., Hsu, N.C., Lau, K.M., Tsay, S.C., Kafatos, M., 2009. Enhanced pre-monsoon warming over the Himalayan-Gangetic region from 1979 to 2007. Geophys. Res. Lett. 36, 1–5. doi:10.1029/2009GL037641

Geethalakshmi, V., Lakshmanan, A., Rajalakshmi, D., Jagannathan, R., Sridhar, G., Ramaraj, A.P., Bhuvaneswari, K., Gurusamy, L., Anbhazhagan, R., 2011. Climate change impact assessment and adaptation strategies to sustain rice production in Cauvery basin of Tamil Nadu. Curr. Sci. 101, 342–347.

Gershunov, A., Schneider, N., Barnett, T., 2001. Low-Frequency Modulation of the ENSO–Indian Monsoon Rainfall Relationship: Signal or Noise? J. Clim. 14, 2486–2492. doi:10.1175/1520-0442(2001)014<2486:LFMOTE>2.0.CO;2

Ghosh, S., Das, D., Kao, S.C., Ganguly, A.R., 2011. Lack of uniform trends but increasing spatial variability in observed Indian rainfall extremes. Nature Clim. Change 2, 86–91.

Ghosh, S., Luniya, V., Gupta, A., 2009. Trend analysis of Indian summer monsoon rainfall at different spatial scales. Atmos. Sci. Lett. 10, 285–290.

Gilroy, K.L., McCuen, R.H., 2012. A nonstationary flood frequency analysis method to adjust for future climate change and urbanization. J. Hydrol. 414–415, 40–48. doi:10.1016/j.jhydrol.2011.10.009

Gosain, A.K., Rao, S., Basuray, D., 2006. Climate change impact assessment on hydrology of Indian river basins. Current 90, 346–353.

Goswami, B.N., Venugopal, V., Sengupta, D., Madhusoodanan, M.S., Xavier, P.K., 2006. Increasing Trend of Extreme Rain Events Over India in a Warming Environment. Science (80). 314, 1442–1445. doi:10.1126/science.1132027

Guhathakurta, P., Rajeevan, M., 2008. Trends in the rainfall pattern over India. Int. J. Climatol. 28, 1453–1469. DOI: 10.1002/joc.1640

Gupta, P.K., Panigrahy, S., Parihar, J.S., 2011. Impact of Climate Change on Runoff of the Major River Basins of India Using Global Circulation Model (HadCM3) Projected Data. J. Indian Soc. Remote Sens. 39, 337–344.

Gupta, S.K., Deshpande, R.D., 2004. Water for India in 2050: First-order assessment of available options. Curr. Sci. 86, 1216–1224.

Hamed, K.H., Rao, A.R., 1998. A modified Mann-Kendall trend test for autocorrelated data. J. Hydrol. 204, 182–196. doi:10.1016/S0022-1694(97)00125-X

Hansen, J., Sato, M., Ruedy, R., 2012. Perception of climate change. Proc. Natl. Acad. Sci. 109, E2415–E2423. doi:10.1073/pnas.1205276109

Harris, I., Jones, P.D., Osborn, T.J., Lister, D.H., 2014. Updated high-resolution grids of monthly climatic observations - the CRU TS3.10 Dataset. Int. J. Climatol. 34, 623–642. doi:10.1002/joc.3711

Hasan, A.B.M.S., Rahman, M.Z., 2013. Change in Temperature over Bangladesh Associated with Degrees of Global Warming. Asian J. Appl. Sci. Eng. 2, 62–75.

He, Y., Bardossy, A., Brommundt, J., 2006. Non-Stationary Flood Frequency Analysis in Soutern Germany. Conf. Hydrosci. Eng. 2006.

Hegerl, G.C., Zwiers, F.W., Braconnot, P., Gillett, N.P., Luo, Y., MarengoOrsini, J.A., Nicholls, N., Penner, J.E., Stott, P.A., 2007. Understanding and attributing climate change, in Climate Change 2007: The Physical Science Basis. Cambridge University Press, Cambridge, United Kingdom and New York, NY, USA.

Heo, J.-H., Kho, Y.W., Shin, H., Kim, S., Kim, T., 2008. Regression equations of probability plot correlation coefficient test statistics from several probability distributions. J. Hydrol. 355, 1–15. doi:10.1016/j.jhydrol.2008.01.027

Hingane, L.S., Kumar, R.K., Murthy, R.B.V., 1985. Long-term trends of surface air temperature in India. Journal of Climatology 5(5), 521–528.

Hirsch, R.M., Alexander, R.B., Smith, A., Geological, U.S., 1991. Selection of Methods for the Detection and Estimation of Trends in Water Quality. Water Resour. Res. 27, 803–813.

Hundal, S.S., Kaur, P., 2007. Climatic variability and its impact on cereal productivity in Indian Punjab. Curr. Sci. 92, 506–512.

Hurst, H.E., 1951. Long term storage capacity of reservoirs. Trans. Am. Soc. Civ. Eng. 116, 770-808.

Intergovernmental Panel on Climate Change (IPCC), 2013. Summary for Policymakers. In: Climate Change 2013: The Physical Science Basis. Contribution of Working Group I to the Fifth Assessment Report of the Intergovernmental Panel on Climate Change [Stocker, T.F., D. Qin, G.-K. Plattner, M. Tignor, S. K. Allen, J. Boschung, A. Nauels, Y. Xia, V. Bex and P.M. Midgley (eds.)]. Cambridge University Press, Cambridge, United Kingdom and New York, NY, USA.

IPCC, 2014. Climate Change 2014: Impacts, Adaptation, and Vulnerability. Part A: Global and Sectoral Aspects. Contribution of Working Group II to the Fifth Assessment Report of the Intergovernmental Panel on Climate Change [Field, C.B., V.R. Barros, D.J. Dokken, K.J. Mach, M.D. Mastrandrea, T.E. Bilir, M. Chatterjee, K.L. Ebi, Y.O. Estrada, R.C. Genova, B. Girma, E.S. Kissel, A.N. Levy, S. MacCracken, P.R. Mastrandrea, and L.L. White (eds.)]. Cambridge University Press, Cambridge, United Kingdom and New York, NY, USA, 1132 pp.

Islam, A., Shirsath, P.B., Kumar, S.N., Subash, N., Sikka, A.K., Aggarwal, P.K., 2014. Modeling Water Management and Food Security in India under Climate Change. In: L. R. Ahuja, L. Ma, R. J. Lascano, editors, Practical Applications of Agricultural System Models to Optimize the Use of Limited Water, Adv. Agric. Syst. Model. 5. ASA, CSSA, and SSSA, Madison, WI. p. 267-316. doi:10.2134/advagricsystmodel5.c11

Jagannathan, P., Parthasarathy, B., 1973. Trends and periodicities of rainfall over India. Mon. Weather Rev. 101, 371–375.

Jain, S.K., Kumar, V., 2012. Trend analysis of rainfall and temperature data for India. Curr. Sci. 102, 37–49.

Jain, S.K., Kumar, V., Saharia, M., 2013. Analysis of rainfall and temperature trends in northeast India. Int. J. Climatol. 33, 968–978. doi:10.1002/joc.3483

Jena, P.P., Chatterjee, C., Pradhan, G., Mishra, A., 2014. Are recent frequent high floods in Mahanadi basin in eastern India due to increase in extreme rainfalls? J. Hydrol. 517, 847–862. doi:10.1016/j.jhydrol.2014.06.021

Jetten, T.H., Focks, D.A., 1997. Potential changes in the distribution of dengue transmission under climate warming. Am. J. Trop. Med. Hyg. 57, 238–287.

Jetten, T.H., Martens, W.J.M., Takken, W., 1996. Model simulations to estimate malaria risk under climate change. J. Med. Entomol. 33, 361–371.

Jhajharia, D., Shrivastava, S.K., Sarkar, D., Sarkar, S., 2009. Temporal characteristics of pan evaporation trends under the humid conditions of northeast India. Agric. For. Meteorol. 149, 763–770. doi:10.1016/j.agrformet.2008.10.024

Jhajharia, D., Singh, V.P., 2011. Trends in temperature, diurnal temperature range and sunshine duration in Northeast India. Int. J. Climatol. 31, 1353–1367. doi:10.1002/joc.2164

Jones, P.D., Moberg, A., 2003. Hemispheric and large-scale surface air temperature variations: An extensive revision and an update to 2001. J. Clim. 16, 206–223. doi:10.1175/1520-0442(2003)016<0206:HALSSA>2.0.CO;2

Joshi, U.R., Rajeevan, M., 2006. Trends in Precipitation Extremes over Southeast Asia. Natl. Clim. Cent. Research Report No: 3/2006, 168–171. doi:10.2151/sola.2009-043

Katz, R.W., Parlange, M.B., Naveau, P., 2002. Statistics of extremes in hydrology. Adv. Water Resour. 25, 1287–1304. doi:10.1016/S0309-1708(02)00056-8

Kellner, O., Niyogi, D., 2015. Climate variability and the U.S. corn belt: Enso and AO episode-dependent hydroclimatic feedbacks to corn production at regional and local scales. Earth Interact. 19, 1–32. doi:10.1175/EI-D-14-0031.1

Kendall, M., Stuart, A., Ord, J.K., 1983. The Advanced Theory of Statistics, vol. 3, Design and Analysis, and Time Series. 4th ed., 780 pp., Oxford Univ. Press, New York

Kendall, M.G., 1955. Rank Correlation Methods. Charles Griffin, London.

Kendall, M.G., Stuart, A., 1968. The Advance Theory of Statistics. vol. 2. Griffin, London.

Kenyon, J., Hegerl, G.C., 2010. Influence of modes of climate variability on global precipitation extremes. J. Clim. 23, 6248–6262. doi:10.1175/2010JCLI3617.1

Khaliq, M.N., Ouarda, T.B.M.J., Ondo, J.C., Gachon, P., Bobée, B., 2006. Frequency analysis of a sequence of dependent and/or non-stationary hydro-meteorological observations: A review. J. Hydrol. 329, 534–552. doi:10.1016/j.jhydrol.2006.03.004

Khan, M.Z.K., Sharma, A., Mehrotra, R., 2017. Global seasonal precipitation forecasts using improved sea surface temperature predictions. J. Geophys. Res. Atmos. 122, 4773–4785. doi:10.1002/2016JD025953

Kiem, A.S., Franks, S.W., Kuczera, G., 2003. Multi-decadal variability of flood risk. Geophys. Res. Lett. 30, 1–4. doi:10.1029/2002GL015992

Kim, H.Y., Ko, J., Kang, S., Tenhunen, J., 2013. Impacts of climate change on paddy rice yield in a temperate climate. Global change biology 19(2), 548–62. DOI: 10.1111/gcb.12047.

Kishtawal, C.M., Niyogi, D., Tewari, M., Pielke, R.A., Shepherd, J.M., 2010. Urbanization signature in the observed heavy rainfall climatology over India. Int. J. Climatol. 30, 1908–1916.

Kothawale, D.R., Munot, A.A., Kumar, K.K., 2010(a). Surface air temperature variability over India during 1901-2007, and its association with enso. Clim. Res. 42, 89–104. doi:10.3354/cr00857

Kothawale, D.R., Revadekar, J.V., Kumar, K.R., 2010(b). Recent trends in pre-monsoon daily temperature extremes over India. J. Earth Syst. Sci. 119, 51–65. doi:10.1007/s12040-010-0008-7

Kothawale, D.R., Rupa Kumar, K., 2005. On the recent changes in surface temperature trends over India. Geophys. Res. Lett. 32. doi:L18714\r10.1029/2005gl023528

Kothyari, U., Singh, V.P., 1996. Rainfall and Temperature Trends in India. Hydrol. Process. 10, 357–372.

Koutsoyiannis, D., 2003. Climate change, the Hurst phenomenon, and hydrological statistics. Hydrol. Sci. J. 48, 3–24. doi:10.1623/hysj.48.1.3.43481

Kulkarni, A., Sabade, S.S., Kripalani, R.H., 2007. Association between extreme monsoons and the dipole mode over the Indian subcontinent. Meteorol. Atmos. Phys. 95, 255–268. doi:10.1007/s00703-006-0204-9

Kumar, S., Merwade, V., Kinter, J.L., Niyogi, D., 2013. Evaluation of temperature and precipitation trends and long-term persistence in CMIP5 twentieth-century climate simulations. J. Clim. 26, 4168–4185. doi:10.1175/JCLI-D-12-00259.1

Kumar, V., Jain, S.K., Singh, Y., 2010. Analysis of long-term rainfall trends in India. Hydrol. Sci. J. 55, 484–496. doi:10.1080/02626667.2010.481373

Kumari, B.P., Londhe, A.L., Daniel, S., Jadhav, D.B., 2007. Observational evidence of solar dimming : Offsetting surface warming over India. Geophys. Res. Lett. 34, 1–5. doi:10.1029/2007GL031133

Kurane, I., 2010. The Effect of Global Warming on Infectious Diseases. Osong Public Heal. Res. Perspect. 1, 4–9.

Labat, D., Goddéris, Y., Probst, J.L., Guyot, J.L., 2004. Evidence for global runoff increase related to climate warming. Adv. Water Resour. 27, 631–642.

Lacombe, G., McCartney, M., 2013. Erratum to: Uncovering consistencies in Indian rainfall trends observed over the last half century. Clim. Change 123(2), 287–299. DOI:10.1007/s10584-013-1036-5

Laio, F., Baldassarre, G. Di, Montanari, A., 2009. Model selection techniques for the frequency analysis of hydrological extremes. Water Resour. Res. 45, 1–11. doi:10.1029/2007WR006666

Lal, M., Singh, K.K., Rathore, L.S., Srinivasan, G., Saseendran, S.A., 1998. Vulnerability of rice and wheat yields in NW India to future changes in climate. Agric. For. Meteorol. 89, 101–114. doi:10.1016/S0168-1923(97)00064-6

Leclerc, M., Ouarda, T.B.M.J., 2007. Non-stationary regional flood frequency analysis at ungauged sites. J. Hydrol. 343, 254–265. doi:10.1016/j.jhydrol.2007.06.021

Legates, D.R., Willmott, C.J., 1990. Mean seasonal and spatial variability in global surface air temperature. Theo. and Appl. Clim. 41, 11–21. doi:10.1007/BF00866198

Lins, H.F., 2012. A Note on Stationarity and Nonstationarity. WMO Report (June 2012).

López, J., Francés, F., 2013. Non-stationary flood frequency analysis in continental Spanish rivers, using climate and reservoir indices as external covariates. Hydrol. Earth Syst. Sci. 17, 3189–3203. doi:10.5194/hess-17-3189-2013

Lye, L.M., Lin, Y., 1994. Long-term dependence in annual peak flows of Canadian rivers. J. Hydrol. 160, 89–103. doi:10.1016/0022-1694(94)90035-3

Machado, M.J., Botero, B.A., López, J., Francés, F., Díez-Herrero, A., Benito, G., 2015. Flood frequency analysis of historical flood data under stationary and non-stationary modelling. Hydrol. Earth Syst. Sci. 19, 2561–2576. doi:10.5194/hess-19-2561-2015

Madansky, A., 1988. Prescriptions for WorkingmStatisticians. Springer, New York, pp. 93-118. DOI:10.1007/978-1-4612-3794-5

Mahato, A., 2014. Climate change and its impact on agriculture in vietnam. Int. J. Sci. Res. Publ. 4, 1–11.

Maity, R., Nagesh Kumar, D., 2006. Bayesian dynamic modeling for monthly Indian summer monsoon rainfall using El Ni??o-Southern Oscillation (ENSO) and Equatorial Indian Ocean Oscillation (EQUINOO). J. Geophys. Res. Atmos. 111, 1-12.

Maity, R., Nagesh Kumar, D., 2008. Probabilistic prediction of hydroclimatic variables with nonparametric quantification of uncertainty. J. Geophys. Res. Atmos. 113, 1–12. doi:10.1029/2008JD009856

Mallya, G., Mishra, V., Niyogi, D., Tripathi, S., Govindaraju, R.S., 2015. Trends and variability of droughts over the Indian monsoon region. Weather Clim. Extrem. 12, 43–68. doi:10.1016/j.wace.2016.01.002

Mann, H.B., 1945. Nonparametric Tests Against Trend. Econometrica 13, 245–259.

McCuen, R.H., 2003. Modeling Hydrologic Change. Department of Civil and Environmental Engineering University of Maryland, Lewis Publishers.

McWilliam, J.R., 1980. Summary and synthesis-adaptation to high temperature stress. In Adaptation of Plants to High Temperature Stress. Turner, N.C., Krammer, P.J., (eds). John Wiley: New York, USA, 444–446.

Meacham, I., 1968. Correlation in sequential data--three sample indicators. Civ. Eng. Trans. Inst. Eng. Aust. CE10(2), 225-228.

Milly, P.C.D., Betancourt, J., Falkenmark, M., Hirsch, R.M., Kundzewicz, Z.W., Lettenmaier, D.P., Stouffer, R.J., 2008. Climate change. Stationarity is dead: whither water management? Science 319, 573–574. doi:10.1126/science.1151915

Milly, P.C.D., Betancourt, J., Falkenmark, M., Hirsch, R.M., Kundzewicz, Z.W., Lettenmaier, D.P., Stouffer, R.J., Dettinger, M.D., Krysanova, V., 2015. On Critiques of '"Stationarity is Dead: WhitherWater Management?" Water Resour. Res. 51, 7785–7789. doi:10.1002/2015WR017408.Received

Mishra, A., Chatterjee, C., 2009. Temporal Changes in Rainfall Occurrence and Distribution in West Midnapore District of West Bengal. J. Indian Water Resour. Soc. 29, 38–48.

Mishra, A., Singh, R., Raghuwanshi, N.S., Chatterjee, C., Froebrich, J., 2013. Spatial variability of climate change impacts on yield of rice and wheat in the Indian Ganga Basin. Sci. Total Environ. 468–469, S132–S138. doi:10.1016/j.scitotenv.2013.05.080

Mishra, A.K., Singh, V.P., 2010. A review of drought concepts. J. Hydrol. 391, 202–216. doi:10.1016/j.jhydrol.2010.07.012

Mittal, N., Bhave, A.G., Mishra, A., Singh, R., 2016. Impact of human intervention and climate change on natural flow regime. Water Resour. Manag. 30, 685–699. doi:10.1007/s11269-015-1185-6

Mittal, N., Mishra, A., Singh, R., Kumar, P., 2014. Assessing future changes in seasonal climatic extremes in the Ganges river basin using an ensemble of regional climate models. Clim. Change 123, 273–286. doi:10.1007/s10584-014-1056-9

Mondal, A., Khare, D., Kundu, S., 2015. Spatial and temporal analysis of rainfall and temperature trend of India. Theor. Appl. Climatol. 122, 143–158. doi:10.1007/s00704-014-1283-z

Mondal, A., Mujumdar, P.P., 2015. Modeling non-stationarity in intensity, duration and frequency of extreme rainfall over India. J. Hydrol. 521, 217–231. doi:10.1016/j.jhydrol.2014.11.071

Mooley, D.A., Parthasarathy, B., 1984. Fluctuations in All-India summer monsoon rainfall during 1871-1978. Clim. Change 6, 287–301. doi:10.1007/BF00142477

Narayana, A.C., 2006. Rainfall variability and its impact on sediment discharge from rivers of Kerala region, southwestern India. J. Geol. Soc. India. 68, 549–558.

National Action Plan on Climate Change, 2008. Government of India. Prime Minister's Council on Climate Change.

National Action Plan on Climate Change, 2010. Government of India. Prime Minister's Council on Climate Change.

National Environment Policy, 2004. Government of India. Ministry of Environment & Forests.

Nayak, S., Mandal, M., 2012. Impact of land-use and land-cover changes on temperature trends over Western India. Curr. Sci. 102, 1166–1173.

New, M., Hulme, M., Jones, P., 1999. Representing Twentieth-Century Space – Time Climate Variability . Part I : Development of a 1961 – 90 Mean Monthly Terrestrial Climatology. J. Clim. 12, 829–856.

Nicholls, R.J., Tol, R.S.J., 2006. Impacts and responses to sea-level rise: a global analysis of the SRES scenarios over the twenty-first century. Philos. Trans. A. Math. Phys. Eng. Sci. 364, 1073–95. doi:10.1098/rsta.2006.1754

Niyogi, D., Chang, H.-I., Chen, F., Gu, L., Kumar, A., Menon, S., A., R., Sr., P., 2007. Potential impacts of aerosol – land – atmosphere interactions on the Indian monsoonal rainfall characteristics. Nat Hazards 42, 345–359. doi:10.1007/s11069-006-9085-y

Niyogi, D., Kishtawal, C., Tripathi, S., Govindaraju, R.S., 2010. Observational evidence that agricultural intensification and land use change may be reducing the Indian summer monsoon rainfall. Water Resour. Res. 46, 1–17. doi:10.1029/2008WR007082

Novotny, E.V., Stefan, H.G., 2007. Stream flow in Minnesota: Indicator of climate change. J. Hydrol. 334, 319–333. doi:10.1016/j.jhydrol.2006.10.011

Olsen, J.R., Lambert, J.H., Haimes, Y.Y., 1998. Risk of extreme events under nonstationary conditions. Risk Anal. 18(4), 497-510.

Otache, M.Y., Li, Z., Bakir, M., 2008. Analysis of long-term dependence phenomenon in Benue River flow process and its hypothesis testing. Chinese J. Oceanol. Limnol. 26, 313–322. doi:10.1007/s00343-008-0313-z

Ouarda, T.B.M.J., El-Adlouni, S., 2011. Bayesian nonstationary frequency analysis of hydrological variables. J. American Water Res. Assoc. 47, 496–505.

Pal, I., Al-Tabbaa, A., 2011. Assessing seasonal precipitation trends in India using parametric and non-parametric statistical techniques. Theor. Appl. Climatol. 103, 1–11. doi:10.1007/s00704-010-0277-8

Pandey, S., 2007. Economic costs of drought and rice farmers' coping mechanisms. Int. Rice Res. News 32, 5-11.

Pant, G.B., Hingane, L.S., 1988. Climatic changes in and around the Rajasthan desert during the 20th century. Int. J. Climatol. 8, 391–401.

Pant, G.B., Kumar, R.K., 1997. Climates of South Asia. John Wiley & Sons 320pp (ISBN 0-471- 94948-5).

Parthasarathy, B., Dhar, O.N., 1974. Secular variations of regional rainfall over India. Q. J. R. Meteorol. Soc. 100, 245–257.

Pathak, A., Ghosh, S., Kumar, P., 2014. Precipitation Recycling in the Indian Subcontinent during Summer Monsoon. J. Hydrometeorol. 15, 2050–2066. doi:10.1175/JHM-D-13-0172.1

Patra, J.P., Mishra, A., Singh, R., Raghuwanshi, N.S., 2012. Detecting rainfall trends in twentieth century (1871-2006) over Orissa State, India. Clim. Change 111, 801–817. doi:10.1007/s10584-011-0215-5

Pattanaik, D.R., 2007. Analysis of rainfall over different homogeneous regions of India in relation to variability in westward movement frequency of monsoon depressions. Nat. Hazards 40, 635–646. doi:10.1007/s11069-006-9014-0

Pattanaik, D.R., Rajeevan, M., 2010. Variability of extreme rainfall events over India during southwest monsoon season. Meteorol. Appl. 17, 88–104. doi:10.1002/met.164

Paul, S., Ghosh, S., Oglesby, R., Pathak, A., Chandrasekharan, A., Ramsankaran, R., 2016. Weakening of Indian Summer Monsoon Rainfall due to Changes in Land Use Land Cover. Sci. Rep. 6, 32177. doi:10.1038/srep32177

Peterson, T.C., Easterling, D.R., Karl, T.R., Groisman, P., Nicholls, N., Plummer, N., Torok, S., Auer, I., Boehm, R., Gullet, D., Vincent, L., Heino, R., Tuomenvirta, H., Mestre, O., Szentimrey, T., Salinger, J., Førland, E.J., Hanssen-Bauer, I., Alexandersson, H., Jones, P., Parker, D., 1998. Homogeneity adjustments of in situ atmospheric climate data: A review. Int. J. Climatol. 18, 1493–1517. doi:10.1002/(SICI)1097-0088(19981115)18:13<1493::AID-JOC329>3.0.CO;2-T

Peterson, T.C., Vose, R.S., 1997. An Overview of the Global Historical Climatology Network Temperature Database. Bull. Am. Meteorol. Soc. 78, 2837–2849. doi:10.1175/JTECH-D-11-00103.1

Pielke Sr., R., Nielsen-Gammon, J., Davey, C., Angel, J., Bliss, O., Doesken, N., Cai, M., Fall, S., Niyogi, D., Gallo, K., Hale, R., Hubbard, K.G.., Lin, X., Li, H., Sr., R. P., Nielsen-Gammon, J., Davey, C., Angel, J., Bliss, O., Doesken, N., Cai, M., Fall, S., Niyogi, D., Gallo, K., Hale, R., Hubbard, K. G. ., Lin, X., Li, H., 2007. Documentation of Uncertainties and Biases Associated with Surface Temperature Measurement Sites for Climate Assessment. Am. Meteorol. Soc. 913–928. doi:10.1175/BAMS-88-6-9I3

Pramanik, S.K., Jagannathan, P., 1954. Climatic changes in India rainfall; Indian. J Meteorol Geophys 4, 291–309.

Radziejewski, M., Kundzewicz, Z.W., 2004. Detectability of changes in hydrological records / Possibilité de détecter les changements dans les chroniques hydrologiques. Hydrol. Sci. J. 49, 39–51. doi:10.1623/hysj.49.1.39.54002

Rajeevan, M., Bhate, J., Jaswal, A.K., 2008. Analysis of variability and trends of extreme rainfall events over India using 104 years of gridded daily rainfall data. Geophysical Res. Lttrs. 35, L18707. doi:10.1029/2008GL035143

Rajeevan, M., Bhate, J., Kale, J.D., Lal, B., 2005. Development of a high resolution daily gridded rainfall data for the Indian region. IMD Met Monograph No: Climatology 22/2005, p. 27.

Rajeevan, M., Bhate, J., Kale, J.D., Lal, B., 2006. High resolution daily gridded rainfall data for the Indian region: Analysis of break and active monsoon spells. Curr. Science 91(3), 296-306.

Rakhecha, P.R., Soman, M.K., 1994. Trends in the annual extreme rainfall events of 1 to 3 days duration over India. Theor. Appl. Climatol. 48, 227–237. doi:10.1007/BF00867053

Ramanathan, V., Chung, C., Kim, D., Bettge, T., Buja, L., Kiehl, J.T., Washington, W.M., Fu, Q., Sikka, D.R., Wild, M., 2005. Atmospheric brown clouds : Impacts on South Asian climate and hydrological cycle. Proc. Natl. Acad. Sci. USA 102, 5326–5333.

Ramanathan, V., Crutzen, P.J., Kiehl, J.T., Rosenfeld, D., 2001. Aerosols, Climate, and the Hydrological Cycle. Science 294, 2119–2124. doi:10.1126/science.1064034

Ranade, A., Singh, N., Singh, H.N., Sontakke, N.A., 2008. On Variability of Hydrological Wet Season, Seasonal Rainfall and Rainwater Potential of the River Basins of India (1813-2006). J. Hydrol. Res. Dev. 23, 79–108.

Rao, A.R., Bhattacharya, D., 1999. Hypothesis testing for long-term memory in hydrologic series. J. Hydrol. 216, 183–196. doi:10.1016/S0022-1694(99)00005-0

Rao, G.S.P., Jaswal, A.K., Kumar, M.S., 2004. Effects of urbanization on meteorological parameters. Mausam 3, 429–440.

Rao, G.S.P., Krishna Murty, M., Joshi, U.R., Thapliyal, V., 2005. Climate Change Over India as Revealed by Critical Extreme Temperature Analysis. Mausam 56, 601–608.

Revadekar, J.V., Kulkarni, A., 2008. The El Nino-Southern Oscillation and winter precipitation extremes over India. Int. J. Climatol. 28, 1445–1452.

Rigby, R.A., Stasinopoulos, D.M., 2005. Generalized additive models for location, scale and shape, (with discussion). Appl. Stat. 54, 507–554. doi:10.18637/jss.v023.i07

Río, S.D., Anjum Iqbal, M., Cano-Ortiz, A., Herrero, L., Hassan, A., Penas, A., 2013. Recent mean temperature trends in Pakistan and links with teleconnection patterns. Int. J. Climatol. 33, 277–290. doi:10.1002/joc.3423

Roth, M., Buishand, T.A., Jongbloed, G., Klein Tank, A.M.G., van Zanten, J.H., 2014. Projections of precipitation extremes based on a regional, non-stationary peaks-over-threshold approach: A case study for the Netherlands and north-western Germany. Weather Clim. Extrem. 4, 1–10. doi:10.1016/j.wace.2014.01.001

Roy, S. Sen, Mahmood, R., Niyogi, D., Lei, M., Foster, S.A., Hubbard, K.G., Douglas, E., Sr, R.P., 2007. Impacts of the agricultural Green Revolution – induced land use changes on air temperatures in India. J. Geophys. Res. 112, 1–13. doi:10.1029/2007JD008834

Roy, S.S., 2008. Impact of aerosol optical depth on seasonal temperatures in India : a spatio-temporal analysis. Int. J. Remote Sens. 29, 37–41. doi:10.1080/01431160701352121

Rudolf, B., Hauschild, H., Rueth, W., Schneider, U., 1994. Terrestrial precipitation analysis: Operational method and required density of point measurements, in Global Precipitations and Climate Change, NATO ASI Ser. I, vol. 26, edited by M. Desbois and F. Desalmond, pp. 173–186, Springer, New York.

Rupa Kumar, K., Kumar, K.K., Pant, G.B., 1994. Diurnal asymmetry of surface temperature trends over India. Geophys. Res. Lett. 21, 677–680. doi:10.1029/94GL00007

Rupa Kumar, K., Pant, G.B., Parthasarathy, B., Sontakke, N.A., 1992. Spatial and sub-seasonal patterns of the long term trends of Indian summer monsoon rainfall. Int. J. Climatol. 12, 257–268.

Rupa Kumar, K., Sahai, A.K., Kumar, K.K., Patwardhan, S.K., Mishra, P.K., Revadekar, J.V., Kamala, K., Pant, G.B., 2006. Climate Change scenarios for 21st Century India.pdf. Curr. Sci. 90(3), 334-345.

Saji, N.H., Goswami, B.N., Vinayachandran, P.N., Yamagata, T., 1999. A dipole mode in the tropical Indian Ocean. Nature 401, 360–363. doi:10.1038/43854

Salas, J.D., Obeysekera, J., 2013. Return period and risk for nonstationary hydrologic extreme events. World Envir. and Water Resour. Cong. 2013: Showcasing the Future, ASCE, 1213–1223.

Salas, J.D., Obeysekera, J., 2014. Revisiting the Concepts of Return Period and Risk for Nonstationary Hydrologic Extreme Events. J. Hydrol. Eng. 19, 554–568.

Salas, J.D., Rajagopalan, B., Saito, L., Brown, C., 2012. Special Section on Climate Change and Water Resources: Climate Nonstationarity and Water Resources Management. J. Water Resour. Plan. Manag. 138, 385–388. doi:10.1061/(ASCE)WR.1943-5452.0000279

Schneider, U., Becker, A., Finger, P., Meyer-Christoffer, A., Ziese, M., 2015. GPCC Monitoring Product: Near Real-Time Monthly Land-Surface Precipitation from Rain-Gauges based on SYNOP and CLIMAT data. DOI: 10.5676/DWD_GPCC/MP_M_V5_100

Sen Roy, S., Balling, R.C., 2005. Analysis of trends in maximum and minimum temperature, diurnal temperature range, and cloud cover over India. Geophys. Res. Lett. 32, 1–4. doi:10.1029/2004GL022201

Sen, P.K., 1968. Estimates of the Regression Coefficient Based on Kendall â€TM s Tau. J. Am. Stat. Assoc. 63, 1379–1389.

Serrano, A., Mateos, V.L., Garcia, J.A., 1999. Trend analysis of monthly precipitation over the Iberian Peninsula for the period 1921-1995. Phys. Chem. Earth, Part B Hydrol. Ocean. Atmos. 24, 85–90. doi:10.1016/S1464-1909(98)00016-1

Shastri, H., Paul, S., Ghosh, S., Karmakar, S., 2014. Impacts of urbanization on Indian summermonsoon rainfall extremes. Journal of Geophysical Research : Atmospheres. J. Geophys. Res. Atmos. 120, 495–516. doi:10.1002/2014JD022061.

Sheehy, J.E., Mitchell, P.L., Ferrer, A.B., 2006. Decline in rice grain yields with temperature: Models and correlations can give different estimates. F. Crop. Res. 98, 151–156. doi:10.1016/j.fcr.2006.01.001

Shepard, D., 1968. A two-dimensional interpolation function for irregularly-spaced data. Proc. 1968 23rd ACM Natl. Conf. 517–524. doi:10.1145/800186.810616

Sherly, M.A., Karmakar, S., Chan, T., Rau, C., 2016. Design Rainfall Framework Using Multivariate Parametric-Nonparametric Approach. J. Hydrol. Eng. 21, 1–17. doi:10.1061/(ASCE)HE.1943-5584.0001256.

Simmons, A.J., Willett, K.M., Jones, P.D., Thorne, P.W., Dee, D.P., 2010. Low-frequency variations in surface atmospheric humidity, temperature, and precipitation: Inferences from reanalyses and monthly gridded observational data sets. J. Geophys. Res. Atmos. 115, 1–21. doi:10.1029/2009JD012442

Singh, J., Hari, V., Sharma, T., Karmakar, S., Ghosh, S., 2016. Signature of Nonstationarity in Precipitation Extremes over Urbanizing Regions in India Identified through a Multivariate Frequency Analyses. EGU Gen. Assem. 2016 18.

Singh, J., Vittal, H., Karmakar, S., Ghosh, S., Niyogi, D., 2016. Urbanization causes nonstationarity in Indian Summer Monsoon Rainfall extremes. Geophys. Res. Lett. 43, 11,269-11,277. doi:10.1002/2016GL071238

Singh, J., Vittal, H., Singh, T., Karmakar, S., Ghosh, S., 2015. A Framework for Investigating the Diagnostic Trend in Stationary and Nonstationary Flood Frequency Analyses Under Changing Climate. J. Clim. Chang. 1, 47–65. doi:10.3233/JCC-150004

Singh, N., Sontakke, N.A., 2002. On climatic fluctuations and environmental changes of the Indo-Gangetic Plains, India. Clim. Change 52, 287–313. doi:10.1023/A:1013772505484

Sinha Ray, K.C., De, U.S., 2003. Climate change in India as evidenced from instrumental records. WMO Bulletin 52(1), 53–59.

Sinha, S.K., Swaminathan, M.S., 1991. Deforestation, climate change and sustainable nutrition security: A case study of India. Clim. Change 19, 201–209.

Spearman, C., 1904. “General Intelligence” Objectively Determined and Measured. American J. Psychology 15, 72–101.

Srivastava, H.N., Dewan, B.N., Dikshit, S.K., Prakash Rao, G.S., Singh, S.S., K. R. Rao, 1992. Decadal trends in climate over India. Mausam, 1992, 43, 7–20.

Srivastava, P.C., Shrivastava, S.K., 2011. Climatic variability and its influence on water availability over eastern Himalayan belt of Arunachal Pradesh. J. of Soil and Water Cons. 10(1), 3-9.

Stedinger, J.R., Griffis, V.W., 2010. Getting From Here to Where? Work. Nonstationarity, Hydrol. Freq. Anal. Water Manag. Colorado Water Institute Information Series No. 109, 99–105.

Steffen, K., Box, J.E., Abdalati, W., 1996. Greenland Climate Network: GC-Net. In S. C.

Strupczewski, W.G., Singh, V.P., Feluch, W., 2001. Non-stationary approach to at-site flood frequency modelling I . Maximum likelihood estimation. J. Hydrol. 248, 123–142.

Strupczewski, W.G., Singh, V.P., Mitosek, H.T., 2001. Non-stationary approach to at-site flood frequency modelling. III. Flood analysis of Polish rivers. J. Hydrol. 248, 152–167.

Subash, N., Sikka, A.K., 2014. Trend analysis of rainfall and temperature and its relationship over India. Theor. Appl. Climatol. 117, 449–462. doi:10.1007/s00704-013-1015-9

Subash, N., Sikka, A.K., Mohan, H.S.R., 2010. An investigation into observational characteristics of rainfall and temperature in Central Northeast India-a historical perspective 1889-2008. Theor. Appl. Climatol. 103, 305–319. doi:10.1007/s00704-010-0299-2

Subash, N., Sikka, A.K., Mohan, H.S.R., 2011. An investigation into observational characteristics of rainfall and temperature in Central Northeast India-a historical perspective 1889-2008. Theor. Appl. Climatol. 103, 305–319. doi:10.1007/s00704-010-0299-2

Subbaramayya, I., Naidu, C.V., 1992. Spatial variations and trends in the Indian monsoon rainfall. Int. J. Climatol. 12, 597–609.

Sugahara, S., Porf´ırio da Rocha, R., Silveira, R., 2009. Non-stationary frequency analysis of extreme daily rainfall in Sao Paulo, Brazil. Int. J. Climatol. 29, 1339–1349. doi: 10.1002/joc.1760

Surendran, S., Gadgil, S., Francis, P.A., Rajeevan, M., 2015. Prediction of Indian rainfall during the summer monsoon season on the basis of links with equatorial Pacific and Indian Ocean climate indices. Environ. Res. Lett. 10, 94004. doi:10.1088/1748-9326/10/9/094004

Tanarhte, M., Hadjinicolaou, P., Lelieveld, J., 2012. Intercomparison of temperature and precipitation data sets based on observations in the Mediterranean and the Middle East. J. Geophys. Res. Atmos. 117. doi:10.1029/2011JD017293

Theil, H., 1950. A rank-invariant method of linear and polynomial regression analysis III. Ned. Akad. Wetenchappen 53, 386–392. doi:10.1007/978-94-011-2546-8

Tramblay, Y., Neppel, L., Carreau, J., Najib, K., 2013. Non-stationary frequency analysis of heavy rainfall events in southern France. Hydrol. Sci. J. 58, 280–294. doi:10.1080/02626667.2012.754988

Trenberth, K.E., 2011. Changes in precipitation with climate change. Clim. Res. 47, 123–138.

Trenberth, K.E., 2012. Framing the way to relate climate extremes to climate change. Clim. Change 115, 283–290. doi:10.1007/s10584-012-0441-5

Trenberth, K.E., Dai, A., Rasmussen, R.M., Parsons, D.B., 2003. The changing character of precipitation. Bull. Am. Meteorol. Soc. 84, 1205–1217+1161. doi:10.1175/BAMS-84-9-1205

UNFCC, 1992. United Nations Framework Convention on Climate Change. Rev. Eur. Community Int. Environ. Law 1, 270–277. doi:10.1111/j.1467-9388.1992.tb00046.x

van Buuren, S., Fredriks, M., 2001. Worm plot: A simple diagnostic device for modelling growth reference curves. Stat. Med. 20, 1259–1277. doi:10.1002/sim.746

van Der Schrier, G., Barichivich, J., Briffa, K.R., Jones, P.D., 2013. A scPDSI-based global data set of dry and wet spells for 1901-2009. J. Geophys. Res. Atmos. 118, 4025–4048. doi:10.1002/jgrd.50355

Villarini, G., Smith, J.A., Serinaldi, F., Bales, J., Bates, P.D., Krajewski, W.F., 2009. Flood frequency analysis for nonstationary annual peak records in an urban drainage basin. Adv. Water Resour. 32, 1255–1266. doi:10.1016/j.advwatres.2009.05.003

Vinvent, L.A., van Wijngaarden, W.A., Hopkinson, R., 2007. Surface temperature and humidity trends in Canada for 1953-2005. J. Clim. 20, 5100–5113. doi:10.1175/JCLI4293.1

Vittal, H., Karmakar, S., Ghosh, S., 2013. Diametric changes in trends and patterns of extreme rainfall over India from pre-1950 to post-1950. Geophys. Res. Lett. 40, 3253–3258.

Vittal, H., Singh, J., Kumar, P., Karmakar, S., 2015. A framework for multivariate data-based at-site flood frequency analysis: Essentiality of the conjugal application of parametric and nonparametric approaches. J. Hydrol. 525, 658–675. doi:10.1016/j.jhydrol.2015.04.024

Vogel, R.M., 1986. The Probability Plot Correlation Coefficient Test for the Normal, Lognormal, and Gumbel Distributional Hypotheses. Water Resour. Res. 22, 587–590. doi:10.1029/WR022i004p00587

Vogel, R.M., 2010. Flood Magnification Factors in the United States. Work. Nonstationarity, Hydrol. Freq. Anal. Water Manag. Colorado Water Institute Information Series No. 109, 140-149.

Vogel, R.M., Kroll, C.N., 1989. Low-Flow Frequency Analysis Using Probability-Plot Correlation Coefficients. J. Water Resour. Plan. Manag. 115, 338–357. doi:10.1061/(ASCE)0733-9496(1989)115:3(338)

Vogel, R.M., McMartin, D.E., 1991. Probability Plot Goodness-of-Fit and Skewness Estimation Procedures for the Pearson Type 3 Distribution. Water Resour. Res. 27, 3149–3158. doi:10.1029/91WR02116

von Neumann, J., 1941. Distribution of the ratio of the mean square successive difference to the variance. Ann. Math. Stat. 12, 367–395. doi:10.1214/aoms/1177731677

Vörösmarty, C.J., McIntyre, P.B., Gessner, M.O., Dudgeon, D., Prusevich, A., Green, P., Glidden, S., Bunn, S.E., Sullivan, C.A., Liermann, C.R., Davies, P.M., 2010. Global threats to human water security and river biodiversity. Nature 468, 334–334. doi:10.1038/nature09549

Wagesho, N., Goel, N.K., Jain, M.K., 2012. Investigation of non-stationarity in hydro-climatic variables at Rift Valley lakes basin of Ethiopia. J. Hydrol. 444–445, 113–133. doi:10.1016/j.jhydrol.2012.04.011

Wagesho, N., Goel, N.K., Jain, M.K., 2013. Temporal and spatial variability of annual and seasonal rainfall over Ethiopia. Hydrol. Sci. J. 58, 354–373. doi:10.1080/02626667.2012.754543

Wallis, J.R., O’connell, P.E., 1973. Firm Reservoir Yield—How Reliable Are Historic Hydrological Records? Hydrol. Sci. Bull. 18, 347–365. doi:10.1080/02626667309494046

Wasko, C., Sharma, A., 2017. Global assessment of flood and storm extremes with increased temperatures. Sci. Rep. 7, 7945. doi:10.1038/s41598-017-08481-1

Wasko, C., Sharma, A., Westra, S., 2016. Reduced spatial extent of extreme storms at higher temperatures. Geophys. Res. Lett. 43, 4026–4032. doi:10.1002/2016GL068509

Westra, S., Alexander, L.V., Zwiers, F.W., 2013. Global increasing trends in annual maximum daily precipitation. J. Clim. 26, 3904–3918. doi:10.1175/JCLI-D-12-00502.1

Wheeler, T., von Braun, J., 2013. Climate Change Impacts on Global Food Security. Science (80). 341, 508–513. doi:10.1126/science.1239402

Willmott, C.J., Matsuura K., 2001. Terrestrial Air Temperature and Precipitation: Monthly and Annual Time Series (1950 - 1999). http://climate.geog.udel.edu/~climate/html_pages/README.ghcn_ts2.html.

Willmott, C.J., Matsuura, K., 1995. Smart Interpolation of Annually Averaged Air Temperature in the United States. J. Appl. Meteorol. doi:10.1175/1520-0450(1995)034<2577:SIOAAA>2.0.CO;2

Willmott, C.J., Robeson, S.M., 1995. Climatologically aided interpolation (CAI) of terrestrial air temperature. Int. J. Climatol. 15, 221–229. doi:10.1002/joc.3370150207

Willmott, C.J., Rowe, C.M., Philpot, W.D., 1985. Small-Scale Climate Maps: A Sensitivity Analysis of Some Common Assumptions Associated with Grid-Point Interpolation and Contouring.

Yaduvanshi, A., Ranade, A., 2015. Effect of Global Temperature Changes on Rainfall Fluctuations over River Basins Across Eastern Indo-GangeticPlains. Aquat. Procedia 4, 721–729. doi:10.1016/j.aqpro.2015.02.093

Yatagai, A., Kamiguchi, K., Arakawa, O., Hamada, A., Yasutomi, N., Kitoh, A., 2012. Aphrodite constructing a long-term daily gridded precipitation dataset for Asia based on a dense network of rain gauges. Bull. Am. Meteorol. Soc. 93, 1401–1415. doi:10.1175/BAMS-D-11-00122.1

Yevjevich, V., 1971. Stochastic Processes in Hydrology. Water Resources Publications, Fort Collins, CO.

Yue, S., Hashino, M., 2003. Long-term trends of annual and monthly precipitation in Japan. Am. Water Resouces Assoc. 39, 587–596.

Yue, S., Pilon, P., Phinney, B., 2003. Canadian streamflow trend detection: impacts of serial and cross-correlation. Hydrol. Sci. J. 48, 51–63. doi:10.1623/hysj.48.1.51.43478

Yue, S., Pilon, P., Phinney, B., Cavadias, G., 2002. The influence of autocorrelation on the ability to detect trend in hydrological series. Hydrol. Process. 16, 1807–1829.

Zaman, R., Malaker, P.K., Murad, K.F.I., Sadat, M.A., 2013. TREND analysis of changing temperature in Bangladesh due to global warming. Journal of Biodiversity and Environmental Sciences (JBES) 3, 32–38.

Zhang, Q., Gu, X., Singh, V.P., Xiao, M., Chen, X., 2015. Evaluation of flood frequency under non-stationarity resulting from climate indices and reservoir indices in the East River basin, China. J. Hydrol. 527, 565–575. doi:10.1016/j.jhydrol.2015.05.029

Zhang, Q., Li, J., Singh, V.P., Xiao, M., 2013. Spatio-temporal relations between temperature and precipitation regimes: Implications for temperature-induced changes in the hydrological cycle. Glob. Planet. Change 111, 57–76. doi:10.1016/j.gloplacha.2013.08.012

Zhang, Q., Xu, C.Y., Singh, V.P., Yang, T., 2009. Multiscale variability of sediment load and streamflow of the lower Yangtze River basin: Possible causes and implications. J. Hydrol. 368, 96–104. doi:10.1016/j.jhydrol.2009.01.030

Zhang, X., Wang, J., Zwiers, F.W., Groisman, P.Y., 2010. The influence of large-scale climate variability on winter maximum daily precipitation over North America. J. Clim. 23, 2902–2915. doi:10.1175/2010JCLI3249.1

Impacts of Increasing Temperature over India

National Environment Policy [128] stated that the anthropogenic climate changes have severe adverse impacts on the country's ecosystems, agricultural potential, forests as well as water and marine resources.

Water resources

The increasing temperature may create myriad of problems in water resources for the country. Increasing temperature will accelerate the hydrologic cycle, altering precipitation and runoff. The intensification of hydrological processes will lead to intense localised rainfall events finally causing floods [212]. The arable lands will be lost due to the riverbank erosion which may result in the failure of the banks and also due to the silt deposited after a flood. The intense rainfall events will also cause heavy erosion, and finally, sedimentation [125; 36] problems in rivers will increase. The increase of flood events and sedimentation problems will change the morphological characteristics of the rivers, and thus the flood will be more devastating in nature due to the reduction in carrying capacity of the rivers. The intense flood events also cause the change of course of rivers affecting human life and displacing many people. In India, many peoples are living on the river bank due to poverty and the change of course of rivers will have a huge impact. In 2008, Kosi river reverted to the 250 years old course and left 30 lakh people homeless in North Bihar in India.

The increasing temperature in summer season may increase the occurrence of droughts. The situation may lead to hydrological and agricultural drought. In the recent year between 2000 to 2015, India has suffered two massive droughts in 2002 and 2013. During drought, the use of groundwater will increase, and it may change the pattern of groundwater use and recharge. The increase of heat wave will also negatively affect the sustenance of ecological flows in the rivers. Both the northern and western India gets less rainfall due to the Indian geographical conditions. The results of the current study are showing more increase of temperature in this region. The combining effect will increase the demand for water and consequently increase the groundwater use in the region. According to Central Ground Water

Board (CGWB), the groundwater is highly depleted on this region. The increasing temperature will create a pressure of water supply on the water resources projects.

The increasing temperature is going to accelerate the retreat of the glaciers of Himalayas and in the Karakoram range. Bahadur [10] reported that at least 500 km^3/yr snow and ice meltwater contributes to the Himalayan streams. The increasing temperature increase the rate of retreat of Himalayan glaciers and almost 67% of the glaciers have retreated in the past decade. Records have been found that the Gangotri glacier is retreating about 28 m per year. The river system like Ganga, Brahmaputra, Indus may benefit from melting snow in the non-monsoon season from increasing temperature, but the snow cover is likely to decrease. The water demand is going to increase in the non-monsoon season for the other rainfed river basins. The alterations of flows of river systems like Ganga, Brahmaputra and Indus due to increasing in snowmelt may significantly influence the countries irrigation system and affect the livelihood of the people living these basins by changing the amount of food production.

The increasing temperature is going to accelerate the rise of sea level. According to IPCC report Summary for Policymakers [65] the global sea level increased by 0.19m during 1901 to 2010 period. World Bank in 2014 reported that a rapid rise in sea level and salinity in the Sundarban regions had triggered migration of inhabitants from several blocks in the forest to other parts of the country. The sea level rise is causing salt intrusion in freshwater sources, mainly groundwater aquifers near the coastal regions of the country [126], affecting the coastal population, agriculture, degrading the quality of groundwater. Groundwater is the backbone for meeting more than 80% domestic needs. The increasing temperature will increase the irrigation demand resulting in the exploitation of groundwater resources, which will continuously decline the groundwater level. The falling groundwater level in various parts of the country has threatened the sustainability of the groundwater resources. It has already been noticed that almost 15% of India's groundwater resources are over-exploited. It can be concluded that the increasing temperature is going to impose multidimensional threat in water resources.

Agriculture

Agriculture forms the backbone of Indian rural livelihood and hence the effects of changing the climate on agricultural production warrants adequate attention. Agricultural production is sensitive to the variability in changing temperature within a season. Higher temperatures are likely to result in a decline in yields, mainly due to the shortening of the crop life cycle especially the grain filling period. McWilliam [112] stated that high temperatures are a major constraint to crop productivity, especially when extreme temperatures coincide with critical stages of the plant development. Sheehy et al. [172] reported rice yield decreases by 0.6 t/ha for every 1ºC increase in temperature. Hundal and Kaur [62] indicated that an increase in temperature between 1°C and 3°C is reduced the rice production by 3%-10% in Punjab. Geethalakshmi et al. [43] found a reduction in rice yield up to 41% due to 4ºC increasing temperature in Tamil Nadu. The increasing temperature may cause droughts in the country. Pandey [136] reported a loss of 40% of total rice production during severe droughts in Jharkhand, Odisha and Chhattisgarh states. Lal et al. [98] reported a decrease in rainfed wheat yield by 0.45 t/ha in India due increase in winter temperature by 0.5ºC. India Agricultural Research Institute (IARI) and others indicated a reduction in wheat production by 4-5 million tonnes (especially in Rabi crops) due to an increase of 1ºC in temperature. Mahato [106] reported that an increase in temperature by 2ºC in Rajasthan is reduced 10 to 15% production of Pearl Millet. From the above discussion, it can be deduced that the increasing temperature trends observed in this study can have severe adverse impacts on the Indian agricultural scenario thus affecting the food security of the nation.

Health

The increasing temperature may increase the incidence of vector-borne diseases like malaria, dengue, chikungunya, Japanese encephalitis, kala-azar and filariasis [19]. It is reported in National Action Plan on Climate Change [127] that an increase of 3.8ºC temperature and 7% relative humidity, the transmission windows of mosquitoes will increase for all the 12 months in 9 states in India. Jetten and Focks [71] reported two to five time more spreadings in dengue transmission due to 4°C increase in temperature in India. Jetten et al. [72] projected two to five times increase in malaria due to an increase of 2 to 4ºC temperature. Hence it can be said that the increasing temperature trends can pose serious public health hazards for the Indian population.

Generalised Additive Models for Location, Scale and Shape (GAMLSS)

The GAMLSS model is capable of doing frequency analysis for non-stationary series. Rigby and Stasinopoulos (2005) proposed the GAMLSS model, which provides a flexible modelling framework for the non-stationary series. In GAMLSS, response variable, 'Y' can be modelled using any general distribution function (e.g. highly skewed and/or kurtotic continuous and discrete distributions) including any of the continuous or discrete distribution. GAMLSS provides the flexibility to modelling the location (related to the mean), scale and shape (related to the dispersion, skewness and kurtosis) parameters of the distribution of any response variable, 'Y' as linear and/or non-linear, parametric and/or additive nonparametric functions of covariates and/or random effects (Rigby and Stasinopoulos, 2005; Stasinopoulos and Rigby, 2007). The theory behind GAMLSS model is briefly described in this section.

In a GAMLSS model, it is assumed that the independent observations y_i, for $i = 1,2, \dots n$ have probability density function $f_y(y_i; \theta^i)$ with $\theta^i = (\theta_1^i, \theta_2^i, \dots \theta_p^i)$ a vector of p distribution parameters accounting for location, scale and shape. Generally, p is not more than four, as four parameters are enough for most of the hydrological applications (Villarini et al., 2009). For a response variable y^T of length n, i.e. $y^T = (y_1, y_{2,} \dots y_n)$, let $g_k(.)$, for $k = 1,2, .. p$, is a monotonic link function, which is used to relate the distribution parameters with the explanatory variables and random effects through an additive model given by:

$$g_k(\theta_k) = \eta_k = X_k\beta_k + \sum_{j=1}^{j_k} Z_{jk}\gamma_{jk} \quad (1)$$

where θ_k and η_k are vectors of length n, β_k for $k = 1,2, .. j_k$, is a parameter vector. X_k is 'n' order known design matrix, Z_{jk} is a fixed known design matrix and γ_{jk} is a random variable. Stasinopoulos and Rigby (2007) discuss the model fitting and selection. In Eq. (1) the linear predictors η_k, for $k = 1,2, \dots p$, are comprised of a parametric component $X_k\beta_k$ (linear functions of covariates) and additive components $Z_{jk}\gamma_{jk}$ (linear functions of random variables).

GAMLSS can derive several sub-models. Most commonly, if $Z_{jk} = I_n$, (I_n is a $n \times n$ identity matrix) and $\gamma_{jk} = h_{jk}(X_{jk})$ for all combinations of j and k in Eq. (1), a semi-parametric additive GAMLSS model is formed as:

$$g_k(\theta_k) = \eta_k = \mathrm{X}_k\beta_k + \sum_{j=1}^{j_k} h_{jk}(x_{jk}) \qquad (2)$$

where, h_{jk} is an unknown function of the explanatory variable X_{jk} and $h_{jk}(x_{jk})$ is the vector which evaluates the function h_{jk} at x_{jk}. The additive terms in Eq. (2) represent smoothing terms (linear or non-linear), which provides additional flexibility for modelling the dependence of the distribution parameters on the covariates. In the present study, this formulation of GAMLSS model is used with the help of cubic spline smoothing technique.

The cubic spline smoothing technique chooses $h(.)$, which maximise a penalised log-likelihood subject to penalty terms of the form $\lambda \int_{-\infty}^{\infty} [h''(t)]^2 dt$, where h'' is the second derivative of h. The smoothing parameter is λ. High values of λ assign a premium on smoothness and heavily penalize functions with large second derivatives. On the other hand, the small values of λ emphasises the goodness of fit.

The GAMLSS model can be fitted using two basic algorithms, namely, CG algorithm and RS algorithm. The CG algorithm is a generalisation of the Cole and Green (1992) algorithm. It uses the first derivatives and the expected values of the second and cross-derivatives of the likelihood function with respect to the location, scale and shape parameters. However, for many population probability density functions, the distribution parameters are information orthogonal (since the expected values of the cross derivatives of the likelihood function are zero). For this situation, the RS algorithm is used. It is a generalised form of the algorithm used by Rigby and Stasinopoulos (1996a, 1996b) for fitting Mean and Dispersion Additive Models, (MADAM). The algorithm does not use the expected values of the cross derivatives.

Annexure 4.2

The results of MK test for AMR series of 239 stations are given in Table 1. This table also provides the results of the change in magnitude of AMR in mm/year for all the stations.

Table 1 Results of MK test, and change in magnitude of AMR in mm/year for 239 stations.

SL. No.	Stations Name	Latitude (Degree)	Longitude (Degree)	Z-values of MK test	Change in Magnitude of AMR (mm/year)
1	Cheyyar	12.67	79.58	-0.679	-0.350
2	Manjallar Head	11.03	79.52	0.588	0.070
3	Minambakkam Aero	13.00	80.18	-0.730	-0.220
4	Pandavar Head	10.78	79.48	-2.347	-1.400
5	Ottapidaram	8.92	78.03	-0.542	-0.080
6	Pakala	15.25	80.00	0.062	0.050
7	Talanayar	10.55	79.78	-1.100	0.080
8	Tanjavur	10.78	79.13	1.293	0.600
9	Vattanam	9.78	79.05	-0.152	0.200
10	Vilathikulam	9.15	78.17	3.210	0.910
11	Aliabad Anicut	12.63	79.23	-1.470	-0.310
12	B.K.Pet	13.67	79.13	0.177	-0.004
13	Cheyyar Anicut	12.60	79.38	-1.239	0.014
14	Cheyyur	12.35	80.02	-0.824	-0.160
15	Chinaganjam	15.70	80.25	0.228	0.010
16	Madurai (T.South)	9.93	78.12	-0.735	-0.020
17	Malaiyur	10.42	79.00	-1.532	-0.054
18	Peranai	10.08	77.93	1.661	0.334
19	Peravoorani	10.28	79.20	1.067	0.186
20	Shatiatope Anicu	11.43	79.57	-2.044	-0.410
21	Sidhout (Siddavat)	14.47	78.97	-1.516	-0.274
22	Srimushnam	11.40	79.42	-2.048	-0.610
23	Iluppur	10.52	78.62	0.112	0.021
24	Sangam	14.60	79.75	-0.208	0.027
25	Kodavasal	10.85	79.48	1.632	0.479
26	Rapur	14.20	79.53	-0.172	0.842
27	Tiruchi.Palli (A)	10.77	78.72	-0.863	-0.161
28	Tirukkattupalli	10.85	78.97	0.302	0.086
29	Vidur Dam-Site	12.07	79.58	0.090	0.114
30	Rajampet	14.20	79.17	0.375	-0.011
31	Pallipattu	13.33	79.45	1.354	0.181
32	Dantan	21.97	87.27	0.370	0.300
33	Daspalla	20.35	84.85	0.902	0.500
34	Sompeta	18.93	84.60	1.417	0.821
35	Tekkali	18.62	84.25	-0.076	0.019

SL. No.	Stations Name	Latitude (Degree)	Longitude (Degree)	Z-values of MK test	Change in Magnitude of AMR (mm/year)
36	Amalapuram	16.57	82.00	-0.008	0.218
37	Rajahmundry	17.00	81.77	0.801	0.414
38	Wallajah	12.93	79.37	2.366	0.446
39	Wandiwash	12.50	79.62	2.579	0.686
40	M.Thurai/Mayuram	11.10	79.65	-1.972	-0.457
41	Melur	10.05	78.33	-2.699	-0.443
42	Thotapalli	18.78	83.52	2.054	0.579
43	Polavaram	17.25	81.65	2.661	0.446
44	Kuppanatham	11.50	79.33	2.073	0.496
45	Pattamundai	20.58	86.57	-1.981	-0.586
46	Echenviduthi	10.40	79.20	2.587	0.300
47	Sunkasula	15.78	79.17	0.887	0.260
48	T.Narsipur	12.20	76.90	2.481	0.300
49	Vempalli	14.37	78.45	1.840	0.414
50	Amritur	12.92	76.92	2.241	0.629
51	Attur	11.60	78.62	-0.450	0.120
52	B.R.Hills	12.00	77.13	-2.489	-0.464
53	Bagur	13.00	76.37	-1.567	-0.343
54	Mahadeswara Hill	12.05	77.60	-1.712	-0.090
55	Pathapalaya	13.75	77.95	-0.882	-0.426
56	Perur	14.37	77.35	0.441	0.177
57	Podanur	10.97	76.98	1.952	0.671
58	Sulebele	13.17	77.80	-1.567	-0.643
59	Sultanpet	10.87	77.20	-2.357	-0.629
60	Dharampuri	12.13	78.17	0.877	0.171
61	Madanapalli	13.55	78.50	-0.733	0.030
62	Maddanur	15.75	78.50	0.308	0.293
63	Madhugiri	13.65	77.20	2.824	0.350
64	Rajali (K.C.C)	14.95	78.52	0.000	-0.219
65	Rasipuram	11.45	78.18	-1.591	-0.186
66	Tavarekere	13.08	77.92	2.134	0.436
67	Periakulam	10.12	77.53	-1.477	-0.143
68	Basaralu	12.70	76.80	-1.308	-0.183
69	Gudibanda	13.63	77.70	-5.247	-0.907
70	Mulanur	10.78	77.70	-1.587	-0.239
71	Magadi	12.95	77.22	-2.565	-0.600
72	Thoppanhalli	12.83	78.20	0.351	0.059
73	Gariabund	20.63	82.07	-0.248	-0.037
74	Deobhog	19.90	82.67	-0.284	0.026
75	Deogarh (Bamra)	21.55	84.73	2.109	0.571
76	Sonepur	20.85	83.98	1.599	0.571
77	Adamabad	20.68	81.25	0.487	-0.120
78	Malegaon	20.55	74.53	0.767	0.343
79	Burhanpur	21.32	76.23	-1.512	-0.343
80	Chalisgaon	20.45	75.02	0.119	0.134

SL. No.	Stations Name	Latitude (Degree)	Longitude (Degree)	Z-values of MK test	Change in Magnitude of AMR (mm/year)
81	Yaval	21.17	75.70	-2.343	-0.379
82	Khargone	21.82	75.62	-1.009	-0.329
83	Mulug	18.18	79.95	1.901	0.586
84	Nirmal	19.10	78.35	0.578	0.200
85	Parbhani	19.27	76.77	0.896	0.088
86	Saoner	21.38	78.92	-1.173	0.129
87	Valapady	11.67	78.42	7.228	0.657
88	Nedungal	12.37	78.27	2.596	0.514
89	Bhavani	11.45	77.72	-0.154	0.051
90	Bindiganavale	12.88	76.63	2.344	-0.043
91	Madakasira	13.93	77.27	-1.999	0.346
92	Bangalore C.O.	12.97	77.58	2.082	0.002
93	Telkoi	21.33	85.33	-0.590	-0.099
94	Nandurbar	21.37	74.25	-1.487	0.113
95	Sindkheda	21.28	74.75	-0.186	-0.290
96	Bhadgaon	20.67	75.23	-1.994	0.264
97	Jamner	20.82	75.78	-2.310	-0.371
98	Pachora	20.67	75.37	0.932	-0.357
99	Chandur Railway	20.82	77.97	-0.958	0.226
100	Hanamkonda	18.02	79.57	0.478	-0.270
101	Jactial	18.80	78.93	-2.678	0.011
102	Nevasa	19.55	74.93	0.728	-0.249
103	Nizamabad	18.67	78.10	-1.268	0.289
104	Bidar	17.87	77.48	-0.270	-0.369
105	Owk	15.22	78.13	1.964	-0.143
106	Hinganghat	20.55	78.83	-0.503	0.118
107	Nanded	19.13	77.33	-0.456	0.207
108	Niphad	20.08	74.12	0.445	-0.151
109	Sangareddi	17.63	78.08	-2.049	0.199
110	Sironcha	18.83	79.97	-1.403	0.506
111	Umrer	20.85	79.33	-0.122	-0.164
112	Yeola	20.05	74.48	-2.477	-0.151
113	Brahmapuri	20.60	79.87	-0.189	-0.857
114	Chandrapur	19.95	79.30	-1.115	-0.017
115	Pathardi	19.17	75.17	-4.108	-0.129
116	Bhadrachalam	17.67	80.90	0.162	0.491
117	Motihari	26.67	84.92	-0.703	0.100
118	Mainpuri	27.23	79.05	0.346	0.023
119	Bahraich	27.57	81.60	1.572	0.564
120	Rajakhera	26.90	78.18	-2.125	-0.200
121	Manohar Thana	24.23	76.80	-0.370	0.057
122	Shahabad	25.25	77.13	-0.343	-0.111
123	Sonkatch	22.97	76.35	-3.746	-1.230
124	Bari	26.65	77.60	-0.188	-0.073
125	Sangod	24.93	76.28	-0.555	-0.059

SL. No.	Stations Name	Latitude (Degree)	Longitude (Degree)	Z-values of MK test	Change in Magnitude of AMR (mm/year)
126	Banswara	23.55	74.45	1.592	0.857
127	Jhabua	22.78	74.58	0.314	0.069
128	Burwaha	22.27	76.03	-1.445	-0.450
129	Daltonganj	24.05	84.07	0.694	0.357
130	Mukteshwar	29.47	79.65	0.249	0.027
131	Jhansi	25.45	78.58	-0.591	-0.187
132	Bharatpur	27.22	77.5	0.078	0.064
133	Fatehpur	25.93	80.83	-1.258	0.036
134	Gohad	26.42	78.45	0.000	-0.016
135	Simdega	22.62	84.57	-0.062	0.150
136	Seorinarayan	21.72	82.60	0.223	-0.057
137	Champua	22.17	85.50	-0.679	0.377
138	Alirajpur	22.30	74.37	0.416	-0.534
139	Harsud	22.12	76.73	-2.162	-0.027
140	Indore	22.72	75.8	0.090	0.241
141	Sagar	23.85	78.75	-1.419	-0.027
142	Satna	24.57	80.83	0.895	-0.377
143	Pendra Road	22.77	81.9	0.282	0.420
144	Raisen	23.33	77.8	0.656	0.089
145	Guna	24.65	77.32	-1.165	0.157
146	Pandaria	22.22	81.42	-2.131	-0.136
147	Niwas	23.05	80.45	0.395	-0.271
148	Dug/Dag	23.93	75.83	-2.277	-0.714
149	Lahar	26.20	78.93	-4.206	-0.557
150	Tezpur	26.62	92.78	1.677	0.250
151	Jalpaiguri	26.53	88.72	1.414	0.771
152	Hazaribagh	23.98	85.37	-1.380	-0.343
153	Alipur	22.53	88.33	0.238	0.287
154	Barhampore	24.13	88.27	1.176	0.614
155	Midnapore	22.42	87.32	0.010	0.027
156	Sonahatu	23.20	85.72	-0.725	-0.186
157	Lumding	25.75	93.18	-2.305	-0.191
158	Gaya Aerodrome	24.75	84.95	-1.647	-0.443
159	Sabour	25.23	87.07	1.041	0.717
160	Silda Belpahari	22.63	86.80	-0.795	-0.189
161	Senha	23.58	84.75	0.038	0.130
162	Agartala Sadar	23.88	91.25	0.863	1.086
163	Cherrapunji	25.25	91.73	0.471	0.189
164	Purnea	25.77	87.47	2.456	1.800
165	Malda	25.03	88.13	0.879	0.337
166	Krishnanagar	23.4	88.52	-1.514	-0.443
167	Jaipur Aero	26.92	76.83	-0.076	0.141
168	Bhim/Dawer	25.75	74.08	-1.364	-0.283
169	Dehra Dun	30.32	78.03	-0.041	-0.109
170	Simla	31.10	77.17	0.456	0.063

SL. No.	Stations Name	Latitude (Degree)	Longitude (Degree)	Z-values of MK test	Change in Magnitude of AMR (mm/year)
171	Kotkhai	31.12	77.53	-0.010	0.026
172	Lachmangarh	27.37	76.87	-2.535	-0.443
173	Mandawar	27.87	76.55	1.144	0.417
174	Nimarana	28.00	76.38	2.091	0.366
175	Kamen	27.65	77.27	-0.279	-0.037
176	Chirawa	28.23	75.65	0.000	-0.023
177	Jhunjhunu	28.13	75.38	0.375	0.077
178	Khetri	28.00	75.80	-0.963	-0.127
179	Hissar	29.17	75.73	1.450	0.514
180	Nimbahera	24.62	74.70	-0.243	0.086
181	Hindoli	25.58	75.50	-3.463	-0.870
182	Patan	25.30	75.95	-2.089	-0.543
183	Bali	25.18	73.28	-1.298	-0.306
184	Bilara	26.18	73.70	-0.335	0.266
185	Desuri	25.28	73.55	-0.189	-0.134
186	Jalore	25.35	72.62	0.175	0.087
187	Nayanagar/Beawar	26.10	74.32	0.641	0.057
188	Pachpadra	25.93	72.27	-0.291	0.343
189	Shergarh	26.33	72.30	-0.517	0.141
190	Merta City	26.63	74.03	-0.899	-0.131
191	Partabgarh	24.05	74.78	0.188	0.004
192	Sheoganj	25.12	73.07	-0.631	-0.186
193	Arthuna	23.50	74.08	0.867	0.429
194	Jodhpur	26.30	73.03	1.586	0.357
195	Barmer	25.75	71.40	-0.259	-0.071
196	Ahmedabad Aero	23.03	72.62	0.462	0.314
197	Deesa	24.20	72.25	-0.492	-0.031
198	Rajkot Aero	22.30	70.77	0.159	0.329
199	Lalsot	26.55	76.33	2.245	0.526
200	Bhuj/R.Mata A.	23.25	69.80	0.164	0.005
201	Chotan	25.48	71.07	2.039	0.414
202	Sathankulam	8.45	77.92	2.123	0.357
203	Srivaikundam	8.63	77.92	-0.911	-0.220
204	Ayikudi	9.00	77.33	0.172	-0.019
205	Manimuthar	8.58	77.42	2.557	0.436
206	Radhapuram	8.27	77.68	-1.340	-0.109
207	Chickmagalur	13.33	75.77	-5.818	-0.857
208	Mudigere T.O.	13.13	75.63	-1.420	-0.257
209	Saklespur	12.95	75.78	-1.176	-0.246
210	Sukravarasathy	12.87	75.80	0.205	-0.174
211	Ammathy	12.23	75.85	0.326	0.080
212	Avandoor	12.38	75.67	0.012	0.014
213	Bhagamandala	12.38	75.52	-0.345	-0.023
214	Harangi	12.50	75.83	2.754	0.800
215	Maladare Forest	12.32	75.97	1.152	0.099

SL. No.	Stations Name	Latitude (Degree)	Longitude (Degree)	Z-values of MK test	Change in Magnitude of AMR (mm/year)
216	Srimangala	12.02	75.98	0.183	-0.117
217	Thittimatti	12.22	76.00	1.698	0.329
218	Periyapatna	12.33	76.10	0.355	0.114
219	Udagamandalam	11.40	76.68	0.000	0.143
220	Kayamkulam	9.18	76.50	-3.007	-0.686
221	Bantwal T.O.	12.88	75.03	1.873	0.271
222	Kozhikode	11.25	75.78	-2.038	-0.486
223	Nedumangad	8.60	77.00	-2.881	-0.414
224	Thiruvananthapur	8.48	76.95	-0.416	-0.139
225	Bombay Colaba	18.98	72.83	2.593	1.143
226	Mundagod Hospita	14.97	75.03	1.009	0.371
227	Panjim	15.48	73.82	3.297	1.157
228	Ratnagiri	16.98	73.30	0.938	0.257
229	Chickmagalur	13.33	75.77	-2.008	-0.529
230	Akola	19.55	74.02	-1.793	-0.271
231	Mercara	12.43	75.73	2.519	0.443
232	Baroda College	22.33	73.27	-1.523	-0.626
233	Veraval	20.90	70.37	1.282	0.731
234	Vada	19.65	73.13	-2.663	-1.014
235	Hoshangabad	22.26	71.19	0.688	0.457
236	Udupi	13.35	74.75	2.704	0.247
237	Yellapur	14.95	74.72	3.335	0.614
238	Dahanu	19.98	72.72	-2.049	-0.686
239	Margon	15.28	73.97	4.209	1.257

Annexure 4.3

The correlation of AMR series with four different covariates (RAT, NINO, IOD, and GAT) are obtained by using the Pearson's correlation test. The results of Pearson's test for 239 stations are given in the Table 1.

Table 1 Pearson's correlation coefficient for AMR series of 239 stations.

SL. No.	Stations Name	Latitude (Degree)	Longitude (Degree)	Pearson's correlation coefficient (r) for covariates			
				RAT	NINO	IOD	GAT
1	Cheyyar	12.67	79.58	-0.156	0.199	0.164	-0.042
2	Manjallar Head	11.03	79.52	0.046	0.117	-0.062	0.166
3	Minambakkam Aero	13.00	80.18	-0.011	0.141	-0.017	-0.044
4	Pandavar Head	10.78	79.48	-0.210	0.112	0.047	-0.200
5	Ottapidaram	8.92	78.03	-0.070	-0.094	-0.021	-0.021
6	Pakala	15.25	80.00	0.189	0.035	-0.024	0.038
7	Talanayar	10.55	79.78	-0.041	-0.128	-0.066	0.100
8	Tanjavur	10.78	79.13	0.185	0.229	-0.055	0.372
9	Vattanam	9.78	79.05	0.028	0.012	0.183	0.027
10	Vilathikulam	9.15	78.17	0.271	0.255	0.263	0.324
11	Aliabad Anicut	12.63	79.23	-0.426	-0.176	-0.166	-0.257
12	B.K.Pet	13.67	79.13	-0.157	0.036	-0.067	0.007
13	Cheyyar Anicut	12.60	79.38	0.024	-0.118	0.136	0.143
14	Cheyyur	12.35	80.02	0.006	0.104	0.027	0.064
15	Chinaganjam	15.70	80.25	-0.113	-0.168	-0.187	-0.024
16	Madurai/T.South	9.93	78.12	0.087	0.007	-0.044	0.054
17	Malaiyur	10.42	79.00	-0.142	-0.005	-0.093	0.057
18	Peranai	10.08	77.93	0.121	0.072	0.052	0.383
19	Peravoorani	10.28	79.20	0.025	0.279	0.101	0.167
20	Shatiatope Anicu	11.43	79.57	-0.262	0.046	0.172	-0.316
21	Sidhout (Siddavat)	14.47	78.97	-0.117	0.058	0.019	-0.128
22	Srimushnam	11.40	79.42	-0.176	0.115	0.062	-0.013
23	Iluppur	10.52	78.62	0.226	-0.144	0.165	0.162
24	Sangam	14.60	79.75	0.056	0.094	0.058	0.010
25	Kodavasal	10.85	79.48	0.070	0.051	-0.006	0.242
26	Rapur	14.20	79.53	0.062	-0.084	0.044	0.136
27	Tiruchi Palli (A)	10.77	78.72	-0.055	-0.033	0.054	-0.010
28	Tirukkattupalli	10.85	78.97	0.017	-0.028	0.075	-0.064
29	Vidur Dam-Site	12.07	79.58	-0.006	0.107	0.117	0.037
30	Rajampet	14.20	79.17	0.068	0.199	0.129	0.126
31	Pallipattu	13.33	79.45	0.061	0.139	-0.088	0.121
32	Dantan	21.97	87.27	0.120	-0.091	0.051	0.268
33	Daspalla	20.35	84.85	0.357	-0.056	0.162	0.432
34	Sompeta	18.93	84.60	0.171	-0.058	-0.033	0.124

SL. No.	Stations Name	Latitude (Degree)	Longitude (Degree)	Pearson's correlation coefficient (r) for covariates			
				RAT	NINO	IOD	GAT
35	Tekkali	18.62	84.25	0.062	0.091	0.118	0.171
36	Amalapuram	16.57	82.00	0.134	-0.182	0.094	0.060
37	Rajahmundry	17.00	81.77	0.087	0.020	0.013	0.155
38	Wallajah	12.93	79.37	0.228	0.207	0.171	0.230
39	Wandiwash	12.50	79.62	0.093	0.212	0.070	0.265
40	M.Thurai/Mayuram	11.10	79.65	-0.207	-0.042	0.046	-0.183
41	Melur	10.05	78.33	-0.139	0.051	0.066	-0.143
42	Thotapalli	18.78	83.52	0.033	0.002	-0.159	0.175
43	Polavaram	17.25	81.65	0.045	0.118	0.019	-0.030
44	Kuppanatham	11.50	79.33	0.204	-0.051	0.357	0.340
45	Pattamundai	20.58	86.57	-0.125	-0.098	-0.035	0.002
46	Echenviduthi	10.40	79.20	0.244	0.149	0.186	0.298
47	Sunkasula	15.78	79.17	-0.105	-0.154	-0.002	0.072
48	T.Narsipur	12.20	76.90	0.085	-0.069	0.038	0.203
49	Vempalli	14.37	78.45	0.291	-0.037	0.030	0.406
50	Amritur	12.92	76.92	0.133	0.004	-0.024	0.401
51	Attur	11.60	78.62	0.229	-0.089	-0.007	0.367
52	B.R.Hills	12.00	77.13	-0.170	-0.166	0.009	-0.262
53	Bagur	13.00	76.37	-0.202	-0.142	-0.003	-0.209
54	Mahadeswara Hill	12.05	77.60	0.258	0.011	0.019	0.120
55	Pathapalaya	13.75	77.95	-0.035	-0.107	-0.115	-0.024
56	Perur	14.37	77.35	0.029	-0.050	0.114	0.028
57	Podanur	10.97	76.98	0.022	0.039	0.153	0.079
58	Sulebele	13.17	77.80	-0.129	0.056	-0.071	-0.195
59	Sultanpet	10.87	77.20	-0.174	-0.021	-0.110	-0.123
60	Dharampuri	12.13	78.17	0.041	0.101	0.134	0.279
61	Madanapalli	13.55	78.50	0.219	0.096	0.075	0.120
62	Maddanur	15.75	78.50	-0.036	0.060	0.011	0.070
63	Madhugiri	13.65	77.20	0.131	-0.003	0.134	0.154
64	Rajali (K.C.C)	14.95	78.52	-0.127	-0.042	0.038	0.013
65	Rasipuram	11.45	78.18	-0.019	0.051	0.090	-0.153
66	Tavarekere	13.08	77.92	0.108	0.074	0.157	0.255
67	Periakulam	10.12	77.53	-0.001	-0.043	0.003	0.060
68	Basaralu	12.70	76.80	0.227	0.102	0.011	0.052
69	Gudibanda	13.63	77.70	-0.134	-0.066	-0.250	-0.444
70	Mulanur	10.78	77.70	-0.138	-0.222	-0.232	-0.106
71	Magadi	12.95	77.22	-0.175	-0.098	-0.099	-0.247
72	Thoppanhalli	12.83	78.20	0.096	-0.226	-0.168	-0.144
73	Gariabund	20.63	82.07	-0.156	-0.096	-0.142	-0.073
74	Deobhog	19.90	82.67	-0.046	-0.069	-0.196	0.181
75	Deogarh (Bamra)	21.55	84.73	0.099	0.185	0.081	0.275
76	Sonepur	20.85	83.98	-0.001	0.035	-0.022	0.146
77	Adamabad	20.68	81.25	0.097	0.252	0.027	0.103
78	Malegaon	20.55	74.53	0.050	0.115	0.187	0.100
79	Burhanpur	21.32	76.23	-0.070	-0.092	-0.102	-0.117

SL. No.	Stations Name	Latitude (Degree)	Longitude (Degree)	Pearson’s correlation coefficient (r) for covariates			
				RAT	NINO	IOD	GAT
80	Chalisgaon	20.45	75.02	-0.055	-0.144	-0.166	0.024
81	Yaval	21.17	75.70	0.050	0.030	-0.132	0.070
82	Khargone	21.82	75.62	-0.153	-0.169	-0.018	0.018
83	Mulug	18.18	79.95	0.208	0.224	-0.055	0.115
84	Nirmal	19.10	78.35	0.080	0.048	0.079	0.115
85	Parbhani	19.27	76.77	-0.176	-0.044	0.059	0.126
86	Saoner	21.38	78.92	0.067	-0.211	-0.097	-0.073
87	Valapady	11.67	78.42	0.179	0.238	0.209	-0.018
88	Nedungal	12.37	78.27	0.121	0.079	0.118	0.191
89	Bhavani	11.45	77.72	-0.045	0.197	0.085	-0.036
90	Bindiganavale	12.88	76.63	-0.098	0.055	-0.078	-0.121
91	Madakasira	13.93	77.27	0.090	-0.001	0.128	0.112
92	Bangalore C.O.	12.97	77.58	0.022	0.122	0.191	-0.040
93	Telkoi	21.33	85.33	0.129	0.139	-0.040	-0.084
94	Nandurbar	21.37	74.25	-0.125	-0.002	-0.100	0.017
95	Sindkheda	21.28	74.75	0.071	-0.007	0.023	0.076
96	Bhadgaon	20.67	75.23	-0.052	-0.002	0.061	0.070
97	Jamner	20.82	75.78	0.207	0.276	-0.039	0.011
98	Pachora	20.67	75.37	-0.096	-0.093	-0.199	-0.111
99	Chandur Railway	20.82	77.97	-0.029	0.046	-0.101	-0.010
100	Hanamkonda	18.02	79.57	-0.160	-0.084	0.081	-0.323
101	Jactial	18.80	78.93	-0.082	0.105	0.150	-0.015
102	Nevasa	19.55	74.93	-0.168	-0.071	0.006	-0.027
103	Nizamabad	18.67	78.10	0.153	-0.066	0.010	0.201
104	Bidar	17.87	77.48	-0.264	-0.212	-0.095	-0.128
105	Owk	15.22	78.13	-0.306	-0.008	0.064	0.043
106	Hinganghat	20.55	78.83	0.097	-0.077	-0.036	0.205
107	Nanded	19.13	77.33	0.095	0.056	-0.068	0.230
108	Niphad	20.08	74.12	-0.106	-0.160	-0.182	-0.012
109	Sangareddi	17.63	78.08	0.143	-0.089	-0.078	0.094
110	Sironcha	18.83	79.97	0.257	0.058	0.110	0.022
111	Umrer	20.85	79.33	0.071	0.104	-0.046	-0.018
112	Yeola	20.05	74.48	0.005	0.142	0.149	-0.052
113	Brahmapuri	20.60	79.87	0.030	-0.013	-0.047	-0.078
114	Chandrapur	19.95	79.30	-0.032	0.012	-0.204	-0.038
115	Pathardi	19.17	75.17	0.087	0.002	0.003	0.076
116	Bhadrachalam	17.67	80.90	0.228	0.056	0.127	0.157
117	Motihari	26.67	84.92	0.008	-0.037	-0.131	-0.091
118	Mainpuri	27.23	79.05	0.154	-0.043	-0.008	-0.005
119	Bahraich	27.57	81.60	-0.031	0.008	0.073	0.049
120	Rajakhera	26.90	78.18	-0.051	-0.049	-0.004	-0.064
121	Manohar Thana	24.23	76.80	0.122	-0.172	-0.095	0.017
122	Shahabad	25.25	77.13	-0.354	-0.004	-0.040	-0.149
123	Sonkatch	22.97	76.35	-0.081	-0.031	0.090	-0.031
124	Bari	26.65	77.60	0.051	0.072	0.228	-0.188

SL. No.	Stations Name	Latitude (Degree)	Longitude (Degree)	Pearson's correlation coefficient (r) for covariates			
				RAT	NINO	IOD	GAT
125	Sangod	24.93	76.28	-0.169	0.095	0.010	-0.016
126	Banswara	23.55	74.45	0.090	0.034	0.091	0.167
127	Jhabua	22.78	74.58	0.025	-0.076	-0.031	0.043
128	Burwaha	22.27	76.03	-0.091	0.002	0.030	0.120
129	Daltonganj	24.05	84.07	0.063	-0.060	0.074	0.113
130	Mukteshwar	29.47	79.65	-0.200	-0.189	-0.236	-0.092
131	Jhansi	25.45	78.58	-0.014	-0.014	0.058	-0.038
132	Bharatpur	27.22	77.5	0.109	0.020	0.098	0.111
133	Fatehpur	25.93	80.83	0.081	0.020	0.076	0.137
134	Gohad	26.42	78.45	0.142	0.045	-0.103	0.008
135	Simdega	22.62	84.57	-0.112	0.128	0.156	-0.108
136	Seorinarayan	21.72	82.60	0.007	-0.087	-0.021	0.201
137	Champua	22.17	85.50	0.001	0.051	0.136	0.000
138	Alirajpur	22.30	74.37	-0.126	-0.052	0.013	-0.194
139	Harsud	22.12	76.73	0.257	-0.069	-0.265	0.057
140	Indore	22.72	75.8	-0.296	0.005	-0.182	0.061
141	Sagar	23.85	78.75	0.020	-0.078	-0.155	-0.012
142	Satna	24.57	80.83	-0.001	-0.117	-0.046	0.017
143	Pendra Road	22.77	81.9	-0.132	0.102	0.074	0.199
144	Raisen	23.33	77.8	-0.004	0.171	0.187	0.057
145	Guna	24.65	77.32	-0.142	-0.119	-0.147	-0.097
146	Pandaria	22.22	81.42	0.081	-0.174	0.097	0.116
147	Niwas	23.05	80.45	0.070	-0.194	-0.065	0.012
148	Dug/Dag	23.93	75.83	0.082	-0.098	-0.059	-0.115
149	Lahar	26.20	78.93	-0.218	0.127	0.020	-0.143
150	Tezpur	26.62	92.78	0.208	-0.007	-0.124	0.136
151	Jalpaiguri	26.53	88.72	0.122	0.031	-0.137	0.237
152	Hazaribagh	23.98	85.37	-0.086	0.153	0.069	-0.062
153	Alipur	22.53	88.33	-0.018	-0.169	-0.170	-0.024
154	Barhampore	24.13	88.27	0.192	-0.181	-0.162	0.299
155	Midnapore	22.42	87.32	-0.107	-0.197	-0.090	-0.108
156	Sonahatu	23.20	85.72	0.071	-0.072	0.075	-0.038
157	Lumding	25.75	93.18	-0.162	-0.120	-0.128	-0.140
158	Gaya Aerodrome	24.75	84.95	-0.147	-0.004	-0.129	-0.146
159	Sabour	25.23	87.07	0.091	0.264	0.130	0.123
160	Silda Belpahari	22.63	86.80	-0.032	-0.083	0.015	-0.092
161	Senha	23.58	84.75	0.007	-0.171	-0.134	0.036
162	Agartala Sadar	23.88	91.25	0.161	-0.053	0.001	-0.025
163	Cherrapunji	25.25	91.73	0.019	-0.029	-0.073	-0.033
164	Purnea	25.77	87.47	0.305	0.160	0.191	0.271
165	Malda	25.03	88.13	0.185	-0.048	0.082	0.311
166	Krishnanagar	23.4	88.52	-0.003	-0.163	-0.102	-0.078
167	Jaipur Aero	26.92	76.83	-0.144	-0.273	-0.250	0.015
168	Bhim/Dawer	25.75	74.08	-0.066	0.039	0.063	0.140
169	Dehra Dun	30.32	78.03	0.125	0.020	-0.059	-0.070

SL. No.	Stations Name	Latitude (Degree)	Longitude (Degree)	Pearson's correlation coefficient (r) for covariates			
				RAT	NINO	IOD	GAT
170	Simla	31.10	77.17	0.065	-0.071	-0.026	0.107
171	Kotkhai	31.12	77.53	0.057	-0.019	-0.144	-0.058
172	Lachmangarh	27.37	76.87	-0.124	-0.146	-0.250	-0.129
173	Mandawar	27.87	76.55	0.155	0.112	0.110	0.227
174	Nimarana	28.00	76.38	0.115	-0.095	-0.034	-0.036
175	Kamen	27.65	77.27	-0.024	-0.076	-0.059	-0.070
176	Chirawa	28.23	75.65	-0.127	-0.180	-0.308	-0.181
177	Jhunjhunu	28.13	75.38	-0.057	-0.268	-0.311	-0.041
178	Khetri	28.00	75.80	-0.208	-0.232	-0.200	-0.238
179	Hissar	29.17	75.73	0.108	-0.109	-0.090	0.144
180	Nimbahera	24.62	74.70	-0.155	-0.055	0.063	0.020
181	Hindoli	25.58	75.50	-0.074	-0.234	-0.121	-0.190
182	Patan	25.30	75.95	-0.278	-0.201	-0.299	-0.213
183	Bali	25.18	73.28	-0.199	-0.013	-0.048	0.069
184	Bilara	26.18	73.70	-0.092	0.204	-0.031	0.194
185	Desuri	25.28	73.55	-0.058	-0.004	-0.060	0.136
186	Jalore	25.35	72.62	-0.211	0.069	-0.122	0.188
187	Nayanagar/Beawar	26.10	74.32	-0.078	0.026	-0.078	-0.045
188	Pachpadra	25.93	72.27	0.000	-0.160	-0.055	0.232
189	Shergarh	26.33	72.30	-0.039	0.067	0.037	0.195
190	Merta City	26.63	74.03	-0.206	0.124	0.004	-0.018
191	Partabgarh	24.05	74.78	0.010	0.005	-0.062	0.060
192	Sheoganj	25.12	73.07	-0.102	-0.173	-0.175	-0.102
193	Arthuna	23.50	74.08	0.120	0.107	0.092	0.239
194	Jodhpur	26.30	73.03	-0.144	0.051	-0.064	0.224
195	Barmer	25.75	71.40	-0.005	0.046	-0.033	0.186
196	Ahmedabad Aero	23.03	72.62	-0.014	-0.087	-0.185	-0.031
197	Deesa	24.20	72.25	-0.104	0.098	0.000	0.108
198	Rajkot Aero	22.30	70.77	-0.001	-0.013	0.005	-0.007
199	Lalsot	26.55	76.33	-0.123	-0.207	-0.142	0.008
200	Bhuj/R.Mata A.	23.25	69.80	-0.155	-0.078	-0.119	-0.017
201	Chotan	25.48	71.07	-0.076	0.014	-0.048	0.306
202	Sathankulam	8.45	77.92	0.244	0.096	0.007	0.277
203	Srivaikundam	8.63	77.92	-0.010	0.066	0.032	-0.099
204	Ayikudi	9.00	77.33	0.034	0.050	0.035	0.013
205	Manimuthar	8.58	77.42	0.155	0.204	0.027	0.377
206	Radhapuram	8.27	77.68	-0.026	0.047	0.011	-0.090
207	Chickmagalur	13.33	75.77	-0.287	0.000	0.076	-0.348
208	Mudigere T.O.	13.13	75.63	-0.087	-0.102	0.101	-0.133
209	Saklespur	12.95	75.78	-0.146	-0.085	0.029	-0.262
210	Sukravarasathy	12.87	75.80	0.179	0.026	0.144	0.098
211	Ammathy	12.23	75.85	0.103	-0.017	0.214	0.201
212	Avandoor	12.38	75.67	0.030	0.061	0.032	-0.028
213	Bhagamandala	12.38	75.52	0.023	0.124	0.055	0.098
214	Harangi	12.50	75.83	0.328	0.338	0.155	0.289

SL. No.	Stations Name	Latitude (Degree)	Longitude (Degree)	Pearson's correlation coefficient (r) for covariates			
				RAT	NINO	IOD	GAT
215	Maladare Forest	12.32	75.97	0.046	0.050	0.045	0.130
216	Srimangala	12.02	75.98	-0.071	0.170	0.140	-0.018
217	Thittimatti	12.22	76.00	0.159	0.065	-0.012	0.157
218	Periyapatna	12.33	76.10	0.020	0.059	-0.049	-0.014
219	Udagamandalam	11.40	76.68	0.045	0.105	0.242	-0.035
220	Kayamkulam	9.18	76.50	-0.233	0.076	-0.094	-0.045
221	Bantwal T.O.	12.88	75.03	0.020	0.128	0.055	0.079
222	Kozhikode	11.25	75.78	-0.150	-0.102	0.034	-0.092
223	Nedumangad	8.60	77.00	-0.086	-0.127	-0.060	-0.007
224	Thiruvananthapur	8.48	76.95	0.066	-0.062	0.104	-0.062
225	Bombay Colaba	18.98	72.83	-0.064	-0.037	-0.162	0.062
226	Mundagod Hospita	14.97	75.03	0.013	0.056	0.079	0.097
227	Panjim	15.48	73.82	0.340	-0.086	-0.038	0.264
228	Ratnagiri	16.98	73.30	0.093	-0.093	0.043	0.195
229	Chickmagalur	13.33	75.77	-0.298	-0.162	-0.124	-0.237
230	Akola	19.55	74.02	-0.213	-0.004	-0.123	-0.343
231	Mercara	12.43	75.73	0.134	0.001	0.003	0.193
232	Baroda College	22.33	73.27	0.074	-0.029	0.224	0.087
233	Veraval	20.90	70.37	-0.269	-0.195	-0.104	-0.138
234	Vada	19.65	73.13	0.050	0.220	0.159	0.290
235	Hoshangabad	22.26	71.19	-0.094	0.011	0.046	-0.057
236	Udupi	13.35	74.75	0.200	-0.002	-0.006	-0.005
237	Yellapur	14.95	74.72	-0.045	-0.138	0.035	-0.015
238	Dahanu	19.98	72.72	0.100	0.073	0.092	0.059
239	Margon	15.28	73.97	0.102	-0.030	-0.089	0.190

The list of communicated manuscripts from the present study are given bellow:

1. RAY, L.K., Goel, N.K. and Arora, M. "Trend analysis and change point detection of temperature over India", Theoretical and Applied Climatology **[Communicated]**

2. RAY, L.K. and Goel, N.K. "Non-stationary frequency analysis of extreme rainfall events across India", Global and Planetary Change **[Communicated]**

3. RAY, L.K. and Goel, N.K. "Flood frequency analysis of Narmada river basin in India under Non-stationary condition", Stochastic Environmental Research and Risk Assessment **[Communicated]**